THE UNIVERSITY OF OKLAHOMA

GRADUATE COLLEGE

A DUAL-POROSITY MODEL FOR TWO-PHASE FLOW IN DEFORMING POROUS MEDIA

A Dissertation

SUBMITTED TO THE GRADUATE FACULTY

in partial fulfillment of the requirements for the

degree of

Doctor of Philosophy

By

ZHENGYING SHU

Norman, Oklahoma

1999

UMI Number: 9930844

A DUAL-POROSITY MODEL FOR TWO-PHASE FLOW IN DEFORMING POROUS MEDIA

A Dissertation APPROVED FOR THE

SCHOOL OF PETROLEUM AND GEOLOGICAL ENGINEERING

BY

Dedication

To my beautiful wife, Hui, and lovely son, David Jiaqi.

Acknowledgments

I would like to express my most sincere gratitude to my advisor Dr. Jean-Claude Roegiers for his invaluable advice, encouragement and guidance throughout this work. His leadership and broad knowledge have been of benefit to me and led to excellence of the Rock Mechanics Institute at the University of Oklahoma.

I also highly appreciated Dr. Mao Bai for his suggestions and help in conducting my research and for drawing me into the field of poroelasticity.

I would like to extend my appreciation to Dr. Roy M. Knapp, Dr. Michael L. Wiggins, Dr. Anuj Gupta and Dr. James M. Forgotson Jr., for serving on my dissertation committee and for their helpful guidance.

A special note of gratitude to all my research group-mates, especially Dr. M. Zaman and Dr. Fanghong Meng, for innumerable discussions from which I learned a lot.

My appreciation goes to my parents, Gengwu Shu and Jinming Zheng, my parents-in-law, Qifan Zhang and Meifang Liu, and my sister-in-law, Jie Zhang, for taking care of my son in both China and the US. I want also to thank my sister, Lianfang Shu, and my brother-in-law, Gaosong Liu, for their encouragement, help and taking part of my responsibility in taking care of our parents.

Contents

List of Figures

List of Tables

Abstract

Only recently has one realized the importance of the coupling of fluid flow with rock matrix deformations for accurately modeling many problems in petroleum, civil, environmental, geological and mining engineering. In the oil industry, problems such as reservoir compaction, ground subsidence, borehole stability and sanding need to be simulated using a coupled approach to make more precise predictions than when each process is considered to be independent of the other. Due to complications associated with multiple physical processes and mathematical representation of a multiphase flow system in deformable fractured reservoirs, very few references, if any, are available in the literature.

In this dissertation, an approach, which is based on the dual-porosity concept and takes into account rock deformations, is presented to derive rigorously a set of coupled differential equations governing the behavior of fractured porous media and two-phase fluid flow. The finite difference numerical method, as an alternative method for finite element, is applied to discretize the governing equations both in time and space domains. Throughout the derived set of equations, the fluid pressures and saturations as well as the solid displacements are considered as the primary unknowns.

The model is tested against the case of single-phase flow in a 1-D consolidation problem for which analytical solutions are available. An example of coupled two-

phase fluid flow and rock deformations for a scenario of a one-dimensional. fractured porous medium is also discussed.

The only paper that proposed a mathematical model for the case of multi-phase flow, and also considered the rock deformations, was published in 1997 by Lewis and Ghafouri. In their model, the derivation of the continuity equations for fluids was carried out by writing out term-by-term the contribution to the fluid accumulation rate. This method was based on the intuitive phenomenological concept, rather than any theoretical reasoning. Hence, some parts in their equations are questionable.

The numerical model and simulator, RFIA (Rock Fluid InterAction), developed in this dissertation can be a powerful tool to solve difficult problems not only in petroleum engineering such as ground subsidence, borehole stability and sand control, but also in civil engineering such as groundwater flow through fractured bedrock and in environmental engineering such as waste deposit concerns in fractured and unconsolidated formations. As an example of application in petroleum engineering, the waterflooding process in a deformable fractured reservoir was numerically simulated and analyzed.

Finally, sensitivity analyses were carried out to investigate the relative importance of some required parameters to the overall behavior of a deformable fractured reservoir.

Chapter 1

Introduction

Natural fractures affect all phases of the petroleum reservoir life-span, from the accumulation of oil to the techniques used to manage production. The existence of fractures in oil reservoirs was known as early as the 1860's. However, only in the last thirty years has significant interest in the effect of fractures on oil production developed.

Naturally-fractured reservoirs can be represented by a dual-porosity system, in which most of the fluid conduction is provided by the fractures, whose permeability k_f is much higher than the permeability of the porous matrix k_m; while most of the fluid storage is provided by the porous blocks, whose porosity ϕ_m is much larger than the porosity of the fractures ϕ_f. For example, the porous blocks may have a porosity of 8-20% and a permeability of the order of a few millidarcys while the porosity of the fractures is at least one order of magnitude less and its permeability is at least ten times greater than the corresponding porous matrix. Thus, while the storage capacity of the matrix is high and the fractures low, the flow in the fractures is high and the blocks act as feeders to the system of fractures. The dual-porosity approach has been used to describe naturally-fractured reservoirs since the 60's.

Withdrawal of hydrocarbons from the reservoir formations may result in an increase in effective stresses on the matrix, leading to collapse of pores; hence, a reduction in porosity and permeability. This phenomenon is called *pore collapse*. It may lead to the compaction of the producing formation and subsidence of the ground surface. Pore collapse in a reservoir affects many aspects of oil and gas production including rock permeability, production rate, wellbore stability, sand production control, reservoir management and ground surface subsidence. Subsidence in turn may affect stability and operability of drilling and production equipment, requiring costly remedial measures.

Numerous problems attributed to pore collapse and deformation of the rock matrix have been reported in different areas of the world, examples of which are Ekofisk field and Valhall fields in the North Sea (Boade *et al.*, 1989; Marius, 1990); Wilmington field, Long Beach, California (Allen, 1968); Bolivar Coast and Lagunillas fields in Venezuela (Merle *et al.*, 1976); Groningen field in Netherlands (Schoonbeek, 1976) and Central Luconia fields in East Malaysia (van Ditzhuijzen and de Waal, 1984). However, in conventional reservoir models, the role of the reservoir rock is often limited to their storage and delivery capabilities and close interaction between fluid flow and rock deformation has been ignored.

Hence, numerical simulation of fluid flow in deformable fractured media is a great challenge and of a great interest for petroleum engineers. Because of complications associated with multiple physical processes in deformable rock masses and mathematical representation of a multiphase flow system, only a few pertinent references are available in the literature, even fewer if the porous media are considered to be fractured.

1.1 Objectives of the Study

The main purpose of this dissertation is to investigate the complex process of two-phase fluid flow in deforming naturally fractured media and the feasibility of applying a finite difference method to solve such types of problems.

The goals of this dissertation are as follows:

1. Derive a set of two-phase fluid flow equations coupled with rock deformations considering the continuity equation, the flow equation, the equation of state, and the solid equilibrium equation to characterize the behavior of fluid flow in deformable naturally fractured media based on the dual-porosity concept.

2. Develop a simulator based on the derived formulations using a finite difference numerical scheme to model the coupled phenomena of immiscible two-phase fluid flow and the deformations of naturally fractured rock.

3. Determine flow, saturation, pore pressure and stress patterns.

4. Use the simulator to study applied problems such as waterflooding process in the petroleum industry.

1.2 Organization of the Dissertation

A brief introduction describing the importance of the present research is presented in Chapter 1 which also includes the goals of this study and outlines the contents of the dissertation.

Chapter 2 gives a thorough critical review of the relevant literature. Reservoir simulation models can be classified according to the type of reservoir they are intended to simulate, or on the basis of a particular reservoir process. Simulators based on the former classification fall generally into three groups: gas reservoir simulators, black-oil reservoir simulators, and compositional reservoir simulators. Particular reservoir processes and phenomena such as wellbore coning, thermal recovery processes, chemical flooding, and miscible displacements categorize other types of reservoir models. The background of this chapter constitutes the basis for the development of most numerical models developed over these past decades.

Chapter 3 derives the governing equations for two-phase fluid flow in a deformable fractured porous medium. The two equilibrium equations for the solid (in x- and y-directions) contain both fluid pressures in the matrix and in the fractures. The four continuity equations for the fluid phases, two for the matrix and another two for the fractures, include the unknown solid displacements. These six equations are fully coupled and the continuity equations in the matrix and in the fractures (for one fluid) are linked by a mass interchange term.

Chapter 4 details the numerical implementation of the governing equations derived in Chapter 4. A finite difference numerical technique is applied as a alternative to the finite element method .

The developed model as well as the simulator are validated by comparing the results from this study with the analytical expressions derived in Chapter 5.

Chapter 6 presents two applications: a fractured rock consolidation problem coupled with two-phase fluid flow; and a deformable fractured reservoir with water injection.

The sensitivity analyses are carried out in Chapter 7 to investigate the relative importance of some required parameters to the overall behavior of a deformable fractured reservoir.

Chapter 8 summarizes the research contributions, conclusions and provides recommendations for future work.

The fundamental and essential ideas needed for this particular research are covered in Appendix A. Reservoir engineering concepts such as capillary pressure and formation volume factor as well as rock mechanics subjects such as stress, strain and poroelasticity are also introduced.

Appendix B lists the special forms of the six discretized governing equations for each boundary and corner point, based on the boundary conditions specified for both validation and application cases, respectively.

Chapter 2

Critical Literature Review

Flow of fluids in fractured porous media was recognized first in the petroleum industry in the 40's. Since then, many researchers have added to the volume of literature on fractured media. The development of models for fluid flow in naturally fractured reservoirs has proceeded along two main different approaches:

1. Statistical approach; and,
2. Enumerative, or discrete approach.

In the first approach, the fractured rock mass is considered as a statistically homogeneous medium consisting of a combination of fractures and a porous rock matrix. The fractures are considered ubiquitous, and the system is called statistically homogeneous because the probability of finding a fracture at any given point in the system is considered the same as finding one at any other point. It relies on the use of the concepts of statistical averaging, volume averaging, and the theory of mixtures.

In the second approach, the fractured reservoir is modeled by attempting to introduce the actual geometry of the discontinuities and the porous rock matrix. The location, orientation, and aperture variations for each individual fracture must be considered in this approach.

Table 2.1 gives a general classification of the existing models used to describe the flow characteristics in naturally fractured reservoirs.

Table 2.1: Naturally Fractured Reservoirs Models

TYPE		CHARACTERISTICS
Statistical Approach	Equivalent porous media	Fluid flow in fracture network can be characterized by an equivalent porous media
	Double porosity	Poorly permeable rock matrix dissected by a network of highly permeable fractures
Enumerative Approach	Isolated fracture	Flow regime in and around a single fracture
	Fracture network	Flow regime in a set of discrete interconnected fractures

The simplest approach has been to use a conventional black-oil simulator, as proposed by Bossie-Codreanu *et al.* (1985), in which the fractures and rock matrix are represented as separated cells. Flow between these cells represents the actual flows between the matrix blocks and their surrounding fractures inside the elements representing the reservoir. This approach is an extreme simplification and is unable to represent certain important physical phenomena such as the transfer of oil from the rock matrix blocks to the fractures. On the other hand, almost all the existing reservoir response models do not include the complex interaction between fluid flow and rock deformations.

2.1 Dual-Porosity Model

2.1.1 Uncoupled Dual-Porosity Model

The dual-porosity approach has been used to describe rigid naturally-fractured reservoirs since the 60's. Barenblatt *et al.* in 1960, Warren and Root in 1963, and several authors later (e.g. Kazemi *et al.* in 1969; Yamamoto *et al.* in 1971) derived an analytical solution for single-phase, unsteady-state flow towards a well in a homogeneous fractured reservoir. These models consider mass transfer between rock matrix blocks and fractures, but no flow is allowed to take place between adjacent rock blocks. All these publications were applying the dual-porosity theory to transient well testing.

Barenblatt *et al.* (1960) formulated the equations of flow for fractured reservoirs of double porosity through the continuum approach. In his model, the two media, fracture network and matrix blocks, were considered to be overlapping continua, whereby the flow and medium parameters were defined at each mathematical point. The equations of motion and of conservation of mass were written independently for each medium, and transfer of liquid between the two media was taken into account by a sink/source term in the equations of conservation of mass. Single-phase, unsteady-state flow within the fractures and quasi-steady state flow from the homogeneous rock blocks to the randomly distributed fractures were considered.

Warren-Root's (1963) model represented the fractured reservoir as an idealized system formed by identical rectangular parallelepipeds, separated by an orthogonal network of fractures. The flow towards the wellbore was considered to take place in the network, while the matrix continuously fed the system of fractures under quasi-steady flow conditions.

Kazemi (1968) developed an ideal theoretical model of a naturally fractured reservoir with a uniform fracture distribution based on the Warren-Root's model; it consisted of a finite circular reservoir with a centrally located well and two distinct porous regions, i.e., matrix and fractures. Later, Dougherty and Babu (1985) extended this model to consider a well that only partially penetrated the formation.

Abdassah and Ershaghi (1986) extended the double porosity model to triple porosity for the analysis of single-phase, unsteady-state flow in naturally fractured reservoirs. A system where fractures have homogeneous properties throughout, and interact with two groups of separate matrix blocks that have distinctly different permeabilities and porosities was considered in their model. They claimed that such a system is a more realistic representation of fractured reservoirs than the traditionally used dual-porosity models and that, in addition, the dual-porosity model is a special case of their proposed triple-porosity model.

de Swaan (1976) developed an analytical solution to the transient flow regime, for a modified dual-porosity model considering the flow from the matrix rocks as unsteady-state. In his model, the shape of the matrix blocks was approximated by regular solids or slabs, instead of rectangular shapes.

Several researchers also studied the flow behavior of an individual rock matrix block and its adjacent fractures. Birks (1955) used a capillary model and a simple relative permeability model to describe the mechanics of oil transfer from the rock matrix to the fractures. Graham and Richardson (1960) used a synthetic model to scale a single element of a fractures-matrix reservoir for predicting imbibition oil recovery behavior. Blair (1960) used numerical techniques to solve the differential equations describing imbibition in linear and radial systems. Mattax and Kyte (1962) proposed a third method for predicting imbibition oil recovery for large reservoir matrix blocks based on scaled imbibition tests on small reservoir core samples. They presented experimental results on water/oil imbibition in laboratory core samples and defined a dimensionless group that related recovery to time. Yamamoto *et al.* (1971) presented a mathematical model for the simulation of pressure, production and saturation behavior of a single block within a fissured system. Variable physical properties, drainage and imbibition capillary pressures, pore compressibility, and gravity were considered in their formulation. Recovery mechanisms for various-size blocks surrounded by oil or gas were studied. Parsons and Chaney (1966) studied the imbibition mechanism in fractured carbonate reservoirs with a bottom waterdrive via laboratory experiments.

Barenblatt (1964) used a different approach to describe the flow from the rock matrix. In his formulation, the flow between the fractures and the matrix blocks was described using source functions derived from dimensional considerations by assuming that it was proportional to the pressure difference. Bokserman *et al.* (1964) took the source function as representing an imbibition process solely and used the experimental data of Mattax and Kyte (1962). Braester (1972) derived the source function by using a conceptual model of a block made up of a bundle of randomly oriented capillary tubes. Rossen (1977) also adopted source functions to consider the flow from the matrix to the fractures. The fundamental advantage of his approach is that these source terms are handled semi-implicitly in both the pressure and saturation calculations involved in the fracture simulation.

All the models mentioned above have been designed to study specific problems and only for a given segment of a reservoir. Simulation of an entire reservoir system with multiple phases further complicated the problem and made additional simulator modifications necessary.

Asfari and Witherspoon (1973) developed a modeling approach for reservoirs with a regular pattern of noncommunicating vertical fractures by assigning constant pressures along each fracture. Kazemi *et al.* (1976) presented a three-dimensional, multiple-well, numerical simulator to represent single or two-phase flow of water and oil in fractured reservoirs. Their equations are two-phase flow extensions of the single-phase equations derived by Warren and Root (1963). The simulator took relative mobilities, gravity force, imbibition and reservoir heterogeneity into account.

Thomas *et al.* (1983) developed a three-dimensional, three-phase model for simulating the flow of water, oil and gas in a naturally fractured reservoir where the dual-porosity system was used to describe the fluids presented in the fractures and matrix blocks. The matrix/fracture transfer function incorporated the effect of pressure on interfacial tension and accounted for capillary pressure, gravity, and viscous forces. Gilman and Kazemi (1982) described a two-phase, three-dimensional simulator similar to that proposed by Thomas *et al.* (1983), in which Kazemi's extension of the Warren-Root model to multiphase flow was used as the basis. Their model accounted for unsteady-state multiphase flow between matrix and fractures, but unsteady-state flow within individual matrix blocks could not be simulated.

Evans (1981) proposed a more general mathematical model than that presented by Thomas *et al.* (1983) for multiphase flow through naturally fractured reservoirs based on Barenblatt's double porous medium concept: one porosity being associated with the rock matrix and the second one relates to the fractures. In his model, flow in the primary pores was described by Darcy's law, while flow in fractures was described using a generalized Darcy's type equation. Time-dependent porosity equations for the rock matrix and the fracture system were derived with the mass conservation equations to complete the governing equations. Nakornthap and Evans (1984) later implemented these formulations into a simulator.

Blaskovitch *et al.* (1983) presented a three-phase, three-dimensional fractured reservoir simulator with the addition of matrix-to-matrix flow and multicomponent fluid representation. Litvak (1985) developed a model to incorporate the special treatment of capillary and gravity forces for the fracture-matrix media into a general purpose dual-porosity, three-phase, three-dimensional reservoir simulator which was designed for field applications.

All of these models, originally developed for the study of hydrocarbon reservoirs, are concerned essentially with the fluid flow, describing the mechanisms that take place during reservoir depletion in different ways and with different degrees of accuracy. The study of the interactions between fluid flow and rock deformability properties in naturally fractured reservoir is not common in the oil industry.

2.1.2 Coupled Single Porosity Models

The study of fluid flow in deformable, saturated, porous media as a coupled flow-deformation phenomenon started with the work of Terzaghi (1943) who developed a one-dimensional consolidation model. An extension to three-dimensional soil consolidation, based on physically consistent assumptions, was given by Biot (1941, 1955, 1956).

Biot presented the first consistent theory formulating the coupled fluid flow and rock deformation processes in fluid-filled porous media, the theory of poroelasticity. Biot's theory of the mechanics of porous media is a major twentieth century extension of theoretical continuum mechanics-a generalization of the elasticity theory which, in its final form, incorporated a complete spectrum of thermodynamical and dissipative effects. It has led to the solution of numerous problems of soil consolidation, dynamics and wave propagation in acoustics, geophysics, engineering and applied physics-problems beyond the scope of traditional methods of the elasticity theory. His first paper established the fundamental field equations for three-dimensional consolidation of an isotropic model representing the settlement of soil under load. These equations gave the stresses and displacements of an elastic matrix, or skeleton, whose voids are filled with a viscous fluid satisfying Darcy's law. Whereas the basic theory is simple and straightforward, its implications were considerable, since it established the conceptual framework from which stems the generalization of Biot's later work. Assuming isotropic, linearity, small strains, reversibility and an incompressible fluid, a system of four linear partial differential equations was obtained for the four unknowns u, v, w, and σ (displacements of the solid matrix in the x-, y-, and z-directions and the fluid pressure). These equations were second-order in x, y and z; and first-order in t; allowed to solve time-dependent diffusion-type settlement problems for concentrated loads and linear boundary conditions. The properties of this system were determined by four distinct physical constants. The paper also demonstrated how a suddenly applied load can be solved in a few lines using elementary Heaviside operational calculus.

Some researchers have studied analytically coupled flow-deformation phenomena in porous media around boreholes. Paslay and Cheatman (1963) studied rock stresses and steady-state flow rates induced by the pressure gradient associated with the flow of formation fluid into a borehole for a permeable, elastic material saturated with an incompressible fluid. Wang and Dusseault (1991) developed a poro-elastoplastic model considering steady fluid flow for a Mohr-Coulomb strain-weakening material. McLellan and Wang (1994) extended this model and studied borehole instability problems. Rudnicky *et al.* (1987) presented an analytical solution for elasto-plasticity around a borehole where permeability was allowed to vary with the radius but symmetry of stresses existed. Detournay and Cheng (1993) used the poroelasticity theory for a borehole in a non-hydrostatic stress field to study the transient flow in the coupled problem around a borehole.

Meanwhile, coupled numerical models have also been developed by other researchers such as Zienkiewicz and Shiomi (1984), Schrefler *et al.* (1990), Li *et al.* (1990), and Li and Zienkiewicz (1992). The formulation of these models was developed within the framework of the continuum theory of mixture, using a spatially-averaged approach. A typical such model is the one developed by Li *et al.* (1990) for immiscible two-phase (water and oil) flow in a deforming porous medium. In this work, they formulated the governing equations on the basis of the generalized Biot theory. The primary unknowns are the displacements of the solid skeleton as well as the pressure and saturation of the wetting fluid. The model considered the effects of fluid and matrix compressibilities, interphase mass exchange and capillary pressure. The mobilities and compressibilities of both fluids phases were assumed to be functions of the porosity, saturation, pressure and temperature. The full mathematical model consisted of two non-linear mass balance equations for the two fluid phases and one non-linear equilibrium equation for the total mixture, subjected to Darcy's law for multiphase flow and the constraint defining capillary pressure between both fluids. They assumed that, in the considered two-phase flow, only one phase (water) is in contact with the solid and that the second phase is entirely contained within this; hence, making no contact with the solid. A generalized Galerkin procedure was followed to discretize the governing equations; and an unconditionally stable direct integration scheme was used to obtain the solution.

Li and Zienkiewicz (1992) extended Li *et al.* (1990) model to simulate multiphase flow in deforming porous media. Unconditionally stable and staggered solution procedures were used and compared for the time-domain numerical solution.

Schrefler and Zhan (1993) developed a fully coupled model for water and air flows in deformable porous media. Slow transient phenomena (consolidation) were considered; the model was of the Biot-type and incorporated the capillary pressure relationship. The finite element method was used for the discretization of the governing equations and a direct method was used for the solution of the resulting system of coupled equations. They assumed that air does not dissolve in water. Hence, this model could not be applied to hydrocarbon systems in which gas can easily dissolve into and/or escape from the oil phase. Gawin *et al.* (1997) also presented a model for numerical simulation of gas and water flow in deformable porous media on the basis of the desaturation experiments performed by Liakopoulos (1965). It consists of three balance equations: mass of dry air, mass of water species and linear momentum of the multiphase medium. An appropriate set of constitutive and state equations, as well as some thermodynamic relationships complete the model. In this model, gas is actually air and can not dissolve into water like in the Schrefler and Zhan's (1993) model, but water can change phase from liquid to vapor and/or from vapor to liquid.

Lewis and Sukirman (1993a) presented an elastoplastic soil model for three-phase, three-dimensional problems based on Mohr-Coulomb's yield surface. The effects of capillary pressure, relative permeability variations and the compressibility factors of rock and fluids were considered on each of the flowing phases. Biot's self-consistent theory was used to develop the governing equations which couple the equilibrium and continuity equations for a deforming saturated oil reservoir. The finite element method was applied to obtain simultaneous solutions to the governing equations where displacements and fluid pressures are the primary unknowns. The final discretized equations were solved by a direct solver using fully implicit procedures.

Sun *et al.* (1997) pointed out that there is some difficulty to deal with the air pressure boundary problem and air injection volume problem using Li *et al.* (1990) model because of taking the pressure and the saturation of the wetting phase as primary unknowns. Hence, they presented a finite element numerical model of two-phase (water and air) flow in deforming porous media in which the displacements, the pressures of air and water were taken as primary unknowns. Again air is considered not dissolving in water.

In their paper, Chin and Prévost (1997) first derived the equations governing isothermal two-phase fluid flow in a deformable porous medium similar to the ones derived by Li *et al.* (1990), but the displacements, the pressures of water and air were taken as primary unknowns. Then, a computer method based on a multistagger solution strategy was used for numerically solving the coupled equations. The full system of coupled equations, defined in the problem domain, was partitioned into smaller subsystems of equations. Each subsystem was then solved separately, assuming the unknowns of the other subsystems were temporarily frozen until (sequentially and repeatedly in a predetermined sequence) all subsystems converged to a self-consistent set of solution variables. Based on the cases investigated and the numerical results obtained, they concluded that this approach was robust, accurate, and efficient for analyzing coupled field problems; it was also more economical in the computational cost compared to the conventional simultaneous procedure.

Dagger (1997) developed a two-dimensional explicit Lagrangian finite difference code, fully-coupled with a two fluid flow system in deformable porous media based on the model derived by Li *et al.* (1990). The solid deformations were considered using the dynamic relaxation procedure which allowed the model to go into the rock's post-peak behavior without creating instabilities. The fluid flow equations were written using mixing laws and the solid was treated as another phase. The primary variables: pore pressure and water saturations, were obtained using Newton's iteration, or a staggered algorithm, to solve the system of nonlinear equations. The code was checked numerically against the analytical solution for single phase flow with consolidation. Examples of coupled fluid flow and rock deformation for a one-dimensional scenario and for a layered oil reservoir compaction are also given.

2.1.3 Coupled Dual-Porosity Models

Single-Phase Fluid Flow Models

Duguid (1973), Duguid and Abel (1974), and Duguid and Lee (1977) proposed a coupled flow-deformation model, explicitly considering the effect of matrix deformations on flow regions. In their model, it was assumed that, for a fully saturated medium, changes in pore volume were equal to the compression of the fluid occupying that space. This assumption is valid only for the situation where fluid is trapped within pores.

Aifantis (1977, 1980) presented a general coupled double-porosity formulation for modeling single-phase in a deformable fissured porous media based on the theory of mixtures. Mixture theory usually adopts a thermodynamic framework and, starting from general constitutive assumptions, produces non-linear governing equations for consolidation which, in their linearized form, are generalizations of Biot's equations. Formulations based on mixture theories are generally useful in practical problems if non-linear or thermal effects are important.

Wilson and Aifantis (1982) obtained the analytical solutions to the column problem in hydro-engineering and the borehole problem in petroleum engineering on the basis of Aifantis' theory of consolidation with double porosity, which is the extension from the Biot's theory of consolidation with single porosity. Khaled *et al.* (1984) published a paper to further elaborate on Aifantis' theory by first providing an alternative derivation of his fissured rock equations through a proper extension of Biot's classical model of flow in single porosity media. They developed a finite element methodology based on the Galerkin's version of the method of weighted residuals for the numerical solution of the relevant equations. This method was used for consolidation problems for the first time and provided some advantages over finite element techniques based on variational principles, such as easy handling of boundary conditions. The above methodology was implemented to numerically solve three examples, namely the one-dimensional column, the two-dimensional layer, and the two-dimensional half-space problems.

Valliappan and Khalili-Naghadeh (1990) derived a set of coupled differential equations governing the behavior of deformable fissured porous media based on the double porosity concept. The coefficients of these coupled differential equations were variables instead of constants which is the case in Aifantis' model. These various coefficients involved in the formulation were explicitly defined in terms of measurable physical parameters. The results obtained from the proposed non-linear formulation were compared with those of previously presented linear formulations.

Elsworth and Bai (1992) and Bai *et al.* (1993, 1994, 1995) presented a constitutive model to define the linear poroelastic response of fractured media to determine the influence of dual porosity effects. Bai and Roegiers (1994, 1995) derived the analytical solutions of single-phase fluid flow and heat flow in deformable fractured media. This seems to be the first analytical attempt made to couple the fluid flow and heat flow with solid deformations in a double-porosity fashion. In the model, Barenblatt *et al.* original approach was modified to provide a physically more sensible characterization of reservoir storage changes. Their formulae and results were in dimensionless form and could be directly pertinent to petroleum engineering.

Ghafouri and Lewis (1996) proposed a finite element double porosity model for heterogeneous deformable porous media on the basis of the similar basic assumptions to those of previous works, but using a different formulations. Most of their expressions were based on the physical understanding of the problem but lacked the support of a rigorous mathematical foundation. The results they obtained were quite meaningful when compared to the equivalent single porosity model. However, the obtained trend was significantly different from what Elsworth and Bai (1992) obtained.

Multiphase Fluid Flow Models (Two- or Three-phase)

Due to complications associated with multiple physical processes and mathematical representations of a multiphase flow system in deformable fractured reservoirs, only one paper has been published by Lewis and Ghafouri (1997). Their model is an extension to multiphase fluid from the single-phase, double porosity model for deformable fractured porous media presented by Ghafouri and Lewis (1996).

2.2 Equivalent Porous Media

Another simple approach to modeling a flow system in fractured porous rock is to treat the entire flow region as an equivalent porous media and adjust the flow coefficients accordingly. Such an approach was developed by Marcus (1962), Parsons (1966), and Snow (1970). It requires only lumped estimates of hydraulic properties, and, thereby, avoids to problem of detailed characterization of the fracture geometry. Long *et al.* (1982) applied the theory of flow through fractured rock and homogeneous anisotropic porous media to determine when a fractured rock behaved as a continuum:

1. When there is an insignificant change in the value of the equivalent permeability when a small addition or subtraction to the test volume occurs; and,

2. When an equivalent permeability tensor exists which predicts the correct flux when the direction of a constant gradient is changed.

Khaleel (1987) applied the porous medium equivalent approach to simulate fluid flow in saturated fractured basalt and predicted flow characteristics. The equivalence was established in terms of the Darcian fluid flux. In evaluating this equivalent porous medium approximation for fluid flow through fractured basalts, a two-dimensional generation region was selected and fracture patterns were produced according to postulated descriptions of the real fracture systems. Within a generation region, a flow region was selected for discrete fracture flow analyses. He got a similar conclusion as Long *et al.* that, from a mathematical standpoint, a fractured basalt can be approximated as an equivalent porous medium if an equivalent hydraulic conductivity tensor exists which produces the correct fluid flux under an arbitrary hydraulic gradient direction.

2.3 Single Fracture Models

Some researchers studied the behavior of a single fracture using numerical models. Conventional analyses (Dietrich *et al.*, 1972; Gale, 1975) assumed that Darcy's law was valid for flow in a fracture, as it is for a homogeneous porous media; that is, the flux is proportional to the pressure gradient. The equivalent permeability of the fracture is usually derived from the *cubic law*, which governs fully-developed laminar flow through parallel plates. Compared to the previous discrete models which assume the fractures to be rigid, Bawden *et al.* (1980) proposed a numerical approach to study the influence of fracture deformations on secondary permeability. As a alternative, analogue models have been used to analyze the behavior of a single fracture. Tsang (1984) proposed a model using the analogy of an electrical resistance network. Walsh (1981) studied the deformations in a fractured rock due to changes in the fluid pressure and applied stresses, finding the solution to the transient flow by analogy between heat transfer in a heterogeneous conductive sheet and deformations in a fractured rock completely filled with an incompressible fluid. Muralidhar and Long (1987) presented an approach to characterize flow in single fractures where the governing flow equations are derived from Newton's second law of motion. Navier-Stoke's equations determined flow for a prescribed pressure drop and, hence, the permeability of the rock fracture. In their work, the flow was taken as one-dimensional steady, laminar and incompressible and the numerical scheme was general and applicable to both two- and three-dimensional problems.

2.4 Fracture Network Models

Snow (1965, 1970), Hudson and Priest (1979) have studied naturally fractured reservoirs with rigid fractures using two-dimensional fracture network models. In the models, stochastic distributions for the fracture sets characteristics, such as spacing, fracture trace density, orientation, size and thickness, were used to estimate the permeability of a fractured rock. Long *et al.* (1985) developed a model for steady fluid flow in random three-dimensional networks of fractures. The fractures were assumed as disc-shaped discontinuities in an impermeable matrix. These fractures can be arbitrarily located within the rock volume and have any desired distribution of aperture, density and radius orientation. A mixed analytical-numerical technique was used to calculate the steady flow through the network. Oda (1985) first defined a crack tensor which is a systemtrical, second-rank tensor relating only to the crack geometry, i.e. to the crack shape, crack size, aperture and orientation. If not all the information concerning cracks is available, which is usually the case in practice, a method using the geometrical probability (stereology) could be employed to predict the crack tensor for rock masses in situ. Then, he formulated the permeability tensor in terms of the crack tensor. Other researchers such as Noorishad *et al.* (1972) and Ayatollahi *et al.* (1983) developed fracture network models where fluid and rock deformation were coupled.

2.5 Models Comparisons

Typical models reviewed before along with the model developed in this dissertation are listed in Table 2.2 according to the following three criteria:

1. Porous media is fractured or not;

2. Number of phase the model can handle; and,

3. Fluid flow is coupled with rock deformations or not.

Table 2.2: Comparisons of Models

Developer	Year	Porosity	Fluid Phase	Rock Deformation
Barenblatt	1960	Dual	Single	No
Warren and Root	1963	Dual	Single	No
Kazemi	1968	Dual	Single	No
Kazemi *et al.*	1976	Dual	Two	No
Thomas *et al.*	1983	Dual	Three	No
Li *et al.*	1990	Single	Two	Yes
Li and Zienkiewicz	1992	Single	Three	Yes
Dagger	1997	Single	Two	Yes
Wilson and Aifantis	1982	Dual	Single	Yes
Elsworth and Bai	1992	Dual	Single	Yes
Bai and Roegiers	1994	Dual	Single	Yes
Ghafouri and Lewis	1996	Dual	Single	Yes
Lewis and Ghafouri*	1997	Dual	Three	Yes
Shu *et al.*	1998	Dual	Two	Yes
Meng**	1998	Dual	Two	Yes
Shu	1999	Dual	Two	Yes

* Based on the intuitive phenomenological concept;
** A finite element model, parallel to present one.

It is noted, from Table 2.2, that some available models dealing with fractured media do not take rock deformations into account; others which can simulate deformable fractured reservoir consider only single-phase fluid flow; and others in which two or three phase fluid flow are coupled with rock deformations are unable to model fractured porous media. The only model which can handle multiphase fluid flow in deformable fractured reservoirs was developed by Lewis and Ghafouri in 1997. However, the model is based on the intuitive phenomenological concept rather than any theoretical reasoning. Hence, the model presented in this dissertation is the first mathematical model for two-phase fluid flow in deformable fractured reservoirs in which the set of coupled differential governing equations are rigorously derived.

Chapter 3

Governing Equations for Two-phase Fluid Flow in a Deformable Fractured Porous Medium

In this chapter, the equilibrium equations for a solid mixture is provided first. Then, continuity equations for fluid phases (water and oil in water-oil system, and oil and gas in oil-gas system) are derived rigorously based on the dual-porosity concept. In the derivation, the formalism presented in Li *et al.* (1990) single-porosity model for two-phase flow (water-oil system) in deforming porous media was creatively extended to dual-porosity model for two-phase flow (water-oil and oil-gas) in deforming fractured porous media.

3.1 Equilibrium Equations for Solid Mixtures (Displacement Equations)

Consider a volume of elastic porous medium filled with a homogeneous fluid. The equilibrium equations for two-dimensional stresses can be obtained by first setting the total forces in the x-direction equal to zero (Fig. 3.1):

$$\left(\sigma_x + \frac{\partial \sigma_x}{\partial x} dx\right) dy - \sigma_x dy + \left(\tau_{yx} + \frac{\partial \tau_{yx}}{\partial y} dy\right) dx - \tau_{yx} dx = 0 \tag{3.1}$$

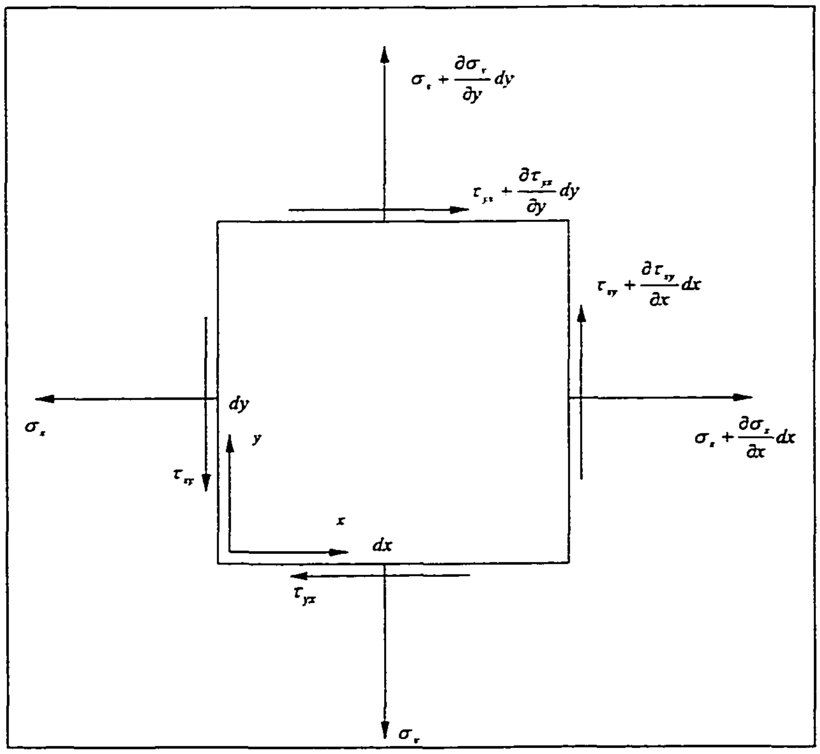

Figure 3.1: Two-Dimensional Stress Components Acting on a Differential Square.

Canceling out terms yields:

$$\frac{\partial \sigma_x}{\partial x} + \frac{\partial \tau_{yx}}{\partial y} = 0 \tag{3.2}$$

Similarly, setting the equilibrium of forces in the y-direction yields:

$$\frac{\partial \sigma_y}{\partial y} + \frac{\partial \tau_{xy}}{\partial x} = 0 \tag{3.3}$$

In compact form:

$$\sum \frac{\partial \tau_{ij}}{\partial x_j} = 0, \ i = 1, 2. \tag{3.4}$$

The total stress τ_{ij} can be expressed as:

$$\tau_{ij} = \sigma_{ij} - \alpha P \delta_{ij} \tag{3.5}$$

where σ_{ij} is referred to as the *effective* stress acting on the solid skeleton, P is the fluid pressure, and α is a physical constant.

The effective stress after an elapsed time t can be expressed as:

$$\sigma_{ij} = \sigma_{ij}^{0} + \Delta\sigma_{ij} \tag{3.6}$$

where σ_{ij}^{0} is the initial effective stress and $\Delta\sigma_{ij}$ is the effective stress increment.

If it is assumed that the porous medium is isotropic, then the linear elastic stress-strain relation takes the form:

$$\Delta\sigma_{ij} = 2G\Delta\varepsilon_{ij} + \lambda\Delta\varepsilon_{kk}\delta_{ij} \tag{3.7}$$

where $\Delta\varepsilon_{ij}$ is the incremental strain of the solid skeleton; G and λ are Lamé's constants. The parameter G is the shear modulus and is defined as:

$$G = \frac{E}{2\,(1+\nu)} \tag{3.8}$$

and λ is identified as:

$$\lambda = \frac{E\nu}{(1+\nu)(1-2\nu)} \tag{3.9}$$

where E is Young's modulus and ν is Poisson's ratio for the solid skeleton.

In general,

$$\Delta\varepsilon_{ij} = \varepsilon_{ij} - \varepsilon_{ij}^{0} \tag{3.10}$$

where ε_{ij}^{0} is the initial strain, which may be caused by such factors as shrinkage, temperature changes, etc. It is assumed in this dissertation that these initial strains are negligible; hence,

$$\Delta\varepsilon_{ij} = \varepsilon_{ij} \tag{3.11}$$

Combining Eqs. (3.2)-(3.7) and (3.11) and assuming $\sigma^0_{ij} = 0$,

$$2G\frac{\partial \varepsilon_{ij}}{\partial x_j} + \lambda\frac{\partial \varepsilon_{jj}}{\partial x_i} - \alpha\frac{\partial P}{\partial x_i} = 0 \tag{3.12}$$

In the case of small deformations, the strain components are related to the displacements by the following linearized relation:

$$\varepsilon_{ij} = \frac{1}{2}\left(\frac{\partial u_i}{\partial x_j} + \frac{\partial u_j}{\partial x_i}\right) \tag{3.13}$$

where u_i is the incremental displacement vector of the solid skeleton. Plugging Eq. (3.13) into (3.12) yields:

$$(\lambda + G)\frac{\partial^2 u_j}{\partial x_i \partial x_j} + G\frac{\partial^2 u_i}{\partial x_j \partial x_j} - \alpha\frac{\partial P}{\partial x_i} = 0 \tag{3.14}$$

This equation forms the required governing equations for the solid matrix displacements. Expanding it to two dimensions gives:

$$(\lambda + G)\left(\frac{\partial^2 u}{\partial x^2} + \frac{\partial^2 v}{\partial x \partial y}\right) + G\left(\frac{\partial^2 u}{\partial x^2} + \frac{\partial^2 u}{\partial y^2}\right) - \alpha\frac{\partial P}{\partial x} = 0 \tag{3.15}$$

$$(\lambda + G)\left(\frac{\partial^2 u}{\partial x \partial y} + \frac{\partial^2 v}{\partial y^2}\right) + G\left(\frac{\partial^2 v}{\partial x^2} + \frac{\partial^2 v}{\partial y^2}\right) - \alpha\frac{\partial P}{\partial y} = 0 \tag{3.16}$$

Eqs. (3.15) and (3.16) are modified to the following forms to be applied to fractured reservoir:

$$(\lambda + G)\left(\frac{\partial^2 u}{\partial x^2} + \frac{\partial^2 v}{\partial x \partial y}\right) + G\left(\frac{\partial^2 u}{\partial x^2} + \frac{\partial^2 u}{\partial y^2}\right) - \alpha_m\frac{\partial P_m}{\partial x} - \alpha_f\frac{\partial P_f}{\partial x} = 0 \tag{3.17}$$

$$(\lambda + G)\left(\frac{\partial^2 u}{\partial x \partial y} + \frac{\partial^2 v}{\partial y^2}\right) + G\left(\frac{\partial^2 v}{\partial x^2} + \frac{\partial^2 v}{\partial y^2}\right) - \alpha_m\frac{\partial P_m}{\partial y} - \alpha_f\frac{\partial P_f}{\partial y} = 0 \tag{3.18}$$

where subscripts, m and f, represent the matrix and fractures, respectively; λ and G are *Lamé's* constants, α is the fluid pressure ratio factor or Biot constant, u and v are the solid displacements in the x- and y-directions, respectively; and P is the fluid pressure.

3.2 Continuity equations for fluid phases

3.2.1 Oil-water system

The continuity equation for the water phase (w) in the matrix (m) is derived, as an example, in this section. The original continuity equation for the water phase is given by:

$$\frac{\partial \phi_m S_{wm} \rho_{wm}}{\partial t} + \frac{\partial \phi_m S_{wm} \rho_{wm} U_{wmi}}{\partial x_i} = 0 \tag{3.19}$$

where ϕ_m is the porosity of the matrix, S_{wm} is the water saturation in the matrix, ρ_{wm} is the water density in the matrix and U_{wmi} is the intrinsic (real) velocity for the water phase in the matrix.

If the solid is considered undeformable, Darcy's velocity for water in more than one phase system is defined as:

$$w_{wmi} = \phi_m S_{wm} U_{wmi} \tag{3.20}$$

In the case where the solid deformations are considered, the above equation should be redefined as:

$$w_{wmi} = \phi_m S_{wm} (U_{wmi} - \dot{u}_i) \tag{3.21}$$

where $\dot{u}_i = \frac{\partial u_i}{\partial t}$, is the solid moving velocity.

According to the definition in Eq. (3.21), Eq. (3.19) can be written as:

$$\frac{\partial \phi_m S_{wm} \rho_{wm}}{\partial t} + \frac{\partial \phi_m S_{wm} \rho_{wm} \, \dot{u}_i}{\partial x_i} + \frac{\partial \rho_{wm} w_{wmi}}{\partial x_i} = 0 \tag{3.22}$$

Now, the mass conservation equation for the solid is given by:

$$\frac{\partial (1-\phi) \rho_s}{\partial t} + \frac{\partial (1-\phi) \rho_s \, \dot{u}_i}{\partial x_i} = 0 \tag{3.23}$$

where ϕ is the total porosity of the porous media, which is equal to the sum of the matrix porosity ϕ_m and the fracture porosity ϕ_f; i.e.:

$$\phi = \phi_m + \phi_f \tag{3.24}$$

Expanding and rearranging Eq. (3.23) yields:

$$\frac{\partial \phi}{\partial t} + \dot{u}_i \frac{\partial \phi}{\partial x_i} = \frac{1-\phi}{\rho_s}\left(\frac{\partial \rho_s}{\partial t} + \dot{u}_i \frac{\partial \rho_s}{\partial x_i}\right) + (1-\phi)\frac{\partial \dot{u}_i}{\partial x_i} \tag{3.25}$$

The following substantial time differential operator:

$$\frac{D}{Dt} = \frac{\partial}{\partial t} + \dot{u}_i \frac{\partial}{\partial x_i} \tag{3.26}$$

is adopted to simplify the expression; and Eq. (3.25) can be reduced to:

$$\frac{D\phi}{Dt} = \frac{1-\phi}{\rho_s}\frac{D\rho_s}{Dt} + (1-\phi)\frac{\partial \dot{u}_i}{\partial x_i} \tag{3.27}$$

or,

$$\frac{D\phi_m}{Dt} = \frac{1-\phi}{\rho_s}\frac{D\rho_s}{Dt} + (1-\phi)\frac{\partial \dot{u}_i}{\partial x_i} - \frac{D\phi_f}{Dt} \tag{3.28}$$

Expanding Eq. (3.22) gives:

$$\phi_m S_{wm}\frac{D\rho_{wm}}{Dt} + \phi_m \rho_{wm}\frac{DS_{wm}}{Dt} + S_{wm}\rho_{wm}\frac{D\phi_m}{Dt}$$

$$+\phi_m S_{wm}\rho_{wm}\frac{\partial \dot{u}_i}{\partial x_i} + \frac{\partial \rho_{wm} w_i}{\partial x_i} = 0 \tag{3.29}$$

Substituting Eq. (3.28) into Eq. (3.29), the following equation is obtained:

$$\phi S_{wm}\frac{D\rho_{wm}}{Dt} + \phi_m \rho_{wm}\frac{DS_{wm}}{Dt} + S_{wm}\rho_{wm}\frac{1-\phi}{\rho_s}\frac{D\rho_s}{Dt}$$

$$+S_{wm}\rho_{wm}(1-\phi_f)\frac{\partial \dot{u}_i}{\partial x_i} - S_{wm}\rho_{wm}\frac{D\phi_f}{Dt} + \frac{\partial \rho_{wm} w_i}{\partial x_i} = 0 \tag{3.30}$$

Another equation relating the change in fracture porosity to the change in fluid pressures is required. This relationship can be derived using the definitions of ϕ and V:

$$\phi_f = \frac{V_f}{V} \tag{3.31}$$

$$V = V_m + V_f + V_s \tag{3.32}$$

where V_m, V_f, V_s and V are the volumes of fluids in the matrix and in the fracture, the volume of solid and the bulk volume of the porous medium, respectively. Differentiation of Eqs. (3.31) and (3.32) with respect to substantial time yields:

$$\frac{D\phi_f}{Dt} = \frac{1}{V}\left[\frac{DV_f}{Dt} - \phi_f \frac{DV}{Dt}\right] \tag{3.33}$$

$$\frac{DV}{Dt} = \frac{DV_m}{Dt} + \frac{DV_f}{Dt} + \frac{DV_s}{Dt} \tag{3.34}$$

Combining the above two equations gives:

$$\frac{D\phi_f}{Dt} = \frac{1}{V}\left[(1-\phi_f)\frac{DV_f}{Dt} - \phi_f\left(\frac{DV_m}{Dt} + \frac{DV_s}{Dt}\right)\right] \tag{3.35}$$

By definition of fluid compressibility, one has:

$$\frac{1}{V_m}\frac{DV_m}{Dt} = -C_m \frac{DP_m}{Dt} \tag{3.36}$$

$$\frac{1}{V_f}\frac{DV_f}{Dt} = -C_f \frac{DP_f}{Dt} \tag{3.37}$$

where C_m and C_f are the comprehensive compressibilities for fluids in the matrix and the fractures, respectively; hence, the saturation-related coefficients are given by:

$$C_m = C_o S_{om} + C_w S_{wm} \tag{3.38}$$

$$C_f = C_o S_{of} + C_w S_{wf} \tag{3.39}$$

where C_o and C_w are the compressibilities for oil and water, respectively defined as:

$$C_o = \frac{1}{V_o}\frac{\partial V_o}{\partial P} \tag{3.40}$$

$$C_w = \frac{1}{V_w}\frac{\partial V_w}{\partial P} \tag{3.41}$$

Combining of Eqs. (3.36), (3.37) and applying the definition of porosity yields:

$$\frac{DV_m}{Dt} = -C_m \phi_m V \frac{DP_m}{Dt} \tag{3.42}$$

$$\frac{DV_f}{Dt} = -C_f \phi_f V \frac{DP_f}{Dt} \tag{3.43}$$

Since (Meng, 1998),

$$\begin{aligned}
\frac{1}{\rho_s}\frac{D\rho_s}{Dt} &= -\frac{1}{V_s}\frac{DV_s}{Dt} \\
&= \frac{1}{1-\phi}\left[\frac{\alpha_{mf}-\phi}{K_s}\frac{DP_m}{Dt} + \frac{\alpha_{mf}-\phi}{K_n s}\frac{DP_f}{Dt} - (1-\alpha_{mf})\,\dot{u}_{i,i}\right]
\end{aligned} \tag{3.44}$$

$$\alpha_{mf} = \frac{\alpha_m \alpha_f}{\alpha_m + \alpha_f} \tag{3.45}$$

Hence, one has:

$$\frac{DV_s}{Dt} = -V\left[-\frac{\alpha_{mf}-\phi}{K_s}\frac{DP_m}{Dt} - \frac{\alpha_{mf}-\phi}{K_n s}\frac{DP_f}{Dt} - (1-\alpha_{mf})\,\dot{u}_{i,i}\right] \tag{3.46}$$

Substituting Eqs. (3.42), (3.43) and (3.46) into Eq. (3.35) gives:

$$\begin{aligned}
\frac{D\phi_f}{Dt} &= -\phi_f C_f (1-\phi_f)\frac{DP_f}{Dt} + \phi_m \phi_f C_m \frac{DP_m}{Dt} + \phi_f \frac{\alpha_{mf}-\phi}{K_s}\frac{DP_m}{Dt} \\
&\quad + \phi_f \frac{\alpha_{mf}-\phi}{K_n s}\frac{DP_f}{Dt} - \phi_f (1-\alpha_{mf})\,\dot{u}_{i,i}
\end{aligned} \tag{3.47}$$

Now, Eqs. (3.44) and (3.47) can be substituted into Eq. (3.30) to give:

$$\begin{aligned}
&\phi_m S_{wm}\frac{D\rho_{wm}}{Dt} + \phi_m \rho_{wm}\frac{DS_{wm}}{Dt} + \alpha_{mf} S_{wm}\rho_{wm}(1-\phi_f)\,\dot{u}_{i,i} \\
&+ S_{wm}\rho_{wm}\left[\frac{\alpha_{mf}-\phi}{K_s}(1-\phi_f) - \phi_m\phi_f C_m\right]\frac{DP_m}{Dt} \\
&+ S_{wm}\rho_{wm}\left[\frac{\alpha_{mf}-\phi}{K_n s}(1-\phi_f) + \phi_f(1-\phi_f)C_f\right]\frac{DP_f}{Dt} + \frac{\partial \rho_{wm} w_{wmi}}{\partial x_i} = 0
\end{aligned} \tag{3.48}$$

Note that in general $\dot{u}_i \frac{\partial}{\partial x_i} \ll \frac{\partial}{\partial t}$ and, therefore, $\frac{D}{Dt} \approx \frac{\partial}{\partial t}$; then, the continuity equation for water phase in matrix becomes:

$$\begin{aligned}
&\phi_m S_{wm}\frac{\partial \rho_{wm}}{\partial t} + \phi_m \rho_{wm}\frac{\partial S_{wm}}{\partial t} + \alpha_{mf} S_{wm}\rho_{wm}(1-\phi_f)\,\dot{u}_{i,i} \\
&+ S_{wm}\rho_{wm}\left[\frac{\alpha_{mf}-\phi}{K_s}(1-\phi_f) - \phi_m\phi_f C_m\right]\frac{\partial P_m}{\partial t} \\
&+ S_{wm}\rho_{wm}\left[\frac{\alpha_{mf}-\phi}{K_n s}(1-\phi_f) + \phi_f(1-\phi_f)C_f\right]\frac{\partial P_f}{\partial t} + \frac{\partial \rho_{wm} w_{wmi}}{\partial x_i} = 0
\end{aligned} \tag{3.49}$$

In a dual-porosity model, one fluid can move from the matrix to the fractures or from the fractures to the matrix, depending on the pressure difference between these two continua for that fluid phase. Therefore, a transfer term (mass exchange term) is needed in Eq. (3.49) to complete the continuity equation. The transfer term for water and oil is calculated by:

$$Q_w = \bar{\alpha}\, \rho_{wm} \frac{k_m k_{rwm}}{\mu_{wm}} \left(P_{wm} - P_{wf}\right) \tag{3.50}$$

$$Q_o = \bar{\alpha}\, \rho_{om} \frac{k_m k_{rom}}{\mu_{om}} \left(P_{om} - P_{of}\right) \tag{3.51}$$

where $\overline{\alpha}$ is the transfer coefficient and μ is the viscosity.

The final continuity equation for the water phase in the matrix of the deforming porous media has the following form:

$$\begin{aligned}
&\phi_m S_{wm} \frac{\partial \rho_{wm}}{\partial t} + \phi_m \rho_{wm} \frac{\partial S_{wm}}{\partial t} + \alpha_{mf} S_{wm} \rho_{wm} (1 - \phi_f)\, \dot{u}_{i,i} \\
&+ S_{wm} \rho_{wm} \left[\frac{\alpha_{mf} - \phi}{K_s} (1 - \phi_f) - \phi_m \phi_f C_m \right] \frac{\partial P_m}{\partial t} \\
&+ S_{wm} \rho_{wm} \left[\frac{\alpha_{mf} - \phi}{K_n s} (1 - \phi_f) + \phi_f (1 - \phi_f) C_f \right] \frac{\partial P_f}{\partial t} \\
&+ \bar{\alpha}\, \rho_{wm} \frac{k_m k_{rwm}}{\mu_{wm}} \left(P_{wm} - P_{wf}\right) + \frac{\partial \rho_{wm} w_{wmi}}{\partial x_i} = 0
\end{aligned} \tag{3.52}$$

Similarly, the continuity equation for oil phase in the matrix:

$$\begin{aligned}
&\phi_m S_{om} \frac{\partial \rho_{om}}{\partial t} + \phi_m \rho_{om} \frac{\partial S_{om}}{\partial t} + \alpha_{mf} S_{om} \rho_{om} (1 - \phi_f)\, \dot{u}_{i,i} \\
&+ S_{om} \rho_{om} \left[\frac{\alpha_{mf} - \phi}{K_s} (1 - \phi_f) - \phi_m \phi_f C_m \right] \frac{\partial P_m}{\partial t} \\
&+ S_{om} \rho_{om} \left[\frac{\alpha_{mf} - \phi}{K_n s} (1 - \phi_f) + \phi_f (1 - \phi_f) C_f \right] \frac{\partial P_f}{\partial t} \\
&+ \bar{\alpha}\, \rho_{om} \frac{k_m k_{rom}}{\mu_{om}} \left(P_{om} - P_{of}\right) + \frac{\partial \rho_{om} w_{omi}}{\partial x_i} = 0
\end{aligned} \tag{3.53}$$

The continuity equation for water phase in the fracture can be written as:

$$\phi_f S_{wf} \frac{\partial \rho_{wf}}{\partial t} + \phi_f \rho_{wf} \frac{\partial S_{wf}}{\partial t} + \alpha_{mf} S_{wf} \rho_{wf} (1 - \phi_m)\, \dot{u}_{i,i}$$

$$+S_{wf}\rho_{wf}\left[\frac{\alpha_{mf}-\phi}{K_s}(1-\phi_m)-\phi_m\phi_f C_f\right]\frac{\partial P_f}{\partial t}$$

$$+S_{wf}\rho_{wf}\left[\frac{\alpha_{mf}-\phi}{K_n s}(1-\phi_m)+\phi_m(1-\phi_m)C_m\right]\frac{\partial P_m}{\partial t}$$

$$+\bar{\alpha}\;\rho_{wm}\frac{k_m k_{rwm}}{\mu_{wm}}(P_{wf}-P_{wm})+\frac{\partial \rho_{wf} w_{wfi}}{\partial x_i}=0 \tag{3.54}$$

The continuity equation for oil phase in the fractures is as follows:

$$\phi_f S_{of}\frac{\partial \rho_{of}}{\partial t}+\phi_f\rho_{of}\frac{\partial S_{of}}{\partial t}+\alpha_{mf}S_{of}\rho_{of}(1-\phi_m)\;\dot{u}_{i,i}$$

$$+S_{of}\rho_{of}\left[\frac{\alpha_{mf}-\phi}{K_s}(1-\phi_m)-\phi_m\phi_f C_f\right]\frac{\partial P_f}{\partial t}$$

$$+S_{of}\rho_{of}\left[\frac{\alpha_{mf}-\phi}{K_n s}(1-\phi_m)+\phi_m(1-\phi_m)C_m\right]\frac{\partial P_m}{\partial t}$$

$$+\bar{\alpha}\;\rho_{om}\frac{k_m k_{rom}}{\mu_{om}}(P_{of}-P_{om})+\frac{\partial \rho_{of} w_{ofi}}{\partial x_i}=0 \tag{3.55}$$

Consequently, there are a total of ten unknowns, which are: solid displacements in x- and y- directions u and v, fluid pressures and saturations in matrix and fractures: P_{wm}, P_{om}, S_{wm}, S_{om}, P_{wf}, P_{of}, S_{wf}, S_{of}. However, one has only six equations, i.e.: (3.17), (3.18), (3.52), (3.53), (3.54), (3.55). Therefore, the following four auxiliary equations for saturation and capillary pressure relationships in matrix and fractures are necessary to solve the problem.

For the matrix:

$$S_{wm}+S_{om}=1 \tag{3.56}$$

$$P_{cm}=P_{om}-P_{wm} \tag{3.57}$$

For the fractures:

$$S_{wf}+S_{of}=1 \tag{3.58}$$

$$P_{cf}=P_{of}-P_{wf} \tag{3.59}$$

3.2.2 Darcy's law

w_i, defined in Eq. (3.21) is calculated using Darcy's law as:

$$w_i = -\frac{kk_r}{\mu}\frac{\partial P}{\partial x_i} \tag{3.60}$$

where k is the absolute permeability of the medium, k_r is the relative permeability of the medium to the fluid phase, and μ is the viscosity of the fluid.

3.2.3 Oil-gas system

Oil-gas system in rigid porous media

The generalized flow equation for component i in a three-phase environment is given by:

$$-\frac{\partial}{\partial x_i}(C_{ig}\rho_g u_g + C_{io}\rho_o u_o + C_{iw}\rho_w u_w) = \frac{\partial}{\partial t}[\phi(C_{ig}\rho_g S_g + C_{io}\rho_o S_o + C_{iw}\rho_w S_w)] \tag{3.61}$$

Where C_{ig} is the mass fraction of the ith component in the gas phase, C_{io} is the mass fraction of the ith component in the oil phase and C_{iw} is the mass fraction of the ith component in the water phase.

This equation for oil-gas system is simplified to:

$$-\frac{\partial}{\partial x_i}(C_{ig}\rho_g u_g + C_{io}\rho_o u_o) = \frac{\partial}{\partial t}[\phi(C_{ig}\rho_g S_g + C_{io}\rho_o S_o)] \tag{3.62}$$

For gas component:

$$-\frac{\partial}{\partial x_i}(C_{gg}\rho_g u_g + C_{go}\rho_o u_o) = \frac{\partial}{\partial t}[\phi(C_{gg}\rho_g S_g + C_{go}\rho_o S_o)] \tag{3.63}$$

For oil component:

$$-\frac{\partial}{\partial x_i}(C_{og}\rho_g u_g + C_{oo}\rho_o u_o) = \frac{\partial}{\partial t}[\phi(C_{og}\rho_g S_g + C_{oo}\rho_o S_o)] \tag{3.64}$$

By definition:

$$C_{gg} = 1 \tag{3.65}$$

$$C_{go} = \frac{m_g}{m_o + m_g} \tag{3.66}$$

$$C_{og} = 0 \tag{3.67}$$

$$C_{oo} = \frac{m_o}{m_o + m_g} \tag{3.68}$$

where m_o and m_g are the masses of oil and gas in oil phase, respectively. Their respective volumes are represented by V_o and V_g.

Since:

$$V_o = \frac{m_o + m_g}{\rho_o} \tag{3.69}$$

$$B_o = \frac{V_o}{V_{os}} = \frac{V_o}{\frac{m_o}{\rho_{os}}} = \frac{\rho_{os}(m_o + m_g)}{m_o \rho_o} \tag{3.70}$$

Where V_{os} is the volume of oil measured at standard conditions.

Hence,

$$C_{oo} = \frac{m_o}{m_o + m_g} = \frac{\rho_{os}}{\rho_o B_o} \tag{3.71}$$

Since:

$$R_s = \frac{V_{gs}}{V_{os}} = \frac{\frac{m_g}{\rho_{gs}}}{\frac{m_o}{\rho_{os}}} = \frac{m_g \rho_{os}}{m_o \rho_{gs}} \tag{3.72}$$

where V_{gs} is the volume of gas measured at standard conditions.

Hence,

$$m_g = \frac{R_s m_o \rho_{gs}}{\rho_{os}} \tag{3.73}$$

From Eq. (3.70),

$$m_o + m_g = \frac{B_o m_o \rho_o}{\rho_{os}} \tag{3.74}$$

So,

$$C_{go} = \frac{m_g}{m_o + m_g} = \frac{\frac{R_s m_o \rho_{gs}}{\rho_{os}}}{\frac{B_o m_o \rho_o}{\rho_{os}}} = \frac{R_s \rho_{gs}}{B_o \rho_o} \tag{3.75}$$

Substitution of Eqs. (3.65) and (3.75) into (3.63) gives the governing equation for the gas component:

$$-\frac{\partial}{\partial x_i}\left(\rho_g u_g + \frac{R_s \rho_{gs}}{B_o} u_o\right) = \frac{\partial}{\partial t}\left[\phi\left(\rho_g S_g + \frac{R_s \rho_{gs}}{B_o} S_o\right)\right] \tag{3.76}$$

Similarly, substitution of Eqs. (3.67) and (3.71) into (3.64) gives the equation for the oil component:

$$-\frac{\partial}{\partial x_i}\left(\frac{u_o}{B_o}\right) = \frac{\partial}{\partial t}\left(\phi \frac{S_o}{B_o}\right) \tag{3.77}$$

Oil-Gas System in Deformable Porous Media

Governing equation for gas The governing equation for gas in the matrix is derived first. Eq. (3.76) is rewritten to be applied to dual porosity model:

$$\frac{\partial}{\partial t}\left(\phi_m \rho_{gm} S_{gm} + \phi_m \frac{R_{sm}\rho_{gsm}}{B_{om}} S_{om}\right) + \frac{\partial}{\partial x_i}\left(\rho_{gm} u_{gm} + \frac{R_{sm}\rho_{gsm}}{B_{om}} u_{om}\right) = 0 \tag{3.78}$$

Darcy's velocities for gas and oil in undeformable solid system are:

$$u_{gm} = \phi_m S_{gm} U_{gmi} \tag{3.79}$$

$$u_{om} = \phi_m S_{om} U_{omi} \tag{3.80}$$

Plugging Eqs. (3.79) and (3.80) into Eq. (3.78) gives

$$\frac{\partial}{\partial t}\left(\phi_m \rho_{gm} S_{gm} + \phi_m \frac{R_{sm}\rho_{gsm}}{B_{om}} S_{om}\right)$$
$$+\frac{\partial}{\partial x_i}\left(\rho_{gm}\phi_m S_{gm} U_{gmi} + \frac{R_{sm}\rho_{gsm}}{B_{om}}\phi_m S_{om} U_{omi}\right) = 0 \tag{3.81}$$

If the solid is considered deformable, Darcy's velocities for gas and oil are defined as:

$$w_{gmi} = \phi_m S_{gm}\left(U_{gmi} - \dot{u}_i\right) \tag{3.82}$$

$$w_{omi} = \phi_m S_{om}\left(U_{omi} - \dot{u}_i\right) \tag{3.83}$$

Manipulating the above equations yields:

$$\phi_m S_{gm} U_{gmi} = w_{gmi} + \phi_m S_{gm}\,\dot{u}_i \tag{3.84}$$

$$\phi_m S_{om} U_{omi} = w_{omi} + \phi_m S_{om}\,\dot{u}_i \tag{3.85}$$

Plugging Eqs. (3.84) and (3.85) into (3.81) yields:

$$\frac{\partial}{\partial t}\left(\phi_m S_{gm}\rho_{gm} + \phi_m S_{om}\rho_{gsm}\frac{R_{sm}}{B_{om}}\right)$$
$$+\frac{\partial}{\partial x_i}\left(\phi_m S_{gm}\rho_{gm}\,\dot{u}_i + \rho_{gm}w_{gmi}\right)$$
$$+\frac{\partial}{\partial x_i}\left(\phi_m S_{om}\rho_{gsm}\frac{R_{sm}}{B_{om}}\,\dot{u}_i + \rho_{gsm}\frac{R_{sm}}{B_{om}}w_{omi}\right) = 0 \tag{3.86}$$

Rearranging and adopting the substantial time differential operator defined in Eq. (3.26), the following equation is obtained:

$$\phi_m S_{gm}\frac{D\rho_{gm}}{Dt} + \phi_m\rho_{gm}\frac{DS_{gm}}{Dt} + S_{gm}\rho_{gm}\frac{D\phi_m}{Dt} + \phi_m S_{gm}\rho_{gm}\frac{\partial\,\dot{u}_i}{\partial x_i} + \frac{\partial}{\partial x_i}\left(\rho_{gm}w_{gmi}\right)$$
$$+\phi_m S_{om}\frac{D}{Dt}\left(\rho_{gsm}\frac{R_{sm}}{B_{om}}\right) + \phi_m\rho_{gsm}\frac{R_{sm}}{B_{om}}\frac{DS_{om}}{Dt} + S_{om}\rho_{gsm}\frac{R_{sm}}{B_{om}}\frac{D\phi_m}{Dt}$$
$$+\phi_m S_{om}\rho_{gsm}\frac{R_{sm}}{B_{om}}\frac{\partial\,\dot{u}_i}{\partial x_i} + \frac{\partial}{\partial x_i}\left(\rho_{gsm}\frac{R_{sm}}{B_{om}}w_{omi}\right) = 0 \tag{3.87}$$

Plugging in Eq. (3.28) and defining:

$$R_m = \rho_{gsm}\frac{R_{sm}}{B_{om}} \tag{3.88}$$

gives:

$$\phi_m S_{gm}\frac{D\rho_{gm}}{Dt} + \phi_m\rho_{gm}\frac{DS_{gm}}{Dt} + S_{gm}\rho_{gm}\frac{1-\phi}{\rho_s}\frac{D\rho_s}{Dt} + S_{gm}\rho_{gm}\left(1-\phi_f\right)\frac{\partial\,\dot{u}_i}{\partial x_i}$$
$$-S_{gm}\rho_{gm}\frac{D\phi_f}{Dt} + \frac{\partial}{\partial x_i}\left(\rho_{gm}w_{gmi}\right) + \phi_m S_{om}\frac{DR_m}{Dt} + \phi_m R_m\frac{DS_{om}}{Dt}$$
$$+S_{om}R_m\frac{1-\phi}{\rho_s}\frac{D\rho_s}{Dt} + S_{om}R_m\left(1-\phi_f\right)\frac{\partial\,\dot{u}_i}{\partial x_i}$$
$$-S_{om}R_m\frac{D\phi_f}{Dt} + \frac{\partial}{\partial x_i}\left(R_m w_{omi}\right) = 0 \tag{3.89}$$

By substituting Eqs. (3.44) and (3.46) into Eq. (3.89), the equation for gas becomes:

$$\phi_m S_{gm}\frac{\partial\rho_{gm}}{\partial t} + \phi_m\rho_{gm}\frac{\partial S_{gm}}{\partial t} + \frac{\partial}{\partial x_i}\left(\rho_{gm}w_{gmi}\right) + \phi_m S_{om}\frac{\partial R_m}{\partial t}$$

$$+\phi_m R_m \frac{\partial S_{om}}{\partial t} + \frac{\partial}{\partial x_i}\left(R_m w_{omi}\right) + \left(S_{gm}\rho_{gm} + S_{om}R_m\right)\left(1-\phi_f\right)\alpha_{mf}\ \dot{u}_{i,i}$$
$$-\left(S_{gm}\rho_{gm} + S_{om}R_m\right)\left[\frac{\alpha_{mf}-\phi}{K_s}\left(\phi_f - 1\right) + \phi_m\phi_f C_m\right]\frac{\partial P_m}{\partial t}$$
$$-\left(S_{gm}\rho_{gm} + S_{om}R_m\right)\left[\frac{\alpha_{mf}-\phi}{K_n s}\left(\phi_f - 1\right) - \phi_f\left(1-\phi_f\right)C_f\right]\frac{\partial P_f}{\partial t} = 0 \tag{3.90}$$

The term $\frac{\partial R_m}{\partial t}$ in Eq. (3.90)can be determined as:

$$\begin{aligned}
\frac{\partial R_m}{\partial t} &= \frac{\partial}{\partial t}\left(\rho_{gsm}\frac{R_{sm}}{B_{om}}\right) \\
&= \rho_{gsm}\frac{\partial}{\partial t}\left(\frac{R_{sm}}{B_{om}}\right) \\
&= \rho_{gsm}\left(\frac{1}{B_{om}}\frac{\partial R_{sm}}{\partial t} - \frac{R_{sm}}{B_{om}^2}\frac{\partial B_{om}}{\partial t}\right) \\
&= \frac{\rho_{gsm}}{B_{om}}\left(\frac{\partial R_{sm}}{\partial P_{gm}}\frac{\partial P_{gm}}{\partial t} - \frac{R_{sm}}{B_{om}}\frac{\partial B_{om}}{\partial P_{om}}\frac{\partial P_{om}}{\partial t}\right)
\end{aligned} \tag{3.91}$$

For the term $\frac{\partial \rho_{gm}}{\partial t}$,

$$\begin{aligned}
\frac{\partial \rho_{gm}}{\partial t} &= \frac{\partial}{\partial t}\left(\frac{\rho_{gsm}}{B_{gm}}\right) \\
&= -\frac{\rho_{gsm}}{B_{gm}^2}\frac{\partial B_{gm}}{\partial t} \\
&= -\frac{\rho_{gsm}}{B_{gm}^2}\frac{\partial B_{gm}}{\partial P_{gm}}\frac{\partial P_{gm}}{\partial t}
\end{aligned} \tag{3.92}$$

Since,

$$w_{gmi} = -\frac{k_m k_{rgm}}{\mu_{gm}}\frac{\partial P_{gm}}{\partial x_i} \tag{3.93}$$

and,

$$\rho_{gm} = \frac{\rho_{gsm}}{B_{gm}} \tag{3.94}$$

So,

$$\begin{aligned}
\frac{\partial}{\partial x_i}\left(\rho_{gm} w_{gmi}\right) &= \frac{\partial}{\partial x_i}\left[\frac{\rho_{gsm}}{B_{gm}}\left(-\frac{k_m k_{rgm}}{\mu_{gm}}\frac{\partial P_{gm}}{\partial x_i}\right)\right] \\
&= -\rho_{gsm}\frac{\partial}{\partial x_i}\left(\frac{k_m k_{rgm}}{\mu_{gm} B_{gm}}\frac{\partial P_{gm}}{\partial x_i}\right)
\end{aligned} \tag{3.95}$$

Since,

$$w_{omi} = -\frac{k_m k_{rom}}{\mu_{om}}\frac{\partial P_{om}}{\partial x_i} \tag{3.96}$$

and,

$$R_m = \rho_{gsm}\frac{R_{sm}}{B_{om}} \tag{3.97}$$

So,

$$\begin{aligned}
\frac{\partial}{\partial x_i}\left(R_m w_{omi}\right) &= \frac{\partial}{\partial x_i}\left[\rho_{gsm}\frac{R_{sm}}{B_{om}}\left(-\frac{k_m k_{rom}}{\mu_{om}}\frac{\partial P_{om}}{\partial x_i}\right)\right] \\
&= -\rho_{gsm}\frac{\partial}{\partial x_i}\left(\frac{R_{sm}}{B_{om}}\frac{k_m k_{rom}}{\mu_{om}}\frac{\partial P_{om}}{\partial x_i}\right)
\end{aligned} \tag{3.98}$$

Plugging Eqs. (3.91), (3.92), (3.95), and (3.98) into Eq. (3.90) yields:

$$\begin{aligned}
&\phi_m \rho_{gm}\frac{\partial S_{gm}}{\partial t} - \rho_{gsm}\frac{\partial}{\partial x_i}\left(\frac{k_m k_{rgm}}{\mu_{gm} B_{gm}}\frac{\partial P_{gm}}{\partial x_i}\right) + \phi_m R_m \frac{\partial S_{om}}{\partial t} \\
&-\rho_{gsm}\frac{\partial}{\partial x_i}\left(\frac{R_{sm}}{B_{om}}\frac{k_m k_{rom}}{\mu_{om}}\frac{\partial P_{om}}{\partial x_i}\right) \\
&+\phi_m \rho_{gsm}\left(\frac{S_{om}}{B_{om}}\frac{\partial R_{sm}}{\partial P_{gm}} - \frac{S_{gm}}{B_g^2}\frac{\partial B_{gm}}{\partial P_{gm}}\right)\frac{\partial P_{gm}}{\partial t} \\
&-\phi_m \rho_{gsm} S_{om}\frac{R_{sm}}{B_{om}^2}\frac{\partial B_{om}}{\partial P_{om}}\frac{\partial P_{om}}{\partial t} \\
&+\left(S_{gm}\rho_{gm} + S_{om}R_m\right)\left(1-\phi_f\right)\alpha_{mf}\, \dot{u}_{i,i} \\
&-\left(S_{gm}\rho_{gm} + S_{om}R_m\right)\left[\frac{\alpha_{mf}-\phi}{K_s}\left(\phi_f - 1\right) + \phi_m \phi_f C_m\right]\frac{\partial P_m}{\partial t} \\
&-\left(S_{gm}\rho_{gm} + S_{om}R_m\right)\left[\frac{\alpha_{mf}-\phi}{K_n s}\left(\phi_f - 1\right) - \phi_f\left(1-\phi_f\right)C_f\right]\frac{\partial P_f}{\partial t} = 0
\end{aligned} \tag{3.99}$$

Similar to a water-oil system in a dual-porosity model, a transfer term is needed to complete the continuity equation. Since gas exist in two forms: free and solution gas, the transfer term for gas consists of two terms; i.e.

$$Q_g = \bar{\alpha}\,\rho_{gm}\frac{k_m k_{rgm}}{\mu_{gm} B_{gm}}\left(P_{gm} - P_{gf}\right) + \bar{\alpha}\,\rho_{gm} R_{sm}\frac{k_m k_{rom}}{\mu_{om} B_{om}}\left(P_{om} - P_{of}\right) \tag{3.100}$$

The first term is the mass exchange between the matrix and the fractures for free gas and the second term is the gas mass exchange caused by oil mass exchange.

The final continuity equation for the gas phase in the matrix of a deforming porous medium is as follows:

$$
\begin{aligned}
&\phi_m \rho_{gm} \frac{\partial S_{gm}}{\partial t} - \rho_{gsm} \frac{\partial}{\partial x_i} \left(\frac{k_m k_{rgm}}{\mu_{gm} B_{gm}} \frac{\partial P_{gm}}{\partial x_i} \right) + \phi_m R_m \frac{\partial S_{om}}{\partial t} \\
&- \rho_{gsm} \frac{\partial}{\partial x_i} \left(\frac{R_{sm}}{B_{om}} \frac{k_m k_{rom}}{\mu_{om}} \frac{\partial P_{om}}{\partial x_i} \right) \\
&+ \phi_m \rho_{gsm} \left(\frac{S_{om}}{B_{om}} \frac{\partial R_{sm}}{\partial P_{gm}} - \frac{S_{gm}}{B_{gm}^2} \frac{\partial B_{gm}}{\partial P_{gm}} \right) \frac{\partial P_{gm}}{\partial t} \\
&- \phi_m \rho_{gsm} S_{om} \frac{R_{sm}}{B_{om}^2} \frac{\partial B_{om}}{\partial P_{om}} \frac{\partial P_{om}}{\partial t} \\
&+ \left(S_{gm} \rho_{gm} + S_{om} R_m \right) \left(1 - \phi_f \right) \alpha_{mf} \, \dot{u}_{i,i} \\
&- \left(S_{gm} \rho_{gm} + S_{om} R_m \right) \left[\frac{\alpha_{mf} - \phi}{K_s} \left(\phi_f - 1 \right) + \phi_m \phi_f C_m \right] \frac{\partial P_m}{\partial t} \\
&- \left(S_{gm} \rho_{gm} + S_{om} R_m \right) \left[\frac{\alpha_{mf} - \phi}{K_n s} \left(\phi_f - 1 \right) - \phi_f \left(1 - \phi_f \right) C_f \right] \frac{\partial P_f}{\partial t} \\
&+ \bar{\alpha} \, \rho_{gm} \frac{k_m k_{rgm}}{\mu_{gm} B_{gm}} \left(P_{gm} - P_{gf} \right) + \bar{\alpha} \, \rho_{gm} R_{sm} \frac{k_m k_{rom}}{\mu_{om} B_{om}} \left(P_{om} - P_{of} \right) = 0
\end{aligned}
\tag{3.101}
$$

The final continuity equation for the gas phase in the fractures can be derived in a similar way:

$$
\begin{aligned}
&\phi_f \rho_{gf} \frac{\partial S_{gf}}{\partial t} - \rho_{gsf} \frac{\partial}{\partial x_i} \left(\frac{k_f k_{rgf}}{\mu_{gf} B_{gf}} \frac{\partial P_{gf}}{\partial x_i} \right) + \phi_f R_f \frac{\partial S_{of}}{\partial t} \\
&- \rho_{gsf} \frac{\partial}{\partial x_i} \left(\frac{R_{sf}}{B_{of}} \frac{k_f k_{rof}}{\mu_{of}} \frac{\partial P_{of}}{\partial x_i} \right) \\
&+ \phi_f \rho_{gsf} \left(\frac{S_{of}}{B_{of}} \frac{\partial R_{sf}}{\partial P_{gf}} - \frac{S_{gf}}{B_{gf}^2} \frac{\partial B_{gf}}{\partial P_{gf}} \right) \frac{\partial P_{gf}}{\partial t} \\
&- \phi_f \rho_{gsf} S_{of} \frac{R_{sf}}{B_{of}^2} \frac{\partial B_{of}}{\partial P_{of}} \frac{\partial P_{of}}{\partial t} \\
&+ \left(S_{gf} \rho_{gf} + S_{of} R_f \right) \left(1 - \phi_m \right) \alpha_{mf} \, \dot{u}_{i,i} \\
&- \left(S_{gf} \rho_{gf} + S_{of} R_f \right) \left[\frac{\alpha_{mf} - \phi}{K_n s} \left(\phi_m - 1 \right) + \phi_m \phi_f C_f \right] \frac{\partial P_f}{\partial t} \\
&- \left(S_{gf} \rho_{gf} + S_{of} R_f \right) \left[\frac{\alpha_{mf} - \phi}{K_s} \left(\phi_m - 1 \right) - \phi_m \left(1 - \phi_m \right) C_m \right] \frac{\partial P_m}{\partial t} \\
&+ \bar{\alpha} \, \rho_{gm} \frac{k_m k_{rgm}}{\mu_{gm} B_{gm}} \left(P_{gf} - P_{gm} \right) + \bar{\alpha} \, \rho_{gm} R_{sm} \frac{k_m k_{rom}}{\mu_{om} B_{om}} \left(P_{of} - P_{om} \right) = 0
\end{aligned}
\tag{3.102}
$$

Governing equation for oil From Eq. (3.77), the governing equation for oil in the matrix is given by:

$$-\frac{\partial}{\partial x_i}\left(\frac{u_{om}}{B_{om}}\right)=\frac{\partial}{\partial t}\left(\phi_m\frac{S_{om}}{B_{om}}\right) \tag{3.103}$$

Moving the right-hand side item to the left and changing the sign yields:

$$\frac{\partial}{\partial t}\left(\phi_m\frac{S_{om}}{B_{om}}\right)+\frac{\partial}{\partial x_i}\left(\frac{u_{om}}{B_{om}}\right)=0 \tag{3.104}$$

Darcy's velocity for oil in an undeformable solid system is again:

$$u_{om}=\phi_m S_{om} U_{omi} \tag{3.105}$$

Plugging this equation into Eq. (3.104) gives:

$$\frac{\partial}{\partial t}\left(\phi_m\frac{S_{om}}{B_{om}}\right)+\frac{\partial}{\partial x_i}\left(\frac{\phi_m S_{om} U_{omi}}{B_{om}}\right)=0 \tag{3.106}$$

Darcy's velocity for oil in a deformable solid system is:

$$w_{omi}=\phi_m S_{om}\left(U_{omi}-\dot{u}\right) \tag{3.107}$$

That is,

$$\phi_m S_{om} U_{omi}=w_{omi}+\phi_m S_{om}\,\dot{u} \tag{3.108}$$

Substituting the above equation into Eq. (3.106) yields:

$$\frac{\partial}{\partial t}(\phi_m\frac{S_{om}}{B_{om}})+\frac{\partial}{\partial x_i}\left(\phi_m\frac{S_{om}}{B_{om}}\,\dot{u}_i\right)+\frac{\partial}{\partial x_i}\left(\frac{w_{omi}}{B_{om}}\right)=0 \tag{3.109}$$

Expanding it gives:

$$\begin{aligned}\phi_m S_{om}\frac{D}{Dt}\left(\frac{1}{B_{om}}\right)+\frac{\phi_m}{B_{om}}\frac{DS_{om}}{Dt}+\frac{S_{om}}{B_{om}}\frac{D\phi_m}{Dt}&\\+\phi_m\frac{S_{om}}{B_{om}}\frac{\partial\,\dot{u}_i}{\partial x_i}+\frac{\partial}{\partial x_i}\left(\frac{w_{omi}}{B_{om}}\right)=0&\end{aligned} \tag{3.110}$$

Plugging Eq. (3.28) into Eq. (3.110) gives:

$$\phi_m S_{om}\frac{D}{Dt}\left(\frac{1}{B_{om}}\right)+\frac{\phi_m}{B_{om}}\frac{DS_{om}}{Dt}+\frac{S_{om}}{B_{om}}\frac{1-\phi}{\rho_s}\frac{D\rho_s}{Dt}$$

$$+\frac{S_{om}}{B_{om}}(1-\phi_f)\frac{\partial\,\dot{u}_i}{\partial x_i}-\frac{S_{om}}{B_{om}}\frac{D\phi_f}{Dt}+\frac{\partial}{\partial x_i}\left(\frac{w_{omi}}{B_{om}}\right)=0 \tag{3.111}$$

Plugging Eqs. (3.44) and (3.47) into Eq. (3.111) yields:

$$\begin{aligned}\phi_m S_{om}\frac{\partial}{\partial t}\left(\frac{1}{B_{om}}\right)+\frac{\phi_m}{B_{om}}\frac{\partial S_{om}}{\partial t}+\frac{S_{om}}{B_{om}}(1-\phi_f)\,\alpha_{mf}\,\dot{u}_{i,i}\\ -S_{om}\frac{1}{B_{om}}\left[\frac{\alpha_{mf}-\phi}{K_s}(\phi_f-1)+\phi_m\phi_f C_m\right]\frac{\partial P_m}{\partial t}\\ -\frac{S_{om}}{B_{om}}\left[\frac{\alpha_{mf}-\phi}{K_n s}(\phi_f-1)-\phi_f(1-\phi_f)C_f\right]\frac{\partial P_f}{\partial t}+\frac{\partial}{\partial x_i}\left(\frac{w_{omi}}{B_{om}}\right)=0\end{aligned} \tag{3.112}$$

For the term $\frac{\partial}{\partial t}\left(\frac{1}{B_{om}}\right)$,

$$\begin{aligned}\frac{\partial}{\partial t}\left(\frac{1}{B_{om}}\right) &= -\frac{1}{B_{om}^2}\frac{\partial B_{om}}{\partial t}\\ &= -\frac{1}{B_{om}^2}\frac{\partial B_{om}}{\partial P_{om}}\frac{\partial P_{om}}{\partial t}\end{aligned} \tag{3.113}$$

For the term $\frac{\partial}{\partial x_i}\left(\frac{w_{omi}}{B_{om}}\right)$,

$$\frac{\partial}{\partial x_i}\left(\frac{w_{omi}}{B_{om}}\right)=-\frac{\partial}{\partial x_i}\left(\frac{k_m k_{rom}}{\mu_{om}B_{om}}\frac{\partial P_{om}}{\partial x_i}\right) \tag{3.114}$$

Plugging Eqs. (3.113) and (3.114) into Eq. (3.112) gives:

$$\begin{aligned}\phi_m\frac{1}{B_{om}}\frac{\partial S_{om}}{\partial t}-\frac{\partial}{\partial x_i}\left(\frac{k_m k_{rom}}{\mu_{om}B_{om}}\frac{\partial P_{om}}{\partial x_i}\right)\\ +S_{om}\frac{1}{B_{om}}(1-\phi_f)\,\alpha_{mf}\,\dot{u}_{i,i}\\ -\phi_m S_{om}\frac{1}{B_{om}^2}\frac{\partial B_{om}}{\partial P_{om}}\frac{\partial P_{om}}{\partial t}\\ -S_{om}\frac{1}{B_{om}}\left[\frac{\alpha_{mf}-\phi}{k_s}(\phi_f-1)+\phi_m\phi_f C_m\right]\frac{\partial P_m}{\partial t}\\ -S_{om}\frac{1}{B_{om}}\left[\frac{\alpha_{mf}-\phi}{k_n S}(\phi_f-1)-\phi_f(1-\phi_f)C_f\right]\frac{\partial P_f}{\partial t}=0\end{aligned} \tag{3.115}$$

The mass transfer term for oil between matrix and fractures is calculated by:

$$Q_o=\overline{\alpha}\frac{k_m k_{rom}}{\mu_{om}B_{om}}(P_{om}-P_{of}) \tag{3.116}$$

The final continuity equation for oil in the matrix can be written as:

$$\phi_m \frac{1}{B_{om}} \frac{\partial S_{om}}{\partial t} - \frac{\partial}{\partial x_i} \left(\frac{k_m k_{rom}}{\mu_{om} B_{om}} \frac{\partial P_{om}}{\partial x_i} \right)$$

$$+ S_{om} \frac{1}{B_{om}} \left(1 - \phi_f\right) \alpha_{mf} \, \dot{u}_{i,i}$$

$$- \phi_m S_{om} \frac{1}{B_{om}^2} \frac{\partial B_{om}}{\partial P_{om}} \frac{\partial P_{om}}{\partial t}$$

$$- S_{om} \frac{1}{B_{om}} \left[\frac{\alpha_{mf} - \phi}{k_s} \left(\phi_f - 1\right) + \phi_m \phi_f C_m \right] \frac{\partial P_m}{\partial t}$$

$$- S_{om} \frac{1}{B_{om}} \left[\frac{\alpha_{mf} - \phi}{k_n S} \left(\phi_f - 1\right) - \phi_f \left(1 - \phi_f\right) C_f \right] \frac{\partial P_f}{\partial t}$$

$$+ \overline{\alpha} \frac{k_m k_{rom}}{\mu_{om} B_{om}} \left(P_{om} - P_{of}\right) = 0 \tag{3.117}$$

The final continuity equation for oil in the fractures is as follows:

$$\phi_f \frac{1}{B_{of}} \frac{\partial S_{of}}{\partial t} - \frac{\partial}{\partial x_i} \left(\frac{k_f k_{rof}}{\mu_{of} B_{of}} \frac{\partial P_{of}}{\partial x_i} \right)$$

$$+ S_{of} \frac{1}{B_{of}} \left(1 - \phi_m\right) \alpha_{mf} \, \dot{u}_{i,i}$$

$$- \phi_f S_{of} \frac{1}{B_{of}^2} \frac{\partial B_{of}}{\partial P_{of}} \frac{\partial P_{of}}{\partial t}$$

$$- S_{of} \frac{1}{B_{of}} \left[\frac{\alpha_{mf} - \phi}{k_n S} \left(\phi_m - 1\right) + \phi_m \phi_f C_f \right] \frac{\partial P_f}{\partial t}$$

$$- S_{of} \frac{1}{B_{of}} \left[\frac{\alpha_{mf} - \phi}{k_s} \left(\phi_m - 1\right) - \phi_m \left(1 - \phi_m\right) C_m \right] \frac{\partial P_m}{\partial t}$$

$$+ \overline{\alpha} \frac{k_m k_{rom}}{\mu_{om} B_{om}} \left(P_{of} - P_{om}\right) = 0 \tag{3.118}$$

Four auxiliary equations are needed to solve the problem, i.e., saturation and capillary pressure relationships in matrix and fracture.

For the matrix:

$$S_{gm} + S_{om} = 1 \tag{3.119}$$

$$P_{cm} = P_{gm} - P_{om} \tag{3.120}$$

For the fractures:

$$S_{gf} + S_{of} = 1 \tag{3.121}$$

$$P_{cf} = P_{gf} - P_{of} \tag{3.122}$$

Chapter 4

Numerical Implementation

Numerical methods must be applied for those problems whose analytical solutions are impossible to obtain. A differential equation expresses a relationship between a function and its derivatives over a continuum; and, therefore, really represents an infinite number of equations with an infinite number of unknowns.

Numerical solutions require only the more modest ability to solve a finite number of equations for a finite number of unknowns. In order to use this ability, one needs to construct a finite system of equations, the solution to which has some relationship with the original infinite system. This process is known as discretization.

Discretization methods fall into two main classes: those methods that approximate the original differential equation itself (usually known as finite difference methods), and those that directly approximate the solution by a function from a finite-dimensional space, using the original differential equation to define the free parameters involved (this group includes the finite element method).

There are currently five widely used numerical methods:

1. Finite difference methods;

2. Galerkin or variational finite element methods;

3. Collocation methods;

4. Method of characteristics; and,
5. Boundary element methods.

These methods are closely related. In several cases the finite difference, finite element, and collocation methods yield the same approximation. The method of characteristics is a variant of the finite difference method and is particularly suitable for solving hyperbolic equations. The boundary element method, a variant of the conventional finite element method, is especially useful in the solution of elliptic equation for which Green's functions exist.

The finite difference and finite element methods are the two most popular numerical approaches for the simulation of reservoir systems. They appear superficially different but are, in fact, closely related. The finite element starts with a variational statement of the problem and introduces piecewise definitions of the functions defined by a set of meshpoint values. The finite difference method starts with a differential statement of the problem and proceeds to replace the derivatives with their discrete analogs.

Both methods result in a set of algebraic equations relating a discrete set of variables in place of the relations in the continuous variables. These algebraic equations are remarkably similar and provide the basis for identifying the methods as essentially similar.

There are two avenues of approach to the simulation of pressure propagation, and mass and energy transport in fractured reservoirs. One requires identification and mathematical definition of the geometry of each fracture in the porous medium. The second assumes the fractures and porous blocks represent two overlapping continua. Finite element methods have been applied to solve the equations arising from both models (Li *et al.*, 1990; Lewis and Ghafouri, 1997) as well as other similar reservoir modeling problems (Zienkiewicz and Parekh, 1970; Neumann and Witherspoon, 1970; Lewis and Schrefler, 1987; Lewis and Sukirman, 1993a and 1993b). The flexibility inherent in the finite element approach is particularly useful in the discrete fracture model. On the other hand, the finite difference methods have a justifiable attraction because of their simplicity and computational efficiency for complex and nonlinear problems (Huyakorn and Pinder, 1983). However, it is noted from the literature review that finite difference methods have never been applied to coupled fractured reservoir models. One of the aims of this dissertation is to test the feasibility of applying such an approach to this kind of models.

4.1 Finite Difference Formulae for Derivatives

The following equations can be derived from the Taylor series:

1. Forward difference in time:

$$\frac{\partial f}{\partial t} = \frac{f_{i,j}^{n+1} - f_{i,j}^{n}}{\Delta t} \tag{4.1}$$

2. Central difference in space:

$$\frac{\partial f}{\partial x} = \frac{f_{i+1,j} - f_{i-1,j}}{2\Delta x} \tag{4.2}$$

$$\frac{\partial f}{\partial y} = \frac{f_{i,j+1} - f_{i,j-1}}{2\Delta y} \tag{4.3}$$

$$\frac{\partial^2 f}{\partial x^2} = \frac{f_{i+1,j} - 2f_{i,j} + f_{i-1,j}}{(\Delta x)^2} \tag{4.4}$$

$$\frac{\partial^2 f}{\partial y^2} = \frac{f_{i,j+1} - 2f_{i,j} + f_{i,j-1}}{(\Delta y)^2} \tag{4.5}$$

3. Mixed partial differential derivatives:

$$\frac{\partial^2 f}{\partial x \partial y} = \frac{f_{i+1,j+1} - f_{i-1,j+1} - f_{i+1,j-1} + f_{i-1,j-1}}{4\Delta x \Delta y} \tag{4.6}$$

$$\frac{\partial^2 f}{\partial x \partial t} = \frac{f_{i+1,j}^{n+1} - f_{i+1,j}^{n} - f_{i-1,j}^{n+1} + f_{i-1,j}^{n}}{2\Delta x \Delta t} \tag{4.7}$$

$$\frac{\partial^2 f}{\partial y \partial t} = \frac{f_{i+1,j}^{n+1} - f_{i+1,j}^{n} - f_{i-1,j}^{n+1} + f_{i-1,j}^{n}}{2\Delta y \Delta t} \tag{4.8}$$

The pressures in the matrix and in the fractures are saturation-averaged pressures of water and oil in that continuum; i.e.:

$$P_m = S_{om} P_{om} + S_{wm} P_{wm} \tag{4.9}$$

$$P_f = S_{of} P_{of} + S_{wf} P_{wf} \tag{4.10}$$

Differentiating Eqs. (4.9) and (4.10) with respect to space (for example, $x-$direction) yields:

$$\frac{\partial P_m}{\partial x} = S_{om}\frac{\partial P_{om}}{\partial x} + P_{om}\frac{\partial S_{om}}{\partial x} + S_{wm}\frac{\partial P_{wm}}{\partial x} + P_{wm}\frac{\partial S_{wm}}{\partial x} \tag{4.11}$$

$$\frac{\partial P_f}{\partial x} = S_{of}\frac{\partial P_{of}}{\partial x} + P_{of}\frac{\partial S_{of}}{\partial x} + S_{wf}\frac{\partial P_{wf}}{\partial x} + P_{wf}\frac{\partial S_{wf}}{\partial x} \tag{4.12}$$

4.2 Finite Difference Approximation of Equilibrium Equations

Based on the finite difference formulae provided in section 5.1, Eq. (3.17) (first equilibrium equation for solid) in finite difference discretization is written as:

$$(\lambda + G)\left[\frac{u_{i+1,j}^{n+1} - 2u_{i,j}^{n+1} + u_{i-1,j}^{n+1}}{(\Delta x)^2} + \frac{v_{i+1,j+1}^{n+1} - v_{i+1,j-1}^{n+1} - v_{i-1,j+1}^{n+1} + v_{i-1,j-1}^{n+1}}{4\Delta x \Delta y}\right]$$

$$+G\left[\frac{u_{i+1,j}^{n+1} - 2u_{i,j}^{n+1} + u_{i-1,j}^{n+1}}{(\Delta x)^2} + \frac{u_{i,j+1}^{n+1} - 2u_{i,j}^{n+1} + u_{i,j-1}^{n+1}}{(\Delta y)^2}\right]$$

$$+\alpha_m\left(S_{om}\frac{p_{omi+1,j}^{n+1} - p_{omi-1,j}^{n+1}}{2\Delta x} + p_{om}\frac{S_{omi+1,j}^{n+1} - S_{omi-1,j}^{n+1}}{2\Delta x}\right.$$

$$\left.+S_{wm}\frac{p_{wmi+1,j}^{n+1} - p_{wmi-1,j}^{n+1}}{2\Delta x} + p_{wm}\frac{S_{wmi+1,j}^{n+1} - S_{wmi-1,j}^{n+1}}{2\Delta x}\right)$$

$$+\alpha_f\left(S_{of}\frac{p^{n+1}_{ofi+1,j}-p^{n+1}_{ofi-1,j}}{2\Delta x}+p_{of}\frac{S^{n+1}_{ofi+1,j}-S^{n+1}_{ofi-1,j}}{2\Delta x}\right.$$

$$\left.+S_{wf}\frac{p^{n+1}_{wfi+1,j}-p^{n+1}_{wfi-1,j}}{2\Delta x}+p_{wf}\frac{S^{n+1}_{wfi+1,j}-S^{n+1}_{wfi-1,j}}{2\Delta x}\right)=0 \tag{4.13}$$

It can be simplified to:

$$\begin{aligned}
& -2(a_1+a_2)u_{i,j}+a_1u_{i+1,j}+a_1u_{i-1,j}+a_2u_{i,j+1}+a_2u_{i,j-1}+a_3v_{i-1,j-1} \\
& -a_3v_{i-1,j+1}+a_3v_{i+1,j+1}-a_3v_{i+1,j-1}-a_4p_{mi-1,j}+a_4p_{mi+1,j}-a_5p_{fi-1,j} \\
& +a_5p_{fi+1,j}-a_{6i,j}S_{mi-1,j}+a_{6i,j}S_{mi+1,j}-a_{7i,j}S_{fi-1,j}+a_{7i,j}S_{fi+1,j} \\
= \; & a_{8i,j}(p_{cmi+1,j}-p_{cmi-1,j})+a_{9i,j}(p_{cfi+1,j}-p_{cfi-1,j})
\end{aligned} \tag{4.14}$$

where,

$$\begin{aligned}
a_1=\frac{\lambda+2G}{(\Delta x)^2},\ a_2=\frac{2G}{(\Delta y)^2},\ a_3=\frac{\lambda+G}{4\Delta x\Delta y} \\
a_4=\frac{\alpha_m}{2\Delta x},\ a_5=\frac{\alpha_f}{2\Delta x} \\
a_{6i,j}=\frac{\alpha_m}{2\Delta x}p_{cmi,j},\ a_{7i,j}=\frac{\alpha_f}{2\Delta x}p_{cfi,j} \\
a_{8i,j}=\frac{\alpha_m}{2\Delta x}(1-S_{mi,j}),\ a_{9i,j}=\frac{\alpha_f}{2\Delta x}(1-S_{fi,j})
\end{aligned} \tag{4.15}$$

Similarly, Eq. (3.18) (second equilibrium equation for solid) becomes:

$$\begin{aligned}
& -2(b_1+b_2)v_{i,j}+b_1v_{i+1,j}+b_1v_{i-1,j}+b_2v_{i,j+1}+b_2v_{i,j-1}+b_3u_{i-1,j-1} \\
& -b_3u_{i-1,j+1}+b_3u_{i+1,j+1}-b_3u_{i+1,j-1}-b_4p_{mi,j-1}+b_4p_{mi,j+1}-b_5p_{fi,j-1} \\
& +b_5p_{fi,j+1}-b_{6i,j}S_{mi,j-1}+b_{6i,j}S_{mi,j+1}-b_{7i,j}S_{fi,j-1}+b_{7i,j}S_{fi,j+1} \\
= \; & b_{8i,j}(p_{cmi,j+1}-p_{cmi,j-1})+b_{9i,j}(p_{cfi,j+1}-p_{cfi,j-1})
\end{aligned} \tag{4.16}$$

where,

$$\begin{aligned}
b_1=\frac{2G}{(\Delta x)^2},\ b_2=\frac{\lambda+2G}{(\Delta y)^2},\ b_3=\frac{\lambda+G}{4\Delta x\Delta y} \\
b_4=\frac{\alpha_m}{2\Delta y},\ b_5=\frac{\alpha_f}{2\Delta y}, \\
b_{6i,j}=\frac{\alpha_m}{2\Delta y}p_{cmi,j},\ b_{7i,j}=\frac{\alpha_f}{2\Delta y}p_{cfi,j}
\end{aligned}$$

$$b_{8i,j} = \frac{\alpha_m}{2\Delta y}(1 - S_{mi,j}),\ b_{9i,j} = \frac{\alpha_f}{2\Delta y}(1 - S_{fi,j}) \tag{4.17}$$

4.3 Finite Difference Approximation of Continuity Equations

4.3.1 Water-Oil System

Applying the chain rule to the derivative of density to time term in the governing equation for water in matrix (Eq. (3.52)) leads to the following:

$$\frac{\partial \rho_w}{\partial t} = \frac{\partial \rho_w}{\partial P_w}\frac{\partial P_w}{\partial t} = \rho_w C_w \frac{\partial P_w}{\partial t} \tag{4.18}$$

where C_w is the compressibility of water, i.e.:

$$C_w = \frac{1}{\rho_w}\frac{\partial \rho_w}{\partial P_w} \tag{4.19}$$

The term $\frac{\partial \rho_w w_i}{\partial x_i}$ in the governing equation consists of two parts in two dimensions:

$$\frac{\partial \rho_w w_i}{\partial x_i} = \frac{\partial \rho_w w_x}{\partial x} + \frac{\partial \rho_w w_y}{\partial y} \tag{4.20}$$

Since,

$$w_x = -\frac{k_m k_{rwm}}{\mu_w}\frac{\partial P_{wm}}{\partial x} \tag{4.21}$$

so,

$$\begin{aligned}
\frac{\partial \rho_w w_x}{\partial x} &= \frac{\partial}{\partial x}\left(-\rho_w \frac{k_m k_{rwm}}{\mu_w}\frac{\partial P_{wm}}{\partial x}\right) \\
&= -\frac{\partial}{\partial x}\left(\lambda_{wxm}\frac{\partial P_{wm}}{\partial x}\right) \\
&= -\frac{1}{\Delta x}\left[\left(\lambda_{wxm}\frac{\partial P_{wm}}{\partial x}\right)_{i+1/2,j} - \left(\lambda_{wxm}\frac{\partial P_{wm}}{\partial x}\right)_{i-1/2,j}\right] \\
&= -\frac{1}{\Delta x}\left(\lambda_{wxmi+1/2,j}\frac{P_{wmi+1,j} - P_{wmi,j}}{\Delta x} - \lambda_{wxmi+1/2,j}\frac{P_{wmi+1,j} - P_{wmi,j}}{\Delta x}\right)
\end{aligned}$$

$$
\begin{aligned}
= & -\Big[T_{wxmi+1/2,j}\left(P_{wmi+1,j}-P_{wmi,j}\right) \\
& -T_{wxmi-1/2,j}\left(P_{wmi,j}-P_{wmi-1,j}\right)\Big]
\end{aligned} \tag{4.22}
$$

where,

$$
\lambda_{wxm}=\rho_w\frac{k_m k_{rwm}}{\mu_w} \tag{4.23}
$$

$$
T_{wxm}=\frac{\lambda_{wxm}}{(\Delta x)^2} \tag{4.24}
$$

Similarly,

$$
\frac{\partial\rho_w w_y}{\partial y}=-\Big[T_{wymi,j+1/2}\left(P_{wmi,j+1}-P_{wmi,j}\right)-T_{wymi,j-1/2}\left(P_{wmi,j}-P_{wmi,j-1}\right)\Big] \tag{4.25}
$$

Then, Eq. (3.52) (the continuity equation for the water phase in the matrix) in finite difference discretization can be written as:

$$
\begin{gathered}
-T_{wxmi+1/2,j}\left(P^{n+1}_{wmi+1,j}-P^{n+1}_{wmi,j}\right)+T_{wxmi-1/2,j}\left(P^{n+1}_{wmi,j}-P^{n+1}_{wmi-1,j}\right) \\
-T_{wxmi,j+1/2}\left(P^{n+1}_{wmi,j+1}-P^{n+1}_{wmi,j}\right)+T_{wxmi,j-1/2}\left(P^{n+1}_{wmi,j}-P^{n+1}_{wmi,j-1}\right) \\
+\phi_m S_{wm}\rho_{wm}C_{wm}\frac{P^{n+1}_{wm}-P^{n}_{wm}}{\Delta t}+\phi_m\rho_{wm}\frac{S^{n+1}_{wm}-S^{n}_{wm}}{\Delta t} \\
+B1_{wm}\frac{S_{wm}}{\Delta t}(P^{n+1}_{wm}-P^{n}_{wm})+B1_{wm}\frac{P_{wm}}{\Delta t}(S^{n+1}_{wm}-S^{n}_{wm})+B1_{wm}\frac{S_{om}}{\Delta t}(P^{n+1}_{om}-P^{n}_{om}) \\
+B1_{wm}\frac{P_{om}}{\Delta t}(S^{n+1}_{om}-S^{n}_{om})+B2_{wm}\frac{S_{wf}}{\Delta t}(P^{n+1}_{wf}-P^{n}_{wf})+B2_{wm}\frac{P_{wf}}{\Delta t}(S^{n+1}_{wf}-S^{n}_{wf}) \\
+B2_{wm}\frac{S_{of}}{\Delta t}(P^{n+1}_{of}-P^{n}_{of})+B2_{wm}\frac{P_{of}}{\Delta t}(S^{n+1}_{of}-S^{n}_{of}) \\
+B3_{wm}\left(\frac{u^{n+1}_{i+1,j}-u^{n}_{i+1,j}-u^{n+1}_{i-1,j}+u^{n}_{i-1,j}}{2\Delta x\Delta t}+\frac{v^{n+1}_{i,j+1}-v^{n}_{i,j+1}-v^{n+1}_{i,j-1}+v^{n}_{i,j-1}}{2\Delta y\Delta t}\right) \\
+B4_{wm}\left(P^{n+1}_{wm}-P^{n+1}_{wf}\right)=0
\end{gathered} \tag{4.26}
$$

where,

$$
B1_{wm}=S_{wm}\rho_{wm}\left[\frac{\alpha_{mf}-\phi}{K_s}\left(\phi_f-1\right)-\phi_m\phi_f C_m\right] \tag{4.27}
$$

$$
B2_{wm}=S_{wm}\rho_{wm}\left[\frac{\alpha_{mf}-\phi}{K_n s}\left(\phi_f-1\right)+\phi_f\left(1-\phi_f\right)C_f\right] \tag{4.28}
$$

$$B3_{wm} = \alpha_{mf}\left(1-\phi_f\right) S_{wm}\rho_{wm} \tag{4.29}$$

$$B4_{wm} = \overline{\alpha}\rho_{wm}\frac{k_m k_{rwm}}{\mu_{wm}} \tag{4.30}$$

It can be further simplified to:

$$\begin{aligned}
& c_{15i,j}p_{mi,j} - c_{1i,j}p_{mi+1,j} - c_{2i,j}p_{mi-1,j} - c_{3i,j}p_{mi,j+1} - c_{4i,j}p_{mi,j-1} \\
& +(c_{10i,j} - c_{7i,j})p_{fi,j} + c_{8i,j}u_{i+1,j} - c_{8i,j}u_{i-1,j} + c_{9i,j}v_{i,j+1} - c_{9i,j}v_{i,j-1} \\
& +c_{11i,j}S_{mi,j} + c_{12i,j}S_{fi,j} \\
= \; & c_{14i,j}p_{mi,j} + c_{10i,j}p_{fi,j} + c_{11i,j}S_{mi,j} + c_{12i,j}S_{fi,j} + c_{8i,j}u_{i+1,j} \\
& -c_{8i,j}u_{i-1,j} + c_{9i,j}v_{i,j+1} - c_{9i,j}v_{i,j-1} + c_{13i,j}p_{cmi,j} - c_{1i,j}p_{cmi+1,j} \\
& -c_{2i,j}p_{cmi-1,j} - c_{3i,j}p_{cmi,j+1} - c_{4i,j}p_{cmi,j-1} - c_{7i,j}p_{cfi,j}
\end{aligned} \tag{4.31}$$

where,

$$\begin{gathered}
c_{1i,j} = \frac{k_m}{(\Delta x)^2}(\frac{\rho_{wm}k_{rwm}}{\mu_{wm}})_{i+\frac{1}{2},j},\ c_{2i,j} = \frac{k_m}{(\Delta x)^2}(\frac{\rho_{wm}k_{rwm}}{\mu_{wm}})_{i-\frac{1}{2},j} \\
c_{3i,j} = \frac{k_m}{(\Delta y)^2}(\frac{\rho_{wm}k_{rwm}}{\mu_{wm}})_{i,j+\frac{1}{2}},\ c_{4i,j} = \frac{k_m}{(\Delta y)^2}(\frac{\rho_{wm}k_{rwm}}{\mu_{wm}})_{i,j-\frac{1}{2}} \\
c_{5i,j} = \frac{\phi_m c_w \rho_{ws}}{\Delta t}(1 - S_{m_{i,j}}) \\
c_{6i,j} = \frac{(1-S_{mi,j})\rho_{wmi,j}}{\Delta t}\left[\frac{\alpha_{mf}-\phi}{K_s}\left(\phi_f - 1\right) - \phi_m\phi_f C_m\right] \\
c_{7i,j} = \overline{\alpha}k_m(\frac{\rho_{wm}k_{rwm}}{\mu_{wm}})_{i,j} \\
c_{8i,j} = \frac{\alpha_{mf}(1-\phi_f)}{2\Delta x\Delta t}\left[\rho_{wm}(1-S_m)\right]_{i,j},\ c_{9i,j} = \frac{\alpha_{mf}(1-\phi_f)}{2\Delta y\Delta t}\left[\rho_{wm}(1-S_m)\right]_{i,j} \\
c_{10i,j} = \frac{\rho_{wm}(1-S_{mi,j})}{\Delta t}\left[\frac{\alpha_{mf}-\phi}{K_n s}\left(\phi_f - 1\right) + \phi_f\left(1-\phi_f\right)C_f\right] \\
c_{11i,j} = c_{6i,j}p_{cmi,j} - \frac{\phi_m}{\Delta t}\rho_{wmij},\ c_{12i,j} = c_{10i,j}p_{cfi,j} \\
c_{13i,j} = c_{1i,j} + c_{2i,j} + c_{3i,j} + c_{4i,j} + c_{7i,j} \\
c_{14i,j} = c_{5i,j} + c_{6i,j},\ c_{15i,j} = c_{13i,j} + c_{14i,j}
\end{gathered} \tag{4.32}$$

Equation (3.53) yields:

$$
\begin{aligned}
& d_{15i,j}p_{mi,j} - d_{1i,j}p_{mi+1,j} - d_{2i,j}p_{mi-1,j} - d_{3i,j}p_{mi,j+1} - d_{4i,j}p_{mi,j-1} \\
& +(d_{10i,j} - d_{7i,j})p_{fi,j} + d_{8i,j}u_{i+1,j} - d_{8i,j}u_{i-1,j} + d_{9i,j}v_{i,j+1} \\
& -d_{9i,j}v_{i,j-1} + d_{11i,j}S_{mi,j} + d_{12i,j}S_{fi,j} \\
= \; & d_{14i,j}p_{mi,j} + d_{10i,j}p_{fi,j} + d_{11i,j}S_{mi,j} + d_{12i,j}S_{fi,j} + d_{8i,j}u_{i+1,j} \\
& -d_{8i,j}u_{i-1,j} + d_{9i,j}v_{i,j+1} - d_{9i,j}v_{i,j-1} \qquad (4.33)
\end{aligned}
$$

where,

$$
\begin{aligned}
d_{1i,j} &= \frac{k_m}{(\Delta x)^2}(\frac{\rho_{om}k_{rom}}{\mu_{om}})_{i+\frac{1}{2},j}, \; d_{2i,j} = \frac{k_m}{(\Delta x)^2}(\frac{\rho_{om}k_{rom}}{\mu_{om}})_{i-\frac{1}{2},j} \\
d_{3i,j} &= \frac{k_m}{(\Delta y)^2}(\frac{\rho_{om}k_{rom}}{\mu_{om}})_{i,j+\frac{1}{2}}, \; d_{4i,j} = \frac{k_m}{(\Delta y)^2}(\frac{\rho_{om}k_{rom}}{\mu_{om}})_{i,j-\frac{1}{2}} \\
d_{5i,j} &= \frac{\phi_m C_o \rho_{os}}{\Delta t} S_{m_{i,j}} \\
d_{6i,j} &= \frac{S_{mi,j}\rho_{omi,j}}{\Delta t}\left[\frac{\alpha_{mf} - \phi}{K_s}(\phi_f - 1) - \phi_m\phi_f C_m\right] \\
d_{7i,j} &= \overline{\alpha}k_m(\frac{\rho_{om}k_{rom}}{\mu_{om}})_{i,j} \\
d_{8i,j} &= \frac{\alpha_{mf}(1-\phi_f)}{2\Delta x\Delta t}(\rho_{om}S_m)_{i,j}, \; d_{9i,j} = \frac{\alpha_{mf}(1-\phi_f)}{2\Delta y\Delta t}(\rho_{om}S_m)_{i,j} \\
d_{10i,j} &= \frac{\rho_{om}S_{mi,j}}{\Delta t}\left[\frac{\alpha_{mf} - \phi}{K_n s}(\phi_f - 1) + \phi_f(1-\phi_f)C_f\right] \\
d_{11i,j} &= d_{6i,j}p_{cmi,j} - \frac{\phi_m}{\Delta t}\rho_{omij}, \; d_{12i,j} = d_{10i,j}p_{cfi,j} \\
d_{13i,j} &= d_{1i,j} + d_{2i,j} + d_{3i,j} + d_{4i,j} + d_{7i,j} \\
d_{14i,j} &= d_{5i,j} + d_{6i,j}, \; d_{15i,j} = d_{13i,j} + d_{14i,j} \qquad (4.34)
\end{aligned}
$$

Equation (3.54) becomes:

$$
\begin{aligned}
& e_{15i,j}p_{fi,j} - e_{1i,j}p_{fi+1,j} - e_{2i,j}p_{fi-1,j} - e_{3i,j}p_{fi,j+1} - e_{4i,j}p_{fi,j-1} \\
& +(e_{10i,j} - e_{7i,j})p_{mi,j} + e_{8i,j}u_{i+1,j} - e_{8i,j}u_{i-1,j} + e_{9i,j}v_{i,j+1} - e_{9i,j}v_{i,j-1} \\
& +e_{11i,j}S_{fi,j} + e_{12i,j}S_{mi,j}
\end{aligned}
$$

$$
\begin{aligned}
= \quad & e_{14i,j}p_{fi,j} + e_{10i,j}p_{mi,j} + e_{11i,j}S_{fi,j} + e_{12i,j}S_{mi,j} + e_{8i,j}u_{i+1,j} - e_{8i,j}u_{i-1,j} \\
& + e_{9i,j}v_{i,j+1} - e_{9i,j}v_{i,j-1} + e_{13i,j}p_{cfi,j} - e_{1i,j}p_{cfi+1,j} - e_{2i,j}p_{cfi-1,j} \\
& - e_{3i,j}p_{cfi,j+1} - e_{4i,j}p_{cfi,j-1} - e_{7i,j}p_{cmi,j} \qquad (4.35)
\end{aligned}
$$

where,

$$
\begin{gathered}
e_{1i,j} = \frac{k_f}{(\Delta x)^2}(\frac{\rho_{wf}k_{rwf}}{\mu_{wf}})_{i+\frac{1}{2},j}, \; e_{2i,j} = \frac{k_f}{(\Delta x)^2}(\frac{\rho_{wf}k_{rwf}}{\mu_{wf}})_{i-\frac{1}{2},j} \\
e_{3i,j} = \frac{k_f}{(\Delta y)^2}(\frac{\rho_{wf}k_{rwf}}{\mu_{wf}})_{i,j+\frac{1}{2}}, \; e_{4i,j} = \frac{k_f}{(\Delta y)^2}(\frac{\rho_{wf}k_{rwf}}{\mu_{wf}})_{i,j-\frac{1}{2}} \\
e_{5i,j} = \frac{\phi_f C_w \rho_{ws}}{\Delta t}(1 - S_{f_{i,j}}) \\
e_{6i,j} = \frac{(1 - S_{fi,j})\rho_{wfi,j}}{\Delta t}\left[\frac{\alpha_{mf} - \phi}{K_s}(\phi_m - 1) - \phi_m \phi_f C_f\right] \\
e_{7i,j} = \overline{\alpha} k_m (\frac{\rho_{wm}k_{rwm}}{\mu_{wm}})_{i,j} \\
e_{8i,j} = \frac{\alpha_{mf}(1 - \phi_m)}{2\Delta x \Delta t}\left[\rho_{wf}(1 - S_f)\right]_{i,j}, \; e_{9i,j} = \frac{\alpha_{mf}(1 - \phi_m)}{2\Delta y \Delta t}\left[\rho_{wf}(1 - S_f)\right]_{i,j} \\
e_{10i,j} = \frac{\rho_{wf}(1 - S_{fi,j})}{\Delta t}\left[\frac{\alpha_{mf} - \phi}{K_n s}(\phi_m - 1) + \phi_m (1 - \phi_m) C_m\right] \\
e_{11i,j} = e_{6i,j}p_{cfi,j} - \frac{\phi_f}{\Delta t}\rho_{wfij}, \; e_{12i,j} = e_{10i,j}p_{cfi,j} \\
e_{13i,j} = e_{1i,j} + e_{2i,j} + e_{3i,j} + e_{4i,j} + e_{7i,j} \\
e_{14i,j} = e_{5i,j} + e_{6i,j}, \; e_{15i,j} = e_{13i,j} + e_{14i,j} \qquad (4.36)
\end{gathered}
$$

Equation (3.55) gives:

$$
\begin{aligned}
& f_{15i,j}p_{fi,j} - f_{1i,j}p_{fi+1,j} - f_{2i,j}p_{fi-1,j} - f_{3i,j}p_{fi,j+1} - f_{4i,j}p_{fi,j-1} \\
& + (f_{10i,j} - f_{7i,j})p_{mi,j} + f_{8i,j}u_{i+1,j} - f_{8i,j}u_{i-1,j} + f_{9i,j}v_{i,j+1} \\
& - f_{9i,j}v_{i,j-1} + f_{11i,j}S_{fi,j} + f_{12i,j}S_{mi,j} \\
= \quad & f_{14i,j}p_{fi,j} + f_{10i,j}p_{mi,j} + f_{11i,j}S_{fi,j} + f_{12i,j}S_{mi,j} + f_{8i,j}u_{i+1,j} \\
& - f_{8i,j}u_{i-1,j} + f_{9i,j}v_{i,j+1} - f_{9i,j}v_{i,j-1} \qquad (4.37)
\end{aligned}
$$

where,

$$f_{1i,j} = \frac{k_f}{(\Delta x)^2}(\frac{\rho_{of}k_{rof}}{\mu_{of}})_{i+\frac{1}{2},j},\ f_{2i,j} = \frac{k_f}{(\Delta x)^2}(\frac{\rho_{of}k_{rof}}{\mu_{of}})_{i-\frac{1}{2},j}$$

$$f_{3i,j} = \frac{k_f}{(\Delta y)^2}(\frac{\rho_{of}k_{rof}}{\mu_{of}})_{i,j+\frac{1}{2}},\ f_{4i,j} = \frac{k_f}{(\Delta y)^2}(\frac{\rho_{of}k_{rof}}{\mu_{of}})_{i,j-\frac{1}{2}}$$

$$f_{5i,j} = \frac{\phi_f C_o \rho_{os}}{\Delta t} S_{f_{i,j}}$$

$$f_{6i,j} = \frac{S_{fi,j}\rho_{ofi,j}}{\Delta t}\left[\frac{\alpha_{mf}-\phi}{K_s}(\phi_m - 1) - \phi_m\phi_f C_f\right]$$

$$f_{7i,j} = \overline{\alpha}k_m(\frac{\rho_{om}k_{rom}}{\mu_{om}})_{i,j}$$

$$f_{8i,j} = \frac{\alpha_{mf}(1-\phi_f)}{2\Delta x\Delta t}(\rho_{of}S_f)_{i,j},\ f_{9i,j} = \frac{\alpha_{mf}(1-\phi_f)}{2\Delta y\Delta t}(\rho_{of}S_f)_{i,j}$$

$$f_{10i,j} = \frac{\rho_{of}S_{fi,j}}{\Delta t}\left[\frac{\alpha_{mf}-\phi}{K_n s}(\phi_m - 1) + \phi_m(1-\phi_m)C_m\right]$$

$$f_{11i,j} = f_{6i,j}p_{cfi,j} - \frac{\phi_f}{\Delta t}\rho_{ofij},\ f_{12i,j} = f_{10i,j}p_{cmi,j}$$

$$f_{13i,j} = f_{1i,j} + f_{2i,j} + f_{3i,j} + f_{4i,j} + f_{7i,j}$$

$$f_{14i,j} = f_{5i,j} + f_{6i,j},\ f_{15i,j} = f_{13i,j} + f_{14i,j} \tag{4.38}$$

4.3.2 Gas-Oil System

Equation (3.101) (the continuity equation for the gas phase in the matrix) in finite difference discretization is written as:

$$-T_{gxmi+1/2,j}\left(P^{n+1}_{gmi+1,j} - P^{n+1}_{gmi,j}\right) + T_{gxmi-1/2,j}\left(P^{n+1}_{gmi,j} - P^{n+1}_{gmi-1,j}\right)$$

$$-T_{gxmi,j+1/2}\left(P^{n+1}_{gmi,j+1} - P^{n+1}_{gmi,j}\right) + T_{gxmi,j-1/2}\left(P^{n+1}_{gmi,j} - P^{n+1}_{gmi,j-1}\right)$$

$$+c_5\frac{P^{n+1}_{gmi,j} - P^{n}_{gmi,j}}{\Delta t} + \frac{\phi_m}{B_{gm}}\frac{S^{n+1}_{gm} - S^{n}_{gm}}{\Delta t}$$

$$-T'_{oxmi+1/2,j}\left(P^{n+1}_{omi+1,j} - P^{n+1}_{omi,j}\right) + T'_{oxmi-1/2,j}\left(P^{n+1}_{omi,j} - P^{n+1}_{omi-1,j}\right)$$

$$-T'_{oxmi,j+1/2}\left(P^{n+1}_{omi,j+1} - P^{n+1}_{omi,j}\right) + T'_{oxmi,j-1/2}\left(P^{n+1}_{omi,j} - P^{n+1}_{omi,j-1}\right)$$

$$+c_5^{'}\frac{P_{omi,j}^{n+1}-P_{omi,j}^{n}}{\Delta t}+\frac{\phi_m}{\rho_{gs}}R_m\frac{S_{om}^{n+1}-S_{om}^{n}}{\Delta t}$$

$$+A1_{gm}\frac{S_{om}}{\Delta t}(P_{om}^{n+1}-P_{om}^{n})+A1_{gm}\frac{P_{om}}{\Delta t}(S_{om}^{n+1}-S_{om}^{n})+A1_{gm}\frac{S_{gm}}{\Delta t}(P_{gm}^{n+1}-P_{gm}^{n})$$

$$+A1_{gm}\frac{P_{gm}}{\Delta t}(S_{gm}^{n+1}-S_{gm}^{n})+A2_{gm}\frac{S_{of}}{\Delta t}(P_{of}^{n+1}-P_{of}^{n})+A2_{gm}\frac{P_{of}}{\Delta t}(S_{of}^{n+1}-S_{of}^{n})$$

$$+A2_{gm}\frac{S_{gf}}{\Delta t}(P_{gf}^{n+1}-P_{gf}^{n})+A2_{gm}\frac{P_{gf}}{\Delta t}(S_{gf}^{n+1}-S_{gf}^{n})$$

$$+A3_{gm}\left(\frac{u_{i+1,j}^{n+1}-u_{i+1,j}^{n}-u_{i-1,j}^{n+1}+u_{i-1,j}^{n}}{2\Delta x\Delta t}+\frac{v_{i,j+1}^{n+1}-v_{i,j+1}^{n}-v_{i,j-1}^{n+1}+v_{i,j-1}^{n}}{2\Delta y\Delta t}\right)$$

$$+A4_{gm}\left(P_{gm}^{n+1}-P_{gf}^{n+1}\right)+A4_{gm}^{'}\left(P_{om}^{n+1}-P_{of}^{n+1}\right)=0 \tag{4.39}$$

where,

$$T_{gxm}=\frac{\lambda_{gxm}}{(\Delta x)^2} \tag{4.40}$$

$$\lambda_{gxm}=\frac{k_m k_{rgm}}{\mu_{gm}B_{gm}} \tag{4.41}$$

$$T_{oxm}^{'}=\frac{\lambda_{oxm}^{'}}{(\Delta x)^2} \tag{4.42}$$

$$\lambda_{oxm}^{'}=\frac{R_{sm}k_m k_{rom}}{\mu_{om}B_{om}} \tag{4.43}$$

$$A1_{gm}=\left(\frac{S_{gm}}{B_{gm}}+\frac{S_{om}}{\rho_{gs}}R_m\right)\left[\frac{\alpha_{mf}-\phi}{K_s}(\phi_f-1)-\phi_m\phi_f C_m\right] \tag{4.44}$$

$$A2_{gm}=\left(\frac{S_{gm}}{B_{gm}}+\frac{S_{om}}{\rho_{gs}}R_m\right)\left[\frac{\alpha_{mf}-\phi}{K_n s}(\phi_f-1)+\phi_f(1-\phi_f)C_f\right] \tag{4.45}$$

$$A3_{gm}=\left(\frac{S_{gm}}{B_{gm}}+\frac{S_{om}}{\rho_{gs}}R_m\right)(1-\phi_f)\alpha_{mf} \tag{4.46}$$

$$A4_{gm}=\frac{\overline{\alpha}k_m k_{rgm}}{\rho_{gs}\mu_{gm}B_{gm}} \tag{4.47}$$

$$A4_{gm}^{'}=\frac{R_{sm}\overline{\alpha}k_m k_{rom}}{\rho_{gs}\mu_{gm}B_{om}} \tag{4.48}$$

It can be further simplified to:

$$c_{15i,j}p_{mi,j}-\left(c_{1i,j}+c_{1i,j}^{'}\right)p_{mi+1,j}-\left(c_{2i,j}+c_{2i,j}^{'}\right)p_{mi-1,j}-\left(c_{3i,j}+c_{3i,j}^{'}\right)p_{mi,j+1}$$

$$-\left(c_{4i,j}+c_{4i,j}^{'}\right)p_{mi,j-1}+(c_{10i,j}-c_{7i,j}-c_{7i,j}^{'})p_{fi,j}+c_{8i,j}u_{i+1,j}-c_{8i,j}u_{i-1,j}$$

$$
\begin{aligned}
&+c_{9i,j}v_{i,j+1} - c_{9i,j}v_{i,j-1} + c_{11i,j}S_{mi,j} + c_{12i,j}S_{fi,j} \\
= \quad & c_{14i,j}p_{mi,j} + c_{10i,j}p_{fi,j} + c_{11i,j}S_{mi,j} + c_{12i,j}S_{fi,j} + c_{8i,j}u_{i+1,j} - c_{8i,j}u_{i-1,j} \\
&+c_{9i,j}v_{i,j+1} - c_{9i,j}v_{i,j-1} + c_1 P_{cmi+1,j} + c_2 P_{cmi-1,j} + c_3 P_{cmi,j+1} \\
&+c_4 P_{cmi,j-1} - c_{13} P_{cmi,j} + c_7 P_{cfi,j} \qquad (4.49)
\end{aligned}
$$

where,

$$c_{1i,j} = T_{gxmi+\frac{1}{2},j}, \; c'_{1i,j} = T'_{oxmi+\frac{1}{2},j}$$

$$c_{2i,j} = T_{gxmi-\frac{1}{2},j}, \; c'_{2i,j} = T'_{oxmi-\frac{1}{2},j}$$

$$c_{3i,j} = T_{gymi,j+\frac{1}{2}}, \; c'_{3i,j} = T'_{oymi,j+\frac{1}{2}}$$

$$c_{4i,j} = T_{gymi,j-\frac{1}{2}}, \; c'_{4i,j} = T'_{oymi,j-\frac{1}{2}}$$

$$c_{5i,j} = \left(\frac{S_{om}}{B_{om}} \frac{\partial R_{sm}}{\partial P_{gm}} - \frac{S_{gm}}{B_{gm}^2} \frac{\partial B_{gm}}{\partial P_{gm}} \right)_{i,j} \frac{\phi_m}{\Delta t}, \; c'_{5i,j} = \frac{\phi_m}{\Delta t} \frac{S_{om} R_{sm}}{B_{om}^2} \frac{\partial B_{om}}{\partial P_{om}}$$

$$c_{6i,j} = \frac{A1_{gm}}{\Delta t}, c_{7i,j} = A4_{gmi,j}$$

$$c_{8i,j} = \frac{A3_{gm}}{2\Delta x \Delta t}, \; c_{9i,j} = \frac{A3_{gm}}{2\Delta y \Delta t}$$

$$c_{10i,j} = \frac{A2_{gm}}{\Delta t}$$

$$c_{11i,j} = \frac{\phi_m R_m}{\rho_{gs} \Delta t} - \frac{\phi_m}{\Delta t B_{gm}} - c_{6i,j} p_{cmi,j}, \; c_{12i,j} = -c_{10i,j} p_{cfi,j}$$

$$c_{13i,j} = c_{1i,j} + c_{2i,j} + c_{3i,j} + c_{4i,j} + c_{7i,j} + c_{6i,j} S_{om}$$

$$c_{14i,j} = c_{5i,j} + c_{6i,j} + c'_{5i,j},$$

$$
\begin{aligned}
c_{15i,j} \quad = \quad & c_{1i,j} + c_{2i,j} + c_{3i,j} + c_{4i,j} + c_{5i,j} + c_{6i,j} + c_{7i,j} \\
& + d'_{1i,j} + d'_{2i,j} + d'_{3i,j} + d'_{4i,j} + d'_{5i,j} + d'_{7i,j} \qquad (4.50)
\end{aligned}
$$

Eq. (3.117) (the continuity equation for the oil phase in the matrix) in finite difference discretization is written as:

$$-T_{oxmi+1/2,j} \left(P_{omi+1,j}^{n+1} - P_{omi,j}^{n+1} \right) + T_{oxmi-1/2,j} \left(P_{omi,j}^{n+1} - P_{omi-1,j}^{n+1} \right)$$

$$
\begin{aligned}
-T_{oxmi,j+1/2}\left(P_{omi,j+1}^{n+1}-P_{omi,j}^{n+1}\right)+T_{oxmi,j-1/2}\left(P_{omi,j}^{n+1}-P_{omi,j-1}^{n+1}\right)\\
+\frac{\phi_m S_{om}}{B_{om}^2}\frac{\partial B_{om}}{\partial P_{om}}\frac{P_{om}^{n+1}-P_{om}^{n}}{\Delta t}+\frac{\phi_m}{B_{om}}\frac{S_{om}^{n+1}-S_{om}^{n}}{\Delta t}\\
+A1_{om}\frac{S_{om}}{\Delta t}(P_{om}^{n+1}-P_{om}^{n})+A1_{om}\frac{P_{om}}{\Delta t}(S_{om}^{n+1}-S_{om}^{n})+A1_{om}\frac{S_{gm}}{\Delta t}(P_{gm}^{n+1}-P_{gm}^{n})\\
+A1_{om}\frac{P_{gm}}{\Delta t}(S_{gm}^{n+1}-S_{gm}^{n})+A2_{om}\frac{S_{of}}{\Delta t}(P_{of}^{n+1}-P_{of}^{n})+A2_{om}\frac{P_{of}}{\Delta t}(S_{of}^{n+1}-S_{of}^{n})\\
+A2_{om}\frac{S_{gf}}{\Delta t}(P_{gf}^{n+1}-P_{gf}^{n})+A2_{om}\frac{P_{gf}}{\Delta t}(S_{gf}^{n+1}-S_{gf}^{n})\\
+A3_{om}\left(\frac{u_{i+1,j}^{n+1}-u_{i+1,j}^{n}-u_{i-1,j}^{n+1}+u_{i-1,j}^{n}}{2\Delta x\Delta t}+\frac{v_{i,j+1}^{n+1}-v_{i,j+1}^{n}-v_{i,j-1}^{n+1}+v_{i,j-1}^{n}}{2\Delta y\Delta t}\right)\\
+A4_{om}\left(P_{om}^{n+1}-P_{of}^{n+1}\right)=0
\end{aligned}
\tag{4.51}
$$

where,

$$
A1_{om}=S_{om}\frac{1}{B_{om}}\left[\frac{\alpha_{mf}-\phi}{K_s}\left(\phi_f-1\right)-\phi_m\phi_f C_m\right]
\tag{4.52}
$$

$$
A2_{om}=S_{om}\frac{1}{B_{om}}\left[\frac{\alpha_{mf}-\phi}{K_n s}\left(\phi_f-1\right)+\phi_f\left(1-\phi_f\right)C_f\right]
\tag{4.53}
$$

$$
A3_{om}=\alpha_{mf}\left(1-\phi_f\right)\frac{S_{om}}{B_{om}}
\tag{4.54}
$$

$$
A4_{om}=\frac{\overline{\alpha}k_m k_{rom}}{\mu_{om}B_{om}}
\tag{4.55}
$$

It can be further simplified to:

$$
\begin{aligned}
& d_{15i,j}p_{mi,j}-d_{1i,j}p_{mi+1,j}-d_{2i,j}p_{mi-1,j}-d_{3i,j}p_{mi,j+1}-d_{4i,j}p_{mi,j-1}\\
& +(d_{10i,j}-d_{7i,j})p_{fi,j}+d_{8i,j}u_{i+1,j}-d_{8i,j}u_{i-1,j}+d_{9i,j}v_{i,j+1}\\
& -d_{9i,j}v_{i,j-1}+d_{11i,j}S_{mi,j}+d_{12i,j}S_{fi,j}\\
= & \ d_{14i,j}p_{mi,j}+d_{10i,j}p_{fi,j}+d_{11i,j}S_{mi,j}+d_{12i,j}S_{fi,j}+d_{8i,j}u_{i+1,j}\\
& -d_{8i,j}u_{i-1,j}+d_{9i,j}v_{i,j+1}-d_{9i,j}v_{i,j-1}
\end{aligned}
\tag{4.56}
$$

where,

$$
d_{1i,j}=\frac{k_m}{(\Delta x)^2}\left(\frac{\rho_{om}k_{rom}}{\mu_{om}}\right)_{i+\frac{1}{2},j},\ d_{2i,j}=\frac{k_m}{(\Delta x)^2}\left(\frac{\rho_{om}k_{rom}}{\mu_{om}}\right)_{i-\frac{1}{2},j}
$$

$$
d_{3i,j}=\frac{k_m}{(\Delta y)^2}\left(\frac{\rho_{om}k_{rom}}{\mu_{om}}\right)_{i,j+\frac{1}{2}},\ d_{4i,j}=\frac{k_m}{(\Delta y)^2}\left(\frac{\rho_{om}k_{rom}}{\mu_{om}}\right)_{i,j-\frac{1}{2}}
$$

$$d_{5i,j} = \frac{\phi_m}{B_{om}^2} S_{m_{i,j}} \frac{\partial B_{om}}{\partial P_{om}}$$

$$d_{6i,j} = \frac{1}{\Delta t} \frac{S_{omi,j}}{B_{om}} \left[\frac{\alpha_{mf} - \phi}{K_s} (\phi_f - 1) - \phi_m \phi_f C_m \right]$$

$$d_{7i,j} = \overline{\alpha} k_m \left(\frac{k_{rom}}{\mu_{om} B_{om}} \right)_{i,j}$$

$$d_{8i,j} = \frac{\alpha_{mf}(1-\phi_f)}{2\Delta x \Delta t} \left(\frac{S_m}{B_{om}} \right)_{i,j}, \; d_{9i,j} = \frac{\alpha_{mf}(1-\phi_f)}{2\Delta y \Delta t} \left(\frac{S_m}{B_{om}} \right)_{i,j}$$

$$d_{10i,j} = \frac{1}{\Delta t} \frac{S_{om}}{B_{om}} \left[\frac{\alpha_{mf} - \phi}{K_n s} (\phi_f - 1) + \phi_f (1 - \phi_f) C_f \right]$$

$$d_{11i,j} = \frac{\phi_m}{\Delta t B_{om}} - d_{6i,j} p_{cmi,j}, \; d_{12i,j} = -d_{10i,j} p_{cfi,j}$$

$$d_{13i,j} = d_{1i,j} + d_{2i,j} + d_{3i,j} + d_{4i,j} + d_{7i,j}$$

$$d_{14i,j} = d_{5i,j} + d_{6i,j}, \; d_{15i,j} = d_{13i,j} + d_{14i,j} \tag{4.57}$$

Similarly, Equation (3.102) (the continuity equation for the gas phase in the fracture) becomes:

$$\begin{aligned}
& e_{15i,j} p_{fi,j} - \left(e_{1i,j} + e'_{1i,j} \right) p_{fi+1,j} - \left(e_{2i,j} + e'_{2i,j} \right) p_{fi-1,j} - \left(e_{3i,j} + e'_{3i,j} \right) p_{fi,j+1} \\
& - \left(e_{4i,j} + e'_{4i,j} \right) p_{fi,j-1} + (e_{10i,j} - e_{7i,j} - e'_{7i,j}) p_{mi,j} + e_{8i,j} u_{i+1,j} - e_{8i,j} u_{i-1,j} \\
& + e_{9i,j} v_{i,j+1} - e_{9i,j} v_{i,j-1} + e_{11i,j} S_{fi,j} + e_{12i,j} S_{mi,j} \\
= \; & e_{14i,j} p_{fi,j} + e_{10i,j} p_{mi,j} + e_{11i,j} S_{fi,j} + e_{12i,j} S_{mi,j} + e_{8i,j} u_{i+1,j} - e_{8i,j} u_{i-1,j} \\
& + e_{9i,j} v_{i,j+1} - e_{9i,j} v_{i,j-1} + e_1 P_{cfi+1,j} + e_2 P_{cfi-1,j} + e_3 P_{cfi,j+1} + e_4 P_{cfi,j-1} \\
& - e_{13} P_{cfi,j} + e_7 P_{cmi,j}
\end{aligned} \tag{4.58}$$

where,

$$e_{1i,j} = T_{gxfi+\frac{1}{2},j}, \; e'_{1i,j} = T'_{oxfi+\frac{1}{2},j}$$

$$e_{2i,j} = T_{gxfi-\frac{1}{2},j}, \; e'_{2i,j} = T'_{oxfi-\frac{1}{2},j}$$

$$e_{3i,j} = T_{gyfi,j+\frac{1}{2}}, \; e'_{3i,j} = T'_{oyfi,j+\frac{1}{2}}$$

$$e_{4i,j} = T_{gyfi,j-\frac{1}{2}}, \; e'_{4i,j} = T'_{oyfi,j-\frac{1}{2}}$$

$$e_{5i,j} = \left(\frac{S_{of}}{B_{of}}\frac{\partial R_{sf}}{\partial P_{gf}} - \frac{S_{gf}}{B_{gf}^2}\frac{\partial B_{gf}}{\partial P_{gf}}\right)_{i,j}\frac{\phi_f}{\Delta t},\ e'_{5i,j} = \frac{\phi_f}{\Delta t}\frac{S_{of}R_{sf}}{B_{of}^2}\frac{\partial B_{of}}{\partial P_{of}}$$

$$e_{6i,j} = \frac{A1_{gf}}{\Delta t}, e_{7i,j} = A4_{gfi,j}$$

$$e_{8i,j} = \frac{A3_{gf}}{2\Delta x\Delta t},\ e_{9i,j} = \frac{A3_{gf}}{2\Delta y\Delta t}$$

$$e_{10i,j} = \frac{A2_{gf}}{\Delta t}$$

$$e_{11i,j} = \frac{\phi_f R_f}{\rho_{gs}\Delta t} - \frac{\phi_f}{\Delta t B_{gf}} - e_{6i,j}p_{cfi,j},\ e_{12i,j} = -e_{10i,j}p_{cmi,j}$$

$$e_{13i,j} = e_{1i,j} + e_{2i,j} + e_{3i,j} + e_{4i,j} + e_{7i,j} + e_{6i,j}S_{of}$$

$$e_{14i,j} = e_{5i,j} + e_{6i,j} + e'_{5i,j},$$

$$\begin{aligned} e_{15i,j} &= e_{1i,j} + e_{2i,j} + e_{3i,j} + e_{4i,j} + e_{5i,j} + e_{6i,j} + e_{7i,j} \\ &+ d'_{1i,j} + d'_{2i,j} + d'_{3i,j} + d'_{4i,j} + d'_{5i,j} + d'_{7i,j} \end{aligned} \tag{4.59}$$

Similarly, Equation (3.118) (the continuity equation for the oil phase in the fracture) becomes:

$$\begin{aligned} & f_{15i,j}p_{fi,j} - f_{1i,j}p_{fi+1,j} - f_{2i,j}p_{fi-1,j} - f_{3i,j}p_{fi,j+1} - f_{4i,j}p_{fi,j-1} \\ & +(f_{10i,j} - f_{7i,j})p_{fi,j} + f_{8i,j}u_{i+1,j} - f_{8i,j}u_{i-1,j} + f_{9i,j}v_{i,j+1} \\ & -f_{9i,j}v_{i,j-1} + f_{11i,j}S_{fi,j} + f_{12i,j}S_{fi,j} \\ = \ & f_{14i,j}p_{fi,j} + f_{10i,j}p_{fi,j} + f_{11i,j}S_{fi,j} + f_{12i,j}S_{fi,j} + f_{8i,j}u_{i+1,j} \\ & -f_{8i,j}u_{i-1,j} + f_{9i,j}v_{i,j+1} - f_{9i,j}v_{i,j-1} \end{aligned} \tag{4.60}$$

where,

$$f_{1i,j} = \frac{k_f}{(\Delta x)^2}(\frac{\rho_{of}k_{rof}}{\mu_{of}})_{i+\frac{1}{2},j},\ f_{2i,j} = \frac{k_f}{(\Delta x)^2}(\frac{\rho_{of}k_{rof}}{\mu_{of}})_{i-\frac{1}{2},j}$$

$$f_{3i,j} = \frac{k_f}{(\Delta y)^2}(\frac{\rho_{of}k_{rof}}{\mu_{of}})_{i,j+\frac{1}{2}},\ f_{4i,j} = \frac{k_f}{(\Delta y)^2}(\frac{\rho_{of}k_{rof}}{\mu_{of}})_{i,j-\frac{1}{2}}$$

$$f_{5i,j} = \frac{\phi_f}{B_{of}^2}S_{fi,j}\frac{\partial B_{of}}{\partial P_{of}}$$

$$f_{6i,j} = \frac{1}{\Delta t}\frac{S_{ofi,j}}{B_{of}}\left[\frac{\alpha_{mf}-\phi}{K_s}\left(\phi_f - 1\right) - \phi_f \phi_f C_f\right]$$

$$f_{7i,j} = \overline{\alpha} k_m \left(\frac{k_{rom}}{\mu_{om} B_{om}}\right)_{i,j}$$

$$f_{8i,j} = \frac{\alpha_{mf}(1-\phi_f)}{2\Delta x \Delta t}\left(\frac{S_f}{B_{of}}\right)_{i,j}, \; f_{9i,j} = \frac{\alpha_{mf}(1-\phi_f)}{2\Delta y \Delta t}\left(\frac{S_f}{B_{of}}\right)_{i,j}$$

$$f_{10i,j} = \frac{1}{\Delta t}\frac{S_{of}}{B_{of}}\left[\frac{\alpha_{mf}-\phi}{K_n s}\left(\phi_f - 1\right) + \phi_f\left(1-\phi_f\right)C_f\right]$$

$$f_{11i,j} = \frac{\phi_f}{\Delta t B_{of}} - f_{6i,j} p_{cfi,j}, \; f_{12i,j} = -f_{10i,j} p_{cfi,j}$$

$$f_{13i,j} = f_{1i,j} + f_{2i,j} + f_{3i,j} + f_{4i,j} + f_{7i,j}$$

$$f_{14i,j} = f_{5i,j} + f_{6i,j}, \; f_{15i,j} = f_{13i,j} + f_{14i,j} \tag{4.61}$$

4.4 Solution procedure

Thus, the finite difference scheme results in a system of algebraic equations in the form of:

$$\begin{bmatrix} a_{1,1} & a_{1,2} & \cdots & a_{1,n-1} & a_{1,n} \\ a_{2,1} & a_{2,2} & \cdots & a_{2,n-1} & a_{2,n} \\ \vdots & & \ddots & & \vdots \\ a_{n-1,1} & a_{n-1,2} & \cdots & a_{n-1,n-1} & a_{n-1,n} \\ a_{n,1} & a_{n,2} & \cdots & a_{n,n-1} & a_{n,n} \end{bmatrix} \begin{bmatrix} u_{1,1} \\ \cdot \\ u_{N_x,N_y} \\ v_{1,1} \\ \cdot \\ v_{N_x,N_y} \\ p_{m1,1} \\ \cdot \\ p_{mN_x,N_y} \\ S_{m1,1} \\ \cdot \\ S_{mN_x,N_y} \\ p_{m1,1} \\ \cdot \\ p_{mN_x,N_y} \\ S_{m1,1} \\ \cdot \\ S_{mN_x,N_y} \end{bmatrix} = \begin{bmatrix} b_1 \\ b_2 \\ \vdots \\ b_{n-1} \\ b_n \end{bmatrix} \tag{4.62}$$

where $[a]$ is a matrix of order $n \times n$ with $n = 6N_xN_y$; and, where N_x and N_y are the nodal numbers along the x- and y-directions, respectively. The coefficient $a_{i,j}$ are those associated with the variables in the finite difference equations, which are constants in case of single-phase flow and dependent variables in the case of two-phase flow. Therefore, the system of equations (Eq. (4.62)) is nonlinear for multi-phase flow.

Zenkiewicz (1977) discussed the advantages and disadvantages between the iteration methods and the direct solution methods. The main advantages of using the iteration method are the reduced central memory storage demands and the elimination of the triangular decomposition which is the most costly part of a direct solution. The disadvantages are:

1. The lack of knowledge on how many iterations are necessary to achieve an acceptable solution, often hundreds or thousands of iterations are required;

2. The value of relaxation factor (ω) which can significantly change the convergence, many people continuously change ω during the solution to achieve an optimal value;

3. The method fails on indefinite or unsymmetrical problems;

4. In non-linear problem, or multiple right-hand sides, no advantage (except perhaps the optimum ω value) can be taken of a previous solution process as the whole iteration process must be repeated.

He concluded that the disadvantages usually far outweigh the advantages for iterative method. Therefore, the Gauss-elimination with pivoting, one of the direct solution, is used in this dissertation to obtain the solution to this system of equations, Eq. (4.62).

Chapter 5

Model Validation

One of the vital tasks which must be carried out before applying a newly-developed model to realistic new problems is to verify the correctness of the model. The mathematical formulation developed in Chapter 3, and numerical techniques used to solve the model described in Chapter 4 were verified using known analytical solutions and the finite element model developed by Meng (1998).

5.1 Comparison with Analytical Solution

A one-dimensional consolidation problem was selected to verify the model. The analytical solution, numerical solution and comparison between these two solutions are presented below.

5.1.1 Analytical Solution

One-dimensional consolidation problems are characterized by only one non-zero normal strain and by field quantities varying only in that direction. Assuming ε_{xx} to be the non-zero strain, the poroelastic constitutive equations are then:

$$\sigma_{xx} = \frac{2G(1-\nu)}{1-2\nu}\varepsilon_{xx} - \alpha p \tag{5.1}$$

$$\sigma_{yy} = \sigma_{zz} = \frac{\nu}{1-\nu}\sigma_{xx} - 2\eta p \tag{5.2}$$

where η is the poroelastic constant. By expressing ε_{xx} in terms of p and σ_{xx} using Eq. (5.1), the diffusion equation for the pore pressure can be written as:

$$\frac{\partial p}{\partial t} - c\frac{\partial^2 p}{\partial x^2} = -\frac{B(1+\nu_u)}{3(1-\nu)}\frac{d\sigma_{xx}}{dt} \tag{5.3}$$

For a constant axial load, σ_{xx}, the right-hand side of Eq. (5.3) drops out to give a homogeneous diffusion equation:

$$\frac{\partial p}{\partial t} - c\frac{\partial^2 p}{\partial x^2} = 0 \tag{5.4}$$

The above differential equation is subjected to the following boundary and initial conditions:

Boundary conditions:

$$p = 0 \text{ at } x = 0 \tag{5.5}$$

$$\frac{\partial p}{\partial x} = 0 \text{ at } x = L \tag{5.6}$$

Initial condition:

$$p_0 = -\frac{B(1+\nu_u)}{3(1-\nu)}\sigma_{xx} \tag{5.7}$$

Then the solution for the pore pressure is:

$$p(x,t) = p_0 \sum_{m=1,3,\cdots}^{\infty} \frac{4}{m\pi} \sin\left(\frac{m\pi x}{2L}\right) \exp\left(-\frac{m^2\pi^2 ct}{4L^2}\right) \tag{5.8}$$

The differential equation for the displacements, u_x, is deduced from Eq. (5.1), by expressing ε_{xx} as $\partial u_x/\partial x$:

$$\frac{2G(1-\nu)}{1-2\nu}\frac{\partial^2 u_x}{\partial x^2} - \alpha\frac{\partial p}{\partial x} = 0 \tag{5.9}$$

subject to the following boundary condition:

$$u_x = 0 \text{ at } x = L \tag{5.10}$$

The solution to this equation is:

$$u_x = u_x^0 + \Delta u_x \tag{5.11}$$

where u_x^0 is calculated by:

$$u_x^0 = -\frac{\sigma_{xx} L(1-2\nu_u)}{2G(1-\nu_u)}\left(1-\frac{x}{L}\right) \tag{5.12}$$

while Δu_x is calculated by:

$$\Delta u_x = -\frac{\sigma_{xx} L(\nu_u - \nu)}{2G(1-\nu)(1-\nu_u)} F(x,t) \tag{5.13}$$

where,

$$F(x,t) = \frac{8}{\pi^2}\sum_{m=1,3,\cdots}^{\infty}\frac{1}{m^2}\cos\left(\frac{m\pi x}{2L}\right)\left[1-\exp\left(-\frac{m^2\pi^2 ct}{4L^2}\right)\right] \tag{5.14}$$

The following equations are needed to calculate B, ν_u, k_u (Detournay and Cheng, 1993):

$$B = \frac{\alpha k_f}{[\alpha - \phi(1-\alpha)]\, k_f + \phi k} \tag{5.15}$$

$$\nu_u = \frac{3k_u - 2G}{2(3k_u + G)} \tag{5.16}$$

$$k_u = k\left[1 + \frac{\alpha^2 k_f}{(1-\alpha)(\alpha-\phi)\, k_f + \phi k}\right] \tag{5.17}$$

where k_f is the fluid compressibility.

The diffusivity coefficient c is given by (Chen, 1996):

$$c = \frac{2G(1-\nu)(\nu_u - \nu)\,\kappa}{\alpha^2(1-2\nu)^2(1-\nu_u)} \tag{5.18}$$

where $\kappa = \frac{k}{\mu}$.

The parameters used for this comparison are listed in Table 5.1.

5.1.2 Numerical Solution

The 2-D, two-phase model developed in this dissertation may, of course, be used to simulate one-dimensional, single-phase consolidation problems.

Table 5.1: Parameters Used in the Comparison

Parameters	Definition	Magnitude	Units
E	modulus of elasticity	3000	MPa
ν	Poisson's ratio	0.2	
k	rock permeability	1.974×10^{-14}	m^2
k_f	fluid compressibility	1.0×10^{-4}	1/MPa
K_s	solid grain bulk modulus	11244	MPa
ϕ	rock porosity	0.2	
μ	fluid viscosity	1.0×10^{-3}	Pa·s
σ	loading stress	2.0	MPa

Initial and Boundary Conditions

Consider a water-saturated column which is suddenly loaded. The fluid in the column is allowed to drain only from the top surface, while all other three surfaces are no-flow boundaries. The axial stress, σ, is a step function applied instantaneously. The initial and boundary conditions needed for modeling this one-dimensional , single-phase consolidation problem are given in Figures 5.1 and 5.2. The discretized domain for the finite difference scheme is shown in Figure 5.3. Only half of original domain is selected for calculations due to the symmetry.

Interior Points

For points within the grid, the six governing equations for solid deformations and two-phase fluid flow in the matrix and in the fractures have already been obtained in finite difference form, i.e., Eqs. (4.14), (4.16), (4.31), (4.33), (4.35), (4.37).

Boundary and Corner Points

However, at the boundaries and at the corners, these six equations have to be rearranged and the following approximation are applied based on the boundary conditions specified:

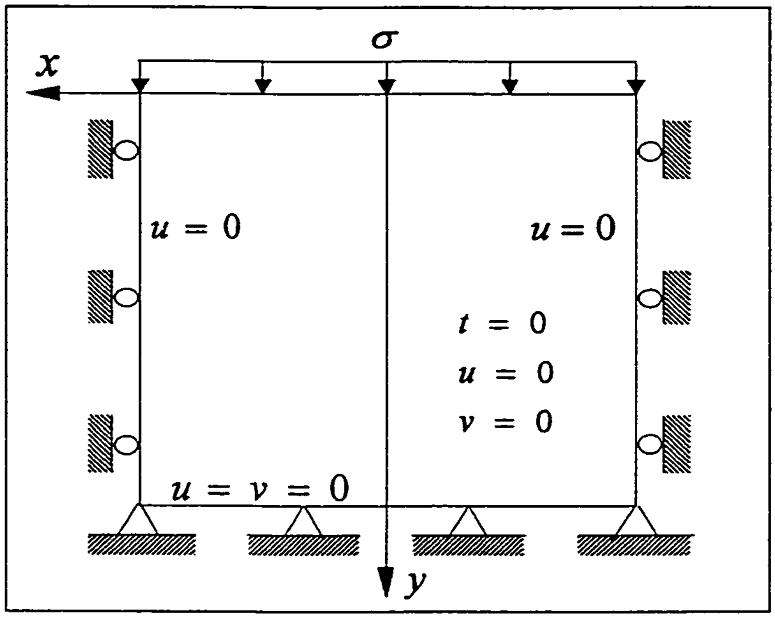

Figure 5.1: Mechanical Boundary and Initial Conditions.

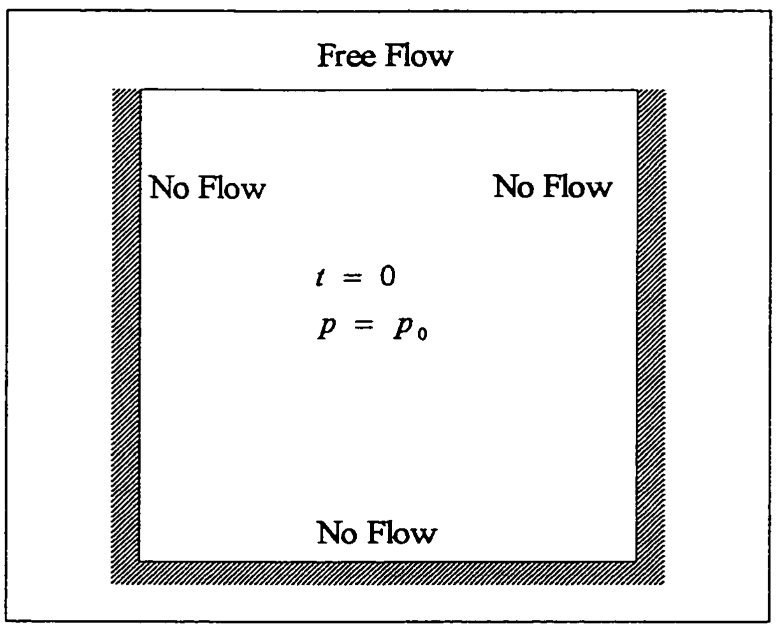

Figure 5.2: Fluid Flow Boundary and Initial Conditions.

- Boundary $i = 1$ (Symmetry line)

$$u_{i-1,j} = u_{i+1,j} \tag{5.19}$$

$$v_{i-1,j} = -v_{i+1,j} \tag{5.20}$$

$$p_{mi-1,j} = p_{mi+1,j} \tag{5.21}$$

$$p_{fi-1,j} = p_{fi+1,j} \tag{5.22}$$

- Boundary $i = N_x$ ($u = 0$ and no flow)

$$u_{i+1,j} = -u_{i-1,j} \tag{5.23}$$

$$v_{i+1,j} = 2v_{i,j} - v_{i-1,j} \tag{5.24}$$

$$p_{mi+1,j} = p_{mi-1,j} \tag{5.25}$$

$$p_{fi+1,j} = p_{fi-1,j} \tag{5.26}$$

- Boundary $j = 1$ (loading stress boundary and open flow)

$$u_{i,j-1} = 2u_{i,j} - u_{i,j+1} \tag{5.27}$$

$$v_{i,j-1} = v_{i,j+1} - 2\Delta y \frac{\sigma}{(\lambda + 2G)} \tag{5.28}$$

$$p_{mi,j-1} = p_{mi,j+1} \tag{5.29}$$

$$p_{fi,j-1} = p_{fi,j+1} \tag{5.30}$$

- Boundary $j = N_y$ ($u = v = 0$ and no flow)

$$u_{i,j+1} = -u_{i,j-1} \tag{5.31}$$

$$v_{i,j+1} = -v_{i,j-1} \tag{5.32}$$

$$p_{mi,j+1} = p_{mi,j-1} \tag{5.33}$$

$$p_{fi,j+1} = p_{fi,j-1} \tag{5.34}$$

- Corner $i = 1$, $j = 1$

$$u_{i-1,j+1} = u_{i+1,j+1} \tag{5.35}$$

$$u_{i-1,j} = u_{i+1,j} \tag{5.36}$$

$$u_{i-1,j-1} = 2u_{i+1,j} - u_{i+1,j+1} \tag{5.37}$$

$$u_{i+1,j-1} = 2u_{i+1,j} - u_{i+1,j+1} \tag{5.38}$$

$$u_{i,j-1} = 2u_{i,j} - u_{i,j+1} \tag{5.39}$$

$$v_{i-1,j+1} = v_{i+1,j+1} \tag{5.40}$$

$$v_{i-1,j} = v_{i+1,j} \tag{5.41}$$

$$v_{i-1,j-1} = 2v_{i+1,j} - v_{i+1,j+1} \tag{5.42}$$

$$v_{i+1,j-1} = v_{i+1,j+1} - 2\Delta y \frac{\sigma}{(\lambda + 2G)} \tag{5.43}$$

$$v_{i,j-1} = v_{i,j+1} - 2\Delta y \frac{\sigma}{(\lambda + 2G)} \tag{5.44}$$

$$p_{mi-1,j} = p_{mi+1,j} \tag{5.45}$$

$$p_{mi,j-1} = -p_{mi,j+1} \tag{5.46}$$

$$p_{fi-1,j} = p_{fi+1,j} \tag{5.47}$$

$$p_{fi,j-1} = -p_{fi,j+1} \tag{5.48}$$

- Corner $i = N_x$, $j = 1$

$$u_{i+1,j+1} = -u_{i-1,j+1} \tag{5.49}$$

$$u_{i+1,j} = -u_{i-1,j} \tag{5.50}$$

$$u_{i+1,j-1} = -2u_{i-1,j} + u_{i-1,j+1} \tag{5.51}$$

$$u_{i,j-1} = 2u_{i,j} - u_{i,j+1} \tag{5.52}$$

$$u_{i-1,j-1} = 2u_{i-1,j} - u_{i-1,j+1} \tag{5.53}$$

$$v_{i+1,j+1} = 2v_{i,j+1} - v_{i-1,j+1} \tag{5.54}$$

$$v_{i+1,j} = 2v_{i,j} - v_{i-1,j} \tag{5.55}$$

$$v_{i+1,j-1} = 4v_{i,j} - 2v_{i-1,j} - 2v_{i,j+1} + v_{i-1,j+1} \tag{5.56}$$

$$v_{i,j-1} = v_{i,j+1} - 2\Delta y \frac{\sigma}{(\lambda + 2G)} \tag{5.57}$$

$$v_{i-1,j-1} = v_{i-1,j+1} - 2\Delta y \frac{\sigma}{(\lambda + 2G)} \tag{5.58}$$

$$p_{mi+1,j} = p_{mi-1,j} \tag{5.59}$$

$$p_{mi,j-1} = -p_{mi,j+1} \tag{5.60}$$

$$p_{fi+1,j} = p_{fi-1,j} \tag{5.61}$$

$$p_{fi,j-1} = -p_{fi,j+1} \tag{5.62}$$

- Corner $i = 1$, $j = N_y$

$$u_{i-1,j-1} = u_{i+1,j-1} \tag{5.63}$$

$$u_{i-1,j} = u_{i+1,j} \tag{5.64}$$

$$u_{i-1,j+1} = -u_{i+1,j-1} \tag{5.65}$$

$$u_{i,j+1} = -u_{i,j-1} \tag{5.66}$$

$$u_{i+1,j+1} = -u_{i+1,j-1} \tag{5.67}$$

$$v_{i-1,j-1} = v_{i+1,j-1} \tag{5.68}$$

$$v_{i-1,j} = v_{i+1,j} \tag{5.69}$$

$$v_{i-1,j+1} = 2v_{i+1,j} - v_{i+1,j-1} \tag{5.70}$$

$$v_{i,j+1} = -v_{i,j-1} \tag{5.71}$$

$$v_{i+1,j+1} = -v_{i+1,j-1} \tag{5.72}$$

$$p_{mi-1,j} = p_{mi+1,j} \tag{5.73}$$

$$p_{mi,j+1} = -p_{mi,j-1} \tag{5.74}$$

$$p_{fi-1,j} = p_{fi+1,j} \tag{5.75}$$

$$p_{fi,j+1} = -p_{fi,j-1} \tag{5.76}$$

- Corner $i = N_x;\ j = N_y$

$$u_{i+1,j-1} = -u_{i-1,j-1} \tag{5.77}$$

$$u_{i+1,j} = -u_{i-1,j} \tag{5.78}$$

$$u_{i+1,j+1} = -2u_{i-1,j} + u_{i-1,j-1} \tag{5.79}$$

$$u_{i,j+1} = -u_{i,j-1} \tag{5.80}$$

$$u_{i-1,j+1} = -u_{i-1,j-1} \tag{5.81}$$

$$v_{i+1,j-1} = 2v_{i,j-1} - v_{i-1,j-1} \tag{5.82}$$

$$v_{i+1,j} = -v_{i-1,j} \tag{5.83}$$

$$v_{i+1,j+1} = -2v_{i-1,j} - 2v_{i,j-1} + v_{i-1,j-1} \tag{5.84}$$

$$v_{i,j+1} = -v_{i,j-1} \tag{5.85}$$

$$v_{i-1,j+1} = -v_{i-1,j-1} \tag{5.86}$$

$$p_{mi+1,j} = p_{mi-1,j} \tag{5.87}$$

$$p_{mi,j+1} = p_{mi,j-1} \tag{5.88}$$

$$p_{fi+1,j} = p_{fi-1,j} \tag{5.89}$$

$$p_{fi,j+1} = p_{fi,j-1} \tag{5.90}$$

Substituting all of these boundary approximations into the six governing Eqs. (4.14), (4.16), (4.31), (4.33), (4.35), and (4.37) yields 6 (number of equations)$\times$8(four boundaries plus four corners) = 48 equations for boundaries and corner points and are listed in the enclosed Appendix B Case 1.

Comparison of Results

Comparison of excess pore pressure along the column depth at different times between the analytical and numerical solutions are shown in Figures 5.4 and 5.5. The evolution of displacements with time, considering two different positions in the column (top and center) , can be determined and excellent agreement is obtained, as shown in Figure 5.6.

5.2 Comparison with a Finite Element Model

Parallel to present study, Meng et al. (1998) and Meng (1998) developed a similar two-phase model for deforming fractured reservoirs and solved it using the finite element method. Meng (1998) compared the results from his model with the results calculated using the present finite difference model and concluded that results from these two models are very similar except for a small difference at early times.

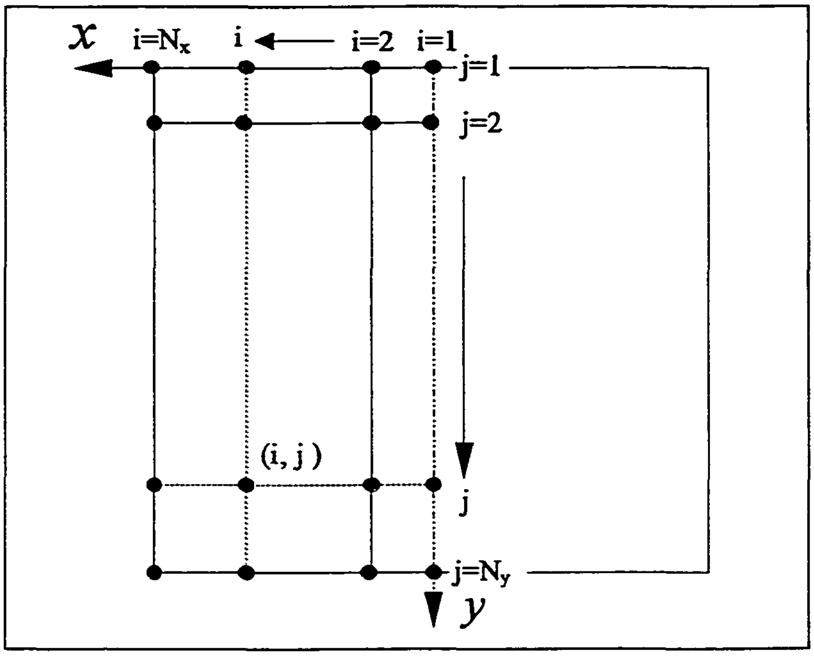

Figure 5.3: Finite Difference Discretized Domain.

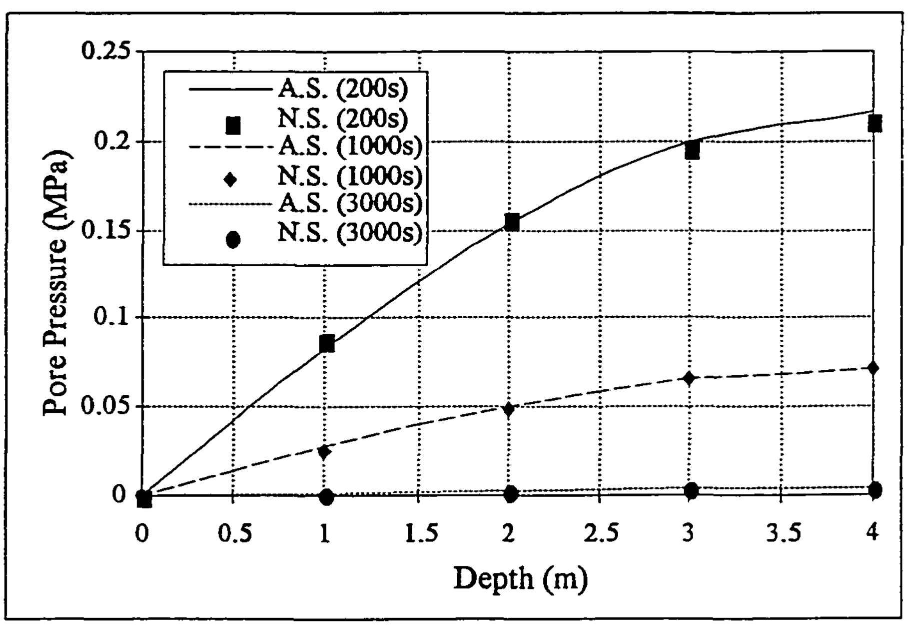

Figure 5.4: Analytical Vs. Numerical Solutions for Pore Pressure.

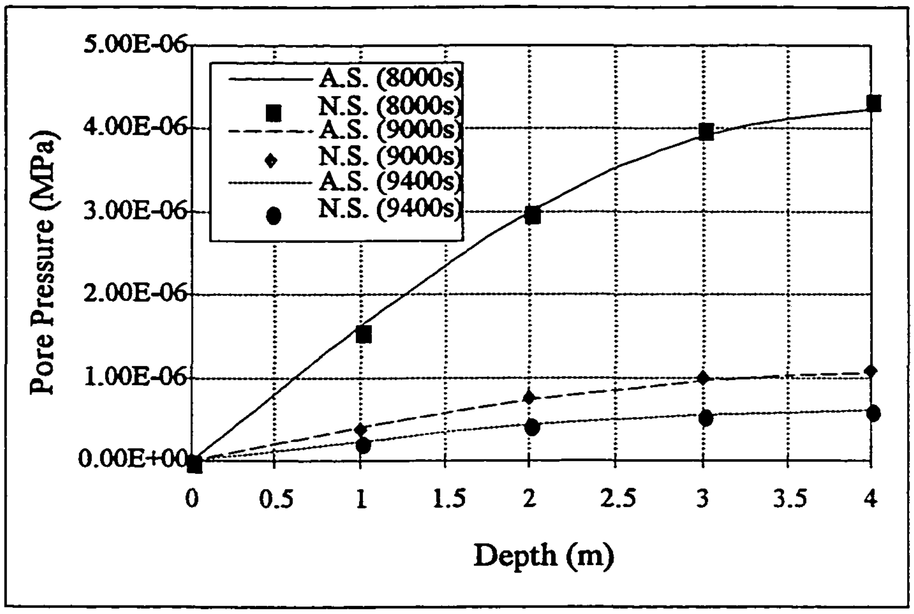

Figure 5.5: Analytical Vs. Numerical Solutions for Pore Pressure.

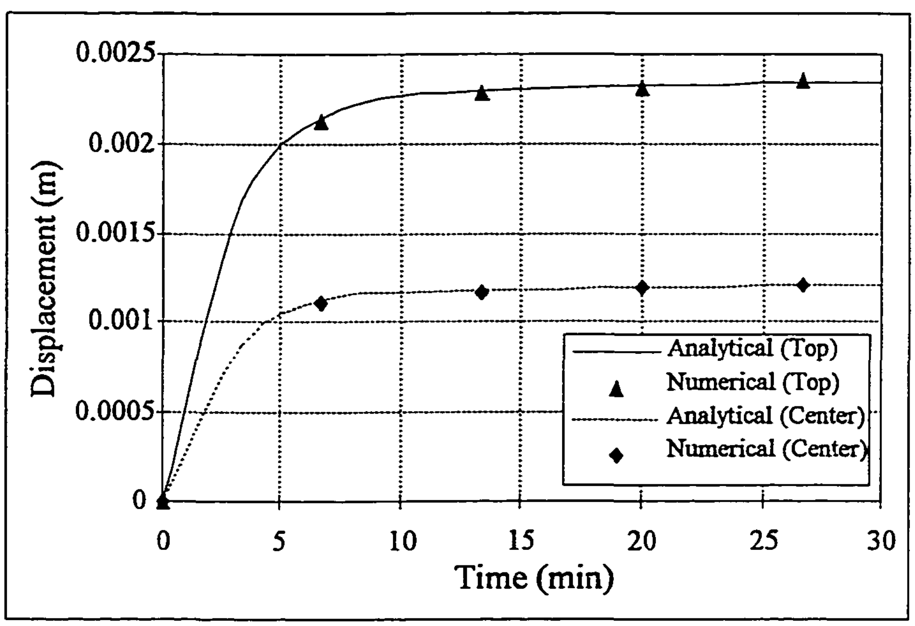

Figure 5.6: Analytical Vs. Numerical Solutions for Displacements.

Chapter 6

Model Applications

The capabilities of the model and the simulator, RFIA (Rock Fluid InterAction), developed in the foregoing chapters have been demonstrated in the following two example problems. First, two-phase flow coupled with solid deformations was considered in a fractured rock for the column problem. Second, a deformable fractured reservoir with a water injection well and an oil production well was investigated. The effect of stress on oil saturation and pressure distributions was studied.

6.1 Two-Phase Flow Coupled with Fractured Rock Consolidation

The column consolidation problem presented in Chapter 6 will be reexamined for modeling the process of simultaneous two-phase flow and solid deformations. The initial and boundary conditions for fluid flow and solid deformations are identical to those shown in Figure 5.1 and 5.2, except that the initial saturations for water and oil are 0.35 and 0.65, respectively. The relative permeability data used in this case are shown in Table 6.1

The following expression is adopted for the capillary pressure-saturation curve

(Dagger, 1997):

$$P_c = \frac{13.159 - 10.8459 S_w}{1 + 3.6262 S_w} \times 6.98 \times 10^{-3} \text{ (MPa)} \tag{6.1}$$

Table 6.1: Relative Permeabilities Data

Water satua. S_w	Oil rel. perm. k_{ro}	Water rel. perm. k_{rw}
0	1	0
0.1	1	0
0.2	1	0
0.3	0.761	0.002
0.4	0.479	0.016
0.5	0.290	0.052
0.6	0.148	0.125
0.7	0.053	0.244
0.8	0.006	0.422
0.9	0	0.670

The parameters used in this case are listed in Table 6.2.

Table 6.2: Parameters Used in the Consolidation Case

Parameters	Definition	Magnitude	Units
E	modulus of elasticity	3000	MPa
ν	Poisson's ratio	0.2	
$\overline{\alpha}$	transfer coefficient	1000	$1/m^2$
k_m	matrix permeability	3.0×10^{-14}	m^2
k_f	fracture permeability	3.0×10^{-12}	m^2
K_s	solid grain bulk modulus	11244	MPa
ϕ_m	matrix porosity	0.2	
ϕ_f	fracture porosity	0.05	
μ_o	oil viscosity	2.0×10^{-3}	Pa·s
μ_w	water viscosity	1.0×10^{-3}	Pa·s
c_o	oil compressibility	1.88×10^{-3}	1/MPa
c_w	water compressibility	4.55×10^{-4}	1/MPa
σ	loading stress	2.0	MPa

Figures 6.1 shows the vertical displacement along the height of the column at

different times after initial loading. It can be seen that the displacements are positively proportional to the time with the largest displacement occurring along the column surface. Figure 6.2 depicts the temporal vertical displacements on the surface and in the middle of the column. The increase of the displacements is also the result of the time increase.

Figures 6.3 and 6.4 illustrate the spatial distributions of the oil-phase pressures along the column at different times for the matrix and for the fractures. In comparison, the pressure in the matrix is larger than that in the fractures. At early times (t=10 sec.), the rate change of the matrix pressure appears to be greater than in the fractures. For the latter, the pressure change is almost linear.

The changes in oil saturations along the column at different times in the matrix and in the fractures are shown in Figures 6.5 and 6.6, respectively. It is of interest to note that the oil saturation for a given depth decreases with time in the matrix while it increases in the fractures because of the mechanism that oil transfers from matrix to fractures.

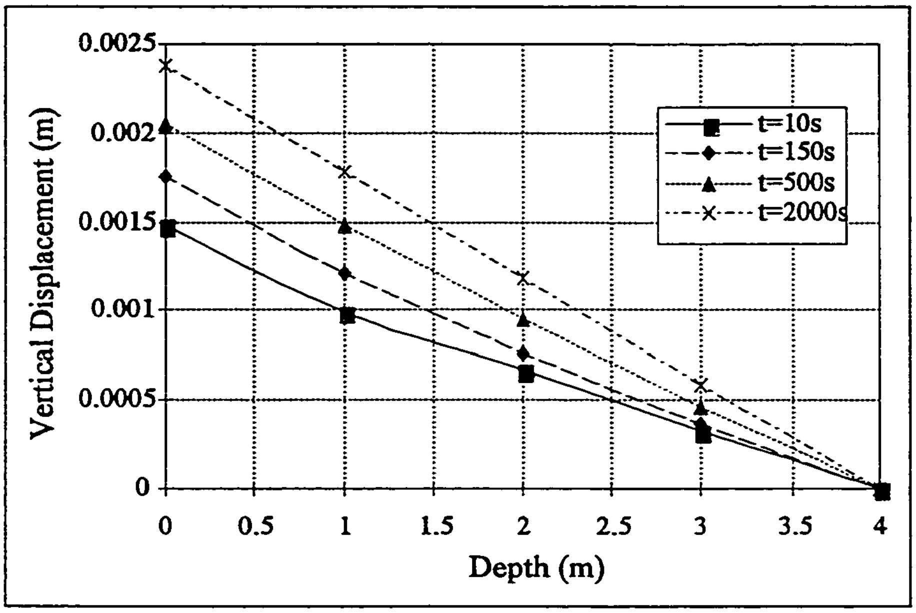

Figure 6.1: Vertical Displacements Vs. Depth.

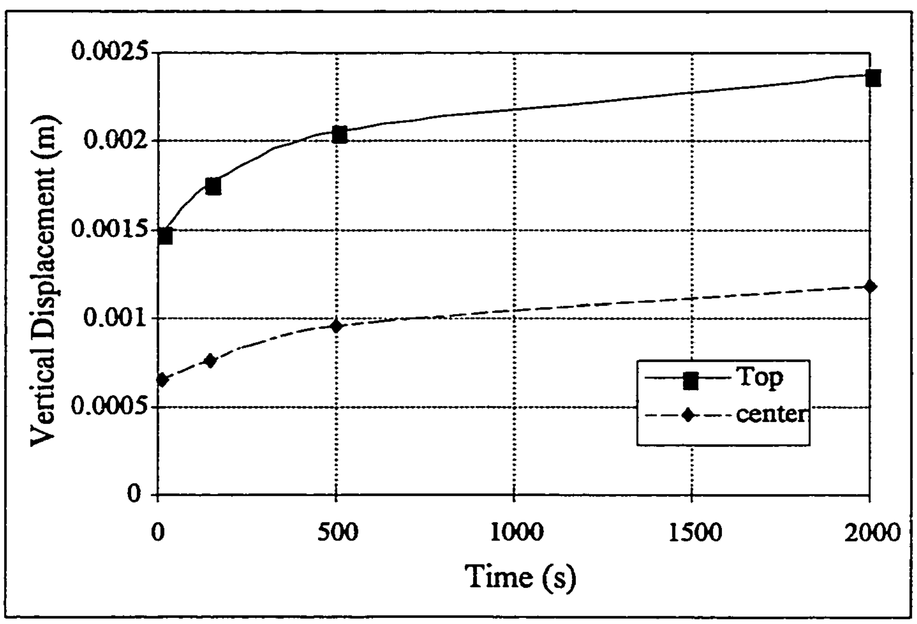

Figure 6.2: Vertical Displacements Vs. Time.

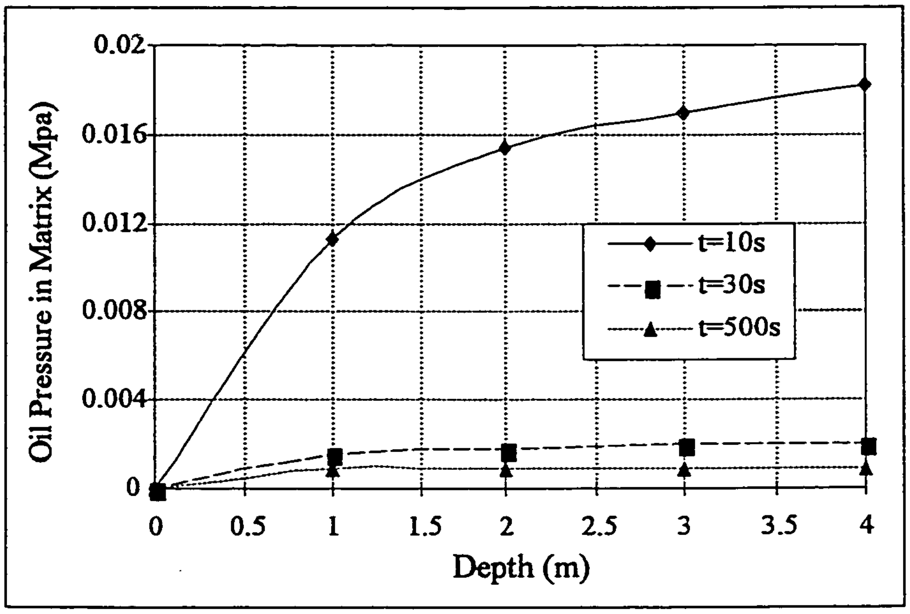

Figure 6.3: Oil Pressure Changes along Depth for Matrix.

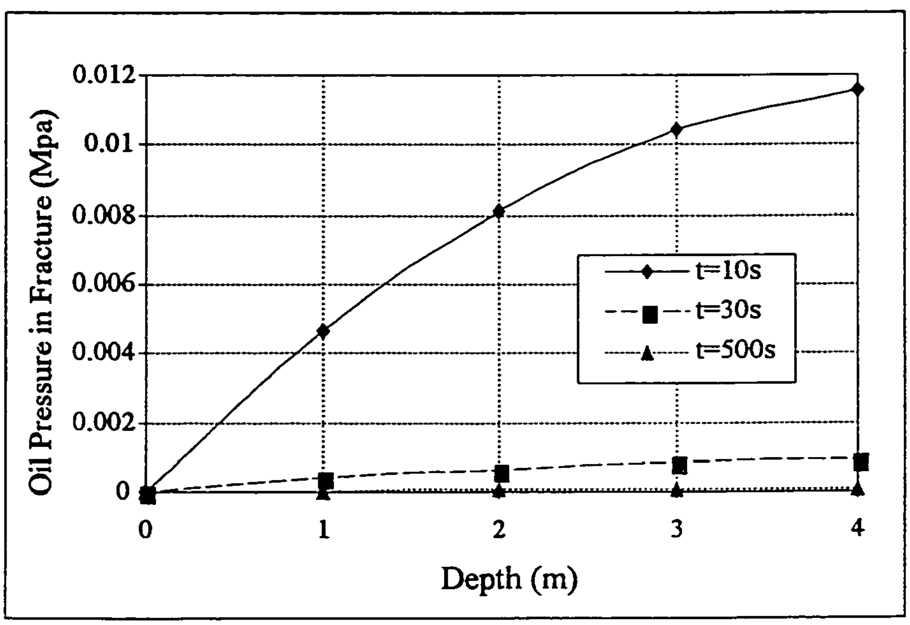

Figure 6.4: Oil Pressure Changes along Depth for Fractures.

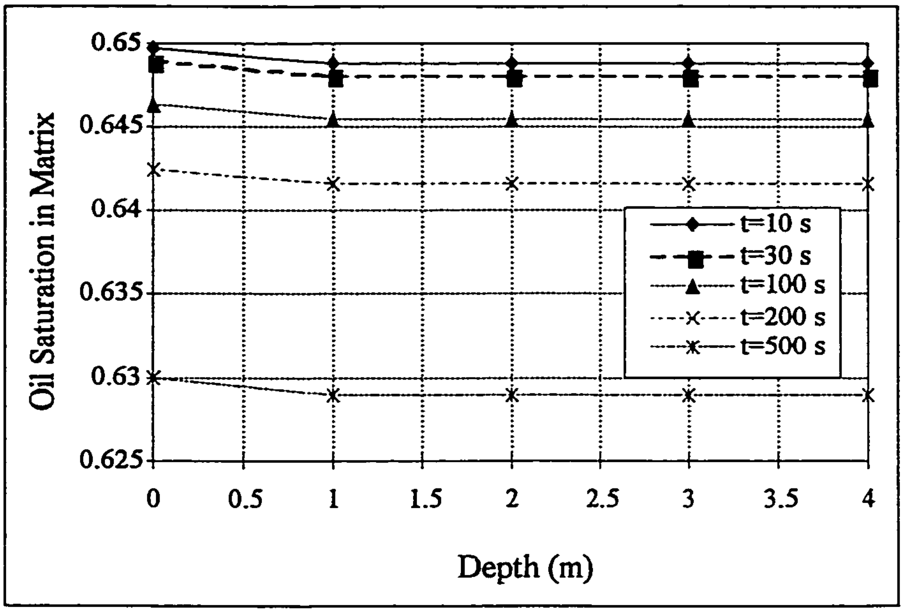

Figure 6.5: Oil Saturation Changes along Depth for Matrix.

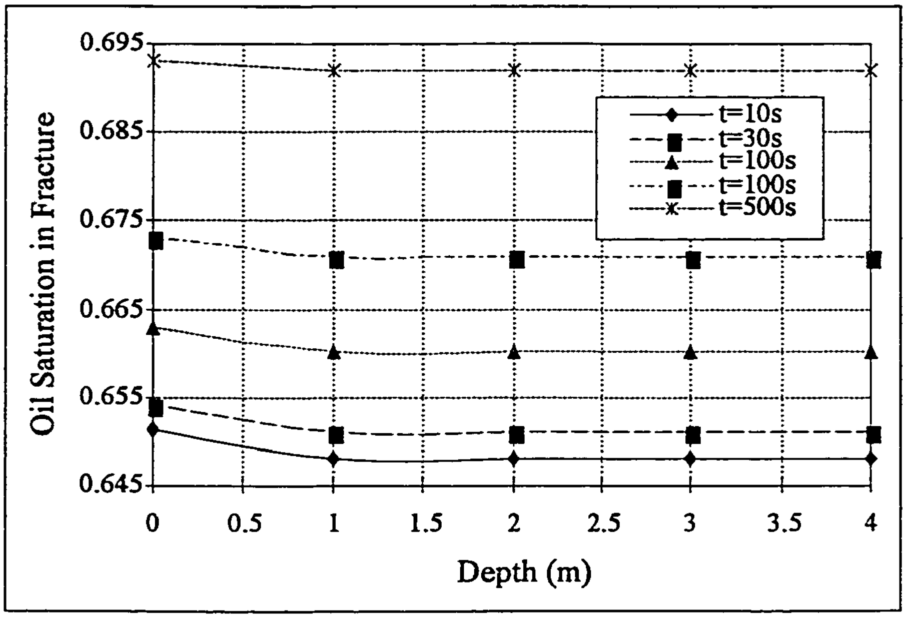

Figure 6.6: Oil Saturation Changes along Depth for Fractures.

6.2 Oil Production from a Deformable Fractured Reservoir with Water Injection

Many different techniques have been applied in reservoir operations to increase the oil production rate. Most common among such production enhancement techniques is waterflooding in which water is injected into the reservoir from different locations than those of hydrocarbon withdrawing boreholes. In the U.S. as much as half of the current oil production is thought to be the result of water injection.

In addition to increasing the output of hydrocarbon, water injection leads to an increase in pore pressure inside the reservoir and the consequent decrease in effective stress on the rock matrix. As a result, compaction of the reservoir and the associated harmful effects are also restrained to some extent.

Both experimental work and numerical simulations indicate that high porosity, weakly- to un-consolidated reservoirs can undergo irreversible deformations or pore collapse beyond a critical effective stress, due to production of hydrocarbons. These pore collapse-related compaction and subsidence problems have been studied conventionally without coupling, where fluid flow and rock deformations are calculated in a staggered manner (Finol and Ali, 1975; Merle *et al.*, 1976; Boade, 1989; Chin and Boade, 1990; Chin *et al.*, 1993; Jones and Mathiesen, 1993). The pore pressures are first calculated using a reservoir simulator which considers just fluid flow or accounts for rock mechanics with rock compressibility as the only parameter. Once the changes in pore pressure distribution are known, the corresponding load vectors and displacements are evaluated using a stress-strain code.

Withdrawing fluids from a reservoir results in an increase in effective stress whereas enhancing oil recovery techniques such as water injection lead to a decrease in effective stress on the reservoir rock matrix. These processes, when implemented in a sequence, introduce a number of loading cycles. The distribution of pore pressure changes due to these processes can be evaluated using the Rock Fluid InterAction simulator, RFIA, developed in this dissertation.

6.2.1 Description of the case studied

A hypothetical example was set up to show that the model can give insights into the effects of stress on the distributions of oil saturation and pressure in a water injection, fractured, deformable reservoir (Figure 6.7). The reservoir size is 200m by 200m in two dimensions. The upper and right sides are subject to a loading stress σ. The left and bottom sides can only move in the y- and x-directions, respectively. Figure 6.8 shows the mechanical boundary conditions. There is no drainage on all boundaries, except two wells at two corners, an oil production well and a water injection well, respectively. The rates for these two wells are given and the parameters used in this case are listed in Table 6.3.

Table 6.3: Parameters Used in the Oil Production Case

Parameters	Definition	Magnitude	Units
E	modulus of elasticity	3000	MPa
ν	Poisson's ratio	0.2	
$\overline{\alpha}$	transfer coefficient	1000	$1/m^2$
k_m	matrix permeability	2.8×10^{-15}	m^2
k_f	fracture permeability	2.8×10^{-13}	m^2
K_s	solid grain bulk modulus	11244	MPa
ϕ_m	matrix porosity	0.2	
ϕ_f	fracture porosity	0.05	
μ_o	oil viscosity	2.0×10^{-3}	Pa·s
μ_w	water viscosity	1.0×10^{-3}	Pa·s
c_o	oil compressibility	1.88×10^{-3}	1/MPa
c_w	water compressibility	4.55×10^{-4}	1/MPa
σ	loading stress	4.0	MPa

6.2.2 Approximation of Boundary Conditions for Boundaries and Corner Points

The six governing equations have to be rearranged and the following approximations were applied based on the boundary conditions specified as in the previous validation case:

- Boundary $i = 1$ (no flow with loading stress σ)

$$u_{i-1,j} = u_{i+1,j} - 2\Delta x \frac{\sigma}{(\lambda + 2G)} \tag{6.2}$$

$$v_{i-1,j} = 2v_{i,j} - v_{i+1,j} \tag{6.3}$$

$$p_{mi-1,j} = p_{mi+1,j} \tag{6.4}$$

$$p_{fi-1,j} = p_{fi+1,j} \tag{6.5}$$

- Boundary $i = N_x$ ($u = 0$ and no flow)

$$u_{i+1,j} = -u_{i-1,j} \tag{6.6}$$

$$v_{i+1,j} = 2v_{i,j} - v_{i-1,j} \tag{6.7}$$

$$p_{mi+1,j} = p_{mi-1,j} \tag{6.8}$$

$$p_{fi+1,j} = p_{fi-1,j} \tag{6.9}$$

- Boundary $j = 1$ (no flow with loading stress σ)

$$u_{i,j-1} = 2u_{i,j} - u_{i,j+1} \tag{6.10}$$

$$v_{i,j-1} = v_{i,j+1} - 2\Delta y \frac{\sigma}{(\lambda + 2G)} \tag{6.11}$$

$$p_{mi,j-1} = p_{mi,j+1} \tag{6.12}$$

$$p_{fi,j-1} = p_{fi,j+1} \tag{6.13}$$

- Boundary $j = N_y$ ($v = 0$ and no flow)

$$u_{i,j+1} = u_{i,j-1} \tag{6.14}$$

$$v_{i,j+1} = -v_{i,j-1} \tag{6.15}$$

$$p_{mi,j+1} = p_{mi,j-1} \tag{6.16}$$

$$p_{fi,j+1} = p_{fi,j-1} \tag{6.17}$$

- Corner $i = 1,\ j = 1$

$$u_{i-1,j+1} = u_{i+1,j+1} - 2\Delta x \frac{\sigma}{(\lambda + 2G)} \tag{6.18}$$

$$u_{i-1,j} = u_{i+1,j} - 2\Delta x \frac{\sigma}{(\lambda + 2G)} \tag{6.19}$$

$$u_{i-1,j-1} = 2u_{i+1,j} - u_{i+1,j+1} - 2\Delta x \frac{\sigma}{(\lambda + 2G)} \tag{6.20}$$

$$u_{i+1,j-1} = 2u_{i+1,j} - u_{i+1,j+1} \tag{6.21}$$

$$u_{i,j-1} = 2u_{i,j} - u_{i,j+1} \tag{6.22}$$

$$v_{i-1,j+1} = 2v_{i,j+1} - v_{i+1,j+1} \tag{6.23}$$

$$v_{i-1,j} = 2v_{i,j} - v_{i+1,j} \tag{6.24}$$

$$v_{i-1,j-1} = 2v_{i,j+1} - v_{i+1,j+1} - 2\Delta y \frac{\sigma}{(\lambda + 2G)} \tag{6.25}$$

$$v_{i+1,j-1} = v_{i+1,j+1} - 2\Delta y \frac{\sigma}{(\lambda + 2G)} \tag{6.26}$$

$$v_{i,j-1} = v_{i,j+1} - 2\Delta y \frac{\sigma}{(\lambda + 2G)} \tag{6.27}$$

$$p_{mi-1,j} = p_{mi+1,j} \tag{6.28}$$

$$p_{mi,j-1} = p_{mi,j+1} \tag{6.29}$$

$$p_{fi-1,j} = p_{fi+1,j} \tag{6.30}$$

$$p_{fi,j-1} = p_{fi,j+1} \tag{6.31}$$

- Corner $i = N_x$, $j = 1$

$$u_{i+1,j+1} = -u_{i-1,j+1} \tag{6.32}$$

$$u_{i+1,j} = -u_{i-1,j} \tag{6.33}$$

$$u_{i+1,j-1} = -2u_{i-1,j} + u_{i-1,j+1} \tag{6.34}$$

$$u_{i,j-1} = 2u_{i,j} - u_{i,j+1} \tag{6.35}$$

$$u_{i-1,j-1} = 2u_{i-1,j} - u_{i-1,j+1} \tag{6.36}$$

$$v_{i+1,j+1} = v_{i-1,j+1} \tag{6.37}$$

$$v_{i+1,j} = v_{i-1,j} \tag{6.38}$$

$$v_{i+1,j-1} = v_{i-1,j-1} \tag{6.39}$$

$$v_{i,j-1} = v_{i,j+1} - 2\Delta y \frac{\sigma}{(\lambda + 2G)} \tag{6.40}$$

$$v_{i-1,j-1} = v_{i-1,j+1} - 2\Delta y \frac{\sigma}{(\lambda + 2G)} \tag{6.41}$$

$$p_{mi+1,j} = p_{mi-1,j} \tag{6.42}$$

$$p_{mi,j-1} = p_{mi,j+1} \tag{6.43}$$

$$p_{fi+1,j} = p_{fi-1,j} \tag{6.44}$$

$$p_{fi,j-1} = p_{fi,j+1} \tag{6.45}$$

- Corner $i = 1$, $j = N_y$

$$u_{i-1,j-1} = u_{i+1,j-1} - 2\Delta x \frac{\sigma}{(\lambda + 2G)} \tag{6.46}$$

$$u_{i-1,j} = u_{i+1,j} - 2\Delta x \frac{\sigma}{(\lambda + 2G)} \tag{6.47}$$

$$u_{i-1,j+1} = u_{i+1,j-1} - 2\Delta x \frac{\sigma}{(\lambda + 2G)} \tag{6.48}$$

$$u_{i,j+1} = u_{i,j-1} \tag{6.49}$$

$$u_{i+1,j+1} = u_{i+1,j-1} \tag{6.50}$$

$$v_{i-1,j-1} = 2v_{i,j-1} - v_{i+1,j-1} \tag{6.51}$$

$$v_{i-1,j} = 2v_{i,j} - v_{i+1,j} \tag{6.52}$$

$$v_{i-1,j+1} = -2v_{i,j-1} + v_{i+1,j-1} \tag{6.53}$$

$$v_{i,j+1} = -v_{i,j-1} \tag{6.54}$$

$$v_{i+1,j+1} = -v_{i+1,j-1} \tag{6.55}$$

$$p_{mi-1,j} = p_{mi+1,j} \tag{6.56}$$

$$p_{mi,j+1} = p_{mi,j-1} \tag{6.57}$$

$$p_{fi-1,j} = p_{fi+1,j} \tag{6.58}$$

$$p_{fi,j+1} = p_{fi,j-1} \tag{6.59}$$

- Corner $i = N_x$, $j = N_y$

$$u_{i+1,j-1} = -u_{i-1,j-1} \tag{6.60}$$

$$u_{i+1,j} = -u_{i-1,j} \tag{6.61}$$

$$u_{i+1,j+1} = u_{i-1,j-1} \tag{6.62}$$

$$u_{i,j+1} = u_{i,j-1} \tag{6.63}$$

$$u_{i-1,j+1} = u_{i-1,j-1} \tag{6.64}$$

$$v_{i+1,j-1} = v_{i-1,j-1} \tag{6.65}$$

$$v_{i+1,j} = v_{i-1,j} \tag{6.66}$$

$$v_{i+1,j+1} = v_{i-1,j+1} \tag{6.67}$$

$$v_{i,j+1} = -v_{i,j-1} \tag{6.68}$$

$$v_{i-1,j+1} = -v_{i-1,j-1} \tag{6.69}$$

$$p_{mi+1,j} = p_{mi-1,j} \tag{6.70}$$

$$p_{mi,j+1} = p_{mi,j-1} \tag{6.71}$$

$$p_{fi+1,j} = p_{fi-1,j} \tag{6.72}$$

$$p_{fi,j+1} = p_{fi,j-1} \tag{6.73}$$

Substituting all of these boundary approximations into the six discretized governing Eqs. (4.14), (4.16), (4.31), (4.33), (4.35), and (4.37) yields 6 (number of equations)×8(four boundaries plus four corners) = 48 equations for boundaries and corners and are listed in the enclosed Appendix A, Case 2.

6.2.3 Analysis of Simulation Results

The displacements in the x- and y-directions for two different times are presented in Figures 6.9 and 6.10. The displacements are the same in the x- and y-directions for same x and y coordinates because of symmetry.

Figure 6.11 depicts the temporal horizontal displacements (u) for three different locations: $x = 0$ m, $x = 50$ m, and $x = 150$ m (shown in Figure 6.12). Obviously, the largest horizontal displacement occurs on $x = 0$ line. The increase of the displacements is also the result of time increasing.

Figures 6.13 and 6.14 show the oil saturations in the matrix and in the fractures, respectively, when there is no stress applied at two boundaries. The water front moves much faster in the fractures than in the matrix because of their much higher permeability.

The oil saturation distribution in the matrix and in the fractures with stress are presented in Figures 6.15 and 6.16. By comparing Figures 6.13 and 6.15, it is noted that stress has a very small effects on the oil saturation distribution. Again, the waterfront moves much faster in the fractures than in the matrix with stress as seen in Figures 6.13 and 6.14.

In Figures 6.16 and 6.17, the waterfront movements can be seen as a function of time in the fractures. The oil pressures for the same time period in the matrix, for cases without and with stress, are shown in Figures 6.18 and 6.19, respectively. It is noted that the pressures with stress are much higher than that without stress.

The oil pressures in the fractures without and with stress after 300 days are presented in Figures 6.20 and 6.21. From Figure 6.21, it seems that the effects of stress on pressures in the fractures is not as large as in the matrix. It should be noted that at early times, for example, $t = 30$ days, pressures in the fractures still increase to very high values because of the applied stress (Figure 6.22).

The effects of stress on pore pressure are further investigated by applying different stresses. Figures 6.23 and 6.24 are the cases for $Q_{in} < Q_{pro}$ and $Q_{in} > Q_{pro}$, respectively. The higher the stress applied, the higher the pore pressure. However, as time goes on, the pore pressure goes to a common point. This indicates that the stress has more impact on pressure at earlier times than later on. These two figures also indicate that withdrawing underground fluids from a reservoir results in an increase in effective stress whereas enhancing oil recovery techniques such as water injection lead to a decrease in effective stress on the reservoir rock matrix. The pore may collapse if the effective stress on the rock matrix exceeds the critical stress (limit of elastic region). When this critical stress is known, the occurrence of the pore collapse can be predicted and may be avoided altogether.

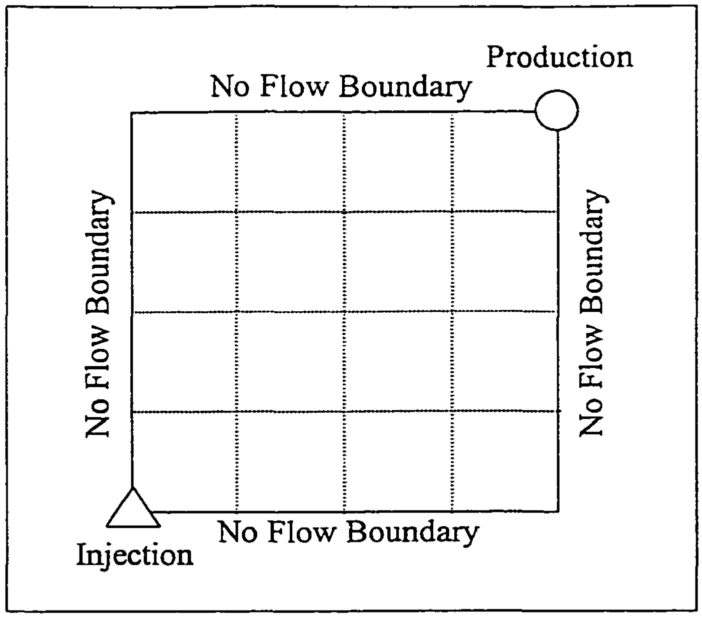

Figure 6.7: Production from a Deformable Fractured Reservoir with Water Injection.

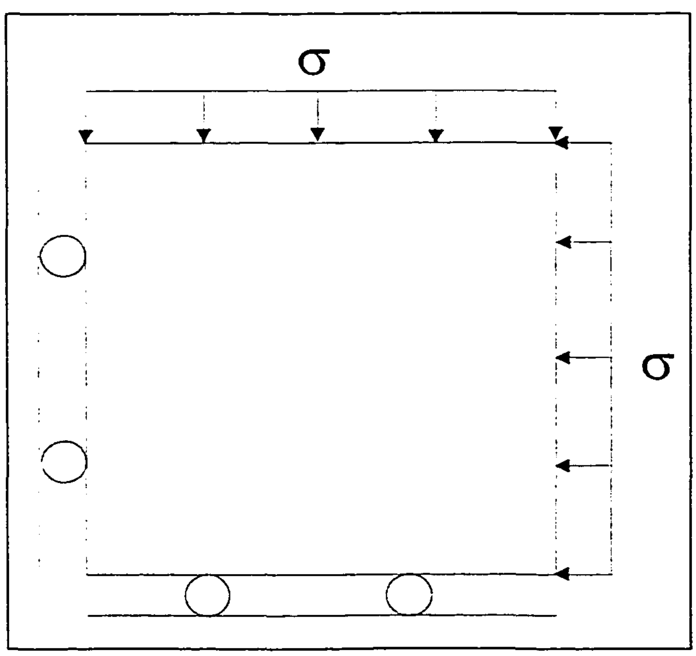

Figure 6.8: Mechanical Boundary Conditions.

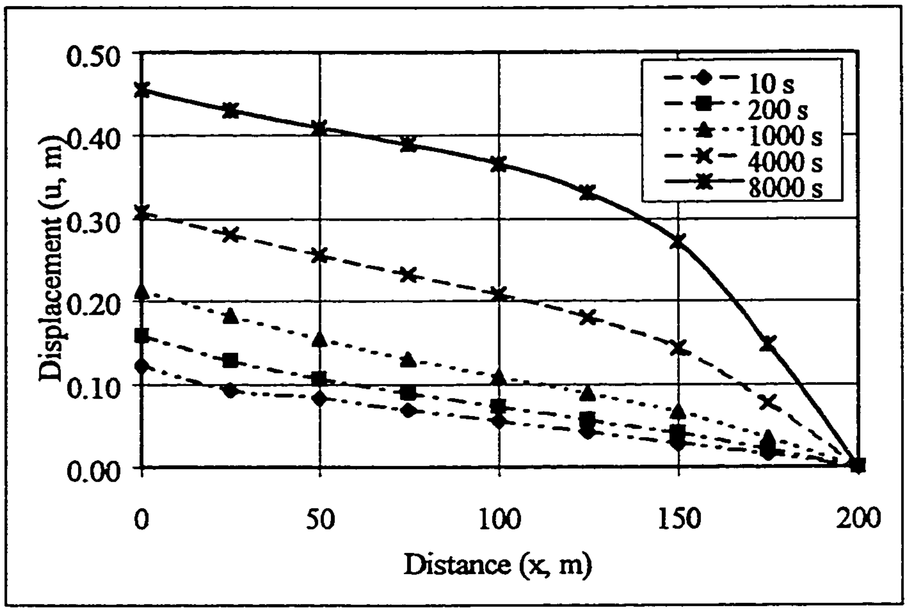

Figure 6.9: Displacements in the x-direction.

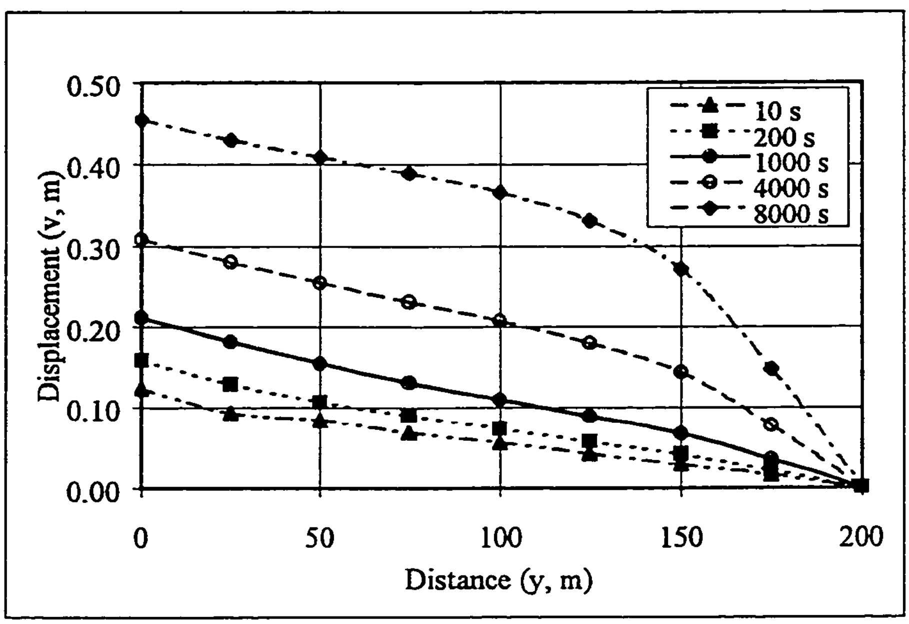

Figure 6.10: Displacements in the y-direction.

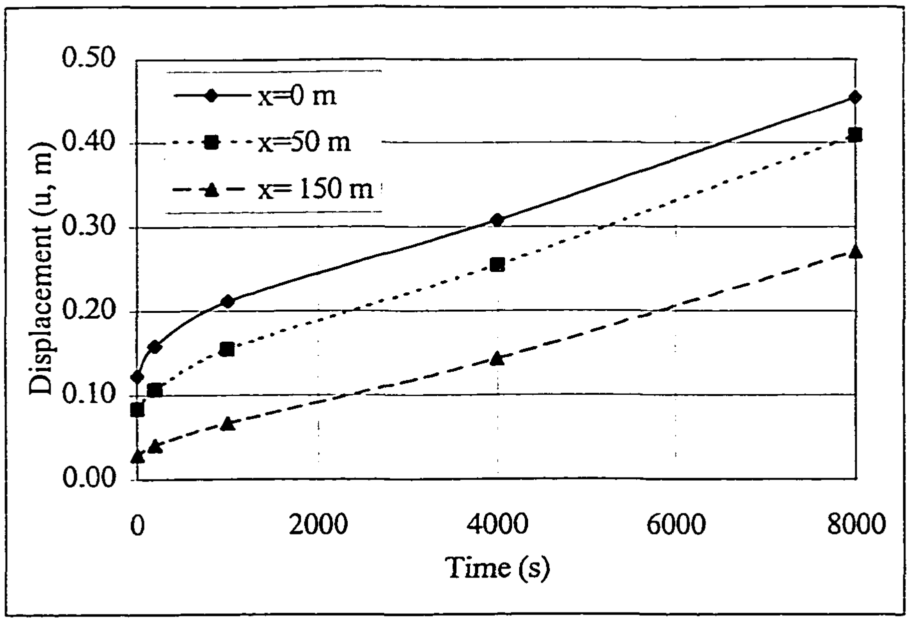

Figure 6.11: Displacements at Different Positions Vs. Time.

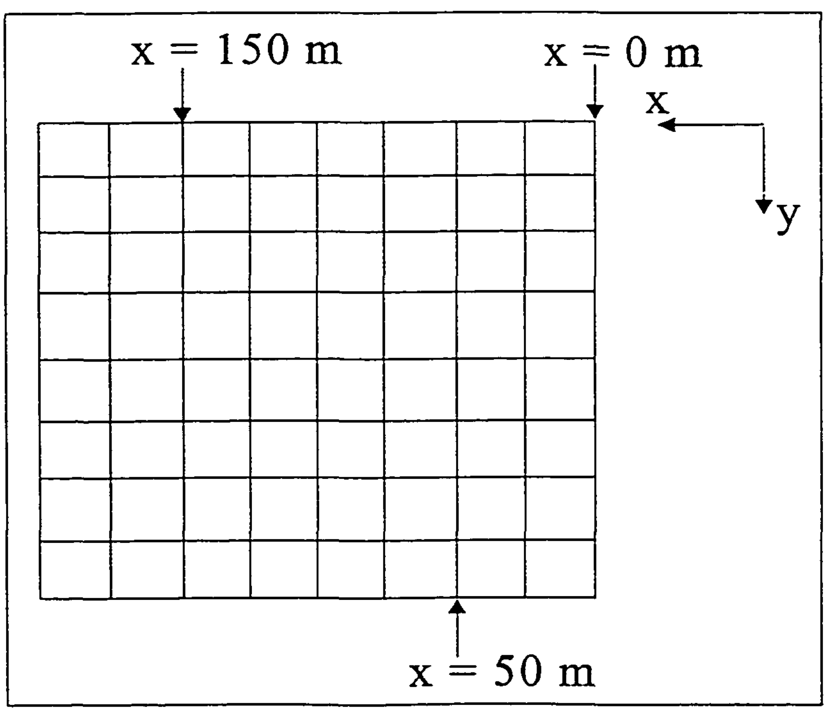

Figure 6.12: Reservoir Grids.

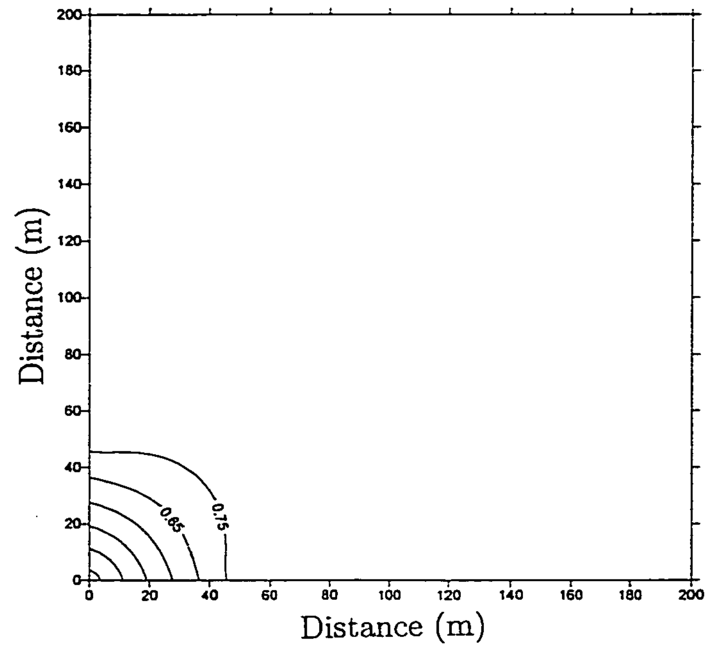

Figure 6.13: Oil Saturation in Matrix (No Stress, Time = 300 days).

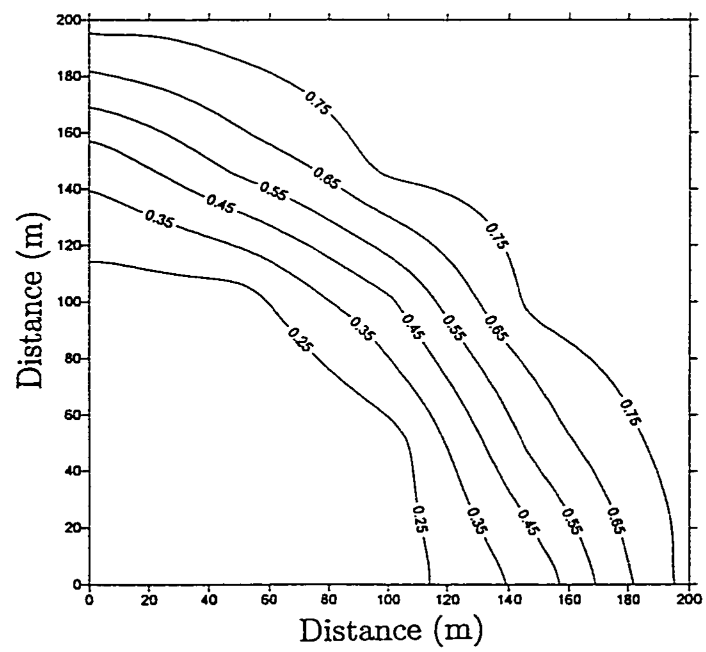

Figure 6.14: Oil Saturation in Fracture (No Stress, Time = 300 days).

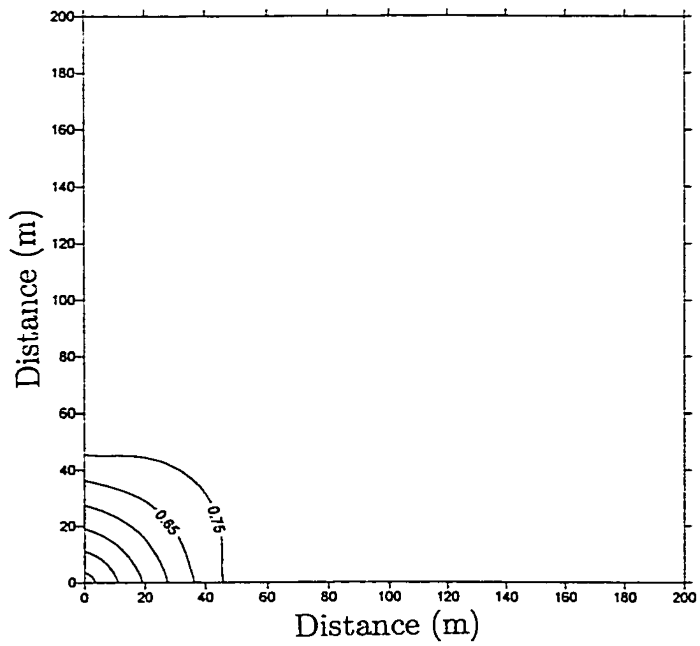

Figure 6.15: Oil Saturation in Matrix (With Stress, Time = 300 days).

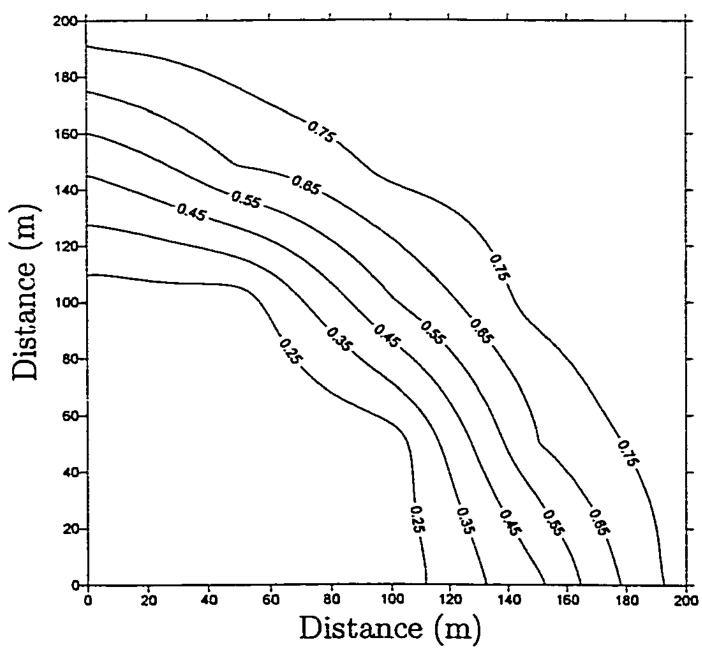

Figure 6.16: Oil Saturation in Fracture (With Stress, Time = 300 days).

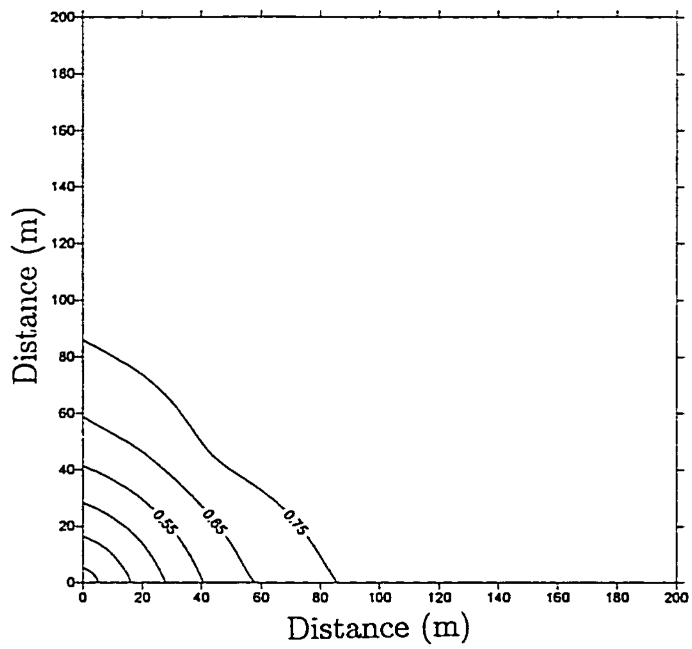

Figure 6.17: Oil Saturation in Fracture (With Stress, Time = 30 days).

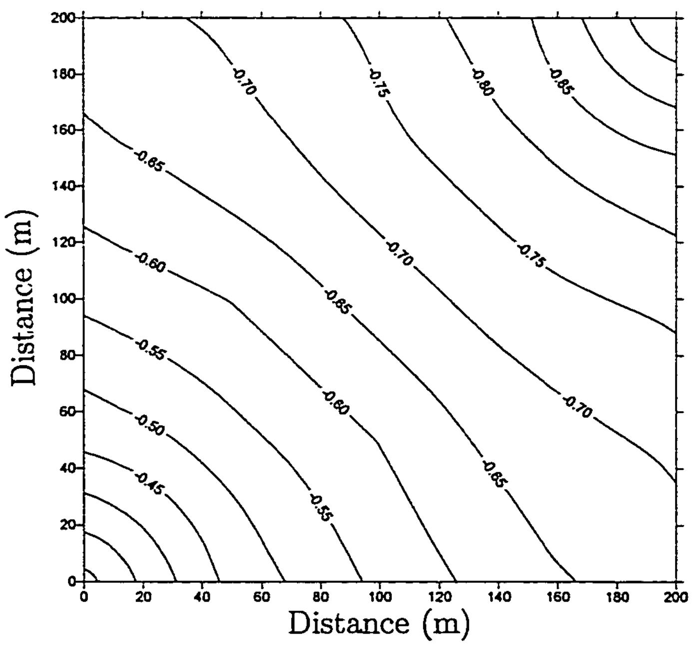

Figure 6.18: Oil Pressure (MPa) in Matrix (No Stress, Time = 300 days).

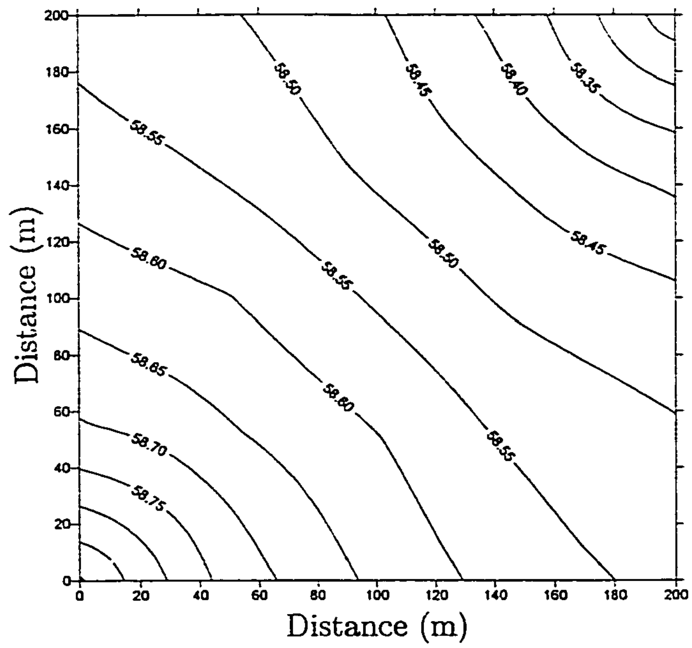

Figure 6.19: Oil Pressure (MPa) in Matrix (With Stress, Time = 300 days).

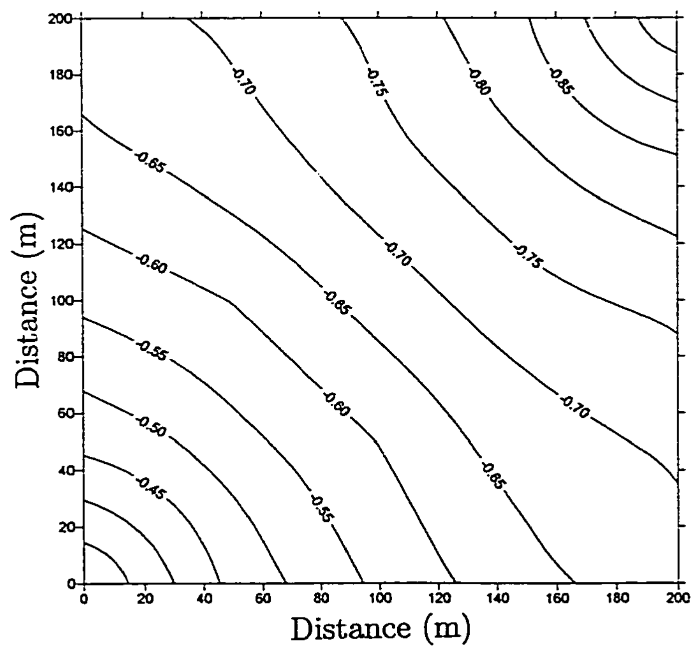

Figure 6.20: Oil Pressure (MPa) in Fracuture(No Stress, Time = 300 days).

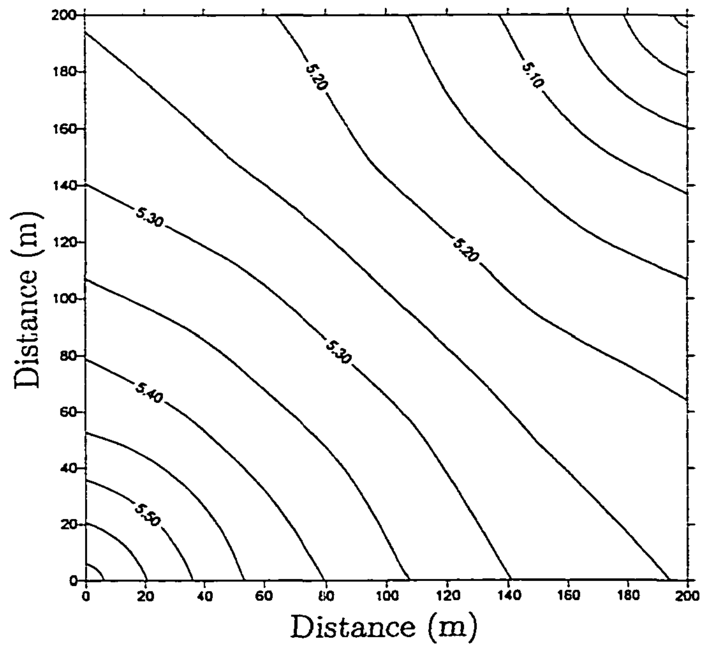

Figure 6.21: Oil Pressure (MPa) in Fracture (With Stress, Time = 300 days).

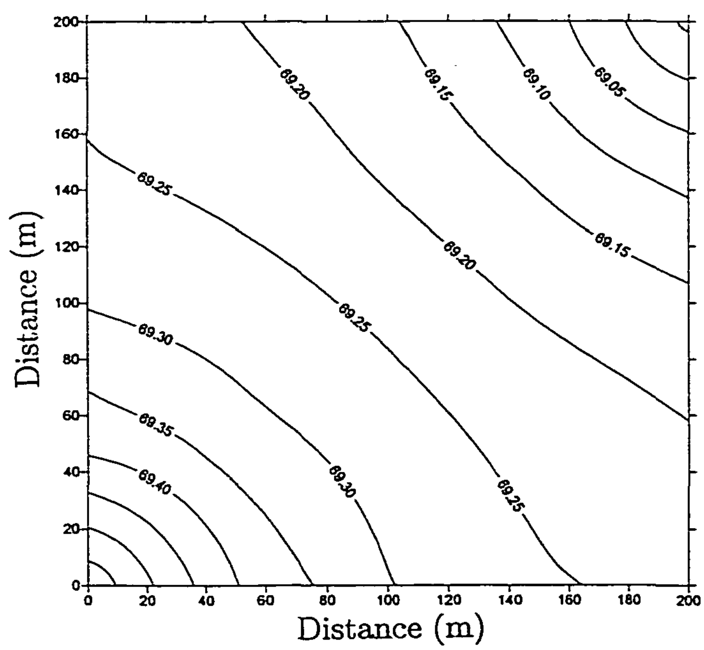

Figure 6.22: Oil Pressure (MPa) in Fracture (With Stress, Time = 30 days).

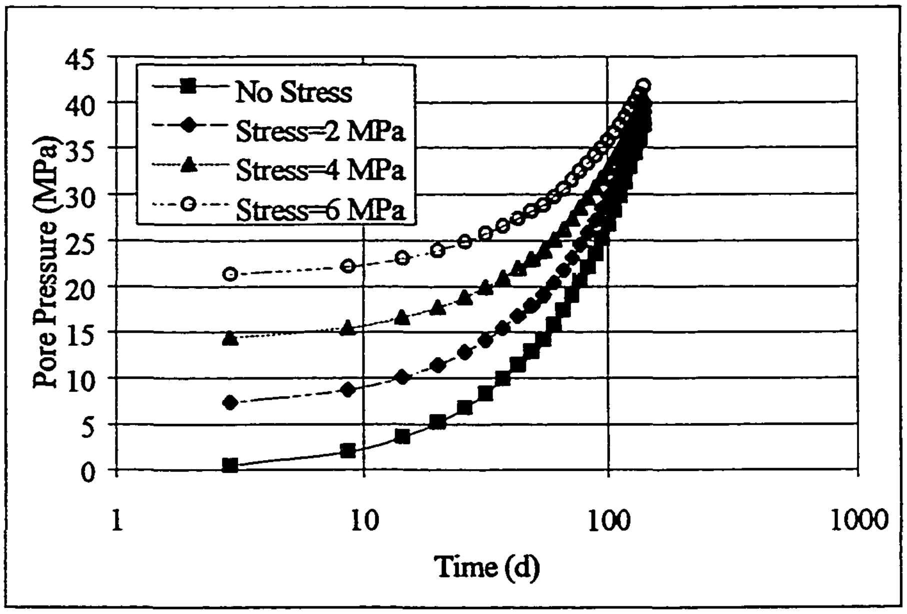

Figure 6.23: Effects of Stress on Pore Pressure.

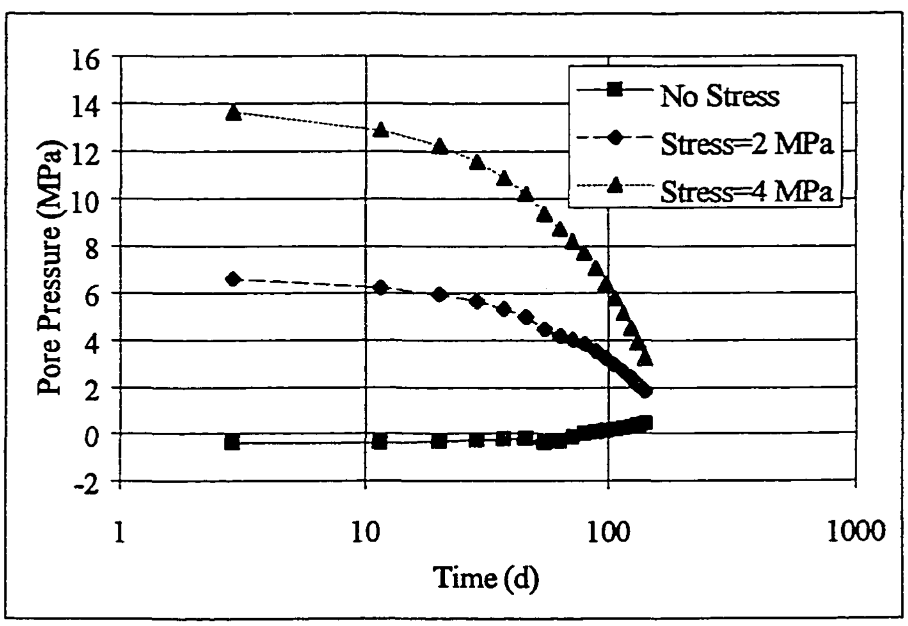

Figure 6.24: Effects of Stress on Pore Pressure.

Chapter 7

Sensitivity Analyses

This last chapter is devoted to sensitivity analyses. Sensitivity analyses (also called what-if analyses) are applied in simulation studies of very different real-life systems, in all kinds of disciplines (that use mathematical models): engineering, chemistry, physics, economics, management science, and so on. Moreover, the theoretical aspects of sensitivity are studied in mathematics and statistics. Unfortunately, the definition of sensitivity analysis varies over and within these many disciplines. In this dissertation, sensitivity analysis is defined as the systematic investigation of the reaction of the simulation response to either extreme values of the model's input variables or to drastic changes in the model's parameters. It is the practice of changing one factor, performing an analysis, and then checking the results to see if they are sensitive to the factor that was changed. Note that the analysis in this chapter concentrates on a single response per run. The effects of the most three important parameters, injection rate, K_s (solid grain bulk modulus), and E (rock's modulus of elasticity) on rock displacements and pore pressure are investigated.

7.1 Description of the Model Used

Figure 7.1 illustrates a five-spot pattern used commonly in waterflooding processes. The reservoir formation is assumed to be naturally fractured and deformable. Only a quarter of one pattern (shaded area in Figure 7.1) is needed due to symmetry. Numbers 1 to 9 are used to indicate the positions of the space domain which will be used in the later analyses (Figure 7.2). For example, point 5 is the center of the quarter. The input parameters used are listed in Table 7.1.

Table 7.1: Parameters Used in the Sensitivity Analyses

Parameters	Definition	Magnitude	Units
E	modulus of elasticity	3000	MPa
ν	Poisson's ratio	0.2	
$\overline{\alpha}$	transfer coefficient	1000	1/m^2
k_m	matrix permeability	3.95×10^{-13}	m^2
k_f	fracture permeability	3.95×10^{-11}	m^2
K_s	solid grain bulk modulus	11244	MPa
ϕ_m	matrix porosity	0.2	
ϕ_f	fracture porosity	0.05	
μ_o	oil viscosity	2×10^{-4}	Pa·s
μ_w	water viscosity	1×10^{-4}	Pa·s
c_o	oil compressibility	2×10^{-3}	1/MPa
c_w	water compressibility	8×10^{-4}	1/MPa

There is no drainage at all along the boundaries (Figure 7.3), except two wells at two opposite corners, an oil production well and a water injection well, respectively. The following three points hold because of symmetry (Figure 7.4):

1. The four corners are fixed, i.e. $u = v = 0$;
2. The left and right sides can move only in the y-direction, i.e. $u = 0$ and $v \neq 0$; and,
3. The upper and bottom sides can move only in the x-direction, i.e. $u \neq 0$ and

$v = 0.$

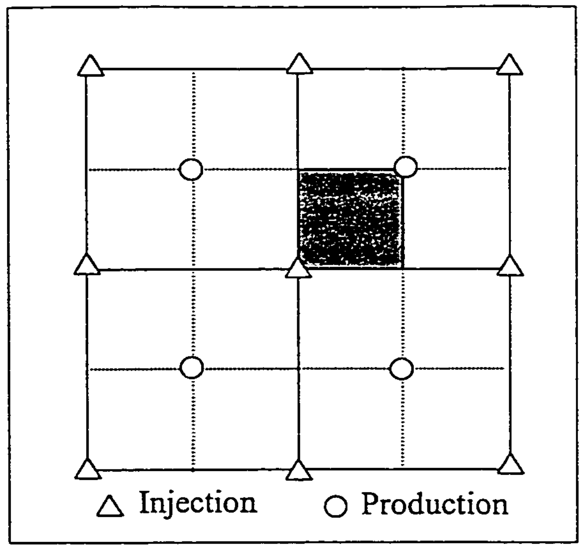

Figure 7.1: Five-Spot Patterns in a Water Flooding Reservoir.

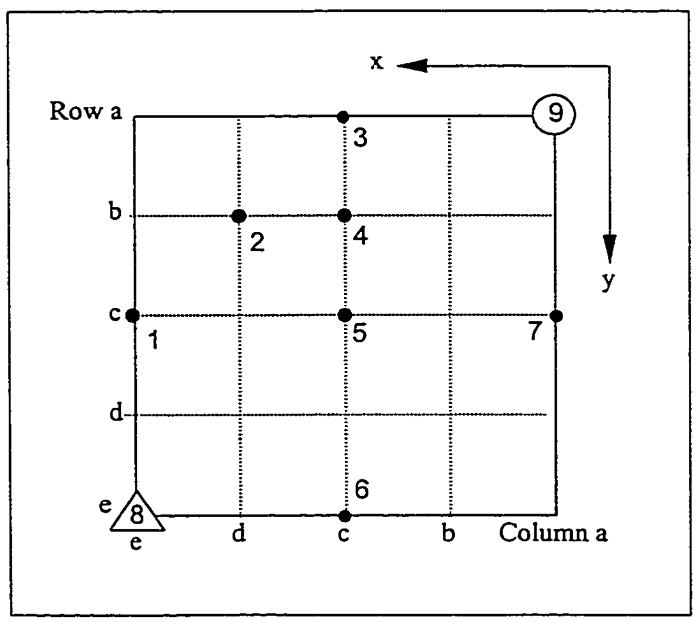

Figure 7.2: A quarter of One Pattern.

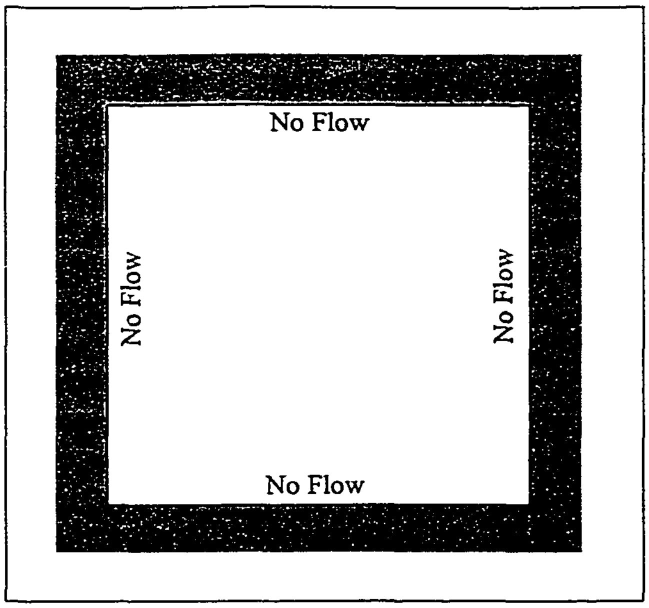

Figure 7.3: Flow Boundaries.

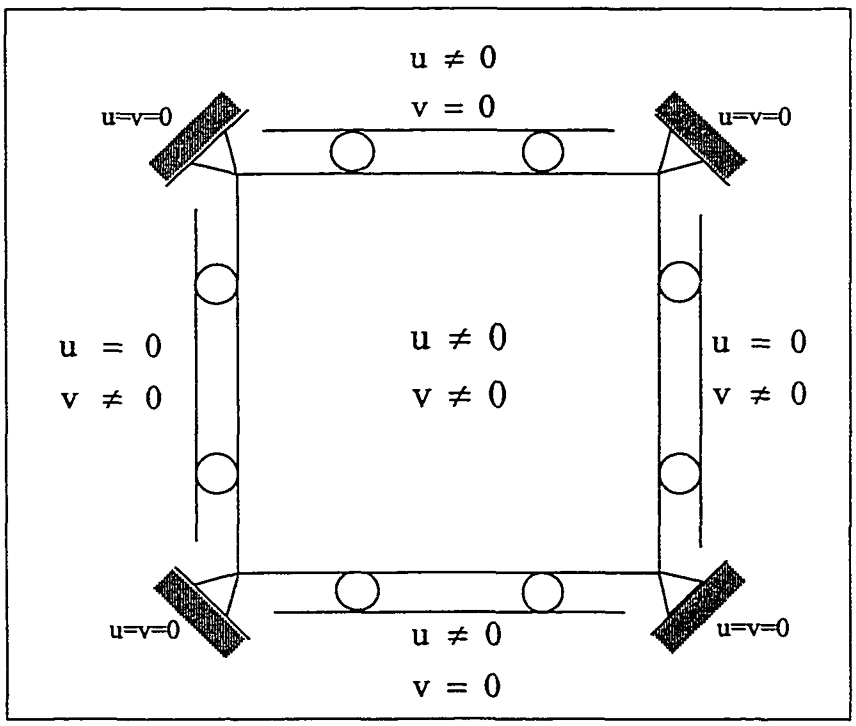

Figure 7.4: Mechanical Boundaries.

7.2 Approximations of Boundary Conditions for Boundaries and Corner Points

The six governing equations have to be re-arranged and the following approximations are applied based on the boundary conditions specified as in the validation and application cases:

- Boundary $i = 1$ ($u = 0$ and no flow)

$$u_{i-1,j} = -u_{i+1,j} \tag{7.1}$$

$$v_{i-1,j} = v_{i+1,j} \tag{7.2}$$

$$p_{mi-1,j} = p_{mi+1,j} \tag{7.3}$$

$$p_{fi-1,j} = p_{fi+1,j} \tag{7.4}$$

- Boundary $i = N_x$ ($u = 0$ and no flow)

$$u_{i+1,j} = -u_{i-1,j} \tag{7.5}$$

$$v_{i+1,j} = v_{i-1,j} \tag{7.6}$$

$$p_{mi+1,j} = p_{mi-1,j} \tag{7.7}$$

$$p_{fi+1,j} = p_{fi-1,j} \tag{7.8}$$

- Boundary $j = 1$ ($v = 0$ and no flow)

$$u_{i,j-1} = u_{i,j+1} \tag{7.9}$$

$$v_{i,j-1} = -v_{i,j+1} \tag{7.10}$$

$$p_{mi,j-1} = p_{mi,j+1} \tag{7.11}$$

$$p_{fi,j-1} = p_{fi,j+1} \tag{7.12}$$

- Boundary $j = N_y$ ($v = 0$ and no flow)

$$u_{i,j+1} = u_{i,j-1} \tag{7.13}$$

$$v_{i,j+1} = -v_{i,j-1} \tag{7.14}$$

$$p_{mi,j+1} = p_{mi,j-1} \tag{7.15}$$

$$p_{fi,j+1} = p_{fi,j-1} \tag{7.16}$$

- Corner $i = 1$, $j = 1$ ($u = 0$ and $v = 0$)

$$u_{i-1,j+1} = -u_{i+1,j+1} \tag{7.17}$$

$$u_{i-1,j} = -u_{i+1,j} \tag{7.18}$$

$$u_{i-1,j-1} = -u_{i+1,j+1} \tag{7.19}$$

$$u_{i+1,j-1} = u_{i+1,j+1} \tag{7.20}$$

$$u_{i,j-1} = u_{i,j+1} \tag{7.21}$$

$$v_{i-1,j+1} = v_{i+1,j+1} \tag{7.22}$$

$$v_{i-1,j} = v_{i+1,j} \tag{7.23}$$

$$v_{i-1,j-1} = -v_{i+1,j+1} \tag{7.24}$$

$$v_{i+1,j-1} = -v_{i+1,j+1} \tag{7.25}$$

$$v_{i,j-1} = -v_{i,j+1} \tag{7.26}$$

$$p_{mi-1,j} = p_{mi+1,j} \tag{7.27}$$

$$p_{mi,j-1} = p_{mi,j+1} \tag{7.28}$$

$$p_{fi-1,j} = p_{fi+1,j} \tag{7.29}$$

$$p_{fi,j-1} = p_{fi,j+1} \tag{7.30}$$

- Corner $i = N_x$, $j = 1$ ($u = 0$ and $v = 0$)

$$u_{i+1,j+1} = -u_{i-1,j+1} \tag{7.31}$$

$$u_{i+1,j} = -u_{i-1,j} \tag{7.32}$$

$$u_{i+1,j-1} = -u_{i-1,j+1} \tag{7.33}$$

$$u_{i,j-1} = u_{i,j+1} \tag{7.34}$$

$$u_{i-1,j-1} = u_{i-1,j+1} \tag{7.35}$$

$$v_{i+1,j+1} = v_{i-1,j+1} \tag{7.36}$$

$$v_{i+1,j} = v_{i-1,j} \tag{7.37}$$

$$v_{i+1,j-1} = -v_{i-1,j+1} \tag{7.38}$$

$$v_{i,j-1} = -v_{i,j+1} \tag{7.39}$$

$$v_{i-1,j-1} = -v_{i-1,j+1} \tag{7.40}$$

$$p_{mi+1,j} = p_{mi-1,j} \tag{7.41}$$

$$p_{mi,j-1} = p_{mi,j+1} \tag{7.42}$$

$$p_{fi+1,j} = p_{fi-1,j} \tag{7.43}$$

$$p_{fi,j-1} = p_{fi,j+1} \tag{7.44}$$

- Corner $i = 1$, $j = N_y$ ($u = 0$ and $v = 0$)

$$u_{i-1,j-1} = -u_{i+1,j-1} \tag{7.45}$$

$$u_{i-1,j} = -u_{i+1,j} \tag{7.46}$$

$$u_{i-1,j+1} = -u_{i+1,j-1} \tag{7.47}$$

$$u_{i,j+1} = u_{i,j-1} \tag{7.48}$$

$$u_{i+1,j+1} = u_{i+1,j-1} \tag{7.49}$$

$$v_{i-1,j-1} = v_{i+1,j-1} \tag{7.50}$$

$$v_{i-1,j} = v_{i+1,j} \tag{7.51}$$

$$v_{i-1,j+1} = -v_{i+1,j-1} \tag{7.52}$$

$$v_{i,j+1} = -v_{i,j-1} \tag{7.53}$$

$$v_{i+1,j+1} = -v_{i+1,j-1} \tag{7.54}$$

$$p_{mi-1,j} = p_{mi+1,j} \tag{7.55}$$

$$p_{mi,j+1} = p_{mi,j-1} \tag{7.56}$$

$$p_{fi-1,j} = p_{fi+1,j} \tag{7.57}$$

$$p_{fi,j+1} = p_{fi,j-1} \tag{7.58}$$

- Corner $i = N_x$, $j = N_y$ ($u = 0$ and $v = 0$)

$$u_{i+1,j-1} = -u_{i-1,j-1} \tag{7.59}$$

$$u_{i+1,j} = -u_{i-1,j} \tag{7.60}$$

$$u_{i+1,j+1} = -u_{i-1,j-1} \tag{7.61}$$

$$u_{i,j+1} = u_{i,j-1} \tag{7.62}$$

$$u_{i-1,j+1} = u_{i-1,j-1} \tag{7.63}$$

$$v_{i+1,j-1} = v_{i-1,j-1} \tag{7.64}$$

$$v_{i+1,j} = v_{i-1,j} \tag{7.65}$$

$$v_{i+1,j+1} = -v_{i-1,j-1} \tag{7.66}$$

$$v_{i,j+1} = -v_{i,j-1} \tag{7.67}$$

$$v_{i-1,j+1} = -v_{i-1,j-1} \tag{7.68}$$

$$p_{mi+1,j} = p_{mi-1,j} \tag{7.69}$$

$$p_{mi,j+1} = p_{mi,j-1} \tag{7.70}$$

$$p_{fi+1,j} = p_{fi-1,j} \tag{7.71}$$

$$p_{fi,j+1} = p_{fi,j-1} \tag{7.72}$$

Substituting all of these boundary approximations into the six discretized governing Eqs. (4.14), (4.16), (4.31), (4.33), (4.35), and (4.37) yields 6 (number of equations)$\times$8 (four boundaries plus four corners) = 48 equations for boundaries and corners to be solved with the other equations for the points within the space domain.

7.3 Analysis of Rock Deformations

The displacements in the x- and y-directions for different positions at different times are presented in Figures 7.5 to 7.10. Some very interesting facts are observed from these graphs. At earlier times, the points in row e have the largest displacements. As time passes, the displacements in row a increase faster than in row e. After 10 days, the curve of displacements for row a is almost symmetrical with the one representing row e. When equilibrium has been reached, the displacements in rows a and e, and the displacements in rows d and b are symmetrical with respect to the central column c. Similar phenomena are also noted for the displacements in y-direction, v.

Because of the symmetric characteristics of the pattern, the reservoir performance should be symmetric to the diagonal line connecting the injection and production wells. However, it should be understood that this means that the displacements of the upper-left part in the x-direction (u) equal the displacements of the

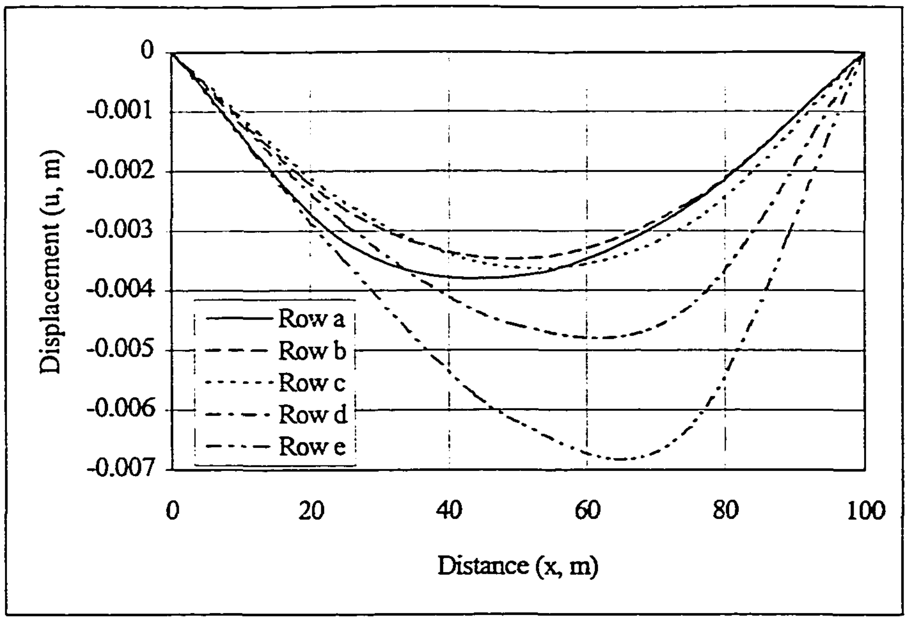

Figure 7.5: Displacements in x-direction (t = 2000 s).

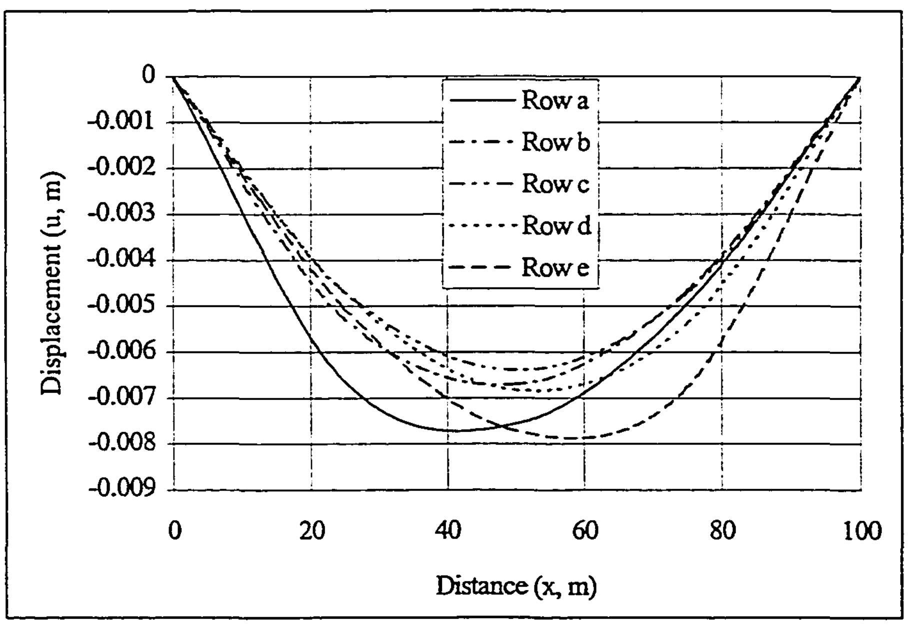

Figure 7.6: Displacements in x-direction (t = 10 d).

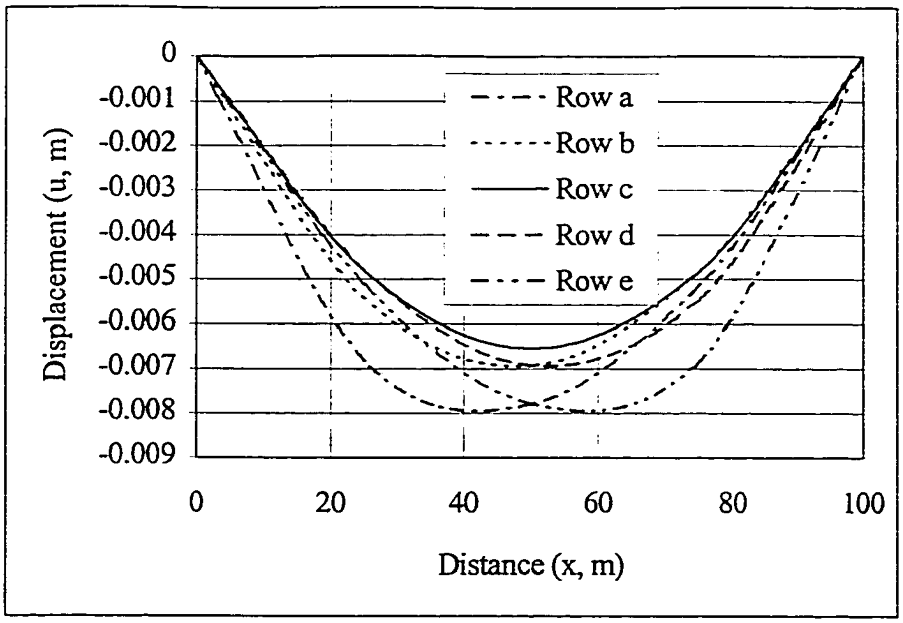

Figure 7.7: Displacements in x-direction (t = 100 d).

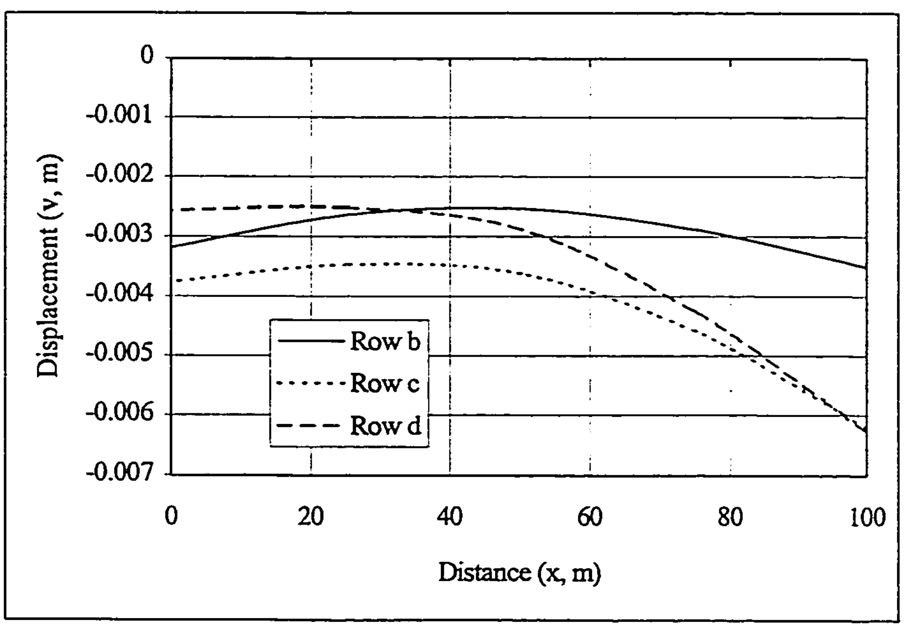

Figure 7.8: Displacements in y-direction (t = 2000 s).

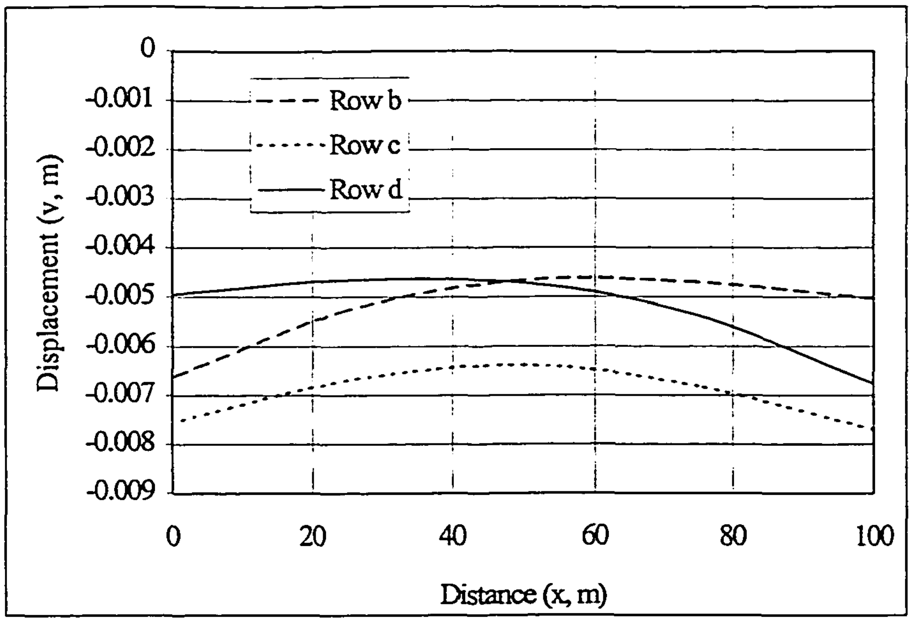

Figure 7.9: Displacements in y-direction (t = 10 d).

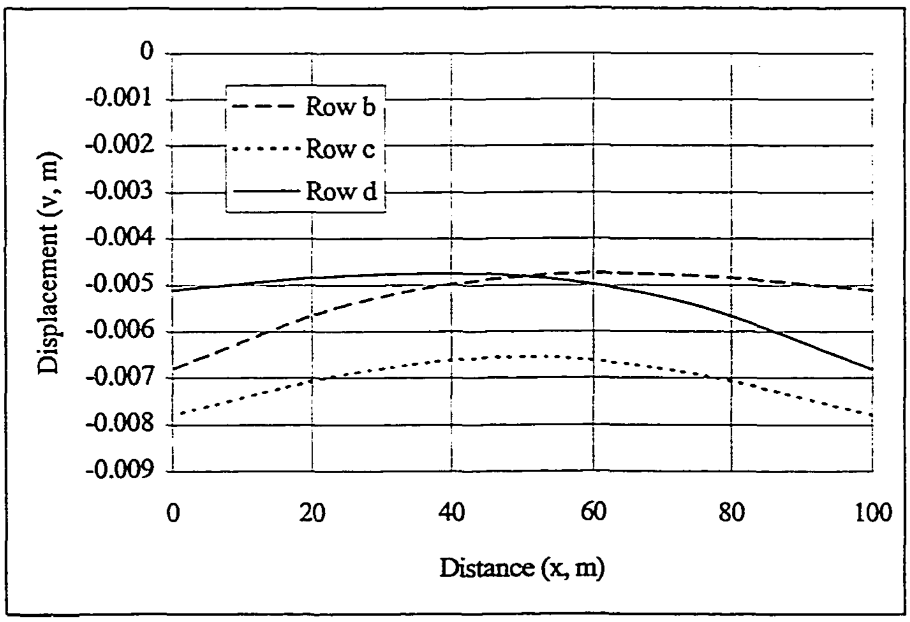

Figure 7.10: Displacements in x-direction (t = 100 d).

lower-right part in the y-direction (v). For example, the displacements of point 3 in the x-direction equals the displacements of point 7 in the y-direction. For the central point 5, the displacements in both directions are the same.

The total displacement can be calculated from the components of displacements in the x- and y-directions as shown, for example, in Figures 7.11 and 7.12 for points 4 and 2, respectively.

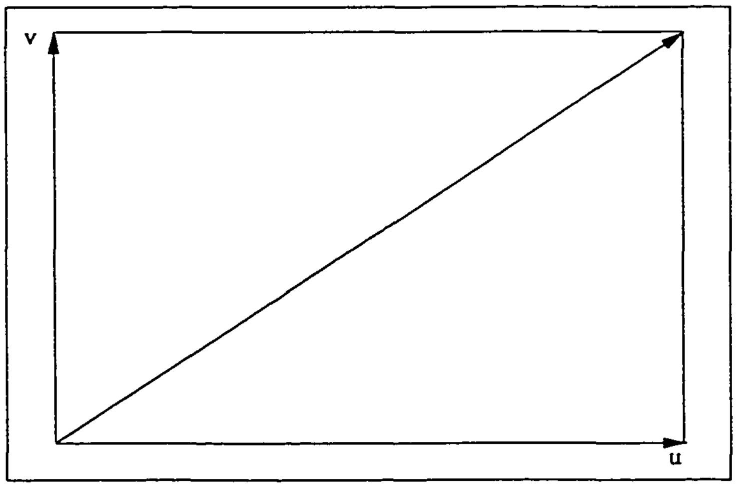

Figure 7.11: Total Displacement in Position 4.

7.4 Effects of Injection Rate on Pore Pressure

The effects of injection rate on pore pressure can be analyzed from the data listed in Table 7.2. The first row is injection rate in bbl/d and the first column is time in days. The negative sign indicates a decrease in pressure. It seems that the pore pressures are extremely sensitive to the injection rate. Under the conditions of these tested cases, a small increase in injection rate would cause a dramatic increase in pore pressure. It should be noted that the pore pressures at positions 1 and 6, and positions 3 and 7 are the same for any times, as expected.

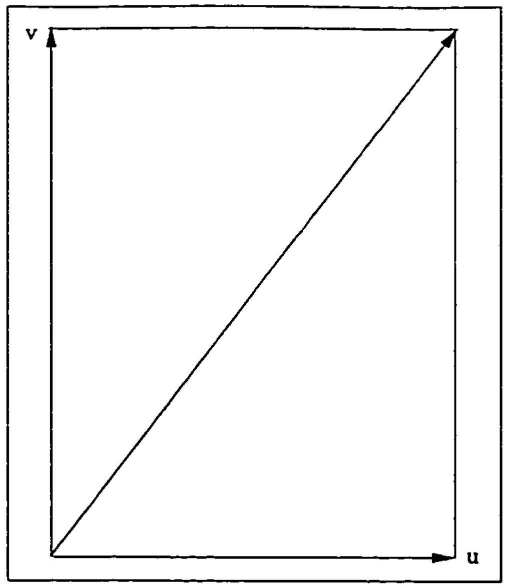

Figure 7.12: Total Displacement in Position 2.

7.5 Effects of K_s (Solid Grain Bulk Modulus) on Displacements and Pore Pressure

The displacements in the x- and y-directions for different positions at different times for various K_s are listed in Tables 7.3 and 7.4. In the table, the first row is time in days and the first column is K_s in MPa. The negative signs indicate that the displacements directions are opposite to the positive directions of the coordinate axes. It is interesting to note that a decrease in K_s results in a decrease in displacements both in the x- and y-directions. When K_s takes the value of 1666.67, the displacements in both directions are zero. The reason is that a decrease in K_s causes the α term to decrease (coefficient of pressure in the governing equations for the matrix displacements). When K_s equals K_t, this α term is zero, meaning that pressure has no effect on rock matrix deformations and, therefore, the displacements in both x- and y-directions are zero.

The effects of K_s on pore pressure can be analyzed from data listed in Table

Table 7.2: Effects of Injection Rate on Pore Pressure

Rate (bbl/d)	1.08	1.09	1.1	Position
1 (day)	-7.1754	0.6503	1.5286	8
	-8.2670	-0.4498	0.4281	1
	-8.2670	-0.4498	0.4281	6
	-8.6493	-0.8366	0.0409	5
	-9.0483	-1.2338	-0.3566	3
	-9.0483	-1.2338	-0.3566	7
	-10.254	-2.4013	-1.5208	9
30 (days)	-319.76	-30.844	1.6153	8
	-321.07	-32.032	0.4381	1
	-321.07	-32.032	0.4380	6
	-321.52	-32.439	0.0347	5
	-321.97	-32.847	-0.3692	3
	-321.97	-32.847	-0.3692	7
	-323.29	-34.038	-1.5462	9
100 (days)	-1131.8	-115.35	1.7542	8
	-1133.0	-116.67	0.4751	1
	-1133.0	-116.67	0.4751	6
	-1133.5	-117.12	0.0365	5
	-1133.8	-117.58	-0.4022	3
	-1133.8	-117.58	-0.4022	7
	-1135.1	-118.90	-1.6821	9

7.5 and Figures 7.13-7.15. It is observed from these graphs that there is a number for K_s above or below which pore pressure would be higher. This number in this analysis is around 17500 MPa.

7.6 Effects of Young's Modulus on Displacements and Pore Pressure

The displacements in the x- and y-directions for different positions at different times for various E are listed in Tables 7.6 and 7.7. The first row is time in days and the first column is E in MPa. It is obvious that a decrease in E results in an increase in displacements in both directions. However, when E increases to a value so that

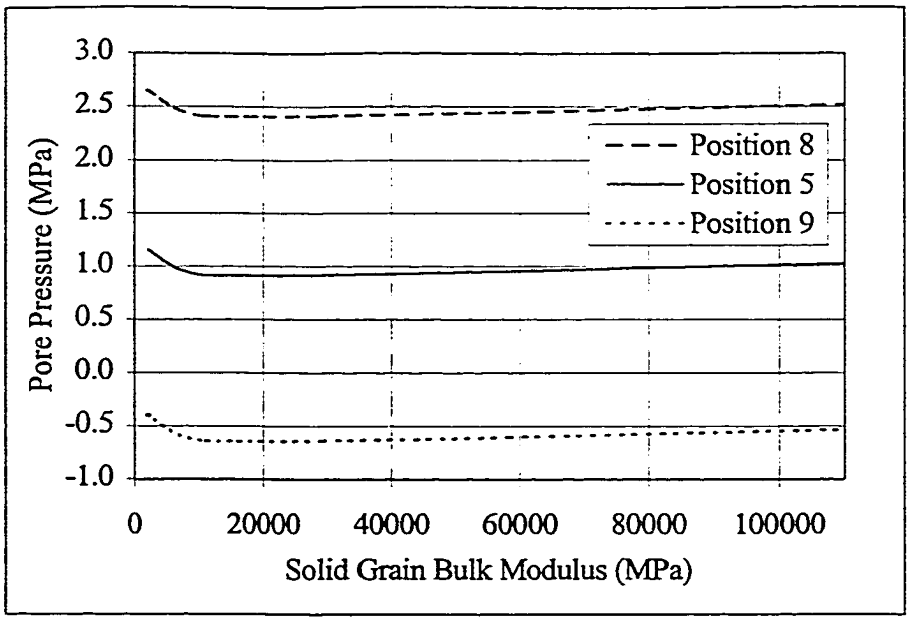

Figure 7.13: Pore Pressure Vs. K_s (t = 1 d).

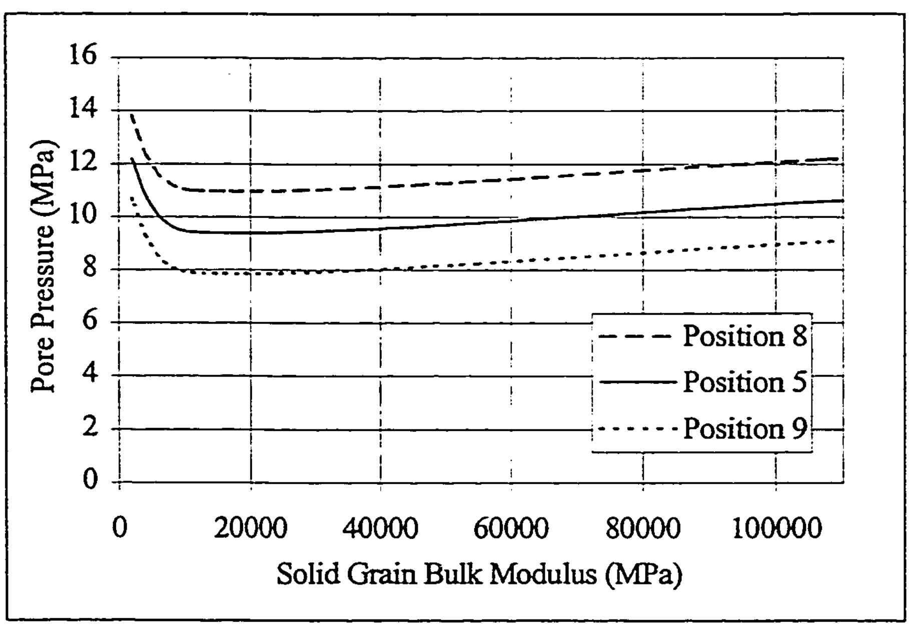

Figure 7.14: Pore Pressure Vs. K_s (t = 10 d).

Table 7.3: Effects of K_s on Displacements in the x-direction (u, m)

Time (days)	**0.023**	**10**	**30**	**100**	Position
1666.7 (MPa)	0	0	0	0	3
	0	0	0	0	5
	0	0	0	0	6
11000 (MPa)	-0.00376	-0.00755	-0.00777	-0.778	3
	-0.00362	-0.00638	-0.00654	-0.00654	5
	-0.00621	-0.00770	-0.00778	-0.00778	6
110000 (MPa)	-0.00436	-0.00876	-0.00902	-0.00903	3
	-0.00420	-0.00741	-0.00759	-0.00759	5
	-0.00720	-0.00893	-0.00903	-0.00903	6

Table 7.4: Effects of K_s on Displacements in the y-direction (v, m)

Time (days)	**0.023**	**10**	**30**	**100**	Position
1666.7 (MPa)	0	0	0	0	1
	0	0	0	0	5
	0	0	0	0	7
11000 (MPa)	-0.00621	-0.00770	-0.00778	-0.00778	1
	-0.00362	-0.00638	-0.00654	-0.00654	5
	-0.00376	-0.00755	-0.00777	-0.00778	7
110000 (MPa)	-0.00720	-0.00893	-0.00903	-0.00903	1
	-0.00420	-0.00741	-0.00759	-0.00759	5
	-0.00436	-0.00876	-0.00902	-0.00903	7

K_t equals to K_s, the displacements in both directions becomes zero because of the same reasons as mentioned above; i.e. α is zero under those conditions.

The pore pressures at different times and positions for various E are listed in Table 7.8 and are plotted in Figures 7.16-7.18. The following two points can be drawn from these graphs:

1. An increase in E results in an increase in pore pressure; and,

2. The effect of E on pore pressure is small. In other words, the pore pressure is not very sensitive to E. However, it becomes more important as time goes on.

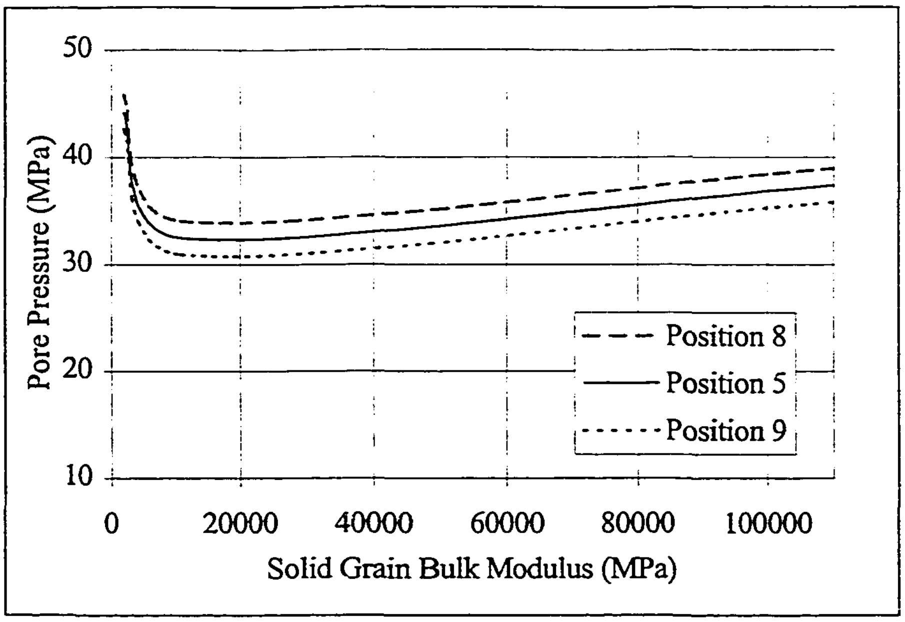

Figure 7.15: Pore Pressure Vs. K_s (t = 100 d).

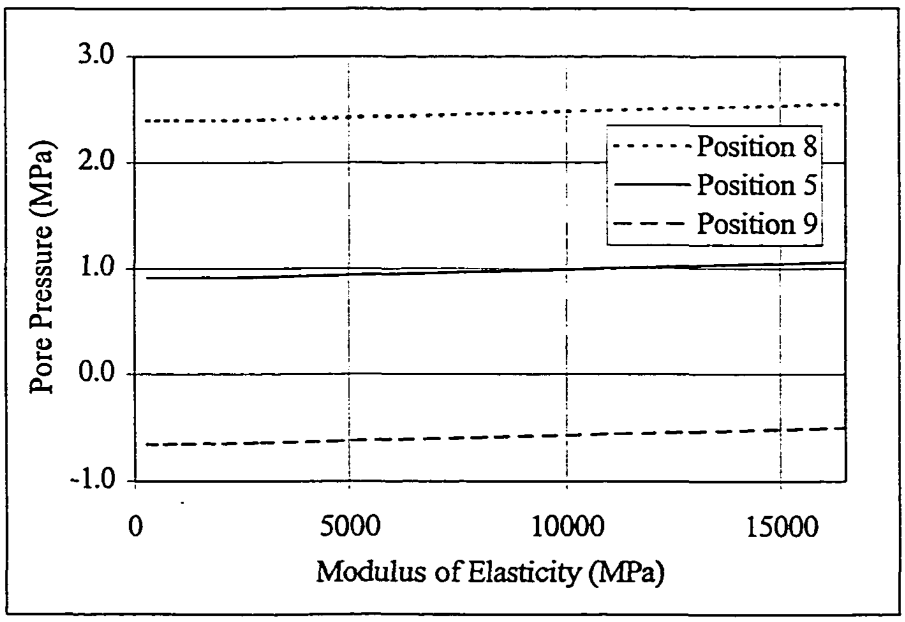

Figure 7.16: Pore Pressure Vs. E (t = 1 d).

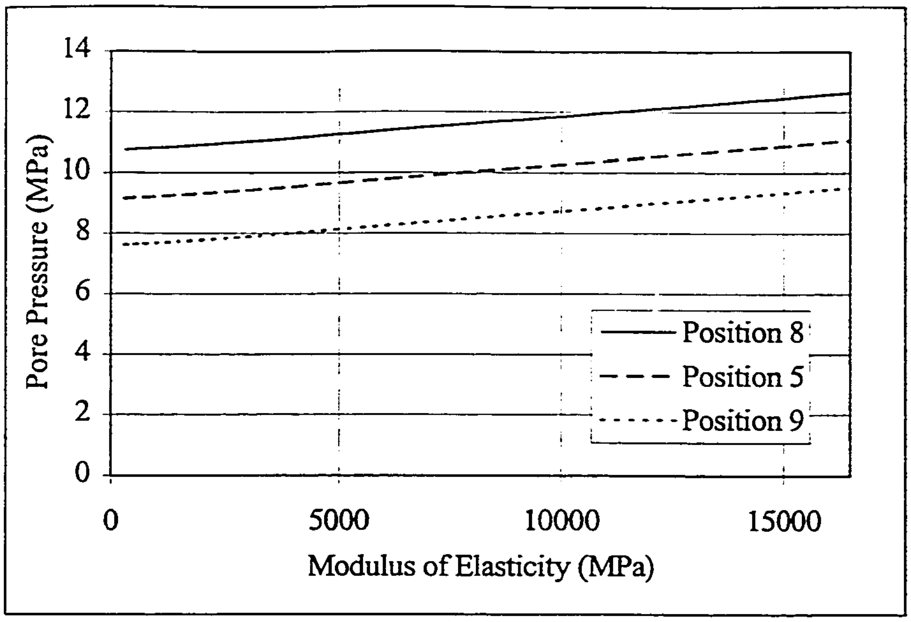

Figure 7.17: Pore Pressure Vs. E (t = 10 d).

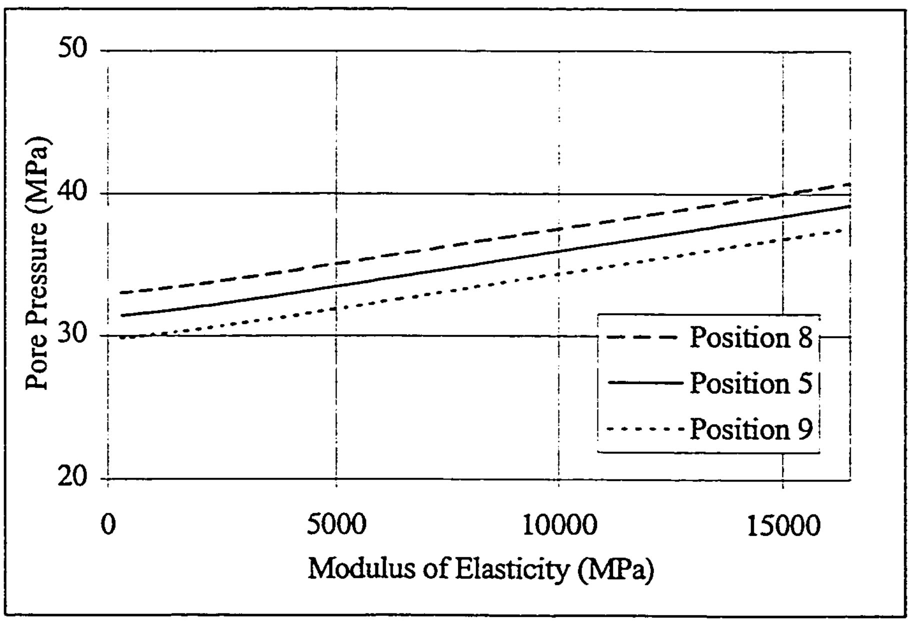

Figure 7.18: Pore Pressure Vs. E (t = 100 d).

Table 7.5: Pore Pressures at Different times and positions for Various K_s

K_s (MPa)	**2000**	**11000**	**110000**	Position
1 (day)	2.6513	2.4084	2.5167	8
	1.1631	0.9202	1.0284	5
	-0.3955	-0.6390	-0.5309	9
10 (days)	13.7940	11.0170	12.2190	8
	12.2130	9.4358	10.6370	5
	10.6780	7.9006	9.1021	9
30 (days)	45.7950	34.0860	38.997	8
	44.2140	32.5040	37.415	5
	42.6350	30.9260	35.837	9

Table 7.6: Effects of E on Displacements in the x-direction (u, m)

Time (days)	**0.023**	**10**	**30**	**100**	Position
300 (MPa)	-0.0428	-0.0876	-0.0902	-0.0903	3
	-0.0400	-0.0742	-0.0759	-0.0759	5
	-0.0668	-0.0894	-0.0903	-0.0903	6
3000 (MPa)	-0.00376	-0.00755	-0.00777	-0.00778	3
	-0.00362	-0.00638	-0.00654	-0.00654	5
	-0.00621	-0.00770	-0.00778	-0.00778	6
19800 (MPa)	0	0	0	0	3
	0	0	0	0	5
	0	0	0	0	6

Table 7.7: Effects of E on Displacements in the y-direction (v, m)

Time (days)	**0.023**	**10**	**30**	**100**	Position
300 (MPa)	-0.0668	-0.0894	-0.0903	-0.0903	1
	-0.0400	-0.0742	-0.0759	-0.0759	5
	-0.0428	-0.0876	-0.0902	-0.0903	7
3000 (MPa)	-0.00621	-0.00770	-0.00778	-0.00778	1
	-0.00362	-0.00638	-0.00654	-0.00654	5
	-0.00376	-0.00755	-0.00777	-0.00778	7
19800 (MPa)	0	0	0	0	1
	0	0	0	0	5
	0	0	0	0	7

Table 7.8: Pore Pressures at Different times and positions for Various E

E (MPa)	**300**	**3000**	**16500**	Position
1 (day)	2.4006	2.4084	2.5505	8
	0.9115	0.9202	1.0624	5
	-0.6518	-0.6390	-0.4963	9
10 (days)	10.7460	11.0170	12.6390	8
	9.1631	9.4358	11.0570	5
	7.6261	7.9006	9.5223	9
30 (days)	33.014	34.0860	40.7700	8
	31.433	32.5040	39.1880	5
	29.854	30.9260	37.6100	9

Chapter 8

Conclusions and Recommendations

Numerical simulation of fluid flow in deformable fractured media is of a great interest for engineers in petroleum, civil, environmental, geological and mining engineering and a challenging area. Because of complications associated with multiple physical processes in deformable fractured rocks and mathematical representation of a multiphase flow system, there is no published literature that derives rigorously the coupled differential equations governing the behavior of deformable fractured porous media and two-phase fluid flow. To the best of the author's knoeledge, this dissertation presents for the first time the theory and formulations in this most advanced area. The following conclusions and recommendations are drawn based on the present research.

8.1 Contributions and Conclusions

1. A two-phase, two-dimensional numerical simulator, RFIA, has been developed to investigate the process of fluids flow in deformable naturally fractured reservoirs and impacts of rock deformations on oil production, effects of withdrawing fluids from underground and/or injecting fluids on pore fluid pressure

and effective stress distributions on rock matrix as well.

2. Mathematical equations incorporated into the simulator included two equilibrium equations for rock deformations and four continuity equations for fluid flow in both matrix and fractures.

3. For each point in the simulated domain, there are ten unknowns: rock deformations in x- and y-directions, two saturations and two pressures in matrix and fractures, respectively. By making use of the capillary pressure and the saturation relationships, four out of these ten unknowns are eliminated to give the final six governing equations needed to be solved.

4. A finite difference numerical scheme, as an alternative method to finite elements, has been applied to discretize the final six governing equations.

5. Comparing to the finite element method, the finite difference method has the advantage of being easy to apply. However, if the resultant nonlinear equations are solved by the direct method, it is tedious to write out the special form of the six governing equations for boundaries and corner points based on the boundary conditions specified.

6. Verification of the finite difference model as well as the simulator is carried out by simulating the consolidation problem in which the analytical solution is available, as well as by comparing the results from a finite element model. Successful agreement was obtained in both cases.

7. The effects of stresses on saturation distribution is small whereas on pore pressure distribution it is quite large. This implies that during oil production, withdraw of underground hydrocarbons for a reservoir formation may cause the effective stress on rock matrix to a content to cause pore collapse.

8. The effective stress that is directly proportional to pore pressure must be controlled within the rock limit in order to prevent the rock from pore collapse. Because pore is most sensitive to injection/production rates, therefore, these rates plays the most important role in controlling pore collapse.

9. An increase in K_s results in an increase in rock displacements in both x- and y-directions. For the pore pressure, there is a value at which the pore pressure is lowest.

10. An increase in E results in a decrease in rock displacements in both x- and y-directions. The pore pressure increases as E increases.

11. The rock fluid interaction simulator, RFIA, can easily simulate different problems by properly setting corresponding coefficients and parameters. These situations include (1) single-phase flow in single-porosity media; (2) single-phase flow in dual-porosity media; (3) two-phase flow in single-porosity media; and (4) two-phase flow in dual-porosity media. In all of the above cases, the porous media can be treated as either deformable or rigid.

12. Dealing with two-phase flow of gas and oil systems in a deforming fractured reservoir is much more complicated and difficult than dealing with oil and water system because of gas solubility in oil. Thus, oil formation volume factor and solution gas-oil ratio must be introduced. Nevertheless, the coupled differential equations governing the behavior of gas and oil flow in a deforming fractured reservoir have been derived, discretized in finite difference format, and are ready to be coded. These formulations are also ready to be discretized using finite element method. Actually, the researchers at Rock Mechanics Institute at the University of Oklahoma are developing a simulator for oil-gas systems based on these formulations presented in this dissertation.

8.2 Recommendations for future work

1. Complete the simulator development of gas-oil flow in deformable naturally fractured reservoir.
2. Try applying iteration methods to solved the resultant system of equations to avoid the painful work to get the special forms of discretized governing equations for boundaries and corner points.
3. Enhance the simulator's interface.
4. The study of reservoir formation permeability is another concern to petroleum engineers because of its direct relationship to oil production rate. In the case of deforming fractured media, the permeability of the porous media is considered stress-dependent as a result of crack aperture changes caused by stress variations. In addition to experimental tests, numerical simulations may be used to predict the stress-dependent permeability under different loading situations. The following relationship relating permeability with porosity, conventionally used in formation damage model, may be adopted in stress-strain model to calculate the instantaneous permeability once the stress-dependent porosity is calculated by a rock fluid interaction simulator, like RFIA developed in this research:

$$k = ak_0 \left(\frac{\phi}{\phi_0} \right)^b \tag{8.1}$$

where k and k_0 are instantaneous and original permeabilities, respectively; and ϕ and ϕ_0 are instantaneous and original porosities, respectively, a and b are proper coefficients.

Nomenclature

A = area, L^2

B_o = oil formation volume fractor

C_{ig} = mass fraction of ith component in gas phase

C_{io} = mass fraction of ith component in oil phase

C_{iw} = mass fraction of ith component in water phase

C_o = oil compressibility, Lt^2/m

C_w = water compressibility, Lt^2/m

C_m = comprehensive compressibility for fluids in matrix, Lt^2/m

C_f = comprehensive compressibility for fluids in fracture, Lt^2/m

E = Young's modulus, m/Lt^2

F = force, mL/t^2

G = Lamé's constant

K = stiffness, m/Lt^2

K_t = bulk moduli of fractured media, m/Lt^2

K_s = bulk moduli of the solid grain, m/Lt^2

k_{rom} = oil relative permeability in rock matrix

k_{rof} = oil relative permeability in fracture

k_{rwm} = water relative permeability in rock matrix

k_{rwf} = water relative permeability in fracture

L = length, L

M = mass, m

P_m = average fluid pressure in rock matrix, m/Lt^2

P_f = average fluid pressure in fracture, m/Lt^2

P_{om} = oil pressure in rock matrix, m/Lt^2

P_{of} = oil pressure in fracture, m/Lt^2

P_{wm} = water pressure in rock matrix, m/Lt^2

P_{wf} = water pressure in fracture, m/Lt^2

P_c = capillary pressure, m/Lt^2

P_{cm} = capillary pressure of rock matrix, m/Lt^2

P_{cf} = capillary pressure of fracture, m/Lt^2

Q_g = mass transfer for gas phase, m/t

Q_o = mass transfer for oil phase, m/t

Q_w = mass transfer for water phase, m/t

R_s = solution gas-oil ratio

S_{om} = oil saturation of rock matrix

S_{of} = oil saturation of fracture

S_{wm} = water saturation of rock matrix

S_{wf} = water saturation of fracture

t = time, t

u = displacement in x-direction, L

v = displacement in y-direction, L

w_{wm} = Darcy's water velocity in rock matrix, L/t

w_{wf} = Darcy's water velocity in fracture, L/t

w_{om} = Darcy's oil velocity in rock matrix, L/t

v_{of} = Darcy's oil velocity in fracture, L/t

U_{wm} = intrinsic water velocity in rock matrix, L/t

U_{wf} = intrinsic water velocity in fracture, L/t

U_{om} = intrinsic oil velocity in rock matrix, L/t

U_{of} = intrinsic oil velocity in fracture, L/t

V = bulkl volume of fractured porous medium, L^3

V_s = solid volume of fractured porous medium, L^3

V_m = pore volume of fractured porous medium, L^3

V_f = fracture volume of fractured porous medium, L^3

V_p = total pore volume, L^3

V_o = volume of oil, L^3

V_w = volume of water, L^3

x, y = $x-$, $y-$direction in a cartesian coordinate system

Greeks

ε = strain

ε_{ij} = strain tensor (i, j=1, ..., 3)

ε_{kk} = volume strain

ν = Poisson's ration

ϕ_m = rock matrix porosity

ϕ_f = fracture matrix porosity

ϕ = total porosity

ρ_s = density of solid, m/L^3

ρ_{wm} = density of water in rock matrix, m/L^3

ρ_{om} = density of oil in rock matrix, m/L^3

ρ_{wf} = density of water in fracture, m/L^3

ρ_{of} = density of oil in fracture, m/L^3

μ_{wm} = water viscosity in rock matrix, m/Lt

μ_{wf} = water viscosity in fracture, m/Lt

μ_{om} = oil viscosity in rock matrix, m/Lt

μ_{of} = oil viscosity in fracture, m/Lt

σ = stress, m/Lt^2

σ_{ij} = stress tensor (i, j=1, ..., 3), m/Lt^2

α = Biot's constant

$\overline{\alpha}$ = transfer coefficient, 1/m^2

Δt = time step, t

References

1. Abdassah, D., and Ershaghi, I., Triple Porosity for Representing Naturally Fractrued Reservoirs, SPE Formation Evaluation, April 1986.

2. Aifantis, E.C., Introducing a Multi-Porous Medium, Developments in Mechanics, Vol. 8, p. 209-211, 1977.

3. Aifantis, E.C., On the Problem of Diffusion in Solids, Acta Mechanica, Vol. 37, p. 265-296, 1980.

4. Allen, D.R., Physical Changes of Reservoir Properties Caused by Subsidence and Repressurizing Operations, Wilmington Field, California, JPT, p. 23-29, 1968.

5. Asfari, A. and Witherspoon, P.A., Numerical Simulation of Naturally Fractured Reservoirs, paper SPE 4290 presented at the SPE-AIME Third Symposium on Numerical Simulation of Reservoir Performance, Houston, Jan. 11-12, 1973.

6. Ayatollahi, M.S. Noorishad, J. and Witherspoon, P.A., Stress-Fluid Flow Analysis of Fractured Rocks, J of Engr. Mech. Vol. 109, p. 1-13, Feb. 1983.

7. Bai, M., Elsworth, D. and Roegiers, J.-C., Multi-Porosity/Multi-Permeability Approach to the Simulation of Naturally Fractured Reservoirs, Water Resour.

Res., Vol. 29, No. 6, p. 1621-1633, 1993.

8. Bai, M., Ma, Q. and Roegiers, J.-C., A Nonlinear Dual-Porosity Model, Appl. Math. Modelling, Vol. 18, p. 602-610, 1994.

9. Bai, M. and Roegiers, J.-C., On the Correlation of Nonlinear Flow and Linear Transport with Application to Dual-Porosity Modeling, JPSE, Vol. 11, p. 63-72, 1994.

10. Bai, M., Roegiers, J.-C. and Elsworth, D., Poromechanical Response of Fractured-Porous Rock Masses, JPSE, Vol. 13, p. 155-168, 1995.

11. Bai, M. and Roegiers, J.-C., Modeling of Heat Flow and Solute Transport in Fractured Rock Masses, Proc. 8th Int. Congress Rock Mechanics, Japan, 1995.

12. Barenblatt, G.I., Zheltov, I.P. and Kochina, I.N., Basic Concepts in the Theory of Seepage of Homogeneous Liquids in Fissured Rocks, Prikl. Mat. Mekh., Vol. 24, No. 5, p. 852-864, 1960.

13. Barenblatt, G.I., On the Motion of a Gas-Liquid Mixture in Porous Fissured Media, Mekh. Machionst., No. 3, p. 47-50, 1964.

14. Bawden, W.F., Curran, J.H., and Roegiers, J-C., Influence of Fracture Deformation on Secondary Permeability - A Numerical Approach, Int. J. Rock Mech. Min. Sci. and Geomech. Abstr., 17, p. 265-279, 1980.

15. Blair, P.M., Caculation of Oil Displacement by Coutercurrent Water Imbibition, Paper 1475-G presented at the Fourth Biennial Secondary Recovery Symposium of SPE in Wichita Falls, TX, May 2-3, 1960.

16. Blaskovitch, F.T., Cain, G.M., Sonier, F., Waldren, D., and Webb, S.J., A Multicomponent Isothermal System for Efficient Reservoir Simulation, SPE Paper, No. 11480, 1983.

17. Biot, M.A., General Theory of Three-Dimensional Consolidation, J. Appl. Phys., Vol. 12, p. 155-164, 1941.

18. Biot, M.A., Theory of Elasticity and Consolidation for a Porous Anisotropic Media, J. Appl. Phys., Vol. 26, p. 182-185, 1955.

19. Biot, M. A.,Theory of Propagation of Elastic Waves in Fluid Saturated Porous Solids, J. Acoustical Society. Am., 28, p. 168-191, 1956.

20. Biot, M. A., Theory of Deformation of a Porous Viscoelastic Anisotropic Solid, J. Appl. Phys., 27, p. 452-469, 1956.

21. Birks, J., A Theoretical Investigation into the Recovery of Oil from Fissured Limestone Formations by Water Drive and Gas-Cap Drive, Proc. 4th World Petr. Cong. Sec. II-F, p. 425-440, 1955.

22. Boade, R.R., Chin, L.Y. and Siemers, W.T., Forecasting of Ekofisk Reservoir Compaction and Subsidence by Numerical Simulation, JPT, p. 723-728, 1989.

23. Bokserman, A.A., Zheltov, I.P. and Kocheshkov, A.A., Motion of Immiscible Liquids in a Cracked Porous Medium, Soviet Physics Dodlady, Vol. 9, No. 4, p. 285-287, 1964.

24. Bossie-Codreanu, D., Bia, P.R. and Sabathier, J.C., The "Checker Model " Improvement in Modeling Naturally Fractured Reservoirs with a Tridimensional, Triphasic, Black-Oil Numerical Model, SPEJ, p. 743-756, 1985.

25. Braester, C., Simultaneous Flow of Immiscible Liquids Through Porous Media, SPEJ, p. 297-305, 1972.

26. Chen, J., An Elastoplastic Model of Fluid-Saturated Porous Media, Ph.D. Dissertation, The University of Oklahoma, 1996.

27. Chin, L.Y. and Boade, R.R, Full-Field, Three-Dimensional Finite-Element Subsidence Model for Ekofisk, Third North Sea Chalk Symposium, Copenhagen, June, 1990.

28. Chin, L.Y., Boade, R.R., Prevost, J.H. and Landa, G.H., Numerical Simulation of Shear-Induced Compaction in the Ekofisk Reservoir, Int. J. Rock Mech. Sci. & Geomech. Abstr., Vol. 30, No. 7, p. 1193-1200, 1993.

29. Chin, L.Y. and Prevost, J.H., Three-Dimensional Computer Modeling of Coupled Geomechanics and Multi-Phase Flow, Computer Methods and Advances in Geomechanics, p. 1171-1176, Balkema, Rotterdam, 1997.

30. Dagger, M.A.S., A Fully-Coupled Two-Phase Flow and Rock Deformation Model for Reservoir Rock, Ph.D dissertation, the University of Oklahoma, 1997.

31. de Swaan, A.O., Analytic Solutions for Determing Naturally Fractured Reservoir properties by Well Testing, SPEJ, p. 117-122, June 1976.

32. Detournay, E. and Cheng, A.H-D., Fundamental of Poroelasticity, Ch.5 in Comprehensive Rock Engineering, Vol. 2, Editor, Fairhurst C., Pergamon Press, 1993.

33. Dietrich, J.H., Raleigh, C.B. and Bredehoeft, J.D., Earthquake Triggering by Fluid Injection at Rangely, Colorado, Paper T2-B, Proc. Symposium on Percolation through Fissured Rock, Int. Soc. Rock Mech., 1972.

34. Dougherty, D.E. and Babu, D.K., Flow to a Partially Penetrating Well in a Double-Porosity Reservoir, Water Res. Research, 21 No. 2. p. 265, 1985.

35. Duguid, J.O., Flow in Fractured Porous Media, Ph.D. Dissertation, Dept. of Civil Engineering, Princeton University, Princeton, N.J., 1973.

36. Duguid, J.O. and Abel, J., Finite Element Galerkin Method for Flow in Fractured Porous Media, in Finite Element Methods in Flow Problems, Oden J.T., Zienkiewicz O.C., Gallagher R.H. and Taylor C., eds., p. 599-615, University of Alabama Press, Huntsville, 1974.

37. Duguid, J.O. and Lee, P.C.Y., Flow in Fractured Porous Media, Water Resources Research, Vol. 13, No. 3, p. 558, 1977.

38. Elsworth, D. and Bai, M., Flow-Deformation Response of Dual-Porosity Media, Journal of Geotechnical Engineering, Vol. 118, No. 1, Jan. 1992.

39. Evans, R.D., A Proposed Model for Multiphase Flow Through Naturally Fractured Reservoirs, SPE Paper, No. 9940, SPE-AIME, Dallas, TX, 1981.

40. Finol, A. and Ali, S.M.F., Numerical Simulation of Oil Production with Simultaneous Ground Subsidence, SPEJ, Vol. 15, p. 411-424, 1975.

41. Friedman, M., Structural Analysis of Fractures in Cores from the Saticoy Field, Ventura County, California, Am. Assoc. Petrol. Geol. Bull., Vol. 53, No. 2, p. 367-389, 1969

42. Friedman, M. and Stearns, D.W., Relations Between Stresses Inferred from calcite Twin Lamellae and Mrofractures, Teton Anticline, Montana, Geol. Soc. Amer. Bull., Vol. 82, No. 11, p. 3151-3162, 1971.

43. Gale, J.E., A Numerical , Field and Laboratory Study of Flow in Rocks with Deformable Fractures, Ph.D. Dissertation, University of California, Berkeley, 1975.

44. Gawin, D., Simoni, L. and Schrefler, B.A., Numerical Model for Hydro-Mechanical Behaviour in Deformable Porous Media: A Benchmark Problem, p. 1171-1176, Balkema, Rotterdam, 1997.

45. Ghafouri, H.R. and Lewis, R.W., A Finite Element Double Porosity Model for Heterogeneous Deformable Porous Media, Int. J. Analytic. Numer. Meth. Geomech., Vol. 20, p. 831-844, 1996.

46. Gilman, J.R. and Kazemi, H., SPE Paper No. 10511 presented at the 6th Symposium on Reservoir Simulation, New Orleans, 1982.

47. Graham, J.W. and Richardson, J.G., Theory and Application of Imbibition Phenomena in Recovery of Oil, Trans., AIME Vol. 216, 377, 1959.

48. Hafner, W., Stress Distributions and Faulting, Bull. Geol. Soc. Amer., Vol. 62, No. 4, p. 373-393, April 1951.

49. Handin, J. and Hager, R.V., Experimental Deformation of Sedimentary Rocks Under Confining Pressure: Test at Room Temperature on Dry Samples, Am. Assoc. Petrol. Geol. Bull., Vol. 41, p. 1-50, 1957.

50. Hudson, J.A. and Priest, S.D., Discontinuities and Rock Mass Geometry, Int. J. Rock Mech. Min. Sci. Geomech. Abstr., 16, p. 135-148, 1979.

51. Huyakorn, P.S. and Pinder, G.F., Computational Methods in Subsurface Flow, Academic Press, Inc., New York, 1983.

52. Jones, M. and Mathiesen, E., Pore Pressure Change and Compaction in North Sea Chalk Hydrocarbon Reservoirs, Int. J. Rock Mech. Min. Sci. & Geomech. Abstr., Vol. 30, No. 7, p. 1205-1208, 1993.

53. Kazemi, H., Pressure Transient Analysis of Naturally Fractured Reservoirs with Uniform Fracture Distribution, SPE 43rd Annual Meeting, Houston, Paper 2156A, Oct., 1968.

54. Kazemi H., Seth M.S. and Thomas G.W., The Interpretation of Interference Tests in Naturally Fractured Reservoirs with Uniform Fracture Distribution, SPEJ, p. 463-472, Sep.1969.

55. Kazemi, H., Merrill, L.S., Porterfield, K.L., and Zeman, P.R., Numerical Simulation of Water-Oil Flow in Naturally Fractured Reservoirs, SPE-AIME 4th Symposium of Numerical Simulation of Reservoir Performance, Los Angeles, Paper No. 5719, Feb. 1976.

56. Khaleel, R., Porous Continuum Models for Fractured Basalts, Flow and Transport through Unrsturated Fractured Rock, Geophysical Monograph 42, R.D. Evans et al. eds. p. 141-148, 1987.

57. Khaled, M.Y., Beskos, D.E. and Aifantis, E.C., On the Theory of Consolidation with Double Porosity - III A Finite Element Formulation, Int. J. Analytic. Numer. Meth. Geomech., Vol. 8, p. 101-123, 1984..

58. Lewis, R.W. and Ghafouri, H.R., A Novel Finite Element Double Porosity Model for Multi-Phase Flow Through Deformable Fractured Porous Media, Int. J. Analytic. Numer. Meth. Geomech., Vol. 21, p. 789-816, 1997.

59. Lewis, R.W. and Schrefler, B.A., The Finite Element Method in the Deformation and Consolidation of Porous Media, Wiley, Chichester, 1987.

60. Lewis, R.W. and Sukirman, Y., Finite Element Modeling of Three-Phase Flow in Deforming Saturated Oil Reservoirs, Int. J. Analytic. Numer. Meth. Geomech., Vol. 17, p. 577-598, 1993a.

61. Lewis, R.W. and Sukirman, Y., Finite Element Modeling for Simulating the Surface Subsidence above a Compacting Hydrocarbon Reservoir, Int. J. Analytic. Numer. Meth. Geomech., Vol. 18, p. 619-639, 1993b.

62. Li, X., Zienkiewicz O.C. and Xie Y.M., A Numerical Model for Immiscible Two-Phase Fluid Flow in a Porous Medium and Its Time Domain Solution, Int. J. for Numer. Meth. in Eng., Vol. 30, p. 1195-1212, 1990.

63. Li, X. and Zienkiewicz, O.C., Multi-phase Flow in Deforming Porous Media and Finite Element Solutions, Computer & Structures, Vol. 45, No. 2, p. 211-227, 1992.

64. Liakopoulos, A.C., Transient Flow through Unsaturated Porous Media, Ph.D. Dissertation, Univ. of California, Berkeley, 1965.

65. Litvak, B., Simulation and Characterization of Naturally Fractured Reservoirs, Paper presented at the 1985 Reservoir Characterization Technical Conference, Dallas, April 1985.

66. Long, J.C.S., Remer, J.S., Wilson, C.R., and Witherspoon, P.A., Porous Media Equivalents for Networks of Discontinuous fractures, Water Resources Research, Vol. 18, No. 3, p. 645-658, June, 1982.

67. Long, J.C.S., Gilmour, P., and Witherspoon, P.A., A Model for Steady Flow in Random, Three Dimensional Networks of Disc-Shaped Fractures, Water Res. Research, Vol. 21, No. 8, p. 1105-1115, Aug. 1985

68. Marcus, H., The Permeability of a Sample of an Anisotropic Porous Medium, J. of Geophysical Research, Vol. 67, No. 13, p. 5215-5225, Dec. 1962.

69. Marius, J.M., Ekofisk Reservoir Voidage and Seabed Subsidence, JPT, p. 1434-1438, 1990.

70. Mattax, C.C. and Kyte, J.R., Imbibition Oil Recovery from Fractured, Water-Drive Reservoirs, Soc. Pet. Eng. J., Trans., AIME, Vol. 225, p. 177-184, 1962.

71. McCaleb, J.A. and Willingham, R.W., Influence of Geologic Heterogeneities on Secondary Recovery from Permian Phosphoria Reservoir, Cottonwood Creek Field, Wyoming, Am. Assoc. Petrol. Geol. Bull., Vol. 51, p. 2122-2132, 1967.

72. McLellan, P.J. and Wang, Y., Predicting the effects of Pore Pressure Penetration on the Extent of Wellbore Instability: Application of a Versatile Poroelastoplastic Model, Eurock'94, Balkema Rotterdam, Holland, 1994.

73. Meng, F.H., Personal Communication, 1998.

74. Meng, F.H., Three-Dimensional Finite Element Modeling of Two-Phase Fluid Flow in Deformable Naturally Fractured Reservoir, Ph.D. Dissertation, The University of Oklahoma, 1998.

75. Meng, F.H. and Bai, M., Two-Phase Fluid Flow in Deformable Fractured Formation: Finite-Element Approach, Report for the Rock Mechanics Research Center, RMRC-98-01, The University of Oklahoma, April, 1998.

76. Merle, A., Kenthie, G.H., Opstal van, G.H.C. and Schneider, G.M.H., The Bachaquero-Study: A Compaction Analysis of the Behavior of a Compaction Drive/Solution Gas Drive Reservoir, JPT, p. 1107-1114, 1976.

77. Muralidhar, K. and Long, J.C.S., A New Approach to Characterizing Flow in Single Fractures, Flow and Transport through Unrsturated Fractured Rock, Geophysical Monograph 42, R.D. Evans et al. eds. p. 141-148, 1987.

78. Nakornthap, K. and Evans, R.D., Numerical Simulation and Reservoir Characterization of Multiphase Fluid Flow in Naturally Fractured Formation, SPE 15130, 1984.

79. Nelson, R.A., Geological Analysis of Naturally Fractured Reservoirs, Gulf Publishing Company, Houston, Texas, 1985

80. Neumann, S.P. and Witherspoon, P.A., Finite Element Method of Analyzing Steady Seepage With a Free Surface, Water Resour. Res., Vol. 6, No. 3, p. 889-897, 1970.

81. Noorishad, J., Ayatollahi M.S. and Witherspoon, P.A., A Finite Element Method for Coupled Stress and Fluid Flow Analysis in Fractured Rock Masses, Int. J. Rock Mech. Min. Sci. & Geomech. Abstr., Vol. 19, p. 185-192, 1982.

82. Oda, M., Permeability Tensor for Discontinuous Rock Masses, Geotechnique, Vol. 35, No. 4, p. 483-495, 1985.

83. Odeh A.S., Unsteady-state Behavior of Naturally Fractured Reservoirs, SPEJ, 5, p. 60-66, 1965.

84. Parsons, R.W., Permeability of Idealized Fractured Rock, SPEJ, p. 126-136. June 1966.

85. Parsons, R.W., and Chaney, P.R., Imbibition Model Studies on Water-Wet Carbonate Rocks, SPEJ, p. 26-34, March 1966.

86. Paslay, P.R. and Cheatham, J.B., Rock Stresses Induced by Flow of Fkuids into Boreholes, SPEJ, p. 85-94, March 1963.

87. Rossen, R.J., Simulation of Naturally Fractured Reservoirs with Semi-Implicit Source Terms, SPEJ, 17, p. 201-210, 1977.

88. Rudnicky, J.W., Fluid Mass Sources and Point Sources in Linear Elastic Diffusive Solids, Mechanics of Material, Vol. 3, p. 243-250, 1987.

89. Schoonbeek, J.B., Land Subsidence as a Result of Natural Gas Extraction in the Province of Groningen, SPE Paper, No. 5751, 1976.

90. Schrefler, B.A. and Zhan, X., A Fully Coupled Model for Water Flow and Airflow in Deformable Porous Media, Water Resour. Res., Vol. 29, No.1, p. 155-167, 1993.

91. Schrefler, B.A., Simoni, L., Li, X. and Zienkiewicz, O.C., Mechanics of Patially Saturated Porous Media, Numerical Methods and Constitutive Modeling in Geomechanics, p. 169-209, 1990.

92. Shu, Z., Bai, M. and Zaman, M., Two-Phase Fluid Flow in Deformable Fractured Formation: Finite-Difference Approach, Report for the Rock Mechanics Research Center, RMRC-98-02, The University of Oklahoma, April, 1998.

93. Snow, D.T., A Parallel Plate Model for Fractured Permeable Media, Ph.D Dissertation, Univ. of California, Berkeley, 1965.

94. Snow, D.T., The Frequency and Apertures of Fractures in Rock, Int. J. Rock Mech. Min. Sci. and Geomech. Abstr., 7, p. 23-40, 1970.

95. Stearns, D.W. and Friedman, M., Reservoirs in Fracture Rock, Am. Assoc. Petrol. Grol., Memoir 16, p. 82-100, 1972.

96. Sun, Y., Sakajo, S. and Nishigaki, M., Application Research on a Numerical Model of Two-Phase Flows in Deformation Porous Medium, Computer Methods and Advances in Geomechanics, p. 1171-1176, Balkema, Rotterdam, 1997.

97. Terzaghi, K., Theory Soil Mechanics, John Wiley & Sons, New York, N.Y., 1943.

98. Thomas, L.K., Dixon, T.N. and Pierson, R.G., Fractured Reservoir Simulation, SPEJ, p. 42-54, 1983.

99. Tsang, Y.W., The Effect of Tortuosity on Fluid Flow Through a Single Fracture, Water REs. Research, 20, No. 9, p. 1209-1215, Sept. 1984.

100. Valliappan, S. and Khalili-Naghadeh, N., Flow through Fissured Porous Media with Deformable Matrix, Int. J. for Num. Methods in Engr., Vol. 29, p. 1079-1094, 1990.

101. van Everdingen, A.F., and Hurst, W., The Application of the Laplace Transformation to Flow Patterns in Reservoirs, Trans. AIME, 186, p. 305-324, 1949.

102. Walsh, J.B., Effect of Pore Pressure and Confining Pressure on Fracture Permeability, Int. J. Rock Mech. Min. Sci. and Geomech. Abstr., 18, p. 429-435, 1981.

103. Wang, Y. and Dusseault, M.B., Borehole Yield and Hydraulic Fracture Initiation in Poorly Consolidation Rock Strata-Part II, Int. J. Rock Mech. Min. Sci. and Geomech. Abstr., Vol. 28, No. 4, p. 247-260, 1991.

104. Warren, J.E. and Root, P.J., The Behavior of Naturally Fractured Reservoirs, SPEJ, Trans., AIME, Vol. 228, p. 245-255, 1963.

105. Wilson, R.K. and Aifantis, E.C., On the Theory of Consolidation with Double Porosity, Int. J. Eng. Sci., Vol. 20, No. 9, p. 1009-1035, 1982.

106. Yamamoto, R.H., Padgett, J.B., Ford, W.J., and Bongeguira, A., Composition Reservoir Simulator for Systems-The Single Block Model, SPEJ, p. 113-128, June 1971.

107. Zienkiewicz, O.C. and Parekh, C.J., Transient Field Problems: Two-Dimensional and Three-Dimensional Analysis by Isoparametric Finite Elements, International Journal of Numerical Methods in Engineering, Vol. 2, p. 61-71, 1970.

108. Zienkiewicz, O.C., The Finite Element Method, McGraw-Hill, 3rd edition, New York, 1977.

109. Zienkiewicz, O.C. and Shiomi, T., Dynamic Behaviour of Saturated Porous Media, the Generalized Biot Formulation and Its Numerical Solution, Int. J. Analytic. Numer. Meth. Geomech., Vol. 8, p. 71-96, 1984.

Appendix A

Fundamental Concepts

In this appendix, a brief explanation of the fundamental concepts which have been used in the foregoing chapters such as porosity and saturation is provided. This would be helpful to someone who is familiar with only part of these concepts. For example, rock mechanics scientists may not know much about reservoir engineering, whereas reservoir engineers may not familiar with rock mechanics terms.

A.1 Porosity

For a rock to form a reservoir, it must have a certain storage capacity, this property is characterized by the *porosity*. This porosity, ϕ, is defined as:

$$\phi = \frac{V_p}{V_t} \times 100\% \tag{A.1}$$

where V_p is the pore volume, and V_t the total volume of the rock.

The porosity of interest to the reservoir engineers, which allows the fluids in the pores to circulate, is the *effective porosity*, ϕ_e, which represents only inter-connected pore spaces.

Also defined is the *total porosity*, ϕ_t, corresponding to all the pores, whether inter-connected or not, and the *residual porosity*, ϕ_r, which only takes account of isolated pores; hence,

$$\phi_t = \phi_e + \phi_r \tag{A.2}$$

The effective porosity of rocks varies between less than 1% to over 40%. It is often stated that the porosity is:

(1) *Low* if $\phi \leq 5\%$;

(2) *Mediocre* if $5\% < \phi \leq 10\%$;

(3) *Average* if $10\% < \phi \leq 20\%$;

(4) *Great* if $20\% < \phi \leq 30\%$; and,

(5) *Excellent* if $\phi > 30\%$.

A distinction is made between intergranular porosity, dissolution porosity (as in limestones, for example), and fractured porosity. For fractured rocks, the fracture porosity related to the rock volume is often much less than 1%.

A.2 Saturation

For a rock to form a reservoir, it must contain a sufficient quantity of hydrocarbons, with a sufficient concentration. In most oil-bearing formations it is believed that the rock was completely saturated with water prior to the invasion and trapping of petroleum. The less dense hydrocarbons are considered to displace water from the interstices of the structurally high part of the formation. However, the oil will not displace all the water which originally occupied these pores. Thus, reservoir rocks normally contain both hydrocarbons and water (frequently referred to as *connate water*) in same or adjacent pores. To determine the quantity of hydrocarbon accumulated in a porous rock formation, it is necessary to determine the fluid saturation (oil, water, and gas) of the rock material.

In the pore volume, V_p, are found a volume V_o of oil, a volume V_w of water, and a volume V_g of gas ($V_p = V_o + V_w + V_g$). The oil, water, and gas saturations are defined as:

$$S_o = \frac{V_o}{V_p} \tag{A.3}$$

$$S_w = \frac{V_w}{V_p} \tag{A.4}$$

$$S_g = \frac{V_g}{V_p} \tag{A.5}$$

expressed in dismal, with:

$$S_o + S_w + S_g = 1.0. \tag{A.6}$$

Knowing the volumes of oil and gas in place in a reservoir requires knowing the saturation at every point, or at least a satisfactory approximation.

A.3 Permeability

For a rock to form a reservoir, the fluids must be able to flow in the rock: this property is characterized by its *permeability*.

The absolute permeability or permeability of a rock represents the ability to allow a fluid to flow through its pores. Permeability can be determined by the experimental Darcy's law.

Consider a sample of length dx and cross-section A, saturated with a fluid of dynamic viscosity μ, and crossed horizontally by a flowrate Q. Under steady-state conditions, the upstream pressure is P, and the downstream pressure is P-dp. The lateral sides are impervious. If the fluid does not react with the rock, which is the general case:

$$Q = -A\frac{k}{\mu}\frac{dp}{dx} \tag{A.7}$$

Equation (A.7) is Darcy's law. k is called the permeability coefficient, and is independent of the type of fluid. It is the absolute or specific permeability of the sample in the direction considered. The range of permeabilities is very wide, it varies from 0.1 mD to more than 10 D. The following terms can be employed to specify the value of the permeability:

(1) ≤ 1 mD: *Very low;*

(2) 1 to 10 mD: *Low;*

(3) 10 to 50 mD: *Mediocre;*

(4) 50 to 200 mD: *Average;*

(5) 200 to 500 mD: *Good; and,*

(6) $>$ 500 mD: *Excellent.*

In hydrocarbon reservoirs, however, the rocks are usually saturated with two or more fluids, such as interstitial water, oil, and gas. It is, therefore, necessary to generalize Darcy's law by introducing the concept of effective permeability to describe the simultaneous flow of more than one fluid. The effective permeability is a relative measure of the conductance of the porous medium to one fluid phase when the medium is saturated with more than one fluid. This definition of effective permeability implies that the medium can have a distinct and measurable conductance to each phase present in the medium. Thus, Darcy's law can be restated as follows:

$$Q_o = -A\frac{k_o}{\mu_o}\frac{dP_o}{dx} \tag{A.8}$$

$$Q_w = -A\frac{k_w}{\mu_w}\frac{dP_w}{dx} \tag{A.9}$$

$$Q_g = -A\frac{k_g}{\mu_g}\frac{dP_g}{dx} \tag{A.10}$$

In the above equation, k_o, k_w, k_g are the effective permeability for oil, water, and gas, respectively.

Effective permeability is a function of the prevailing fluid saturation, the rock-wetting characteristics, and the geometry of the pores in the rock. Owing to the many possible combinations of saturation for a single medium, laboratory data are usually summarized and reported as relative permeability. *Relative permeability* is defined as the ratio of the effective permeability of a fluid at a given value of saturation to the effective permeability of that fluid at 100 percent saturation (absolute permeability). Relative permeability can be expressed symbolically as:

$$k_{ro} = \frac{k_o}{k} \tag{A.11}$$

$$k_{rw} = \frac{k_w}{k} \tag{A.12}$$

$$k_{rg} = \frac{k_g}{k} \tag{A.13}$$

A typical relative permeability curves for oil and water is shown in Figure A.1.

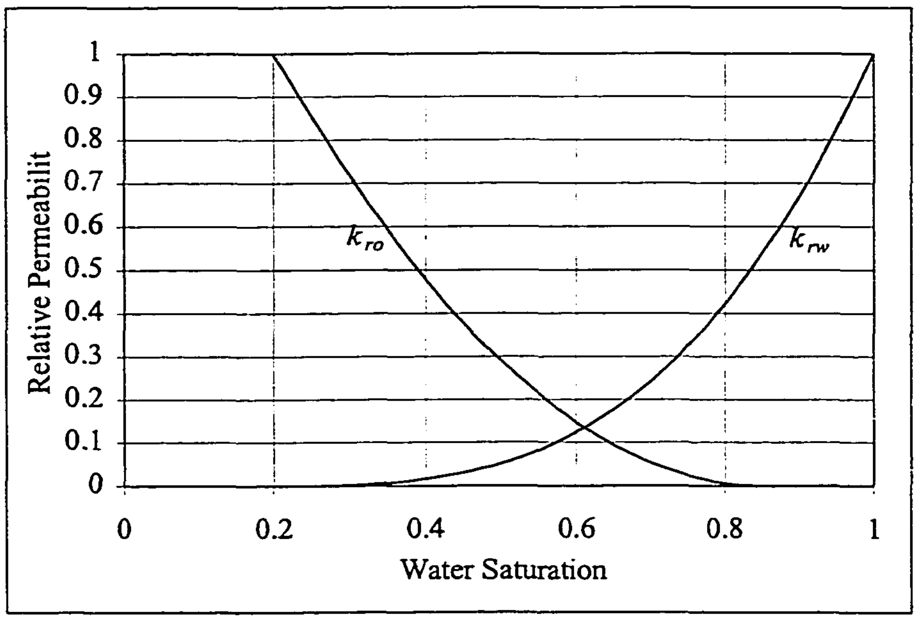

Figure A.1: Typical Relative Permeability Curves.

A.4 Capillary Pressure

Capillary pressure can be qualitatively expressed as the difference in pressure which exists across the interface which separates two immiscible fluids. Conceptually, it is perhaps easier to think of it as the suction capacity of a rock for a fluid that wets the rock, or the capacity of a rock to repel a non-wetting fluid. Quantitatively, capillary pressure will be defined as the difference between pressure in the oil phase and pressure in the water phase, i.e.,

$$P_c = P_o - P_w \tag{A.14}$$

The importance of capillary pressure to reservoir engineering is as follows:

1. Capillary pressure data are needed to describe waterflood behavior in more complex prediction models;
2. Capillary forces, along with gravity forces, control the vertical distribution of fluids in a reservoir. Capillary pressure data can be used to predict the vertical water distribution in a water-wet system;
3. Capillary pressure data provided an indication of the pore size distribution in a reservoir;
4. Capillary forces influence the movement of a waterflood front and, consequently, the ultimate displacement efficiency; and,
5. Capillary forces determine connate water saturation.

Figure A.2 shows a typical capillary pressure curve for a water-air system.

A.5 Formation Volume Factor

The volume of oil which enters the stock tank at the surface is less that the volume of oil which flows into the wellbore from the reservoir. This change in oil volume which accompanies the change from reservoir to surface conditions is due to the following three factors:

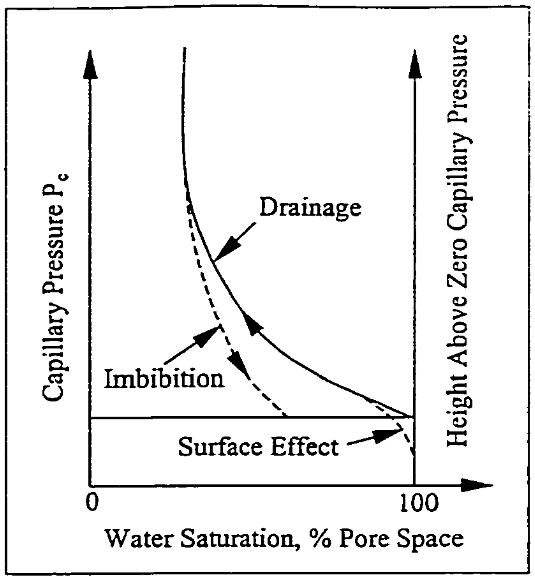

Figure A.2: Capillary Pressure Curve.

1. evolution of gas from the oil as pressure is decreased from reservoir to surface pressure. This causes a rather large decrease in volume of the oil when there is a significant amount of dissolved gas;

2. reduction in pressure also causes the remaining oil to expand slightly, but this is somewhat offset by the following factor.

3. contraction of the oil due to the reduction of temperature; and,

The change in oil volume due to these three factors is expressed in terms of the *formation volume factor* of oil. It is defined as the volume of reservoir oil required to produce one barrel of oil in the stock tank. Because the reservoir oil includes dissolved gas,

$$B_o = \frac{\text{Volume of oil + dissolved gas leaving at reservoir conditions}}{\text{Volume of oil entering stock tank at standard conditions}} \tag{A.15}$$

Another way to express the formation volume factor of oil is that it is the volume of reservoir occupied by one stock tank barrel plus the gas in solution at reservoir temperature and pressure.

The relationship of formation volume factor of oil to reservoir pressure for a typical black oil is given in Figure A.3.

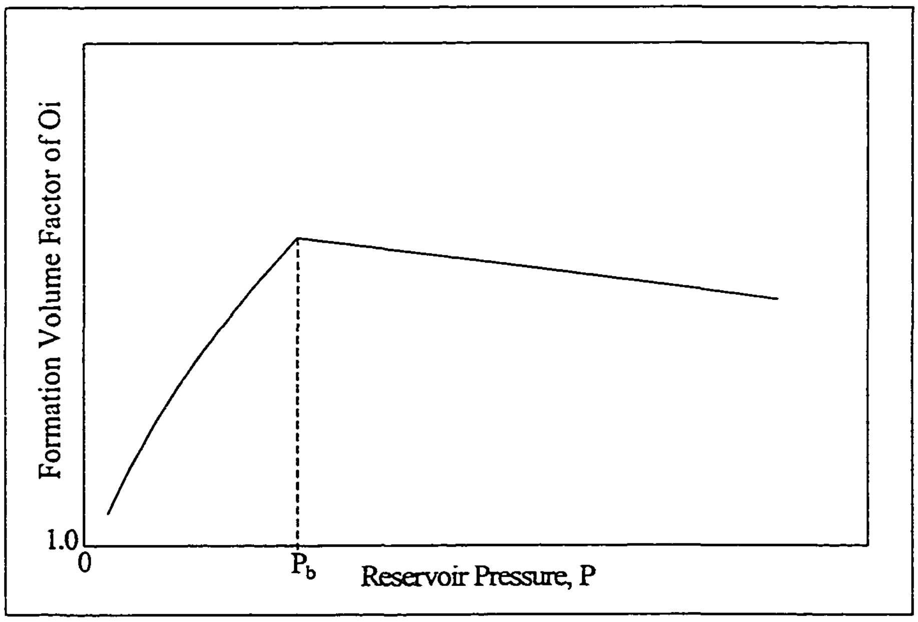

Figure A.3: Typical Shape of Formation Volume Factor of a Black Oil.

This figure shows the initial reservoir pressure to be above the bubble-point pressure of the oil. As reservoir pressure is decreased from initial pressure to bubble-point pressure, the formation volume factor increases slightly because of the expansion of the liquid in the reservoir.

A reduction in reservoir pressure below bubble-point pressure results in the evolution of gas in the pore spaces of the reservoir. The liquid remaining in the reservoir has less gas in solution and, consequently, a smaller formation volume factor. Formation volume factor is also sometimes called *reservoir volume factor*.

A.6 Solution Gas-Oil Ratio

The quantity of gas dissolved in oil at reservoir conditions is called *solution gas-oil ratio*. The solution gas-oil ratio is the amount of gas that evolves from the oil as oil is transported from reservoir to surface conditions. This ratio is defined in terms of the quantities of gas and oil which appears at the surface during production.

$$R_s = \frac{\text{Volume of gas produced at surface at standard conditions}}{\text{Volume of oil entering stock tank at stand conditions}} \tag{A.16}$$

Solution gas-oil ratio is also called *dissolved gas-oil ratio* and occasionally *gas solubility*.

Figure A.4 shows the way the solution gas-oil ratio of a typical black oil changes as reservoir pressure is reduced at constant temperature. The line is horizontal at pressures above the bubble-point pressure, P_b, because at these pressures no gas is released in the pore space and the entire liquid mixture is produced into the wellbore. When reservoir pressure is reduced below this bubble-point pressure, gas evolves in the reservoir, leaving less gas dissolved in the liquid.

A.7 Fractured Reservoirs

A.7.1 Definition

A reservoir fracture is a naturally occurring macroscopic planar discontinuity in the rock mass due to deformations or physical diageneses. For practical reasons, it is assumed to have been initially open, but may have been subsequently altered or mineralized. It may, therefore, have either a positive or negative effect on fluid flow within the formation. A fractured reservoir is a reservoir in which naturally occurring fractures have a significant effect on reservoir fluid flow either in the form of increased reservoir permeability and/or porosity or increased permeability

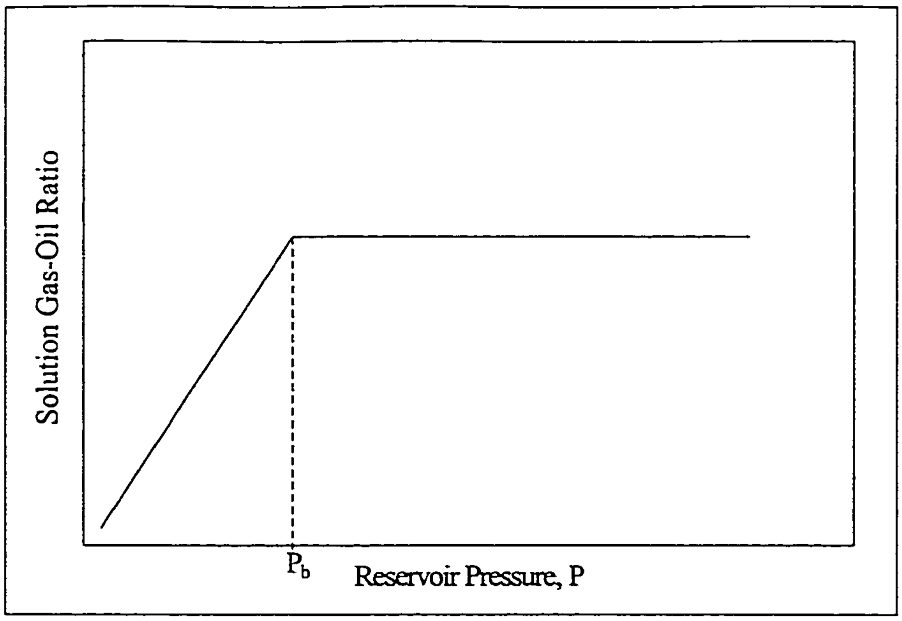

Figure A.4: Typical Shape of Solution Gas-Oil Ratio of a Black Oil.

anisotropy.

A.7.2 Origin

The origin of the fracture system is postulated from data on fracture dip, morphology, strike (if available), relative abundance, and the angular relationships between fractures sets. These data can be obtained from full-diameter core (oriented or conventional), borehole televiewer output, or other less oriented logging tools, and applied to empirical models of fracture generation. Available fracture models range from tectonic to others that are primarily diagenetic in origin. It is only by a proper fit of fracture data to one of these genetic models that any effective extrapolation or intrapolation of fracture distributions can be made. The interpretation of the fractures origin involves a combined geological/rock mechanics approach to the problem. It is assumed that natural fracture patterns depict the local state of stress at the time of fracturing, and that subsurface rocks fracture in a manner qualitatively similar to equivalent rocks in laboratory tests performed at analogous simulated environmental conditions. Natural fracture patterns are interpreted in light of laboratory-derived fracture patterns (Handin and Hager, 1957), and in terms of postulated paleostress fields and strain distributions at the time of fracturing. In general, any physical or mathematical model of deformations that depicts stress or strain fields can, by various levels of extrapolation, be used as a fracture distribution model (Hafner, 1951).

A genetic classification scheme for natural fracture systems, which is an expansion of that found in Stearns and Friedman (1972), permits separation of complicated natural fracture systems into superimposed components of different origin. Such partitioning can make delineation of structures (Friedman, 1969; Friedman and Stearns, 1971) and prediction of increased fractured-related reservoir quality (McCaleb and Willingham, 1967; Stearns and Friedman, 1972) from fracture data more tractable. Stearns and Friedman (1972) classify fractures into those observed in laboratory experiments and those observed in outcrop and subsurface settings. Their classification scheme, together with modifications suggested by Nelson (1985), forms a useful basis for fracture models (Table A.1). Nelson's major modification to Stearns's and Friedman's scheme is the addition of two categories of naturally occurring fractures: contractional fractures and surface-related fractures. A minor modification to the experimental fracture classification is the addition of a category similar to extension fractures in morphology and orientation but having a different stress state at generation time.

Table A.1: Experimental and Natural Fracture Classification

Experimental Fracture Classification	1. Shear fractures
	2. Extension fractures
	3. Tension fractures
Naturally Occurring Fracture Classification	1. Tectonic fractures (due to surface forces)
	2. Regional fractures (due to surface forces)
	3. Contractional fractures (due to body forces)
	4. Surface related fractures (due to body firces)

A.8 Stress and Strain

The concepts of stress and strain, in their simplest form, involve a mathematical abstraction for specifying the interaction between one part of a continuous material body and another. These abstractions involve the ideas of vector and tensor fields. Recall that a scalar is a mathematical entity that has only a magnitude assigned to it; temperature for example. Scalar quantities are treated mathematically as a tensor of rank zero. Vector quantities, on the other hand, possess a magnitude and a direction of action. Velocity, for example, is a vector quantity and can be treated mathematically as a tensor of rank 1.

Stress, σ, is defined as the amount of forces ΔF applied on an area ΔA as ΔA approaches zero:

$$\sigma = \lim_{\Delta A \to 0} \frac{\Delta F}{\Delta A} \tag{A.17}$$

Stress is frequently measured in Pa (= Pascal = N/m^2), bar, atmosphere, psi(= lb/inch^2), or dynes/cm^2. The SI unit Pa is most comfortable, while the others are mostly used in engineering calculations.

The sign of the stress σ is not uniquely defined by the physics of the situation, and has, therefore, to be defined by convention: in rock mechanics, compressive stresses are taken as positive. The historical reason for this is probably that the stresses in the earth's crust are almost exclusively compressive.

An ordered arrangement of vectors about a point can be treated mathematically as a tensor of rank two. The state of stress, for example, is a shorthand way of describing the infinite array of force vectors about an infinitesimal point within a body. This mathematical description of a vector array requires the definition of only nine vector components of the infinite array in order to define all others. At equilibrium, the nine vector components needed to describe the state of stress reduce to six. Of these six, three are defined as normal stress components (σ) and three are defined as shear stress components (τ) as shown in Equations A.18-A.20. In one particular frame of reference, the normal stresses become principal normal stresses ($\sigma_1, \sigma_2, \sigma_3$ or maximum, intermediate, and minimum normal components), and effectively reduce the tensor to three components.

In general,

$$\sigma_{i,j} = \begin{vmatrix} \sigma_{11} & \tau_{12} & \tau_{13} \\ \tau_{13} & \sigma_{22} & \tau_{23} \\ \tau_{31} & \tau_{32} & \sigma_{33} \end{vmatrix} \tag{A.18}$$

When at equilibrium $\tau_{12} = \tau_{21}, \tau_{13} = \tau_{31}, \tau_{23} = \tau_{32}$,

$$\sigma_{i,j} = \begin{vmatrix} \sigma_{11} & \tau_{12} & \tau_{13} \\ - & \sigma_{22} & \tau_{23} \\ - & - & \sigma_{33} \end{vmatrix} \tag{A.19}$$

When the coordinate axes are the principal axes and the remaining components are the principal stresses,

$$\sigma_{i,j} = \begin{vmatrix} \sigma_{11} & 0 & 0 \\ 0 & \sigma_{22} & 0 \\ 0 & 0 & \sigma_{33} \end{vmatrix} \tag{A.20}$$

The state of strain involves a similar treatment using a tensor of rank two to describe the infinite array of displacement vectors about a similar infinitesimal point within a deformed body.

Strain, ε, is defined as the amount of elongation of a fiber, $\Delta\delta$, divided by its original length, ΔL as ΔL approach zero,

$$\varepsilon = \lim_{\Delta L \to 0} \frac{\Delta\delta}{\Delta L} \tag{A.21}$$

The entities that describe the changes in the state of stress and strain and their vector components from point to point within the body are the stress and strain fields (tensor fields). A feeling for fields and the vector components that make up the state of stress or strain in a body can be gained through the manipulation of small magnets. If one slowly brings the two like poles of a pair of magnets together from various directions, holding one stationary and moving the other, a tactile sense of the infinite array of magnetic force vectors can be obtained. The perception of force intensity changes with varying distance and orientation of the magnets gives one a physical analogy to the stress-field concept.

A.8.1 Stress-Strain Relationships

The state of stress at a point and the stress field throughout a body are mathematical descriptions of the forces within a body and how they interact and change from point to point. The state of strain at a point and the strain field mathematical descriptions of the displacements due to temporary or permanent deformations within a body and how they interact and change from point to point. The states of stress and strain and their fields within a body are not independent but are directly related to one another. The functional relationships relating stress and strain in various types of materials are defined by *constitutive equations.* These constitutive relationships include those defined by the theories of elasticity, plasticity, viscosity and various syntheses of the three.

The constitutive equations are, for the most part, based ultimately on empiricism or experimentation. Material samples are subjected to loads of various magnitudes and configurations and particular subsequent displacements measured. The loads and displacements are equated to stress and strain components and generally plotted graphically in a manner similar to that shown in Figure A.5. It is the form of curves like these that are the basis of most constitutive equations.

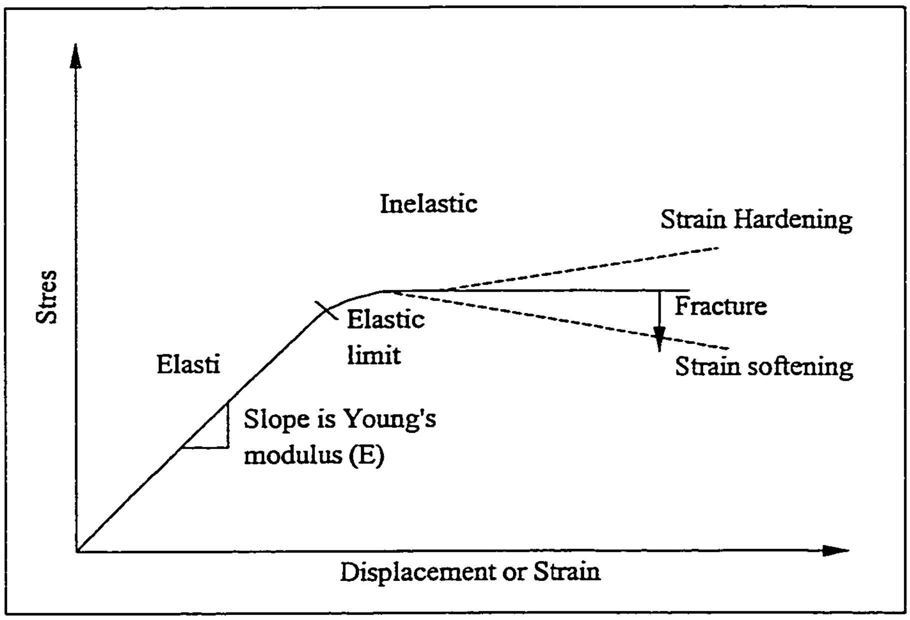

Figure A.5: General Form of Stress-Strain Curve for Rock with Both Elastic and Inelastic Portions Shown.

Elasticity

Elasticity is a theory that entails a constitutive relationship for a solid body that obeys Hooke's law or behaves elastically. This law states that the stress tensor (state of stress at an infinitesimal point) is linearly proportional to the strain tensor (state of strain at an infinitesimal point) and that the body return to its original shape and dimensions when all external loads are removed. Mathematically,

$$\sigma_{i,j} = E_{ijkl}\varepsilon_{kl} \tag{A.22}$$

Where $\sigma_{i,j}$ is the stress tensor, E_{ijkl} is the elastic moduli and ε_{kl} is the strain tensor. The stress and strain tensors contain nine vector components each, while the elastic moduli tensor (a tensor of rank three) contains eighty-one such components. However, assumptions involving equilibrium, symmetry, and isotropy can reduce the stress and strain tensors to six independent components each and the elastic constant tensor to two (the Lamé's constants).

Perfectly elastic behavior would be characterized by a stress-strain curve that is linear, with a positive slope (constant and positive Young's modulus) and an immediate return to its initial stress-strain point upon complete unloading, Figure A.6. Modification of ideal elasticity include *hysteresis* in the unloading curve, Figure A.7, and time-dependent recovery of all strains or displacements with a nonlinear but complete recoverable portion to the stress-strain curve, Figure A.8.

Plasticity

Plasticity is a theory that entails a constitutive relationship for a solid body that behaves in a fully ductile manner (flow), or plastically. Ideally, upon loading the material deforms elastically up to a yield stress past which the material displaces or strains indefinitely without sustaining additional load (σ_1 = yield stress). The characteristic stress-strain behavior is indicated by a horizontal portion of the stress-strain curve, Figure A.9. Modification to this behavior include positive slope, strain hardening, Figure A.10. All plastic strains or displacements are nonrecoverable. True plastic behavior in rocks is generally restricted to relatively weak, ductile rocks, such as clay-rich shales and some unconsolidated sands and tuffs.

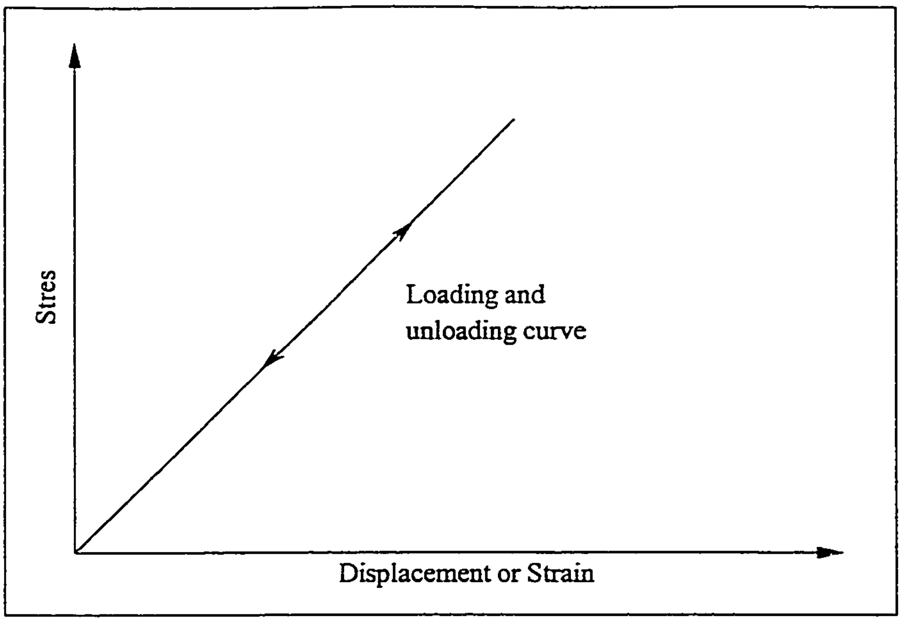

Figure A.6: Perfectly Linear Elastic Behavior.

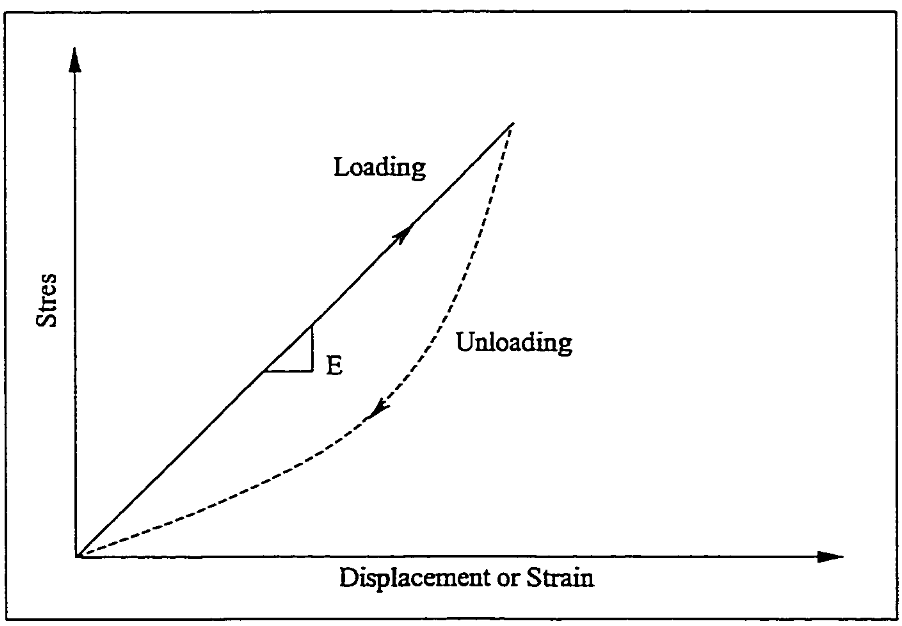

Figure A.7: Linear Elastic Behavior with Hysteresis in the Unloading Curve.

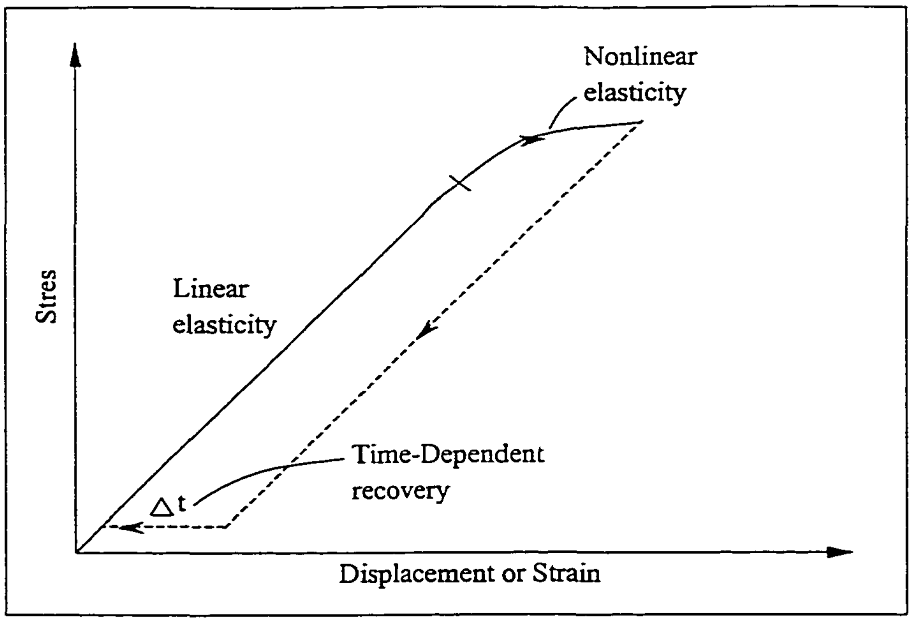

Figure A.8: Non-Linear Elastic Behavior with a Time-Dependent Recovery.

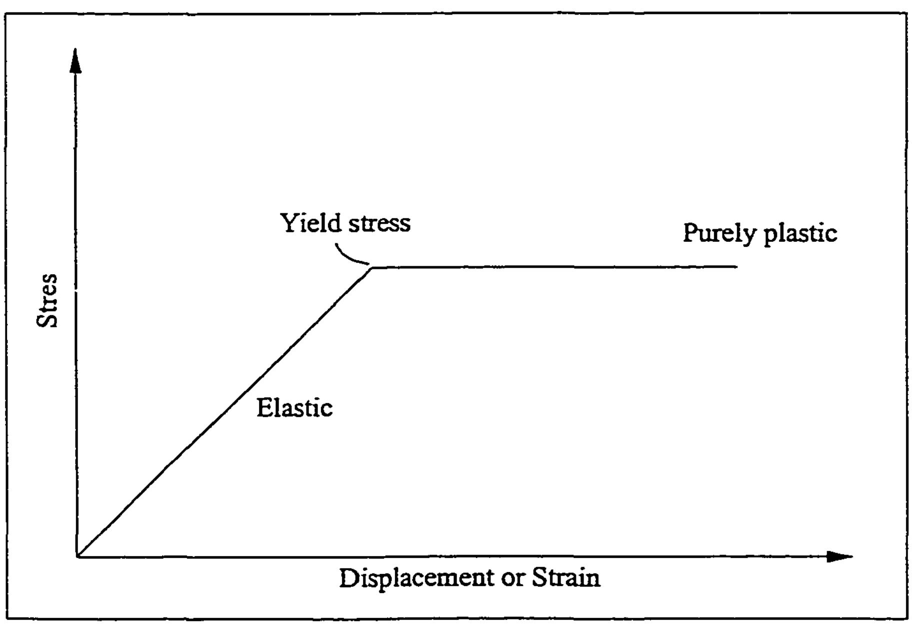

Figure A.9: Purely Plastic Behavior.

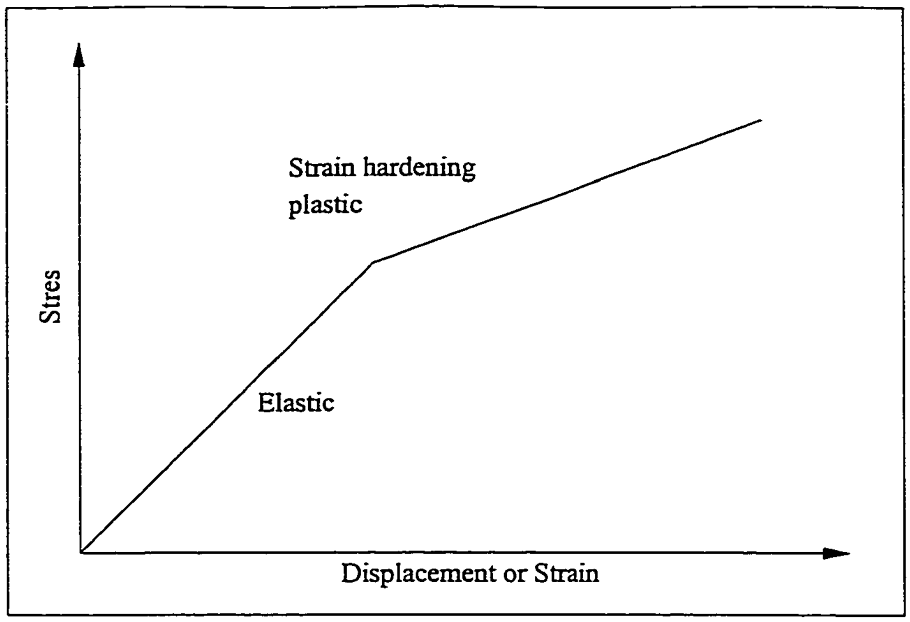

Figure A.10: Strain Hardening Plactic Behavior.

Viscosity

Viscosity is a theory that entails a constitutive relationship for a solid body that behaves like a Newtonian viscous fluid or in a viscous manner. Ideally, it relates stress to strain rate in a linear manner (refer to Figure A.11), i.e.:

$$\sigma_{i,j} = n_{ijkl}\, \dot{\varepsilon}_{kl} \tag{A.23}$$

Where n_{ijkl} is the viscosity tensor and $\dot{\varepsilon}_{kl}$ is the strain rate tensor

The viscosity of rocks is hard to determine. It is usually derived from long-term creep tests at either constant load or constant strain rate. For simplicity, assumptions of isotropy and incompressibility allow the viscosity tensor to be reduced to a single value for any particular rock.

The viscous constitutive relationship is generally applied to the response of rocks to long-term loading, such as over geological time. Modifications of this constitutive relationship include nonlinear viscosity and temperature-dependent viscosity (refer to Figure A.12).

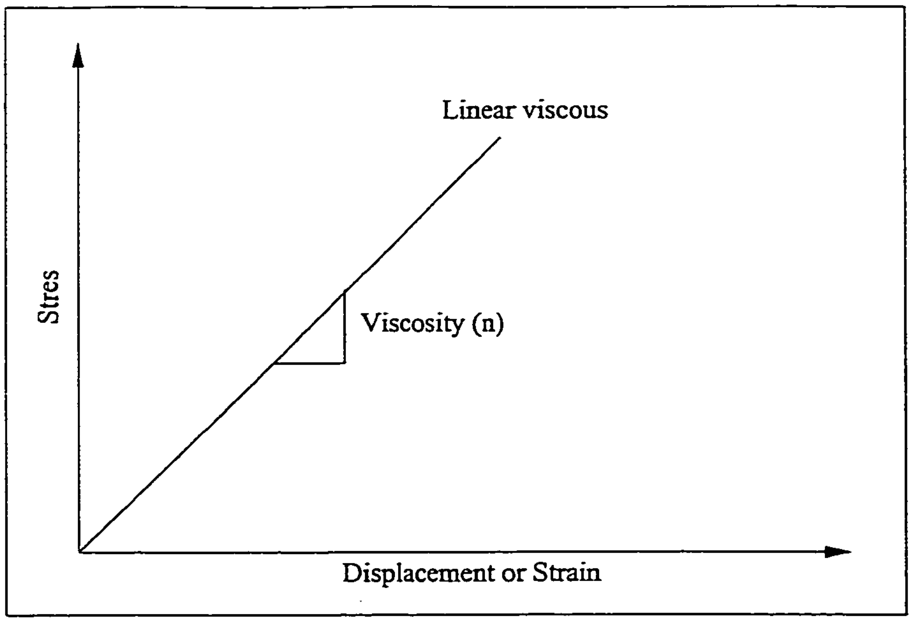

Figure A.11: Linear Viscous Behavior.

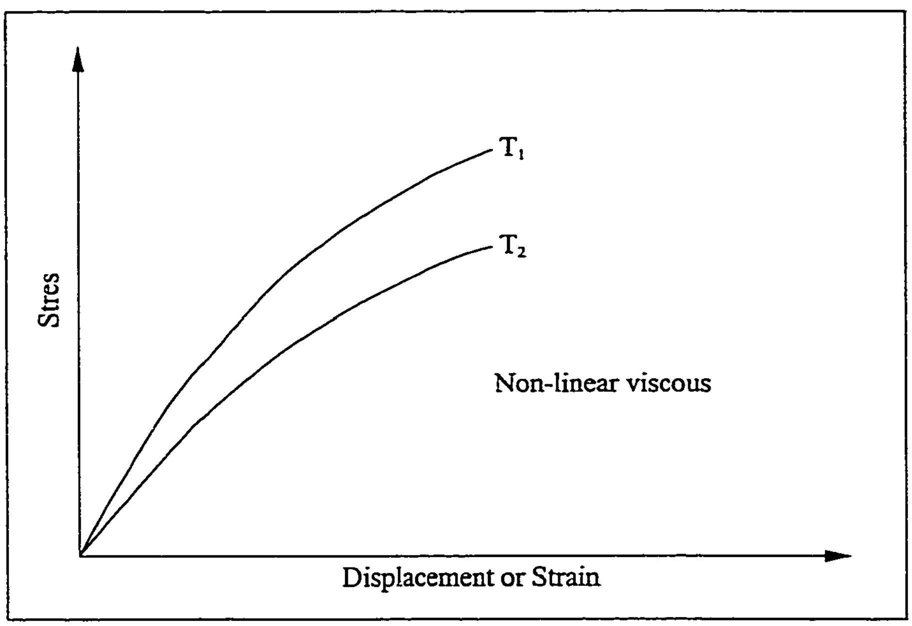

Figure A.12: Non-Linear Viscous Behavior with the Effect of Tepperature ($T_1 < T_2$).

Mixtures

Most rocks do not strain in response to stress (or vice versa) according to any of the three ideal constitutive relationships. Indeed, most rocks exhibit much more complex behavior than any of the simple ones discussed above. As a result, experimentalists and theoreticians often model rock stress-strain behavior with a mixture of the ideal relationships, such as viscoelastic, elastico-plastic, and visco-plastic behavior, to name a few. In these approaches, portions of the stress-strain curves for a rock are assigned a constitutive behavior analogous to its form, and these behavior elements are added or amalgamated into a combined relationship meant to mimic the real rock response.

In this dissertation, a rock is assumed, for simplicity, to behave elastically.

A.9 Poroelasticity

In most petroleum engineering applications, rocks are expected to have their pore spaces saturated with liquids and/or gases. When fluid permeates, rocks undergo a disturbance from their initial state of stress or pore pressure, and intricate coupled mechanical and hydraulic processes will occur. For example, a perturbation in the fluid pore pressure, in a saturated rock, will cause fluid flow towards the least pressurized regions, while simultaneously the rock under the *effective stress* disturbance will undergo deformations. The simplest theory that would take into account of the coupled deformation-diffusion phenomena in rock masses, is the theory of poroelasticity derived by Biot in 1941.

According to this theory, when a porous material of connective solid structure, such as rock, is subjected to an increment in compressive stress, a volumetric deformation will take place. The deformation actually consists of two components:

1. deformations of the solid skeleton; and,

2. change in the pore spaces.

If the rock pore spaces are permeated by a compressible fluid, the fluid will initially resist deformation, and give rise to an uneven fluid pore pressure whose magnitude is inversely proportional to the fluid compressibility. Whenever there is a change in fluid pore pressure, a variation in the effective stress applied on the solid skeleton will take place. The solid must further deform to accommodate the equilibrium and the compatibility requirements.

From the solid deformation point of view, two material coefficients, Young's modulus E and Poisson's ratio ν, are necessary and sufficient to describe the linear, isotropic mechanical deformation. For the fluid flow in porous media, the mobility coefficient, κ, alone characterizes the dissipative fluid flow effect. However, these three parameters are not sufficient to characterize a poroelastic material. Two more independent coefficients, Skempton's pore pressure coefficient, B, and Biot's effective stress coefficient, α, are needed for describing the coupling phenomena between the mechanical and hydraulic processes.

Skempton's pore pressure coefficient, B, is defined as the ratio of the induced pore pressure P_p over the increment of the average confining pressure P under undrained condition, i.e.,

$$B = \frac{P_p}{P} \tag{A.24}$$

Its value is related to the compressibility of the solid, fluid, and skeleton, and normally varies between the range $0 \leq B \leq 1$. The upper rage B=1 is reached for an incompressible fluid. On the other hand, $B \approx 0$ if the fluid is considered very compressible (such as gas).

As an extension of the linear theory of elasticity, Biot derived the theory of poroelasticity, assuming an elastic continuous porous medium, fully saturated with fluid.

The Biot's effective stress $\sigma'_{i,j}$ is defined as :

$$\sigma'_{i,j} = \sigma_{i,j} - \alpha\delta_{i,j}P \tag{A.25}$$

where $\sigma_{i,j}$ is the total stress, P is the pore pressure acting on the solid grains, and α is known as the Biot's constant, which can be evaluated approximately by:

$$\alpha = 1 - \frac{K_t}{K_s} \tag{A.26}$$

where K_s and K_t are the bulk moduli of solid grains and the skeleton respectively.

Appendix B

Forty-eight equations for the boundaries and the corners

B.1 Case 1 Two-Phase Flow Coupled with Solid Deformations in a Fractured Rock

- Boundary $i = 1$

Equation 1

$$-2(a_1 + a_2)u_{i,j} + 2a_1 u_{i+1,j} + a_2 u_{i,j+1} + a_2 u_{i,j-1} = 0 \tag{B.1}$$

Equation 2

$$\begin{aligned}
& -2(b_1 + b_2)v_{i,j} + 2b_1 v_{i+1,j} + b_2 v_{i,j+1} + b_2 v_{i,j-1} - b_4 p_{mi,j-1} + b_4 p_{mi,j+1} \\
& -b_5 p_{fi,j-1} + b_5 p_{fi,j+1} - b_{6i,j} S_{mi,j-1} + b_{6i,j} S_{mi,j+1} - b_{7i,j} S_{fi,j-1} + b_{7i,j} S_{fi,j+1} \\
= \; & b_{8i,j}(p_{cmi,j+1} - p_{cmi,j-1}) + b_{9i,j}(p_{cfi,j+1} - p_{cfi,j-1})
\end{aligned} \tag{B.2}$$

Equation 3

$$\begin{aligned}
& c_{15i,j} p_{mi,j} - (c_{1i,j} + c_{2i,j}) p_{mi+1,j} - c_{3i,j} p_{mi,j+1} - c_{4i,j} p_{mi,j-1} \\
& +(c_{10i,j} - c_{7i,j}) p_{fi,j} + c_{9i,j} v_{i,j+1} - c_{9i,j} v_{i,j-1} + c_{11i,j} S_{mi,j} + c_{12i,j} S_{fi,j} \\
= \; & c_{14i,j} p_{mi,j} + c_{10i,j} p_{fi,j} + c_{11i,j} S_{mi,j} + c_{12i,j} S_{fi,j} \\
& +c_{9i,j} v_{i,j+1} - c_{9i,j} v_{i,j-1} + c_{13i,j} p_{cmi,j} - (c_{1i,j} + c_{2i,j}) p_{cmi+1,j} \\
& -c_{3i,j} p_{cmi,j+1} - c_{4i,j} p_{cmi,j-1} - c_{7i,j} p_{cfi,j}
\end{aligned} \tag{B.3}$$

Equation 4

$$
\begin{aligned}
& d_{15i,j}p_{mi,j} - (d_{1i,j} + d_{2i,j})p_{mi+1,j} - d_{3i,j}p_{mi,j+1} - d_{4i,j}p_{mi,j-1} \\
& +(d_{10i,j} - d_{7i,j})p_{fi,j} + d_{9i,j}v_{i,j+1} - d_{9i,j}v_{i,j-1} + d_{11i,j}S_{mi,j} + d_{12i,j}S_{fi,j} \\
= \; & d_{14i,j}p_{mi,j} + d_{10i,j}p_{fi,j} + d_{11i,j}S_{mi,j} \\
& +d_{12i,j}S_{fi,j} + d_{9i,j}v_{i,j+1} - d_{9i,j}v_{i,j-1} \qquad \text{(B.4)}
\end{aligned}
$$

Equation 5

$$
\begin{aligned}
& e_{15i,j}p_{fi,j} - (e_{1i,j} + e_{2i,j})p_{fi+1,j} - e_{3i,j}p_{fi,j+1} - e_{4i,j}p_{fi,j-1} \\
& +(e_{10i,j} - e_{7i,j})p_{mi,j} + e_{9i,j}v_{i,j+1} - e_{9i,j}v_{i,j-1} + e_{11i,j}S_{fi,j} + e_{12i,j}S_{mi,j} \\
= \; & e_{14i,j}p_{fi,j} + e_{10i,j}p_{mi,j} + e_{11i,j}S_{fi,j} + e_{12i,j}S_{mi,j} + e_{9i,j}v_{i,j+1} \\
& -e_{9i,j}v_{i,j-1} + e_{13i,j}p_{cfi,j} - (e_{1i,j} + e_{2i,j})p_{cfi+1,j} \\
& -e_{3i,j}p_{cfi,j+1} - e_{4i,j}p_{cfi,j-1} - e_{7i,j}p_{cmi,j} \qquad \text{(B.5)}
\end{aligned}
$$

Equation 6

$$
\begin{aligned}
& f_{15i,j}p_{fi,j} - (f_{1i,j} + f_{2i,j})p_{fi+1,j} - f_{3i,j}p_{fi,j+1} - f_{4i,j}p_{fi,j-1} \\
& +(f_{10i,j} - f_{7i,j})p_{mi,j} + f_{9i,j}v_{i,j+1} - f_{9i,j}v_{i,j-1} + f_{11i,j}S_{fi,j} + f_{12i,j}S_{mi,j} \\
= \; & f_{14i,j}p_{fi,j} + f_{10i,j}p_{mi,j} + f_{11i,j}S_{fi,j} \\
& +f_{12i,j}S_{mi,j} + f_{9i,j}v_{i,j+1} - f_{9i,j}v_{i,j-1} \qquad \text{(B.6)}
\end{aligned}
$$

- Boundary $i = N_x$

Equation 1

$$
\begin{aligned}
& -2(a_1 + a_2)u_{i,j} + a_2u_{i,j+1} + a_2u_{i,j-1} + 2a_3v_{i-1,j-1} - 2a_3v_{i-1,j+1} \\
& \qquad +2a_3v_{i,j+1} - 2a_3v_{i,j-1} = 0 \qquad \text{(B.7)}
\end{aligned}
$$

Equation 2

$$\begin{aligned}
& -2b_2v_{i,j} + b_2v_{i,j+1} + b_2v_{i,j-1} + 2b_3u_{i-1,j-1} - 2b_3u_{i-1,j+1} \\
& -b_4p_{mi,j-1} + b_4p_{mi,j+1} - b_5p_{fi,j-1} + b_5p_{fi,j+1} - b_{6i,j}S_{mi,j-1} \\
& +b_{6i,j}S_{mi,j+1} - b_{7i,j}S_{fi,j-1} + b_{7i,j}S_{fi,j+1} \\
= \; & b_{8i,j}(p_{cmi,j+1} - p_{cmi,j-1}) + b_{9i,j}(p_{cfi,j+1} - p_{cfi,j-1}) \qquad \text{(B.8)}
\end{aligned}$$

Equation 3

$$\begin{aligned}
& c_{15i,j}p_{mi,j} - (c_{1i,j} + c_{2i,j})p_{mi-1,j} - c_{3i,j}p_{mi,j+1} - c_{4i,j}p_{mi,j-1} \\
& +(c_{10i,j} - c_{7i,j})p_{fi,j} - 2c_{8i,j}u_{i-1,j} + c_{9i,j}v_{i,j+1} - c_{9i,j}v_{i,j-1} \\
& +c_{11i,j}S_{mi,j} + c_{12i,j}S_{fi,j} \\
= \; & c_{14i,j}p_{mi,j} + c_{10i,j}p_{fi,j} + c_{11i,j}S_{mi,j} + c_{12i,j}S_{fi,j} - 2c_{8i,j}u_{i-1,j} \\
& +c_{9i,j}v_{i,j+1} - c_{9i,j}v_{i,j-1} + c_{13i,j}p_{cmi,j} - (c_{1i,j} + c_{2i,j})p_{cmi-1,j} \\
& -c_{3i,j}p_{cmi,j+1} - c_{4i,j}p_{cmi,j-1} - c_{7i,j}p_{cfi,j} \qquad \text{(B.9)}
\end{aligned}$$

Equation 4

$$\begin{aligned}
& d_{15i,j}p_{mi,j} - (d_{1i,j} + d_{2i,j})p_{mi-1,j} - d_{3i,j}p_{mi,j+1} - d_{4i,j}p_{mi,j-1} \\
& +(d_{10i,j} - d_{7i,j})p_{fi,j} - 2d_{8i,j}u_{i-1,j} + d_{9i,j}v_{i,j+1} - d_{9i,j}v_{i,j-1} \\
& +d_{11i,j}S_{mi,j} + d_{12i,j}S_{fi,j} \\
= \; & d_{14i,j}p_{mi,j} + d_{10i,j}p_{fi,j} + d_{11i,j}S_{mi,j} + d_{12i,j}S_{fi,j} - 2d_{8i,j}u_{i-1,j} \\
& +d_{9i,j}v_{i,j+1} - d_{9i,j}v_{i,j-1} \qquad \text{(B.10)}
\end{aligned}$$

Equation 5

$$\begin{aligned}
& e_{15i,j}p_{fi,j} - (e_{1i,j} + e_{2i,j})p_{fi-1,j} - e_{3i,j}p_{fi,j+1} - e_{4i,j}p_{fi,j-1} \\
& +(e_{10i,j} - e_{7i,j})p_{mi,j} - 2e_{8i,j}u_{i-1,j} + e_{9i,j}v_{i,j+1} - e_{9i,j}v_{i,j-1} \\
& +e_{11i,j}S_{fi,j} + e_{12i,j}S_{mi,j}
\end{aligned}$$

$$
\begin{aligned}
= \ & e_{14i,j}p_{fi,j} + e_{10i,j}p_{mi,j} + e_{11i,j}S_{fi,j} + e_{12i,j}S_{mi,j} - 2e_{8i,j}u_{i-1,j} \\
& + e_{9i,j}v_{i,j+1} - e_{9i,j}v_{i,j-1} + e_{13i,j}p_{cfi,j} - (e_{1i,j} + e_{2i,j})p_{cfi-1,j} \\
& - e_{3i,j}p_{cfi,j+1} - e_{4i,j}p_{cfi,j-1} - e_{7i,j}p_{cmi,j} \qquad \text{(B.11)}
\end{aligned}
$$

Equation 6

$$
\begin{aligned}
& f_{15i,j}p_{fi,j} - (f_{1i,j} + f_{2i,j})p_{fi-1,j} - f_{3i,j}p_{fi,j+1} - f_{4i,j}p_{fi,j-1} \\
& + (f_{10i,j} - f_{7i,j})p_{mi,j} - 2f_{8i,j}u_{i-1,j} + f_{9i,j}v_{i,j+1} - f_{9i,j}v_{i,j-1} \\
& + f_{11i,j}S_{fi,j} + f_{12i,j}S_{mi,j} \\
= \ & f_{14i,j}p_{fi,j} + f_{10i,j}p_{mi,j} + f_{11i,j}S_{fi,j} + f_{12i,j}S_{mi,j} - 2f_{8i,j}u_{i-1,j} \\
& + f_{9i,j}v_{i,j+1} - f_{9i,j}v_{i,j-1} \qquad \text{(B.12)}
\end{aligned}
$$

- Boundary $j = 1$

Equation 1

$$
\begin{aligned}
& -2a_1u_{i,j} + a_1u_{i+1,j} + a_1u_{i-1,j} - a_4p_{mi-1,j} + a_4p_{mi+1,j} - a_5p_{fi-1,j} \\
& + a_5p_{fi+1,j} - a_{6i,j}S_{mi-1,j} + a_{6i,j}S_{mi+1,j} - a_{7i,j}S_{fi-1,j} + a_{7i,j}S_{fi+1,j} \\
= \ & a_{8i,j}(p_{cmi+1,j} - p_{cmi-1,j}) + a_{9i,j}(p_{cfi+1,j} - p_{cfi-1,j}) \qquad \text{(B.13)}
\end{aligned}
$$

Equation 2

$$
\begin{aligned}
& -2(b_1 + b_2)v_{i,j} + b_1v_{i+1,j} + b_1v_{i-1,j} + 2b_2v_{i,j+1} - b_2c \\
& + 2b_3u_{i-1,j} - 2b_3u_{i-1,j+1} + 2b_3u_{i+1,j+1} - 2b_3u_{i+1,j} \\
& + 2b_4p_{mi,j+1} + 2b_5p_{fi,j+1} + 2b_{6i,j}S_{mi,j+1} + 2b_{7i,j}S_{fi,j+1} \\
= \ & 2b_{8i,j}p_{cmi,j+1} + 2b_{9i,j}p_{cfi,j+1} \qquad \text{(B.14)}
\end{aligned}
$$

Equation 3

$$
c_{15i,j}p_{mi,j} - c_{1i,j}p_{mi+1,j} - c_{2i,j}p_{mi-1,j} - (c_{3i,j} - c_{4i,j})p_{mi,j+1}
$$

$$
\begin{aligned}
&+(c_{10i,j} - c_{7i,j})p_{fi,j} + c_{8i,j}u_{i+1,j} - c_{8i,j}u_{i-1,j} + c_{11i,j}S_{mi,j} + c_{12i,j}S_{fi,j} \\
= \;& c_{14i,j}p_{mi,j} + c_{10i,j}p_{fi,j} + c_{11i,j}S_{mi,j} + c_{12i,j}S_{fi,j} + c_{8i,j}u_{i+1,j} \\
&-c_{8i,j}u_{i-1,j} + c_{13i,j}p_{cmi,j} - c_{1i,j}p_{cmi+1,j} - c_{2i,j}p_{cmi-1,j} \\
&-(c_{3i,j} - c_{4i,j})p_{cmi,j+1} - c_{7i,j}p_{cfi,j}
\end{aligned} \tag{B.15}
$$

Equation 4

$$
\begin{aligned}
&d_{15i,j}p_{mi,j} - d_{1i,j}p_{mi+1,j} - d_{2i,j}p_{mi-1,j} - (d_{3i,j} - d_{4i,j})p_{mi,j+1} \\
&+(d_{10i,j} - d_{7i,j})p_{fi,j} + d_{8i,j}u_{i+1,j} - d_{8i,j}u_{i-1,j} + d_{11i,j}S_{mi,j} + d_{12i,j}S_{fi,j} \\
= \;& d_{14i,j}p_{mi,j} + d_{10i,j}p_{fi,j} + d_{11i,j}S_{mi,j} \\
&+d_{12i,j}S_{fi,j} + d_{8i,j}u_{i+1,j} - d_{8i,j}u_{i-1,j}
\end{aligned} \tag{B.16}
$$

Equation 5

$$
\begin{aligned}
&e_{15i,j}p_{fi,j} - e_{1i,j}p_{fi+1,j} - e_{2i,j}p_{fi-1,j} - (e_{3i,j} - e_{4i,j})p_{fi,j+1} \\
&+(e_{10i,j} - e_{7i,j})p_{mi,j} + e_{8i,j}u_{i+1,j} - e_{8i,j}u_{i-1,j} + e_{11i,j}S_{fi,j} + e_{12i,j}S_{mi,j} \\
= \;& e_{14i,j}p_{fi,j} + e_{10i,j}p_{mi,j} + e_{11i,j}S_{fi,j} + e_{12i,j}S_{mi,j} + e_{8i,j}u_{i+1,j} \\
&-e_{8i,j}u_{i-1,j} + e_{13i,j}p_{cfi,j} - e_{1i,j}p_{cfi+1,j} - e_{2i,j}p_{cfi-1,j} \\
&-(e_{3i,j} - e_{4i,j})p_{cfi,j+1} - e_{7i,j}p_{cmi,j}
\end{aligned} \tag{B.17}
$$

Equation 6

$$
\begin{aligned}
&f_{15i,j}p_{fi,j} - f_{1i,j}p_{fi+1,j} - f_{2i,j}p_{fi-1,j} - (f_{3i,j} - f_{4i,j})p_{fi,j+1} \\
&+(f_{10i,j} - f_{7i,j})p_{mi,j} + f_{8i,j}u_{i+1,j} - f_{8i,j}u_{i-1,j} + f_{11i,j}S_{fi,j} + f_{12i,j}S_{mi,j} \\
= \;& f_{14i,j}p_{fi,j} + f_{10i,j}p_{mi,j} + f_{11i,j}S_{fi,j} \\
&+f_{12i,j}S_{mi,j} + f_{8i,j}u_{i+1,j} - f_{8i,j}u_{i-1,j}
\end{aligned} \tag{B.18}
$$

- Boundary $j = N_y$

Equation 1

$$
\begin{aligned}
& -2(a_1+a_2)u_{i,j} + a_1 u_{i+1,j} + a_1 u_{i-1,j} + 2a_3 v_{i-1,j-1} - 2a_3 v_{i+1,j-1} \\
& -a_4 p_{mi-1,j} + a_4 p_{mi+1,j} - a_5 p_{fi-1,j} + \ a_5 p_{fi+1,j} - a_{6i,j} S_{mi-1,j} \\
& +a_{6i,j} S_{mi+1,j} - a_{7i,j} S_{fi-1,j} + a_{7i,j} S_{fi+1,j} \\
= \ & a_{8i,j}(p_{cmi+1,j} - p_{cmi-1,j}) + a_{9i,j}(p_{cfi+1,j} - p_{cfi-1,j})
\end{aligned}
\tag{B.19}
$$

Equation 2

$$
-2(b_1+b_2)v_{i,j} + b_1 v_{i+1,j} + b_1 v_{i-1,j} + 2b_3 u_{i-1,j-1} - 2b_3 u_{i+1,j-1} = 0 \tag{B.20}
$$

Equation 3

$$
\begin{aligned}
& c_{15i,j} p_{mi,j} - c_{1i,j} p_{mi+1,j} - c_{2i,j} p_{mi-1,j} - (c_{3i,j} + c_{4i,j}) p_{mi,j-1} \\
& +(c_{10i,j} - c_{7i,j}) p_{fi,j} + c_{8i,j} u_{i+1,j} - c_{8i,j} u_{i-1,j} - 2c_{9i,j} v_{i,j-1} \\
& +c_{11i,j} S_{mi,j} + c_{12i,j} S_{fi,j} \\
= \ & c_{14i,j} p_{mi,j} + c_{10i,j} p_{fi,j} + c_{11i,j} S_{mi,j} + c_{12i,j} S_{fi,j} + c_{8i,j} u_{i+1,j} \\
& -c_{8i,j} u_{i-1,j} - 2c_{9i,j} v_{i,j-1} + c_{13i,j} p_{cmi,j} - c_{1i,j} p_{cmi+1,j} \\
& -c_{2i,j} p_{cmi-1,j} - (c_{3i,j} + c_{4i,j}) p_{cmi,j-1} - c_{7i,j} p_{cfi,j}
\end{aligned}
\tag{B.21}
$$

Equation 4

$$
\begin{aligned}
& d_{15i,j} p_{mi,j} - d_{1i,j} p_{mi+1,j} - d_{2i,j} p_{mi-1,j} - (d_{3i,j} + d_{4i,j}) p_{mi,j-1} \\
& +(d_{10i,j} - d_{7i,j}) p_{fi,j} + d_{8i,j} u_{i+1,j} - d_{8i,j} u_{i-1,j} - 2d_{9i,j} v_{i,j-1} \\
& +d_{11i,j} S_{mi,j} + d_{12i,j} S_{fi,j} \\
= \ & d_{14i,j} p_{mi,j} + d_{10i,j} p_{fi,j} + d_{11i,j} S_{mi,j} + d_{12i,j} S_{fi,j} \\
& +d_{8i,j} u_{i+1,j} - d_{8i,j} u_{i-1,j} - 2d_{9i,j} v_{i,j-1}
\end{aligned}
\tag{B.22}
$$

Equation 5

$$
e_{15i,j} p_{fi,j} - e_{1i,j} p_{fi+1,j} - e_{2i,j} p_{fi-1,j} - (e_{3i,j} + e_{4i,j}) p_{fi,j-1}
$$

$$
\begin{aligned}
&+(e_{10i,j} - e_{7i,j})p_{mi,j} + e_{8i,j}u_{i+1,j} - e_{8i,j}u_{i-1,j} - 2e_{9i,j}v_{i,j-1} \\
&+e_{11i,j}S_{fi,j} + e_{12i,j}S_{mi,j} \\
= \;& e_{14i,j}p_{fi,j} + e_{10i,j}p_{mi,j} + e_{11i,j}S_{fi,j} + e_{12i,j}S_{mi,j} + e_{8i,j}u_{i+1,j} \\
&-e_{8i,j}u_{i-1,j} - 2e_{9i,j}v_{i,j-1} + e_{13i,j}p_{cfi,j} - e_{1i,j}p_{cfi+1,j} \\
&-e_{2i,j}p_{cfi-1,j} - (e_{3i,j} + e_{4i,j})p_{cfi,j-1} - e_{7i,j}p_{cmi,j} \qquad \text{(B.23)}
\end{aligned}
$$

Equation 6

$$
\begin{aligned}
&f_{15i,j}p_{fi,j} - f_{1i,j}p_{fi+1,j} - f_{2i,j}p_{fi-1,j} - (f_{3i,j} + f_{4i,j})p_{fi,j-1} \\
&+(f_{10i,j} - f_{7i,j})p_{mi,j} + f_{8i,j}u_{i+1,j} - f_{8i,j}u_{i-1,j} - 2f_{9i,j}v_{i,j-1} \\
&+f_{11i,j}S_{fi,j} + f_{12i,j}S_{mi,j} \\
= \;& f_{14i,j}p_{fi,j} + f_{10i,j}p_{mi,j} + f_{11i,j}S_{fi,j} + f_{12i,j}S_{mi,j} + f_{8i,j}u_{i+1,j} \\
&-f_{8i,j}u_{i-1,j} - 2f_{9i,j}v_{i,j-1} \qquad \text{(B.24)}
\end{aligned}
$$

- Corner $i = 1$, $j = 1$

Equation 1

$$
-2a_1u_{i,j} + 2a_1u_{i+1,j} + 2a_3v_{i+1,j} - 2a_3v_{i+1,j+1} + a_3c = 0 \qquad \text{(B.25)}
$$

Equation 2

$$
\begin{aligned}
&-2(b_1 + b_2)v_{i,j} + 2b_1v_{i+1,j} + 2b_2v_{i,j+1} - b_2c \\
&+2b_4p_{mi,j+1} + 2b_5p_{fi,j+1} + 2b_{6i,j}S_{mi,j+1} + 2b_{7i,j}S_{fi,j+1} \\
= \;& 2b_{8i,j}p_{cmi,j+1} + 2b_{9i,j}p_{cfi,j+1} \qquad \text{(B.26)}
\end{aligned}
$$

Equation 3

$$
\begin{aligned}
&c_{15i,j}p_{mi,j} - (c_{1i,j} + c_{2i,j})p_{mi+1,j} - (c_{3i,j} - c_{4i,j})p_{mi,j+1} \\
&+(c_{10i,j} - c_{7i,j})p_{fi,j} + c_{11i,j}S_{mi,j} + c_{12i,j}S_{fi,j}
\end{aligned}
$$

$$
\begin{aligned}
= \; & c_{14i,j}p_{mi,j} + c_{10i,j}p_{fi,j} + c_{11i,j}S_{mi,j} + c_{12i,j}S_{fi,j} \\
& -(c_{1i,j} + \; c_{2i,j})p_{cmi+1,j} + c_{13i,j}p_{cmi,j} \\
& -(c_{3i,j} - c_{4i,j})p_{cmi,j+1} - c_{7i,j}p_{cfi,j}
\end{aligned} \tag{B.27}
$$

Equation 4

$$
\begin{aligned}
& d_{15i,j}p_{mi,j} - (d_{1i,j} + d_{2i,j})p_{mi+1,j} - (d_{3i,j} - d_{4i,j})p_{mi,j+1} \\
& +(d_{10i,j} - d_{7i,j})p_{fi,j} + d_{11i,j}S_{mi,j} + d_{12i,j}S_{fi,j} \\
= \; & d_{14i,j}p_{mi,j} + d_{10i,j}p_{fi,j} + d_{11i,j}S_{mi,j} + d_{12i,j}S_{fi,j}
\end{aligned} \tag{B.28}
$$

Equation 5

$$
\begin{aligned}
& e_{15i,j}p_{fi,j} - (e_{1i,j} + e_{2i,j})p_{fi+1,j} - (e_{3i,j} - e_{4i,j})p_{fi,j+1} \\
& +(e_{10i,j} - e_{7i,j})p_{mi,j} + e_{11i,j}S_{fi,j} + e_{12i,j}S_{mi,j} \\
= \; & e_{14i,j}p_{fi,j} + e_{10i,j}p_{mi,j} + e_{11i,j}S_{fi,j} + e_{12i,j}S_{mi,j} - e_{7i,j}p_{cmi,j} \\
& -(e_{1i,j} + \; e_{2i,j})p_{cfi+1,j} + e_{13i,j}p_{cfi,j} - (e_{3i,j} - e_{4i,j})p_{cfi,j+1}
\end{aligned} \tag{B.29}
$$

Equation 6

$$
\begin{aligned}
& f_{15i,j}p_{fi,j} - (f_{1i,j} + f_{2i,j})p_{fi+1,j} - (f_{3i,j} - f_{4i,j})p_{fi,j+1} \\
& +(f_{10i,j} - f_{7i,j})p_{mi,j} + f_{11i,j}S_{fi,j} + f_{12i,j}S_{mi,j} \\
= \; & f_{14i,j}p_{fi,j} + f_{10i,j}p_{mi,j} + f_{11i,j}S_{fi,j} + f_{12i,j}S_{mi,j}
\end{aligned} \tag{B.30}
$$

- Corner $i = 1$, $j = N_y$

Equation 1

$$
-2(a_1 + a_2)u_{i,j} + 2a_1u_{i+1,j} - 2a_3v_{i+1,j} = 0 \tag{B.31}
$$

Equation 2

$$
-2(b_1 + b_2)v_{i,j} + 2b_1v_{i+1,j} = 0 \tag{B.32}
$$

Equation 3

$$
\begin{aligned}
& c_{15i,j}p_{mi,j} - (c_{1i,j} + c_{2i,j})p_{mi+1,j} - (c_{4i,j} + c_{3i,j})p_{mi,j-1} \\
& +(c_{10i,j} - c_{7i,j})p_{fi,j} - 2c_{9i,j}v_{i,j-1} + c_{11i,j}S_{mi,j} + c_{12i,j}S_{fi,j} \\
= \; & c_{14i,j}p_{mi,j} + c_{10i,j}p_{fi,j} + c_{11i,j}S_{mi,j} + c_{12i,j}S_{fi,j} - 2c_{9i,j}v_{i,j-1} \\
& +c_{13i,j}p_{cmi,j} - (c_{1i,j} + c_{2i,j})p_{cmi+1,j} - (c_{4i,j} + c_{3i,j})p_{cmi,j-1} \\
& -c_{7i,j}p_{cfi,j}
\end{aligned} \tag{B.33}
$$

Equation 4

$$
\begin{aligned}
& d_{15i,j}p_{mi,j} - (d_{1i,j} + d_{2i,j})p_{mi+1,j} - (d_{4i,j} + d_{3i,j})p_{mi,j-1} \\
& +(d_{10i,j} - d_{7i,j})p_{fi,j} - 2d_{9i,j}v_{i,j-1} + d_{11i,j}S_{mi,j} + d_{12i,j}S_{fi,j} \\
= \; & d_{14i,j}p_{mi,j} + d_{10i,j}p_{fi,j} + d_{11i,j}S_{mi,j} + d_{12i,j}S_{fi,j} - 2d_{9i,j}v_{i,j-1}
\end{aligned} \tag{B.34}
$$

Equation 5

$$
\begin{aligned}
& e_{15i,j}p_{fi,j} - (e_{1i,j} + e_{2i,j})p_{fi+1,j} - (e_{4i,j} + e_{3i,j})p_{fi,j-1} \\
& +(e_{10i,j} - e_{7i,j})p_{mi,j} - 2e_{9i,j}v_{i,j-1} + e_{11i,j}S_{fi,j} + e_{12i,j}S_{mi,j} \\
= \; & e_{14i,j}p_{fi,j} + e_{10i,j}p_{mi,j} + e_{11i,j}S_{fi,j} + e_{12i,j}S_{mi,j} + e_{13i,j}p_{cfi,j} \\
& -(e_{1i,j} + e_{2i,j})p_{cfi+1,j} - (e_{4i,j} + e_{3i,j})p_{cfi,j-1} - e_{7i,j}p_{cmi,j} \\
& -2e_{9i,j}v_{i,j-1}
\end{aligned} \tag{B.35}
$$

Equation 6

$$
\begin{aligned}
& f_{15i,j}p_{fi,j} - (f_{1i,j} + f_{2i,j})p_{fi+1,j} - (f_{4i,j} + f_{3i,j})p_{fi,j-1} \\
& +(f_{10i,j} - f_{7i,j})p_{mi,j} - 2f_{9i,j}v_{i,j-1} + f_{11i,j}S_{fi,j} + f_{12i,j}S_{mi,j} \\
= \; & f_{14i,j}p_{fi,j} + f_{10i,j}p_{mi,j} + f_{11i,j}S_{fi,j} + f_{12i,j}S_{mi,j} - 2f_{9i,j}v_{i,j-1}
\end{aligned} \tag{B.36}
$$

- Corner $i = N_x$, $j = 1$

Equation 1

$$
\begin{aligned}
&-2(a_1+a_2)u_{i,j}+a_2u_{i,j+1}-a_3c-2a_3v_{i-1,j+1}\\
&\quad+4a_3v_{i,j+1}-4a_3v_{i,j}+2a_3v_{i-1,j}=0 \qquad \text{(B.37)}
\end{aligned}
$$

Equation 2

$$
\begin{aligned}
&-2b_2v_{i,j}+2b_2v_{i,j+1}-b_2c+4b_3u_{i-1,j}-4b_3u_{i-1,j+1}\\
&+2b_4p_{mi,j+1}+2b_5p_{fi,j+1}+2b_{6i,j}S_{mi,j+1}+2b_{7i,j}S_{fi,j+1}\\
= \;& 2b_{8i,j}p_{cmi,j+1}+2b_{9i,j}p_{cfi,j+1} \qquad \text{(B.38)}
\end{aligned}
$$

Equation 3

$$
\begin{aligned}
&c_{15i,j}p_{mi,j}-(c_{1i,j}+c_{2i,j})p_{mi-1,j}-(c_{3i,j}-c_{4i,j})p_{mi,j+1}\\
&+(c_{10i,j}-c_{7i,j})p_{fi,j}-2c_{8i,j}u_{i-1,j}+c_{11i,j}S_{mi,j}+c_{12i,j}S_{fi,j}\\
= \;& -2c_{8i,j}u_{i-1,j}+c_{11i,j}S_{mi,j}+c_{12i,j}S_{fi,j}+c_{13i,j}p_{cmi,j}\\
&+c_{14i,j}p_{mi,j}+c_{10i,j}p_{fi,j}-(c_{2i,j}+c_{1i,j})p_{cmi-1,j}\\
&-(c_{3i,j}-c_{4i,j})p_{cmi,j+1}-c_{7i,j}p_{cfi,j} \qquad \text{(B.39)}
\end{aligned}
$$

Equation 4

$$
\begin{aligned}
&d_{15i,j}p_{mi,j}-(d_{1i,j}+d_{2i,j})p_{mi-1,j}-(d_{3i,j}-d_{4i,j})p_{mi,j+1}\\
&+(d_{10i,j}-d_{7i,j})p_{fi,j}-2d_{8i,j}u_{i-1,j}+d_{11i,j}S_{mi,j}+d_{12i,j}S_{fi,j}\\
= \;& d_{14i,j}p_{mi,j}+d_{10i,j}p_{fi,j}+d_{11i,j}S_{mi,j}\\
&+d_{12i,j}S_{fi,j}-2d_{8i,j}u_{i-1,j} \qquad \text{(B.40)}
\end{aligned}
$$

Equation 5

$$
\begin{aligned}
&e_{15i,j}p_{fi,j}-(e_{1i,j}+e_{2i,j})p_{fi-1,j}-(e_{3i,j}-e_{4i,j})p_{fi,j+1}\\
&+(e_{10i,j}-e_{7i,j})p_{mi,j}-2e_{8i,j}u_{i-1,j}+e_{11i,j}S_{fi,j}+e_{12i,j}S_{mi,j}\\
= \;& -2e_{8i,j}u_{i-1,j}+e_{11i,j}S_{fi,j}+e_{12i,j}S_{mi,j}+e_{13i,j}p_{cfi,j}
\end{aligned}
$$

$$+e_{14i,j}p_{fi,j} + e_{10i,j}p_{mi,j} - (e_{2i,j} + e_{1i,j})p_{cfi-1,j}$$
$$-(e_{3i,j} - e_{4i,j})p_{cfi,j+1} - e_{7i,j}p_{cmi,j} \tag{B.41}$$

Equation 6

$$\begin{aligned} & f_{15i,j}p_{fi,j} - (f_{1i,j} + f_{2i,j})p_{fi-1,j} - (f_{3i,j} - f_{4i,j})p_{fi,j+1} \\ & +(f_{10i,j} - f_{7i,j})p_{mi,j} - 2f_{8i,j}u_{i-1,j} - f_{10i,j}S_{fi,j} \\ = \; & f_{14i,j}p_{fi,j} + f_{10i,j}p_{mi,j} + f_{11i,j}S_{fi,j} + f_{12i,j}S_{mi,j} - 2f_{8i,j}u_{i-1,j} \end{aligned} \tag{B.42}$$

- Corner $i = N_x,\ j = N_y$

Equation 1

$$-2(a_1 + a_2)u_{i,j} + 4a_3v_{i-1,j-1} - 4a_3v_{i,j-1} - 2a_3v_{i-1,j} = 0 \tag{B.43}$$

Equation 2

$$-2(b_1 + b_2)v_{i,j} + 4b_3u_{i-1,j-1} = 0 \tag{B.44}$$

Equation 3

$$\begin{aligned} & c_{15i,j}p_{mi,j} - (c_{2i,j} + c_{1i,j})p_{mi-1,j} - (c_{4i,j} + c_{3i,j})p_{mi,j-1} \\ & +(c_{10i,j} - c_{7i,j})p_{fi,j} - 2c_{8i,j}u_{i-1,j} - 2c_{9i,j}v_{i,j-1} + c_{11i,j}S_{mi,j} + c_{12i,j}S_{fi,j} \\ = \; & c_{14i,j}p_{mi,j} + c_{10i,j}p_{fi,j} + c_{11i,j}S_{mi,j} + c_{12i,j}S_{fi,j} - 2c_{8i,j}u_{i-1,j} \\ & -2c_{9i,j}v_{i,j-1} + c_{13i,j}p_{cmi,j} - (c_{2i,j} + c_{1i,j})p_{cmi-1,j} \\ & -(c_{4i,j} + c_{3i,j})p_{cmi,j-1} - c_{7i,j}p_{cfi,j} \end{aligned} \tag{B.45}$$

Equation 4

$$\begin{aligned} & d_{15i,j}p_{mi,j} - (d_{1i,j} + d_{2i,j})p_{mi-1,j} - (d_{3i,j} + d_{4i,j})p_{mi,j-1} \\ & +(d_{10i,j} - d_{7i,j})p_{fi,j} - 2d_{8i,j}u_{i-1,j} - 2d_{9i,j}v_{i,j-1} + d_{11i,j}S_{mi,j} + d_{12i,j}S_{fi,j} \\ = \; & d_{14i,j}p_{mi,j} + d_{10i,j}p_{fi,j} + d_{11i,j}S_{mi,j} \\ & +d_{12i,j}S_{fi,j} - 2d_{8i,j}u_{i-1,j} - 2d_{9i,j}v_{i,j-1} \end{aligned} \tag{B.46}$$

Equation 5

$$
\begin{aligned}
& e_{15i,j}p_{fi,j} - (e_{2i,j} + e_{1i,j})p_{fi-1,j} - (e_{4i,j} + e_{3i,j})p_{fi,j-1} \\
& +(e_{10i,j} - e_{7i,j})p_{mi,j} - 2e_{8i,j}u_{i-1,j} - 2e_{9i,j}v_{i,j-1} + e_{11i,j}S_{fi,j} + e_{12i,j}S_{mi,j} \\
= \; & e_{14i,j}p_{fi,j} + e_{10i,j}p_{mi,j} + e_{11i,j}S_{fi,j} + e_{12i,j}S_{mi,j} - 2e_{8i,j}u_{i-1,j} - 2e_{9i,j}v_{i,j-1} \\
& +e_{13i,j}p_{cfi,j} - (e_{2i,j} + e_{1i,j})p_{cfi-1,j} \\
& -(e_{4i,j} + e_{3i,j})p_{cfi,j-1} - e_{7i,j}p_{cmi,j} \qquad \text{(B.47)}
\end{aligned}
$$

Equation 6

$$
\begin{aligned}
& f_{15i,j}p_{fi,j} - (f_{2i,j} + f_{1i,j})p_{fi-1,j} - (f_{4i,j} + f_{3i,j})p_{fi,j-1} \\
& +(f_{10i,j} - f_{7i,j})p_{mi,j} - 2f_{8i,j}u_{i-1,j} - 2f_{9i,j}v_{i,j-1} + f_{11i,j}S_{fi,j} + f_{12i,j}S_{mi,j} \\
= \; & f_{14i,j}p_{fi,j} + f_{10i,j}p_{mi,j} + f_{11i,j}S_{fi,j} \\
& +f_{12i,j}S_{mi,j} - 2f_{8i,j}u_{i-1,j} - 2f_{9i,j}v_{i,j-1} \qquad \text{(B.48)}
\end{aligned}
$$

B.2 Case 2 Oil Production from a Deformable Fractured Reservoir with Water Injection

- Boundary $i = 1$

Equation 1

$$
\begin{aligned}
&-2(a_1 + a_2)u_{i,j} + 2a_1 u_{i+1,j} - a_1 c_1 + a_2 u_{i,j+1} + a_2 u_{i,j-1} \\
&2a_3 v_{i,j-1} - 2a_3 v_{i+1,j-1} - 2a_3 v_{i,j+1} + 2a_3 u_{i+1,j+1} = 0
\end{aligned} \tag{B.49}
$$

Equation 2

$$
\begin{aligned}
&-2b_2 v_{i,j} + b_1 v_{i+1,j} - b_1 v_{i+1,j} + b_2 v_{i,j+1} - b_2 v_{i,j-1} - b_4 p_{mi,j-1} + b_4 p_{mi,j+1} \\
&-b_5 p_{fi,j-1} + b_5 p_{fi,j+1} - b_{6i,j} S_{mi,j-1} + b_{6i,j} S_{mi,j+1} - b_{7i,j} S_{fi,j-1} + b_{7i,j} S_{fi,j+1} \\
= \; & b_{8i,j}(p_{cmi,j+1} - p_{cmi,j-1}) + b_{9i,j}(p_{cfi,j+1} - p_{cfi,j-1})
\end{aligned} \tag{B.50}
$$

Equation 3

$$
\begin{aligned}
&c_{15i,j} p_{mi,j} - (c_{1i,j} + c_{2i,j}) p_{mi+1,j} - c_{3i,j} p_{mi,j+1} - c_{4i,j} p_{mi,j-1} \\
&+(c_{10i,j} - c_{7i,j}) p_{fi,j} + c_{9i,j} v_{i,j+1} - c_{9i,j} v_{i,j-1} + c_{11i,j} S_{mi,j} + c_{12i,j} S_{fi,j} \\
= \; & c_{14i,j} p_{mi,j} + c_{10i,j} p_{fi,j} + c_{11i,j} S_{mi,j} + c_{12i,j} S_{fi,j} \\
&+c_{9i,j} v_{i,j+1} - c_{9i,j} v_{i,j-1} + c_{13i,j} p_{cmi,j} - (c_{1i,j} + c_{2i,j}) p_{cmi+1,j} \\
&-c_{3i,j} p_{cmi,j+1} - c_{4i,j} p_{cmi,j-1} - c_{7i,j} p_{cfi,j}
\end{aligned} \tag{B.51}
$$

Equation 4

$$
\begin{aligned}
&d_{15i,j} p_{mi,j} - (d_{1i,j} + d_{2i,j}) p_{mi+1,j} - d_{3i,j} p_{mi,j+1} - d_{4i,j} p_{mi,j-1} \\
&+(d_{10i,j} - d_{7i,j}) p_{fi,j} + d_{9i,j} v_{i,j+1} - d_{9i,j} v_{i,j-1} + d_{11i,j} S_{mi,j} + d_{12i,j} S_{fi,j} \\
= \; & d_{14i,j} p_{mi,j} + d_{10i,j} p_{fi,j} + d_{11i,j} S_{mi,j} \\
&+d_{12i,j} S_{fi,j} + d_{9i,j} v_{i,j+1} - d_{9i,j} v_{i,j-1}
\end{aligned} \tag{B.52}
$$

Equation 5

$$\begin{aligned}
& e_{15i,j}p_{fi,j} - (e_{1i,j} + e_{2i,j})p_{fi+1,j} - e_{3i,j}p_{fi,j+1} - e_{4i,j}p_{fi,j-1} \\
& +(e_{10i,j} - e_{7i,j})p_{mi,j} + e_{9i,j}v_{i,j+1} - e_{9i,j}v_{i,j-1} + e_{11i,j}S_{fi,j} + e_{12i,j}S_{mi,j} \\
= \; & e_{14i,j}p_{fi,j} + e_{10i,j}p_{mi,j} + e_{11i,j}S_{fi,j} + e_{12i,j}S_{mi,j} + e_{9i,j}v_{i,j+1} \\
& -e_{9i,j}v_{i,j-1} + e_{13i,j}p_{cfi,j} - (e_{1i,j} + e_{2i,j})p_{cfi+1,j} \\
& -e_{3i,j}p_{cfi,j+1} - e_{4i,j}p_{cfi,j-1} - e_{7i,j}p_{cmi,j} \qquad \text{(B.53)}
\end{aligned}$$

Equation 6

$$\begin{aligned}
& f_{15i,j}p_{fi,j} - (f_{1i,j} + f_{2i,j})p_{fi+1,j} - f_{3i,j}p_{fi,j+1} - f_{4i,j}p_{fi,j-1} \\
& +(f_{10i,j} - f_{7i,j})p_{mi,j} + f_{9i,j}v_{i,j+1} - f_{9i,j}v_{i,j-1} + f_{11i,j}S_{fi,j} + f_{12i,j}S_{mi,j} \\
= \; & f_{14i,j}p_{fi,j} + f_{10i,j}p_{mi,j} + f_{11i,j}S_{fi,j} \\
& +f_{12i,j}S_{mi,j} + f_{9i,j}v_{i,j+1} - f_{9i,j}v_{i,j-1} \qquad \text{(B.54)}
\end{aligned}$$

- Boundary $i = N_x$

Equation 1

$$-2(a_1 + a_2)u_{i,j} + a_2u_{i,j+1} + a_2u_{i,j-1} = 0 \qquad \text{(B.55)}$$

Equation 2

$$\begin{aligned}
& -2\left(b_1 + b_2\right)v_{i,j} + 2b_1v_{i-1,j} + b_2v_{i,j+1} + b_2v_{i,j-1} \\
& +2b_3u_{i-1,j-1} - 2b_3u_{i-1,j+1} - b_4p_{mi,j-1} + b_4p_{mi,j+1} - b_5p_{fi,j-1} \\
& +b_5p_{fi,j+1} - b_{6i,j}S_{mi,j-1} + b_{6i,j}S_{mi,j+1} - b_{7i,j}S_{fi,j-1} + b_{7i,j}S_{fi,j+1} \\
= \; & b_{8i,j}(p_{cmi,j+1} - p_{cmi,j-1}) + b_{9i,j}(p_{cfi,j+1} - p_{cfi,j-1}) \qquad \text{(B.56)}
\end{aligned}$$

Equation 3

$$c_{15i,j}p_{mi,j} - (c_{1i,j} + c_{2i,j})p_{mi-1,j} - c_{3i,j}p_{mi,j+1} - c_{4i,j}p_{mi,j-1}$$

$$
\begin{aligned}
&+(c_{10i,j} - c_{7i,j})p_{fi,j} - 2c_{8i,j}u_{i-1,j} + c_{9i,j}v_{i,j+1} - c_{9i,j}v_{i,j-1} \\
&+c_{11i,j}S_{mi,j} + c_{12i,j}S_{fi,j} \\
= \;& c_{14i,j}p_{mi,j} + c_{10i,j}p_{fi,j} + c_{11i,j}S_{mi,j} + c_{12i,j}S_{fi,j} - 2c_{8i,j}u_{i-1,j} \\
&+c_{9i,j}v_{i,j+1} - c_{9i,j}v_{i,j-1} + c_{13i,j}p_{cmi,j} - (c_{1i,j} + c_{2i,j})p_{cmi-1,j} \\
&-c_{3i,j}p_{cmi,j+1} - c_{4i,j}p_{cmi,j-1} - c_{7i,j}p_{cfi,j} \qquad (B.57)
\end{aligned}
$$

Equation 4

$$
\begin{aligned}
&d_{15i,j}p_{mi,j} - (d_{1i,j} + d_{2i,j})p_{mi-1,j} - d_{3i,j}p_{mi,j+1} - d_{4i,j}p_{mi,j-1} \\
&+(d_{10i,j} - d_{7i,j})p_{fi,j} - 2d_{8i,j}u_{i-1,j} + d_{9i,j}v_{i,j+1} - d_{9i,j}v_{i,j-1} \\
&+d_{11i,j}S_{mi,j} + d_{12i,j}S_{fi,j} \\
= \;& d_{14i,j}p_{mi,j} + d_{10i,j}p_{fi,j} + d_{11i,j}S_{mi,j} + d_{12i,j}S_{fi,j} - 2d_{8i,j}u_{i-1,j} \\
&+d_{9i,j}v_{i,j+1} - d_{9i,j}v_{i,j-1} \qquad (B.58)
\end{aligned}
$$

Equation 5

$$
\begin{aligned}
&e_{15i,j}p_{fi,j} - (e_{1i,j} + e_{2i,j})p_{fi-1,j} - e_{3i,j}p_{fi,j+1} - e_{4i,j}p_{fi,j-1} \\
&+(e_{10i,j} - e_{7i,j})p_{mi,j} - 2e_{8i,j}u_{i-1,j} + e_{9i,j}v_{i,j+1} - e_{9i,j}v_{i,j-1} \\
&+e_{11i,j}S_{fi,j} + e_{12i,j}S_{mi,j} \\
= \;& e_{14i,j}p_{fi,j} + e_{10i,j}p_{mi,j} + e_{11i,j}S_{fi,j} + e_{12i,j}S_{mi,j} - 2e_{8i,j}u_{i-1,j} \\
&+e_{9i,j}v_{i,j+1} - e_{9i,j}v_{i,j-1} + e_{13i,j}p_{cfi,j} - (e_{1i,j} + e_{2i,j})p_{cfi-1,j} \\
&-e_{3i,j}p_{cfi,j+1} - e_{4i,j}p_{cfi,j-1} - e_{7i,j}p_{cmi,j} \qquad (B.59)
\end{aligned}
$$

Equation 6

$$
\begin{aligned}
&f_{15i,j}p_{fi,j} - (f_{1i,j} + f_{2i,j})p_{fi-1,j} - f_{3i,j}p_{fi,j+1} - f_{4i,j}p_{fi,j-1} \\
&+(f_{10i,j} - f_{7i,j})p_{mi,j} - 2f_{8i,j}u_{i-1,j} + f_{9i,j}v_{i,j+1} - f_{9i,j}v_{i,j-1} \\
&+f_{11i,j}S_{fi,j} + f_{12i,j}S_{mi,j}
\end{aligned}
$$

$$
\begin{aligned}
= \quad & f_{14i,j}p_{fi,j} + f_{10i,j}p_{mi,j} + f_{11i,j}S_{fi,j} + f_{12i,j}S_{mi,j} \\
& -2f_{8i,j}u_{i-1,j} + f_{9i,j}v_{i,j+1} - f_{9i,j}v_{i,j-1} \qquad \text{(B.60)}
\end{aligned}
$$

- Boundary $j = 1$

Equation 1

$$
\begin{aligned}
& -2a_1u_{i,j} + a_1u_{i+1,j} + a_1u_{i-1,j} - a_4p_{mi-1,j} + a_4p_{mi+1,j} - a_5p_{fi-1,j} \\
& +a_5p_{fi+1,j} - a_{6i,j}S_{mi-1,j} + a_{6i,j}S_{mi+1,j} - a_{7i,j}S_{fi-1,j} + a_{7i,j}S_{fi+1,j} \\
= \quad & a_{8i,j}(p_{cmi+1,j} - p_{cmi-1,j}) + a_{9i,j}(p_{cfi+1,j} - p_{cfi-1,j}) \qquad \text{(B.61)}
\end{aligned}
$$

Equation 2

$$
\begin{aligned}
& -2(b_1 + b_2)v_{i,j} + b_1v_{i+1,j} + b_1v_{i-1,j} + 2b_2v_{i,j+1} - b_2c \\
& +2b_3u_{i-1,j} - 2b_3u_{i-1,j+1} + 2b_3u_{i+1,j+1} - 2b_3u_{i+1,j} = 0 \qquad \text{(B.62)}
\end{aligned}
$$

Equation 3

$$
\begin{aligned}
& c_{15i,j}p_{mi,j} - c_{1i,j}p_{mi+1,j} - c_{2i,j}p_{mi-1,j} - (c_{3i,j} + c_{4i,j})p_{mi,j+1} \\
& +(c_{10i,j} - c_{7i,j})p_{fi,j} + c_{8i,j}u_{i+1,j} - c_{8i,j}u_{i-1,j} + c_{11i,j}S_{mi,j} + c_{12i,j}S_{fi,j} \\
= \quad & c_{14i,j}p_{mi,j} + c_{10i,j}p_{fi,j} + c_{11i,j}S_{mi,j} + c_{12i,j}S_{fi,j} + c_{8i,j}u_{i+1,j} \\
& -c_{8i,j}u_{i-1,j} + c_{13i,j}p_{cmi,j} - c_{1i,j}p_{cmi+1,j} - c_{2i,j}p_{cmi-1,j} \\
& -(c_{3i,j} - c_{4i,j})p_{cmi,j+1} - c_{7i,j}p_{cfi,j} \qquad \text{(B.63)}
\end{aligned}
$$

Equation 4

$$
\begin{aligned}
& d_{15i,j}p_{mi,j} - d_{1i,j}p_{mi+1,j} - d_{2i,j}p_{mi-1,j} - (d_{3i,j} + d_{4i,j})p_{mi,j+1} \\
& +(d_{10i,j} - d_{7i,j})p_{fi,j} + d_{8i,j}u_{i+1,j} - d_{8i,j}u_{i-1,j} + d_{11i,j}S_{mi,j} + d_{12i,j}S_{fi,j} \\
= \quad & d_{14i,j}p_{mi,j} + d_{10i,j}p_{fi,j} + d_{11i,j}S_{mi,j} \\
& +d_{12i,j}S_{fi,j} + d_{8i,j}u_{i+1,j} - d_{8i,j}u_{i-1,j} \qquad \text{(B.64)}
\end{aligned}
$$

Equation 5

$$
\begin{aligned}
& e_{15i,j}p_{fi,j} - e_{1i,j}p_{fi+1,j} - e_{2i,j}p_{fi-1,j} - (e_{3i,j} + e_{4i,j})p_{fi,j+1} \\
& +(e_{10i,j} - e_{7i,j})p_{mi,j} + e_{8i,j}u_{i+1,j} - e_{8i,j}u_{i-1,j} + e_{11i,j}S_{fi,j} + e_{12i,j}S_{mi,j} \\
= \; & e_{14i,j}p_{fi,j} + e_{10i,j}p_{mi,j} + e_{11i,j}S_{fi,j} + e_{12i,j}S_{mi,j} + e_{8i,j}u_{i+1,j} \\
& -e_{8i,j}u_{i-1,j} + e_{13i,j}p_{cfi,j} - e_{1i,j}p_{cfi+1,j} - e_{2i,j}p_{cfi-1,j} \\
& -(e_{3i,j} - e_{4i,j})p_{cfi,j+1} - e_{7i,j}p_{cmi,j}
\end{aligned}
\tag{B.65}
$$

Equation 6

$$
\begin{aligned}
& f_{15i,j}p_{fi,j} - f_{1i,j}p_{fi+1,j} - f_{2i,j}p_{fi-1,j} - (f_{3i,j} + f_{4i,j})p_{fi,j+1} \\
& +(f_{10i,j} - f_{7i,j})p_{mi,j} + f_{8i,j}u_{i+1,j} - f_{8i,j}u_{i-1,j} + f_{11i,j}S_{fi,j} + f_{12i,j}S_{mi,j} \\
= \; & f_{14i,j}p_{fi,j} + f_{10i,j}p_{mi,j} + f_{11i,j}S_{fi,j} \\
& +f_{12i,j}S_{mi,j} + f_{8i,j}u_{i+1,j} - f_{8i,j}u_{i-1,j}
\end{aligned}
\tag{B.66}
$$

- Boundary $j = N_y$

Equation 1

$$
\begin{aligned}
& -2(a_1 + a_2)u_{i,j} + a_1u_{i+1,j} + a_1u_{i-1,j} + 2a_2u_{i,j-1} + 2a_3v_{i-1,j-1} \\
& -2a_3v_{i+1,j-1} - a_4p_{mi-1,j} + a_4p_{mi+1,j} - a_5p_{fi-1,j} + a_5p_{fi+1,j} \\
& -a_{6i,j}S_{mi-1,j} + a_{6i,j}S_{mi+1,j} - a_{7i,j}S_{fi-1,j} + a_{7i,j}S_{fi+1,j} \\
= \; & a_{8i,j}(p_{cmi+1,j} - p_{cmi-1,j}) + a_{9i,j}(p_{cfi+1,j} - p_{cfi-1,j})
\end{aligned}
\tag{B.67}
$$

Equation 2

$$
-2(b_1 + b_2)v_{i,j} + b_1v_{i+1,j} + b_1v_{i-1,j} = 0 \tag{B.68}
$$

Equation 3

$$
c_{15i,j}p_{mi,j} - c_{1i,j}p_{mi+1,j} - c_{2i,j}p_{mi-1,j} - (c_{3i,j} + c_{4i,j})p_{mi,j-1}
$$

$$
\begin{aligned}
&+(c_{10i,j} - c_{7i,j})p_{fi,j} + c_{8i,j}u_{i+1,j} - c_{8i,j}u_{i-1,j} - 2c_{9i,j}v_{i,j-1} \\
&+c_{11i,j}S_{mi,j} + c_{12i,j}S_{fi,j} \\
= \; & c_{14i,j}p_{mi,j} + c_{10i,j}p_{fi,j} + c_{11i,j}S_{mi,j} + c_{12i,j}S_{fi,j} + c_{8i,j}u_{i+1,j} \\
&-c_{8i,j}u_{i-1,j} - 2c_{9i,j}v_{i,j-1} + c_{13i,j}p_{cmi,j} - c_{1i,j}p_{cmi+1,j} \\
&-c_{2i,j}p_{cmi-1,j} - (c_{3i,j} + c_{4i,j})p_{cmi,j-1} - c_{7i,j}p_{cfi,j}
\end{aligned} \tag{B.69}
$$

Equation 4

$$
\begin{aligned}
&d_{15i,j}p_{mi,j} - d_{1i,j}p_{mi+1,j} - d_{2i,j}p_{mi-1,j} - (d_{3i,j} + d_{4i,j})p_{mi,j-1} \\
&+(d_{10i,j} - d_{7i,j})p_{fi,j} + d_{8i,j}u_{i+1,j} - d_{8i,j}u_{i-1,j} - 2d_{9i,j}v_{i,j-1} \\
&+d_{11i,j}S_{mi,j} + d_{12i,j}S_{fi,j} \\
= \; & d_{14i,j}p_{mi,j} + d_{10i,j}p_{fi,j} + d_{11i,j}S_{mi,j} + d_{12i,j}S_{fi,j} \\
&+d_{8i,j}u_{i+1,j} - d_{8i,j}u_{i-1,j} - 2d_{9i,j}v_{i,j-1}
\end{aligned} \tag{B.70}
$$

Equation 5

$$
\begin{aligned}
&e_{15i,j}p_{fi,j} - e_{1i,j}p_{fi+1,j} - e_{2i,j}p_{fi-1,j} - (e_{3i,j} + e_{4i,j})p_{fi,j-1} \\
&+(e_{10i,j} - e_{7i,j})p_{mi,j} + e_{8i,j}u_{i+1,j} - e_{8i,j}u_{i-1,j} - 2e_{9i,j}v_{i,j-1} \\
&+e_{11i,j}S_{fi,j} + e_{12i,j}S_{mi,j} \\
= \; & e_{14i,j}p_{fi,j} + e_{10i,j}p_{mi,j} + e_{11i,j}S_{fi,j} + e_{12i,j}S_{mi,j} + e_{8i,j}u_{i+1,j} \\
&-e_{8i,j}u_{i-1,j} - 2e_{9i,j}v_{i,j-1} + e_{13i,j}p_{cfi,j} - e_{1i,j}p_{cfi+1,j} \\
&-e_{2i,j}p_{cfi-1,j} - (e_{3i,j} + e_{4i,j})p_{cfi,j-1} - e_{7i,j}p_{cmi,j}
\end{aligned} \tag{B.71}
$$

Equation 6

$$
\begin{aligned}
&f_{15i,j}p_{fi,j} - f_{1i,j}p_{fi+1,j} - f_{2i,j}p_{fi-1,j} - (f_{3i,j} + f_{4i,j})p_{fi,j-1} \\
&+(f_{10i,j} - f_{7i,j})p_{mi,j} + f_{8i,j}u_{i+1,j} - f_{8i,j}u_{i-1,j} - 2f_{9i,j}v_{i,j-1} \\
&+f_{11i,j}S_{fi,j} + f_{12i,j}S_{mi,j}
\end{aligned}
$$

$$
\begin{aligned}
&= f_{14i,j}p_{fi,j} + f_{10i,j}p_{mi,j} + f_{11i,j}S_{fi,j} + f_{12i,j}S_{mi,j} + f_{8i,j}u_{i+1,j} \\
&\quad -f_{8i,j}u_{i-1,j} - 2f_{9i,j}v_{i,j-1}
\end{aligned} \tag{B.72}
$$

- Corner $i = 1,\ j = 1$

Equation 1

$$
-2a_1u_{i,j} + 2a_1u_{i+1,j} - a_1c = 0 \tag{B.73}
$$

Equation 2

$$
-2b_2v_{i,j} + 2b_2v_{i,j+1} - b_2c = 0 \tag{B.74}
$$

Equation 3

$$
\begin{aligned}
& c_{15i,j}p_{mi,j} - (c_{1i,j} + c_{2i,j})p_{mi+1,j} - (c_{3i,j} + c_{4i,j})p_{mi,j+1} \\
& +(c_{10i,j} - c_{7i,j})p_{fi,j} + c_{11i,j}S_{mi,j} + c_{12i,j}S_{fi,j} \\
= \ & c_{14i,j}p_{mi,j} + c_{10i,j}p_{fi,j} + c_{11i,j}S_{mi,j} + c_{12i,j}S_{fi,j} \\
& -(c_{1i,j} + c_{2i,j})p_{cmi+1,j} + c_{13i,j}p_{cmi,j} \\
& -(c_{3i,j} - c_{4i,j})p_{cmi,j+1} - c_{7i,j}p_{cfi,j}
\end{aligned} \tag{B.75}
$$

Equation 4

$$
\begin{aligned}
& d_{15i,j}p_{mi,j} - (d_{1i,j} + d_{2i,j})p_{mi+1,j} - (d_{3i,j} + d_{4i,j})p_{mi,j+1} \\
& +(d_{10i,j} - d_{7i,j})p_{fi,j} + d_{11i,j}S_{mi,j} + d_{12i,j}S_{fi,j} \\
= \ & d_{14i,j}p_{mi,j} + d_{10i,j}p_{fi,j} + d_{11i,j}S_{mi,j} + d_{12i,j}S_{fi,j}
\end{aligned} \tag{B.76}
$$

Equation 5

$$
\begin{aligned}
& e_{15i,j}p_{fi,j} - (e_{1i,j} + e_{2i,j})p_{fi+1,j} - (e_{3i,j} + e_{4i,j})p_{fi,j+1} \\
& +(e_{10i,j} - e_{7i,j})p_{mi,j} + e_{11i,j}S_{fi,j} + e_{12i,j}S_{mi,j} \\
= \ & e_{14i,j}p_{fi,j} + e_{10i,j}p_{mi,j} + e_{11i,j}S_{fi,j} + e_{12i,j}S_{mi,j} - e_{7i,j}p_{cmi,j} \\
& -(e_{1i,j} + e_{2i,j})p_{cfi+1,j} + e_{13i,j}p_{cfi,j} - (e_{3i,j} - e_{4i,j})p_{cfi,j+1}
\end{aligned} \tag{B.77}
$$

Equation 6

$$
\begin{aligned}
& f_{15i,j}p_{fi,j} - (f_{1i,j} + f_{2i,j})p_{fi+1,j} - (f_{3i,j} + f_{4i,j})p_{fi,j+1} \\
& +(f_{10i,j} - f_{7i,j})p_{mi,j} + f_{11i,j}S_{fi,j} + f_{12i,j}S_{mi,j} \\
= \; & f_{14i,j}p_{fi,j} + f_{10i,j}p_{mi,j} + f_{11i,j}S_{fi,j} + f_{12i,j}S_{mi,j}
\end{aligned} \tag{B.78}
$$

- Corner $i = 1$, $j = N_y$

Equation 1

$$
\begin{aligned}
& -2(a_1 + a_2)u_{i,j} + 2a_1u_{i+1,j} - a1c \\
& +2a_2u_{i,j-1} + 4a_3v_{i,j-1} - 4a_3v_{i+1,j-1} = 0
\end{aligned} \tag{B.79}
$$

Equation 2

$$
v_{i,j} = 0 \tag{B.80}
$$

Equation 3

$$
\begin{aligned}
& c_{15i,j}p_{mi,j} - (c_{1i,j} + c_{2i,j})p_{mi+1,j} - (c_{4i,j} + c_{3i,j})p_{mi,j-1} \\
& +(c_{10i,j} - c_{7i,j})p_{fi,j} - 2c_{9i,j}v_{i,j-1} + c_{11i,j}S_{mi,j} + c_{12i,j}S_{fi,j} \\
= \; & c_{14i,j}p_{mi,j} + c_{10i,j}p_{fi,j} + c_{11i,j}S_{mi,j} + c_{12i,j}S_{fi,j} - 2c_{9i,j}v_{i,j-1} \\
& +c_{13i,j}p_{cmi,j} - (c_{1i,j} + c_{2i,j})p_{cmi+1,j} - (c_{4i,j} + c_{3i,j})p_{cmi,j-1} \\
& -c_{7i,j}p_{cfi,j}
\end{aligned} \tag{B.81}
$$

Equation 4

$$
\begin{aligned}
& d_{15i,j}p_{mi,j} - (d_{1i,j} + d_{2i,j})p_{mi+1,j} - (d_{4i,j} + d_{3i,j})p_{mi,j-1} \\
& +(d_{10i,j} - d_{7i,j})p_{fi,j} - 2d_{9i,j}v_{i,j-1} + d_{11i,j}S_{mi,j} + d_{12i,j}S_{fi,j} \\
= \; & d_{14i,j}p_{mi,j} + d_{10i,j}p_{fi,j} + d_{11i,j}S_{mi,j} + d_{12i,j}S_{fi,j} - 2d_{9i,j}v_{i,j-1}
\end{aligned} \tag{B.82}
$$

Equation 5

$$
\begin{aligned}
& e_{15i,j}p_{fi,j} - (e_{1i,j} + e_{2i,j})p_{fi+1,j} - (e_{4i,j} + e_{3i,j})p_{fi,j-1} \\
& +(e_{10i,j} - e_{7i,j})p_{mi,j} - 2e_{9i,j}v_{i,j-1} + e_{11i,j}S_{fi,j} + e_{12i,j}S_{mi,j} \\
= \; & e_{14i,j}p_{fi,j} + e_{10i,j}p_{mi,j} + e_{11i,j}S_{fi,j} + e_{12i,j}S_{mi,j} + e_{13i,j}p_{cfi,j} \\
& -(e_{1i,j} + e_{2i,j})p_{cfi+1,j} - (e_{4i,j} + e_{3i,j})p_{cfi,j-1} - e_{7i,j}p_{cmi,j} \\
& -2e_{9i,j}v_{i,j-1}
\end{aligned}
\tag{B.83}
$$

Equation 6

$$
\begin{aligned}
& f_{15i,j}p_{fi,j} - (f_{1i,j} + f_{2i,j})p_{fi+1,j} - (f_{4i,j} + f_{3i,j})p_{fi,j-1} \\
& +(f_{10i,j} - f_{7i,j})p_{mi,j} - 2f_{9i,j}v_{i,j-1} + f_{11i,j}S_{fi,j} + f_{12i,j}S_{mi,j} \\
= \; & f_{14i,j}p_{fi,j} + f_{10i,j}p_{mi,j} + f_{11i,j}S_{fi,j} + f_{12i,j}S_{mi,j} - 2f_{9i,j}v_{i,j-1}
\end{aligned}
\tag{B.84}
$$

- Corner $i = N_x$, $j = 1$

Equation 1

$$u_{i,j} = 0 \tag{B.85}$$

Equation 2

$$
\begin{aligned}
& -2\left(b_1 + b_2\right)v_{i,j} + 2b_1 v_{i-1,j} + 2b_2 v_{i,j+1} \\
& -b_2 c + 4b_3 u_{i-1,j} - 4b_3 u_{i-1,j+1} = 0
\end{aligned}
\tag{B.86}
$$

Equation 3

$$
\begin{aligned}
& c_{15i,j}p_{mi,j} - (c_{1i,j} + c_{2i,j})p_{mi-1,j} - (c_{3i,j} + c_{4i,j})p_{mi,j+1} \\
& +(c_{10i,j} - c_{7i,j})p_{fi,j} - 2c_{8i,j}u_{i-1,j} + c_{11i,j}S_{mi,j} + c_{12i,j}S_{fi,j} \\
= \; & -2c_{8i,j}u_{i-1,j} + c_{11i,j}S_{mi,j} + c_{12i,j}S_{fi,j} + c_{13i,j}p_{cmi,j} \\
& +c_{14i,j}p_{mi,j} + c_{10i,j}p_{fi,j} - (c_{2i,j} + c_{1i,j})p_{cmi-1,j} \\
& -(c_{3i,j} - c_{4i,j})p_{cmi,j+1} - c_{7i,j}p_{cfi,j}
\end{aligned}
\tag{B.87}
$$

Equation 4

$$\begin{aligned}
& d_{15i,j}p_{mi.j} - (d_{1i,j} + d_{2i,j})p_{mi-1,j} - (d_{3i,j} + d_{4i,j})p_{mi,j+1} \\
& +(d_{10i,j} - d_{7i,j})p_{fi,j} - 2d_{8i,j}u_{i-1,j} + d_{11i,j}S_{mi,j} + d_{12i,j}S_{fi,j} \\
= \;& d_{14i,j}p_{mi,j} + d_{10i,j}p_{fi,j} + d_{11i,j}S_{mi,j} \\
& +d_{12i,j}S_{fi,j} - 2d_{8i,j}u_{i-1,j} \qquad \text{(B.88)}
\end{aligned}$$

Equation 5

$$\begin{aligned}
& e_{15i,j}p_{fi.j} - (e_{1i,j} + e_{2i,j})p_{fi-1,j} - (e_{3i,j} + e_{4i,j})p_{fi,j+1} \\
& +(e_{10i,j} - e_{7i,j})p_{mi,j} - 2e_{8i,j}u_{i-1,j} + e_{11i,j}S_{fi,j} + e_{12i,j}S_{mi,j} \\
= \;& -2e_{8i,j}u_{i-1,j} + e_{11i,j}S_{fi,j} + e_{12i,j}S_{mi,j} + e_{13i,j}p_{cfi,j} \\
& +e_{14i,j}p_{fi,j} + e_{10i,j}p_{mi,j} - (e_{2i,j} + e_{1i,j})p_{cfi-1,j} \\
& -(e_{3i,j} - e_{4i,j})p_{cfi,j+1} - e_{7i,j}p_{cmi,j} \qquad \text{(B.89)}
\end{aligned}$$

Equation 6

$$\begin{aligned}
& f_{15i,j}p_{fi,j} - (f_{1i,j} + f_{2i,j})p_{fi-1,j} - (f_{3i,j} + f_{4i,j})p_{fi,j+1} \\
& +(f_{10i,j} - f_{7i,j})p_{mi,j} - 2f_{8i,j}u_{i-1,j} - f_{10i,j}S_{fi,j} \\
= \;& f_{14i,j}p_{fi,j} + f_{10i,j}p_{mi,j} + f_{11i,j}S_{fi,j} + f_{12i,j}S_{mi,j} - 2f_{8i,j}u_{i-1,j} \qquad \text{(B.90)}
\end{aligned}$$

- Corner $i = N_x$, $j = N_y$

Equation 1

$$-2(a_1 + a_2)u_{i,j} + 2a_2u_{i,j-1} = 0 \qquad \text{(B.91)}$$

Equation 2

$$-2(b_1 + b_2)v_{i,j} + 2b_1u_{i-1,j} + 2b_3u_{i-1,j-1} = 0 \qquad \text{(B.92)}$$

Equation 3

$$c_{15i,j}p_{mi,j} - (c_{2i,j} + c_{1i,j})p_{mi-1,j} - (c_{4i,j} + c_{3i,j})p_{mi,j-1}$$

$$
\begin{aligned}
& +(c_{10i,j} - c_{7i,j})p_{fi,j} - 2c_{8i,j}u_{i-1,j} - 2c_{9i,j}v_{i,j-1} + c_{11i,j}S_{mi,j} + c_{12i,j}S_{fi,j} \\
= \;& c_{14i,j}p_{mi,j} + c_{10i,j}p_{fi,j} + c_{11i,j}S_{mi,j} + c_{12i,j}S_{fi,j} - 2c_{8i,j}u_{i-1,j} \\
& -2c_{9i,j}v_{i,j-1} + c_{13i,j}p_{cmi,j} - (c_{2i,j} + c_{1i,j})p_{cmi-1,j} \\
& -(c_{4i,j} + c_{3i,j})p_{cmi,j-1} - c_{7i,j}p_{cfi,j}
\end{aligned} \tag{B.93}
$$

Equation 4

$$
\begin{aligned}
& d_{15i,j}p_{mi,j} - (d_{1i,j} + d_{2i,j})p_{mi-1,j} - (d_{3i,j} + d_{4i,j})p_{mi,j-1} \\
& +(d_{10i,j} - d_{7i,j})p_{fi,j} - 2d_{8i,j}u_{i-1,j} - 2d_{9i,j}v_{i,j-1} + d_{11i,j}S_{mi,j} + d_{12i,j}S_{fi,j} \\
= \;& d_{14i,j}p_{mi,j} + d_{10i,j}p_{fi,j} + d_{11i,j}S_{mi,j} \\
& +d_{12i,j}S_{fi,j} - 2d_{8i,j}u_{i-1,j} - 2d_{9i,j}v_{i,j-1}
\end{aligned} \tag{B.94}
$$

Equation 5

$$
\begin{aligned}
& e_{15i,j}p_{fi,j} - (e_{2i,j} + e_{1i,j})p_{fi-1,j} - (e_{4i,j} + e_{3i,j})p_{fi,j-1} + (e_{10i,j} - e_{7i,j})p_{mi,j} \\
& -2e_{8i,j}u_{i-1,j} - 2e_{9i,j}v_{i,j-1} + e_{11i,j}S_{fi,j} + e_{12i,j}S_{mi,j} \\
= \;& e_{14i,j}p_{fi,j} + e_{10i,j}p_{mi,j} + e_{11i,j}S_{fi,j} + e_{12i,j}S_{mi,j} - 2e_{8i,j}u_{i-1,j} \\
& -2e_{9i,j}v_{i,j-1} + e_{13i,j}p_{cfi,j} - (e_{2i,j} + e_{1i,j})p_{cfi-1,j} \\
& -(e_{4i,j} + e_{3i,j})p_{cfi,j-1} - e_{7i,j}p_{cmi,j}
\end{aligned} \tag{B.95}
$$

Equation 6

$$
\begin{aligned}
& f_{15i,j}p_{fi,j} - (f_{2i,j} + f_{1i,j})p_{fi-1,j} - (f_{4i,j} + f_{3i,j})p_{fi,j-1} + (f_{10i,j} - f_{7i,j})p_{mi,j} \\
& -2f_{8i,j}u_{i-1,j} - 2f_{9i,j}v_{i,j-1} + f_{11i,j}S_{fi,j} + f_{12i,j}S_{mi,j} \\
= \;& f_{14i,j}p_{fi,j} + f_{10i,j}p_{mi,j} + f_{11i,j}S_{fi,j} \\
& +f_{12i,j}S_{mi,j} - 2f_{8i,j}u_{i-1,j} - 2f_{9i,j}v_{i,j-1}
\end{aligned} \tag{B.96}
$$

IMAGE EVALUATION TEST TARGET (QA-3)

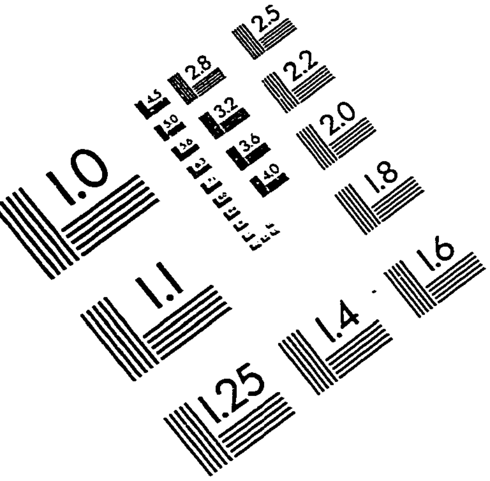

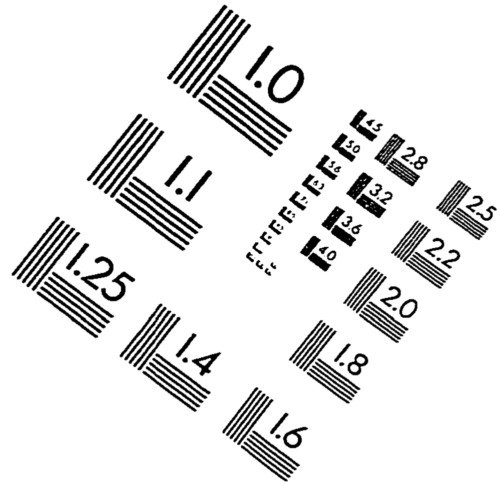

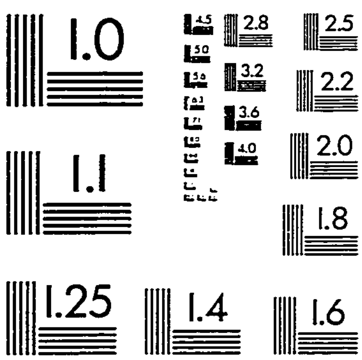

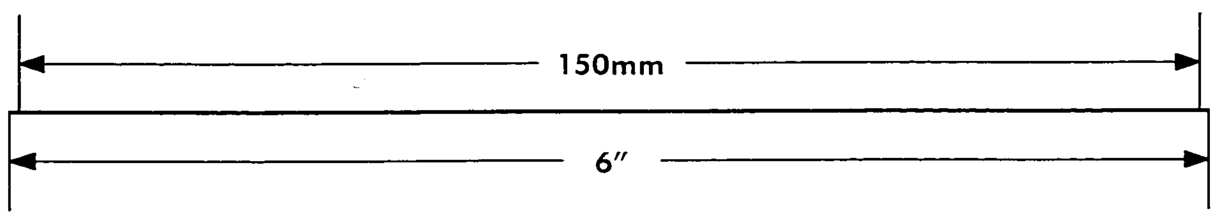

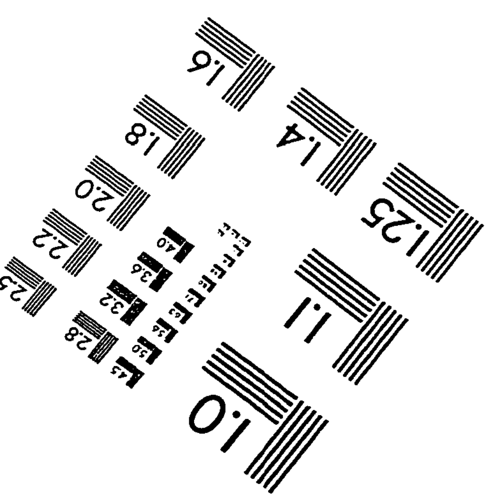

APPLIED IMAGE . Inc
1653 East Main Street
Rochester, NY 14609 USA
Phone: 716/482-0300
Fax: 716/288-5989